



**HAL**  
open science

## Impact of the wind during a building airleakage measurement

Adeline Bailly Mélois

► **To cite this version:**

Adeline Bailly Mélois. Impact of the wind during a building airleakage measurement. Thermics [physics.class-ph]. Université de Lyon, 2020. English. NNT : 2020LYSET017 . tel-03450967

**HAL Id: tel-03450967**

**<https://theses.hal.science/tel-03450967>**

Submitted on 26 Nov 2021

**HAL** is a multi-disciplinary open access archive for the deposit and dissemination of scientific research documents, whether they are published or not. The documents may come from teaching and research institutions in France or abroad, or from public or private research centers.

L'archive ouverte pluridisciplinaire **HAL**, est destinée au dépôt et à la diffusion de documents scientifiques de niveau recherche, publiés ou non, émanant des établissements d'enseignement et de recherche français ou étrangers, des laboratoires publics ou privés.



N°d'ordre NNT : 2020LYSET017

**THÈSE de DOCTORAT DE L'UNIVERSITÉ DE LYON**  
opérée au sein de  
**l'École de l'aménagement durable des territoires ENTPE**

**École Doctorale N° 162**  
**(Ecole Mécanique, Énergétique, Génie Civil, Acoustique)**

**Spécialité / discipline de doctorat :**  
Sciences pour l'ingénieur / Thermique Energétique

par :  
**Adeline Bailly, ép. Mélois**

---

**Impact of the wind during a building  
airleakage measurement**

Impact du vent pendant une mesure d'étanchéité à  
l'air de l'enveloppe des bâtiments

---

Devant le jury composé de :

Bastide, Alain, Professeur, Université de La Réunion  
Jansens, Arnold, Professeur, Ghent University  
Wood, Christopher, Professeur ass.  
Meslem, Amina, Professeure, IUT de Rennes  
Leprince, Valérie, Docteure, société PLEIAQ

Président  
Rapporteur  
Rapporteur  
Examinatrice  
Examinatrice

El Mankibi, Mohamed, Professeur, ENTPE  
Carrié, François Rémi, Docteur, Société ICEE  
Moujalled, Bassam, Docteur, Cerema

Directeur de thèse  
Co-directeur de thèse  
Co-directeur de thèse



# Remerciements

*Je remercie tout d'abord mes 3 directeurs de thèse, Mohamed, Rémi et Bassam pour m'avoir guidée et soutenue pendant ces 4 années. Merci à Rémi de m'avoir choisie pour ce projet, de m'avoir guidée dans toutes les épreuves, et d'avoir été présent tout au long de cette aventure. Merci à Mohamed de m'avoir accueillie, et d'avoir mobilisé toutes les ressources dont j'ai pu avoir besoin. Merci à Bassam, d'avoir rempli un rôle de co-directeur, de collègue et d'ami pendant toute cette thèse.*

*Je tiens ensuite à remercier les membres du jury : Arnold Janssens, Christopher Wood, Alain Bastide, Amina Meslem, et Valérie Leprince. Merci pour leurs conseils et le temps qu'ils m'ont accordé.*

*Je remercie chaleureusement les experts de l'AIVC m'ayant consacré du temps pour me conseiller lors d'étapes importantes de mon travail : Max Sherman, Iain Walker, Benjamin Jones, Gary Nelson, Stefanie Rolfsmeier, Valérie Leprince, Christophe Delmotte, Jiri Novak, Steven Rogers et Bill Graber.*

*Merci également aux chercheurs du CETIAT, Isabelle Caré, Laure Mouradian et Alain Guedel, ainsi que du CSTB, François Demouges, pour leurs conseils précieux, leurs critiques avisées et leur temps.*

*Merci à l'ENTPE de m'avoir accueillie, aux chercheurs et aux doctorants pour tous ces moments partagés pendant cette thèse, à l'équipe logistique et la mission technique pour m'avoir accompagnée sur ce gros projet, et à l'équipe qui m'a permis de réaliser le film de ma thèse. Merci en particulier à Joachim Blanc Gonnet et Bernard Lorient.*

*Je remercie ma direction au Cerema Centre-Est pour m'avoir permis de réaliser cette thèse. Merci particulièrement à Myriam Olivier, qui m'a soutenue dès le début du projet, puis à Julie Tissot, Cédric Lentillon et Laurent Deleersnyder pour avoir rendu cette thèse possible et pour m'avoir permis de consacrer tout mon temps à ce projet. Merci à la DRII du Cerema pour son soutien.*

*Je remercie mes collègues du CECP d'Angers pour leur aide précieuse et leur participation à ce projet, grâce à la conception et la réalisation de la maquette, et en particulier Xavier Bertrand et Anthony Colin.*

*Merci aux chercheurs de l'équipe BPE pour leur soutien et pour la construction de cette équipe qui me permet de continuer mon travail en tant que chercheuse au sein du Cerema.*

*Je remercie mon stagiaire, Anh Dung Tran, sur qui j'ai pu compter pendant 5 mois et qui était un véritable binôme pendant la phase expérimentale.*

*Merci à l'équipe Bâtiments du Cerema, qui m'a accueillie en tant que stagiaire et qui m'a ensuite fait grandir dans la famille des maçons, qui m'a fait découvrir la perméabilité à l'air, la ventilation mais également des valeurs de travail uniques. Merci en particulier à mon collègue Pierre, mon papi au travail. Un très grand merci également à mes deux mentores : Valérie et Gaëlle, qui m'ont formée depuis les bancs de l'école, m'ont donné le goût de la recherche et de la natation, m'ont soutenue et m'ont poussée à me dépasser, en véritables amies. Un merci très particulier à Bassam, qui en plus d'être devenu co-directeur de thèse, a été*

*mon soutien quotidien durant cette longue aventure : merci pour toutes ces discussions culinaires indispensables pour garder le moral !*

*Je tiens enfin à remercier ma famille pour m'avoir soutenue et suivie dans cette aventure, sans comprendre tout à fait ce que je faisais : mes parents, mes sœurs et mon frère. Un très grand merci à Elie et à Coline d'avoir rempli cette aventure d'amour, et au petit Cornichon qui a animé mes derniers mois de thèse de ses petits coups de pieds.*



## Abstract

To reach the nearly zero energy building level for new buildings, minimizing and controlling envelope airleakage has become one of the major levers to reduce the energy use in buildings. It is then crucial to perform reliable building airtightness measurements. Nevertheless, windy conditions during fan pressurization tests, which is the most commonly used test method and is described by the standard ISO9972, may strongly impact the test results and then lead to significant errors. As these errors are yet not well qualified and quantified, this thesis aims at characterizing the error induced by a steady wind during building airleakage measurements through laboratory experiments on a reduced model in a wind tunnel.

The analysis of 219,000 onsite tests performed on French buildings leads to the identification of factors that can significantly impact the envelope airtightness, such as the nature of the main construction material, the technique of thermal insulation, and the ventilation system, and levers to improve the practices of stakeholders and testers. Whereas many fields are included in the national database, we have very poor information regarding the uncertainty of the measurement results and thus their reliability. Our evaluation of the current knowledge regarding airtightness test uncertainty shows that several sources of error lie in the measurement itself whereas numerous sources are linked to the flow model. As no holistic approach proposes a global qualification and quantification of these errors, there remains a considerable need for research to assess the uncertainty of a test, including exploratory theoretical and experimental work.

Thus, we designed and constructed an experimental facility to reproduce pressurization tests on a reduced scale during steady wind conditions, under laboratory controlled conditions. We first present the physical model of a test we developed to conduct a dimensional analysis, leading to the definition of similarity conditions between reduced scale and full scale. Secondly, we present the design characteristic of our facility that includes a model of a simplified single-zone house with two leaks (scale 1/25<sup>th</sup>), a pressurization device with an airflow controller, and a 4.11 m long wind tunnel. We then analyze 96 pressurization tests we performed according to ISO 9972 on our facility, which include 864 measurements under steady conditions: for nine configurations of leakage distribution of our model and under eight different wind speeds (from 0 to 7 m s<sup>-1</sup>). We observed that the variation of the zero-flow pressure difference induced by strong winds depends on the leakage distribution: from 1 Pa to more than 16 Pa, which indicates that the zero-flow pressure difference is not always a relevant indicator of the windy conditions. The error due to wind we evaluated for these strong wind speeds depends on the leakage distribution, especially for the 4 Pa indicator  $q_4$ , with a maximal error varying from 2% (leaks equally distributed) to 35% (60% of the leakage on the windward facade). We tested alternative analysis methods that yet did not provide more reliable results. Nevertheless, many other analysis methods should be tested from these experimental data, and many new data should be obtained using this experimental facility, leading hopefully to more reliable protocols for building airtightness tests.



# Résumé

## 1.1 Introduction

La directive Européenne 2010/31/EU, qui doit être appliquée par les états membres de l'Union Européenne fin 2020, rend obligatoire le niveau « zéro-énergie » pour la construction de nouveaux bâtiments. Cette exigence est un vrai challenge pour l'ensemble des acteurs de la construction, qui doivent désormais mettre en œuvre des solutions pour assurer la bonne qualité de l'air intérieur et le confort thermique dans les bâtiments, tout en réduisant l'impact environnemental et énergétique pour faire face au réchauffement climatique. Depuis plusieurs dizaines d'années, réduire et maîtriser les infiltrations d'air à travers l'enveloppe des bâtiments est devenu un des leviers principaux pour la réduction des consommations d'énergie. Ainsi, le renforcement de l'étanchéité à l'air de l'enveloppe des bâtiments devient crucial pour la construction de nouveaux bâtiments.

En France, l'actuelle réglementation thermique RT2012 rend déjà obligatoire le traitement de la perméabilité à l'air de l'enveloppe pour les bâtiments résidentiels, en imposant une valeur limite réglementaire, ainsi qu'une mesure à réception (ou dans certains cas, l'application d'une démarche qualité certifiée) pour justifier du respect de cette limite. Cette mesure doit être réalisée conformément à la norme internationale ISO 9972 par un opérateur autorisé. Si le cadre réglementaire et normatif est très précis en France, les opérateurs de mesure ainsi que les maîtres d'ouvrage sont régulièrement confrontés sur le terrain à des situations particulières rendant la mesure impossible. En effet, afin de limiter les incertitudes de mesure liées au vent, la norme ISO 9972 et son guide d'application FD P50-784 n'autorisent la mesure que dans des conditions de vent calme. Suivant la situation géographique du bâtiment, il est régulièrement impossible de respecter l'obligation réglementaire de mesure dans ces conditions de vent. Il y a donc un besoin important de faire évoluer le protocole de mesure pour le rendre moins impacté par le vent, ou mieux prendre en compte les erreurs induites par le vent. Cependant, malgré une communauté internationale de chercheurs actifs sur le sujet depuis plusieurs dizaines d'années, la complexité des phénomènes physiques et la diversité des situations rencontrées sur le terrain ne permettent pas aujourd'hui de quantifier cette erreur, ni de proposer de méthode plus fiable.

Ainsi, cette thèse vise à caractériser l'impact induit par le vent pendant une mesure d'étanchéité à l'air, à travers l'analyse de mesures expérimentales réalisées à échelle réduite dans une soufflerie en laboratoire.

## 1.2 Etats des lieux des mesures d'étanchéité à l'air en France

Le chapitre 2 de ce manuscrit présente dans un premier temps un état des lieux des mesures d'étanchéité à l'air en France, à travers l'analyse de la base de données nationale qui comprend 219 000 mesures réalisées sur site par des opérateurs autorisés. Plus de

96% des mesures enregistrées dans cette base de données ont été réalisées sur des bâtiments résidentiels : nous présentons ici uniquement les résultats concernant ces bâtiments. Premièrement, nous avons mis en avant plusieurs facteurs qui peuvent impacter de façon importante l'étanchéité à l'air de l'enveloppe des bâtiments :

- la nature du matériau de construction principal : les constructions en bois sont généralement moins étanches que les bâtiments construits en brique ou en béton. Nous observons notamment une valeur médiane de l'indicateur français de perméabilité à l'air  $Q_{Pa-surf}$  15% plus élevée pour les maisons individuelles construites en bois, 20% pour les bâtiments de logements collectifs. Bien que les bâtiments en bois soient équipés d'un pare-vapeur qui devrait renforcer l'étanchéité à l'air, le manque d'expérience sur ce type de principe constructif en France expliquerait ces moins bons résultats pour ces bâtiments ;
- le type d'isolation thermique : nous observons que les logements collectifs isolés par l'extérieur présentent une meilleure étanchéité à l'air, ce qui peut s'expliquer par l'utilisation plus courante de béton cellulaire, plus étanche, pour ces constructions ;
- le type de système de ventilation : nous observons, également uniquement pour les logements collectifs, que la présence de système de ventilation double-flux s'associe d'une meilleure étanchéité à l'air (-17% sur la valeur médiane de  $Q_{Pa-surf}$  par rapport aux bâtiments équipés de systèmes simple-flux). Cela s'explique par le suivi d'une démarche globale de renforcement de la qualité de la construction qui accompagne en général le choix d'un système double-flux dans les bâtiments de logements collectifs.

Une analyse des fuites détectées dans les bâtiments de la base de données a permis de mettre en avant d'une part les fuites les plus souvent rencontrées (les plus fréquemment identifiées sont les fuites au niveau des traversées de planchers, murs et cloisons), mais également d'identifier des fuites qui, lorsqu'elles sont présentes, sont en général un indicateur d'une moins bonne étanchéité à l'air. On observe notamment que lorsque des fuites dues à l'éclairage sont détectées dans des maisons (ce qui est le cas pour 109 224 maisons de la base de données), la valeur médiane de  $Q_{Pa-surf}$  est 18% plus élevée que la médiane de l'ensemble des maisons. Ces résultats sont très utiles pour renforcer l'étanchéité à l'air des futures constructions, en intégrant des points d'attention particuliers dans les phases de conception et de réalisation des bâtiments.

Nous observons également que l'introduction d'une valeur limite réglementaire encourage la mise en œuvre de corrections de dernière minute au moment du test, ce qui peut avoir un impact important sur la durabilité de l'étanchéité à l'air de l'enveloppe.

Finalement, nous observons que malgré la quantité d'information dans cette base de données, nous ne disposons pas d'éléments permettant d'évaluer la fiabilité de ces mesures. Le seul indicateur que nous avons pu calculer, c'est l'écart entre les résultats des différentes saisons : nous n'avons observé aucun impact saisonnier sur le résultat des mesures.

L'analyse de cette base de données montre que de nombreux tests sont réalisés tous les ans en France, et environ 65 000 nouveaux tests sont attendus chaque année. Ces tests sont utilisés pour justifier du respect de l'exigence réglementaire, et leurs résultats sont

utilisés dans le calcul thermique des bâtiments. Il est donc essentiel de pouvoir garantir la fiabilité des résultats des mesures d'étanchéité à l'air de l'enveloppe des bâtiments.

### **1.3 Sources d'incertitudes pendant une mesure d'étanchéité à l'air : connaissances et lacunes**

Les premières mesures d'étanchéité à l'air des bâtiments ont été réalisées dans les années 1950 et 1960 en utilisant des méthodes de gaz traceurs, très longues et très coûteuses. Des prototypes ont alors été développés à partir de la fin des années 1960 aux Etats-Unis, au Canada et au Royaume-Uni pour mesurer la perméabilité à l'air de l'enveloppe d'un bâtiment en se basant sur la méthode de pressurisation, qui se base sur la loi puissance ci-dessous :

$$q = C * \Delta p^n$$

avec :

- $q$  le débit de fuite volumique [ $\text{m}^3 \text{h}^{-1}$ ]
- $\Delta p$  la différence de pression entre l'intérieur et l'extérieur du bâtiment [Pa]
- $C$  le coefficient de fuite d'air [ $\text{m}^3 \text{h}^{-1} \text{Pa}^{-n}$ ]
- $n$  l'exposant de débit d'air [-].

La méthode multi-points de pressurisation, qui est la méthode la plus couramment utilisée et décrite dans les normes ISO 9972 et ASTM 779-19, exige d'imposer plusieurs différences de pression et de mesurer les débits de fuite correspondants. Un débit de fuite à une pression de référence peut alors être extrapolé en réalisant une régression linéaire. Différentes pressions de référence sont utilisées dans le monde, notamment 4 Pa (en France pour le calcul du  $Q_{4\text{Pa-surf}}$ , et aux Etats-Unis) et 50 Pa (dans de nombreux pays). Cette technique de mesure est aujourd'hui réalisée avec une « blowerdoor ».

L'analyse de 39 études dédiées à la caractérisation des incertitudes de mesure de perméabilité à l'air nous ont permis de classer les nombreuses sources d'incertitudes en deux familles.

#### *1.3.1 Les sources liées à la réalisation de la mesure*

Ces sources rassemblent notamment les incertitudes des appareils de mesure, la préparation du bâtiment par l'opérateur, la règle d'échantillonnage lorsque seule une partie du bâtiment est soumise à l'essai, ou encore la méthode d'analyse des données mesurées. Les erreurs dues à certaines de ces erreurs peuvent être réduites, en mettant en place par exemple une qualification des opérateurs et des exigences concernant l'étalonnage du matériel de mesure. D'autres, comme l'impact de la méthode d'analyse, font aujourd'hui l'objet de travaux de recherche qui nécessitent encore des études numériques et des tests expérimentaux.

#### *1.3.2 Les sources liées au modèle physique*

La méthode basée sur la loi puissance suppose que l'ensemble des débits d'air passant à travers les fuites de l'enveloppe peuvent être vus comme un seul débit passant par une

unique fuite équivalente, qui est soumise à une unique différence de pression. La méthode de mesure inclut des corrections pour tenir compte de l'hétérogénéité des différences de pression tout autour du bâtiment, et également des différences de température ou l'impact du vent. Cependant, ces corrections ne sont pas complètes, ni parfois physiquement correctes. Il existe donc des erreurs qui ne sont pas corrigées, et qui peuvent engendrer une incertitude importante sur le résultat de la mesure. Bien que la communauté scientifique travaille activement pour améliorer ces corrections, de nombreux travaux de recherche théoriques, numériques et expérimentaux sont encore nécessaires pour identifier l'ensemble des sources d'erreurs, leur impact aux différentes étapes d'une mesure et quantifier ces erreurs. En particulier, nous avons besoin de mieux comprendre les variations des différences de pression dans le temps et l'espace, et proposer une correction plus exacte que la correction par la pression à débit nul qui est aujourd'hui réalisée.

## **1.4 Définition des critères de similitudes et des rapports d'échelles pour le dimensionnement d'un banc expérimental à échelle réduite**

Afin de mieux comprendre l'impact du vent pendant une mesure de perméabilité à l'air du bâtiment, nous avons choisi de réaliser des tests à échelle réduite dans des conditions de laboratoire maîtrisées, sur une maquette dont l'étanchéité réelle est parfaitement connue. La reproduction de phénomènes physiques à échelle réduite nécessite la définition de critères de similitudes, afin de s'assurer que les résultats de l'expérimentation seront transposables à échelle réelle.

### *1.4.1 Modèle d'un test de perméabilité à l'air*

Le chapitre 4 de ce mémoire présente tout d'abord les équations qui décrivent un test de perméabilité à l'air. Pour développer ce modèle nous faisons les hypothèses suivantes :

- un bâtiment peut être représenté par une unique zone présentant deux types de façades : les façades exposées au vent et les façades à l'abri du vent ;
- pour une direction de vent donnée,
  - o les fuites présentes sur les façades exposées peuvent être représentées par une seule fuite ;
  - o les fuites présentes sur les façades abritées peuvent être représentées par une seule fuite.

En appliquant ces hypothèses, notre modèle est constitué de :

- deux équations décrivant la différence de pression de part et d'autre de la fuite exposée et de la fuite abritée respectivement ;
- deux équations décrivant le débit d'air à travers la fuite exposée et la fuite abritée respectivement;
- un bilan de masse sur notre système ;
- et une équation de conservation d'énergie dans notre système.

#### 1.4.2 Définition des critères de similitude

Après avoir simplifié notre modèle d'équations en se plaçant en conditions initiales isothermes qui seront assurées dans le laboratoire, nous avons appliqué le théorème de Washy-Buckingham. Ce théorème permet, à partir de la définition du phénomène observé (ici, l'erreur induite par le vent sur le résultat de la mesure), de définir les nombres adimensionnels qui devront avoir la même valeur entre l'échelle réelle et l'échelle de l'expérimentation. Dans notre cas, nous devons conserver 4 nombres adimensionnels faisant intervenir les variables suivantes :

- les différences de pression  $\Delta p$  ;
- la masse volumique de l'air  $\rho$  ;
- la vitesse du vent à la hauteur du bâtiment  $U$  ;
- le temps  $t$  ;
- les surfaces des fuites  $A$  ;
- les débits volumiques  $q$  ;
- les longueurs  $L$  ;
- le volume interne  $V$ .

La conservation de ces nombres adimensionnels entre les deux échelles conduit aux équations entre les rapports d'échelle suivant (avec pour une variable  $X$ ,  $\bar{X}$  le rapport entre la valeur à échelle réduite et la valeur à échelle réelle) :

$$\bar{U}^2 = \bar{p}$$

$$\bar{p} \cdot \bar{A}^2 = \bar{q}^2$$

$$\bar{A}^{0,5} = \bar{L}$$

$$\bar{V} \cdot \bar{U} = \bar{L} \cdot \bar{q}$$

Ces critères de similitude permettent de réaliser une expérimentation à échelle réduite en imposant un rapport d'échelle égal à 1 pour la vitesse de vent et les différences de pression ( $\bar{U} = 1$  et  $\bar{p} = 1$ ) : à échelle réduite, la vitesse de vent et les différences de pression imposées seront les mêmes qu'à échelle réelle.

### **1.5 Reproduction de tests de perméabilité à l'air à échelle réduite dans une soufflerie : conception et caractérisation d'un nouveau banc expérimental**

L'objectif du chapitre 5 de ce mémoire est de présenter les étapes du dimensionnement du banc expérimental à échelle réduite qui doivent permettre de :

- réaliser des mesures de perméabilité à l'air de l'enveloppe de bâtiment à échelle réduite ;
- générer un vent constant, pour différentes vitesses de vent ;
- mesurer précisément des différences de pressions, des vitesses de vent et des débits d'air.

Le banc expérimental comprend :

- une maquette de bâtiment une zone ;
- un appareil de pressurisation et de mesure ;
- une soufflerie ;
- un ensemble de capteurs et d'appareils de mesure.

Afin de concevoir à la fois une soufflerie de taille raisonnable et une maquette de taille suffisante, l'échelle 1/25<sup>e</sup> est retenue pour les dimensions de la maquette. Les autres rapports d'échelle ont alors été déduits à partir du chapitre 4.

### *1.5.1 Conception du banc experimental*

#### *1.5.1.1 La maquette*

La maquette est conçue à partir d'une maison individuelle fictive comprenant un RDC et un étage, avec une perméabilité à l'air correspondant au niveau limite imposé par la RT2012, ce qui correspond à une surface équivalente de fuite à 4 Pa  $ELA_4 = 0,0142 \text{ m}^2$ . La maquette est un parallélépipède de dimensions 0,24x0,40x0,2 m<sup>3</sup> avec deux fuites sur deux façades opposées dont l'une correspond à la façade exposée et l'autre à la façade abritée. La somme des surfaces des deux fuites correspond à la valeur de  $ELA_4$  en considérant différents ratios de distribution de  $ELA_4$  sur les deux façades (10% à 90%) afin de pouvoir étudier l'impact de la distribution des fuites. Des mesures préliminaires avec une version provisoire de la maquette et des modélisations CFD ont permis de définir la position des fuites : pour chacune des deux façades concernées, la fuite est positionnée à 13 cm du plancher de la maquette et à 7 cm du bord droit, afin d'éviter à la fois les effets de la couche limite de la soufflerie et l'impact direct de la fuite opposée.

La maquette doit tout d'abord être très robuste : sa perméabilité à l'air ne doit pas s'altérer dans le temps, d'une mesure sur l'autre. D'autre part, afin de permettre de nombreuses expérimentation dans le futur, la maquette doit facilement permettre des évolutions. La maquette est donc constituée d'un squelette en métal et de façades amovibles en Plexiglas®. Les deux façades exposée et abritée incluent une ouverture circulaire dans laquelle s'installent des cylindres métalliques percés à différents diamètres correspondants aux différentes tailles de fuite. Le plancher de la maquette est muni d'un grand panneau circulaire équipé de système de fixations permettant de placer précisément la maquette dans la soufflerie dans différentes positions avec un angle variant de 0° à 360°. Le socle inclut également différentes connections étanches permettant notamment d'accueillir des tubes de pression et un thermomètre, ainsi que de connecter l'appareil de pressurisation.

#### *1.5.1.2 L'appareil de pressurization*

L'appareil de pressurisation doit permettre à la fois d'imposer des différences de pression entre l'intérieur et l'extérieur de la maquette de 10 Pa à 100 Pa, et de mesurer précisément le débit d'air qu'il fournit. A partir du système d'équations défini dans le chapitre 4, nous avons calculé les débits théoriques pour des vitesses de vent nulle à 7 m s<sup>-1</sup> pour cet

intervalle de différence de pression. L'appareil de mesure doit alors être capable de fournir des débits stables de  $3,0 \cdot 10^{-5}$  à  $3,0 \cdot 10^{-4} \text{ m}^3 \text{ s}^{-1}$ .

L'appareil de mesure que nous avons assemblé comprend :

- un contrôleur de flux massique qui fournit et mesure des débits de  $0,4 \text{ l min}^{-1}$  à  $100 \text{ l min}^{-1}$  ( $6,7 \cdot 10^{-6}$  à  $1,7 \cdot 10^{-3} \text{ m}^3 \text{ s}^{-1}$ ) avec une précision de  $\pm 5\%$  de la valeur mesurée ;
- un compresseur qui fournit de l'air comprimé à 3 bar au contrôleur ;
- un manomètre qui mesure la différence de pression entre l'intérieur et l'extérieur de la maquette.

L'ensemble du dispositif est piloté par une application développée avec le logiciel Labview, qui est appelée par un programme VBA qui permet de reproduire automatiquement de nombreux tests de perméabilité dans des conditions de répétabilité pour différentes vitesses de vent.

Contrairement à une blowerdoor, notre appareil de mesure ne permettra de réaliser des mesures qu'en pressurisation. D'autre part, il sera connecté au socle de la maquette : aucun impact du vent directement sur l'appareil de mesure ne sera donc reproduit pendant les mesures de perméabilité à l'air à échelle réduite.

#### *1.5.1.3 La soufflerie*

La soufflerie doit permettre de reproduire des vents stables de 0 à  $7 \text{ m s}^{-1}$ . La soufflerie doit comprendre :

- une chambre de tranquillisation avec 1 nid d'abeille et 2 écrans ;
- un convergent ;
- une chambre d'essai ;
- un diffuseur ;
- un ventilateur.

Des simulations CFD ont été réalisées premièrement pour évaluer les champs de pression et de vitesse dans la chambre d'essai, afin de les comparer aux champs théoriques à échelle réelle. Aucune différence significative n'a été identifiée, ce qui a permis de valider les dimensions de la chambre d'essai. Deuxièmement, la forme idéale du convergent étant très coûteuse à fabriquer (forme de Bell-Metha), des formes simplifiées ont été étudiées grâce à de nouvelles simulations CFD. Une forme simplifiée, avec un angle de  $30^\circ$ , a été retenue.

Les plans finaux de la soufflerie prévoient une soufflerie de 4,11 m de longueur, 2 m de hauteur maximale, 2 m de largeur maximale avec une chambre d'essai de  $1,5 \times 1 \times 1 \text{ m}^3$ .

#### *1.5.2 Caractérisation du banc expérimental*

La maquette présente une très bonne étanchéité à l'air sans les deux fuites volontaires, et un débit de fuite à 4 Pa  $q_4=0,17 \text{ m}^3 \text{ h}^{-1}$  pour les 9 configurations de répartition de fuites. Le débit à travers chaque fuite a été caractérisé et correspond à un régime turbulent, avec un exposant  $n = 0,5$ . Les coefficients d'exposition au vent  $C_p$  ont été évalués au niveau des deux fuites opposées et correspondent aux valeurs de la littérature.

L'appareil de pressurisation a permis d'imposer des différences de pression stables entre l'intérieur et l'extérieur de la maquette de 10 à 100 Pa pour toutes les vitesses de vent possibles dans la soufflerie. L'appareil est automatiquement piloté et permet de réaliser rapidement des tests en séries.

La soufflerie a été installée dans une pièce dédiée du laboratoire, et permet de reproduire des vents constants stables à des vitesses inférieures à  $1 \text{ m s}^{-1}$  jusqu'à  $7,5 \text{ m s}^{-1}$ . Les vitesses de vent mesurées dans la chambre d'essai sont stables dans le temps et dans l'espace.

## **1.6 Évaluation de l'impact du vent pendant une mesure de perméabilité à l'air**

Dans le chapitre 6, nous étudions l'impact du vent pour les 9 configurations de répartition de fuite pour des vents stables allant de 0 à  $7 \text{ m s}^{-1}$ . Les tests sont réalisés à échelle réduite sur notre banc expérimental, avec des vitesses de vent et des différences de pression similaires à celles rencontrées à échelle réelle (rapports d'échelle = 1). Le protocole de test est le protocole décrit dans la norme ISO 9972, avec des différences de pression allant de 10 à 100 Pa. Afin d'analyser l'impact de différentes restrictions du protocole normatif, des tests sont réalisés même lorsque la limite de 5 Pa pour la valeur de pression à débit nul  $\Delta p_0$  est dépassé. Nous avons réalisé 96 tests de perméabilité à l'air, ce qui représentent 864 mesures. Ces tests ont été réalisés grâce aux applications Labview et au programme VBA que nous avons développés pour piloter le banc expérimental et enregistrer toutes les données expérimentales.

### *1.6.1 Impact du vent sur la valeur de pression à débit nul $\Delta p_0$*

Nous avons tout d'abord analysé les différences de pression à débit nul pour les 9 configurations de répartition de fuite et pour 8 vitesses de vent (de 0 à  $7 \text{ m s}^{-1}$ ). La différence de pression à débit nul  $\Delta p_0$  est considérée comme un indicateur des conditions de vent. Sa valeur doit être inférieure en valeur absolue à 5 Pa pour que le test soit valide selon la norme ISO 9972.

Nous observons que la valeur de  $\Delta p_0$  dépend de façon très importante de la répartition des fuites : les valeurs de  $\Delta p_0$  varient de -16,7 Pa à +11,6 Pa pour un vent de  $7 \text{ m s}^{-1}$ . De plus, nous obtenons pour certaines configurations des valeurs très faibles (inférieur en valeur absolue à 1 Pa) pour des vitesses de vents élevées, ce qui montre que la différence de pression à débit nul n'est pas toujours un indicateur pertinent des conditions de vent.

Nous avons également montré que la limite de 5 Pa n'invalide pas les mêmes conditions de vent pour toutes les répartitions de fuite :

- lorsque les fuites sont majoritairement sur la façade abritée au vent, seuls les tests réalisés pour des vents faibles sont valides selon l'ISO 9972 ;
- lorsque les fuites sont majoritairement sur la façade exposée au vent, des tests peuvent être valides jusqu'à  $5 \text{ m s}^{-1}$  ;

- pour la répartition particulière avec 60% de la surface totale de fuite sur la façade exposée et 40% sur celle abritée, toutes les vitesses de vent étudiées conduisent à des tests valides.

Ces résultats montrent que la limite de 5 Pa ne reflète pas toujours les conditions de vents forts.

### *1.6.2 Impact du vent sur le résultat du test*

Nous avons calculé l'erreur induite par le vent pour les tests réalisés selon le protocole de l'ISO 9972, en comparant le résultat du test à la valeur réelle de perméabilité à l'air de la maquette à 4 Pa ( $q_4$ ) et à 50 Pa ( $q_{50}$ ). Nous observons tout d'abord que l'erreur dépend du choix de l'indicateur : à 50 Pa, l'erreur induite par le vent reste inférieure à 6% pour toutes les configurations de répartitions de fuite et pour des vents jusqu'à  $7 \text{ m s}^{-1}$ . A 4 Pa, l'erreur maximale pour chaque configuration varie de 2% (fuites équitablement réparties, pour une vitesse de vent de  $6 \text{ m s}^{-1}$ ) à 35% (60% des fuites sur la façade exposée, pour un vent de  $7 \text{ m s}^{-1}$ ). Lorsque les fuites sont très majoritairement (à 80% et 90%) sur la façade exposée, l'erreur maximale reste élevée autour de 18%. Ces résultats remettent en question la limite de 5 Pa pour  $\Delta p_0$ , qui ne garantit pas ici la fiabilité du résultat.

Nous avons enfin testé des protocoles de mesure alternatifs afin de réduire l'erreur induite par le vent. A partir des mêmes données expérimentales, nous avons calculé les valeurs de  $q_4$  et  $q_{50}$  pour 3 protocoles de tests à 1 point de mesures (10 Pa, 50 Pa et 100 Pa respectivement) avec un exposant  $n$  égal à 0,5, et 3 protocoles de tests à 2 points de mesure (10/50 Pa, 10/100 Pa et 50/100 Pa respectivement). Nous avons alors comparé les erreurs induites par le vent pour les tests réalisés en appliquant ces 6 protocoles aux résultats obtenus avec le protocole de l'ISO 9972. Pour des tests réalisés à échelle réduite, sur notre maquette, avec des vents stables, on observe que le protocole de l'ISO 9972 induit généralement des erreurs plus faibles que les protocoles alternatifs que nous avons testés. Nous observons tout de même des cas particuliers : lorsque les fuites sont majoritairement sur la façade exposée, les protocoles 1-point à 50 Pa et à 100 Pa induisent des erreurs plus faibles que l'ISO 9972 pour des vitesses de vents supérieures à  $4 \text{ m s}^{-1}$ . Cette analyse montre qu'appliquer une méthode de traitement des données différentes pourrait permettre de réduire les erreurs importantes induites par le vent.

## **1.7 Conclusions et perspectives**

Nous avons observé, alors que le renforcement de l'étanchéité à l'air de l'enveloppe des bâtiments est indispensable pour réduire les consommations d'énergie des bâtiments et améliorer la qualité des constructions, que nous avons besoin d'évaluer les performances des enveloppes afin d'améliorer les bâtiments existants et les futures constructions. Il est donc nécessaire de quantifier les infiltrations d'air et donc de réaliser des mesures de perméabilité à l'air fiables.

Le vent étant identifié comme une source importante d'erreur pour le résultat de la mesure, nous avons besoin de quantifier cette erreur, pour ensuite améliorer le protocole de mesure afin de réduire l'impact du vent.

Notre approche pour contribuer à cette recherche a été d'évaluer l'impact du vent en réalisant des tests expérimentaux à échelle réduite. Notre contribution principale à la recherche est la conception, l'installation et la caractérisation d'un nouveau banc expérimental qui permet de réaliser des tests de perméabilité à l'air de l'enveloppe à échelle réduite. Les avantages de ce nouveau banc expérimental sont :

- les conditions de laboratoire maîtrisées ;
- les caractéristiques prédéfinies de la maquette en terme de perméabilité à l'air ;
- la plage de vitesse de vent générées dans la chambre d'essai de la soufflerie ;
- les performances de l'appareil de pressurisation.

A travers l'analyse de 96 tests de perméabilité à l'air réalisés sur ce banc expérimental, nous avons montré que :

- la limite de 5 Pa pour la différence de pression à débit nul ne permet pas d'éviter toutes les conditions de vent fort ;
- l'erreur induite par le vent sur le résultat calculé à 4 Pa  $q_4$  dépend de façon très importante de la répartition des fuites sur l'enveloppe des bâtiments, avec une erreur pouvant atteindre 35%.

Ainsi, nous avons montré qu'il est indispensable d'améliorer le protocole de mesure afin d'obtenir des résultats plus fiables. Une des pistes d'amélioration concerne la méthode d'analyse des données mesurées.

Afin de définir un protocole plus fiable, nous avons besoin maintenant de consolider nos travaux de recherche. Tout d'abord, nous devons caractériser avec précision les incertitudes de nos résultats, notamment à partir des incertitudes liées aux différents appareils de mesure que nous avons utilisés. Deuxièmement, nous devons continuer à tester différentes méthodes d'analyse des données mesurées. Enfin, nous prévoyons de réaliser de nouveaux tests sur notre banc d'essai :

- des tests multiples en conditions de répétabilité ;
- avec des fuites de forme différentes et avec des matériaux différents ;
- avec plus de fuites.

Enfin, nous allons étudier la possibilité de générer des conditions de vents instables dans notre soufflerie, afin d'évaluer l'impact des fluctuations du vent. Notre dernière perspective de travail aujourd'hui est la confrontation de nos résultats avec des tests réalisés à échelle réelle.

# Table of contents

<b><u>ABSTRACT .....</u></b>	<b><u>3</u></b>
<b>TABLE OF CONTENTS .....</b>	<b>12</b>
<b>LIST OF FIGURES.....</b>	<b>24</b>
<b>LIST OF TABLES .....</b>	<b>28</b>
<b>ABBREVIATIONS .....</b>	<b>29</b>
<b>NOMENCLATURE .....</b>	<b>30</b>
<b><u>1. INTRODUCTION.....</u></b>	<b><u>32</u></b>
<b>1.1 THESIS CONTEXT.....</b>	<b>32</b>
<b>1.2 RESEARCH PROBLEMATIC.....</b>	<b>34</b>
<b>1.3 THESIS METHODOLOGY .....</b>	<b>35</b>
<b><u>2. IMPROVING BUILDING ENVELOPE KNOWLEDGE FROM ANALYSIS OF 219,000 CERTIFIED ON-SITE AIRLEAKAGE MEASUREMENTS IN FRANCE.....</u></b>	<b><u>38</u></b>
<b>2.1 INTEGRATION OF AIRTIGHTNESS REQUIREMENTS IN ENERGY REGULATIONS AND PROGRAMS .....</b>	<b>38</b>
<b>2.2 FRENCH REQUIREMENTS AND DATABASE DEVELOPMENT.....</b>	<b>39</b>
<b>2.3 FRENCH DATABASE ANALYSIS.....</b>	<b>41</b>
<b>2.3.1 OVERVIEW OF NEW FRENCH BUILDING STOCK.....</b>	<b>41</b>
<b>2.3.2 IDENTIFICATION OF FACTORS IMPACTING BUILDING AIRLEAKAGE AND MEASUREMENT RESULTS .....</b>	<b>43</b>
<b>2.3.3 IDENTIFYING AREAS OF IMPROVEMENT FOR BUILDING CONSTRUCTION STAKEHOLDERS AND MEASUREMENT TESTERS.....</b>	<b>51</b>
<b>2.4 LIMITS AND APPLICATIONS OF THE DATABASE ANALYSIS .....</b>	<b>57</b>
<b>2.4.1 BARRIERS IN COMPARISON WITH OTHER DATABASES .....</b>	<b>57</b>

2.4.2	FEEDBACK TO TESTERS AND STAKEHOLDERS .....	57
2.4.3	IMPROVEMENT OF DATABASES IN FRANCE AND THROUGHOUT THE WORLD.....	57
<b>2.5</b>	<b>CONCLUSIONS .....</b>	<b>58</b>
<b>3.</b>	<b><u>UNCERTAINTY SOURCES IN BUILDING PRESSURIZATION TESTS: REVIEW AND RESEARCH</u></b>	
	<b><u>GAPS.....</u></b>	<b><u>60</u></b>
<b>3.1</b>	<b>BACKGROUND .....</b>	<b>60</b>
3.1.1	PRESSURIZATION TEST PRINCIPLE .....	60
3.1.2	DEVELOPMENT OF MEASURING DEVICE PROTOTYPES.....	61
3.1.3	PRESSURIZATION TEST METHOD AT LARGE SCALE TESTING .....	64
3.1.4	STANDARDS AND METHODS .....	65
3.1.5	OBJECTIVES AND APPROACH OF THE LITERATURE REVIEW ANALYSIS .....	69
<b>3.2</b>	<b>UNCERTAINTIES DUE TO INTRINSIC MODEL ASSUMPTIONS.....</b>	<b>71</b>
3.2.1	VARIABILITY OF THE INDOOR-OUTDOOR PRESSURE DIFFERENCE.....	72
3.2.2	FLOW EQUATION .....	73
3.2.3	ZERO-FLOW PRESSURE CORRECTION AND MEASUREMENT .....	76
<b>3.3</b>	<b>UNCERTAINTIES DUE TO MEASURING PROTOCOL, EQUIPMENT, AND ANALYSIS .....</b>	<b>78</b>
3.3.1	BUILDING PREPARATION .....	78
3.3.2	SAMPLING PROCEDURE .....	79
3.3.3	PRESSURE MEASUREMENT AND AIRFLOW MEASUREMENT UNCERTAINTIES.....	80
3.3.4	REGRESSION ANALYSIS METHODS.....	81
3.3.5	REFERENCE VALUES FOR DERIVED QUANTITIES .....	83
<b>3.4</b>	<b>MAPPING OF THE CURRENT KNOWLEDGE REGARDING THE SOURCES OF ERRORS CHARACTERIZATION ..</b>	<b>83</b>
<b>3.5</b>	<b>CONCLUSION.....</b>	<b>92</b>

**4. DEFINITION OF THE SIMILARITY CONDITIONS AND THE SCALE RATIOS FOR THE REDUCED SCALE EXPERIMENTAL FACILITY.....93**

**4.1 MODELING BUILDING AIRTIGHTNESS PRESSURIZATION TESTS WITH SHARP-EDGED OPENINGS .....94**

4.1.1 INTRODUCTION ..... 94

4.1.2 IDEALIZED BUILDING ..... 94

4.1.3 TEMPERATURE AND DENSITY OF AIRFLOWS ENTERING AND LEAVING THE BUILDING ..... 95

4.1.4 PRESSURE DIFFERENCE AT LEAKAGE SITES ..... 95

4.1.5 FLOW THROUGH LEAKAGE SITES ..... 96

4.1.6 EQUATION OF STATE..... 96

4.1.7 CONTINUITY EQUATION ..... 97

4.1.8 ENERGY CONSERVATION EQUATION ..... 97

**4.2 DEFINITION OF SIMILARITY CONDITIONS .....99**

4.2.1 SIMPLIFICATION OF THE MODEL..... 99

4.2.2 DEFINITION OF DIMENSIONLESS NUMBERS ..... 100

**4.3 DEFINITION OF THE SCALE RATIOS .....103**

4.3.1 GENERAL CONFIGURATION ..... 103

4.3.2 SIMPLIFICATION FOR STEADY CONDITIONS..... 103

**4.4 CONCLUSIONS ..... 104**

**5. REDUCED SCALE REPRODUCTION OF BUILDING FAN PRESSURIZATION TESTS IN A WIND TUNNEL: DESIGN AND CHARACTERIZATION OF A NEW EXPERIMENT FACILITY.....105**

**5.1 DESIGN AND SIZING OF THE EXPERIMENT ..... 105**

5.1.1 DEFINITION OF THE REFERENCE FULL SCALE BUILDING..... 105

5.1.2 DESIGN OF THE REDUCED BUILDING MODEL..... 105

5.1.3 SPECIFICATIONS FOR THE PRESSURIZATION DEVICE..... 109

5.1.4	DESIGN OF THE WIND TUNNEL.....	110
<b>5.2</b>	<b>RESULTS: EXPERIMENT FACILITY INSTALLATION, VALIDATION, AND LESSONS FOR ISO 9972 PROTOCOL IMPLEMENTATION.....</b>	<b>118</b>
5.2.1	INSTALLATION OF THE EXPERIMENT FACILITY.....	118
5.2.2	VALIDATION OF THE MODEL CHARACTERISTICS.....	120
5.2.3	WIND SPEED FIELD IN THE TESTING CHAMBER.....	124
5.2.4	PRESSURE DIFFERENCE FIELD IN THE TESTING CHAMBER.....	128
<b>5.3</b>	<b>CONCLUSIONS.....</b>	<b>131</b>
<b>6.</b>	<b><u>EVALUATION OF THE IMPACT OF THE WIND DURING A PRESSURIZATION MEASUREMENT</u></b>	<b><u>132</u></b>
<b>6.1</b>	<b>REPRODUCTION OF PRESSURIZATION TESTS.....</b>	<b>132</b>
6.1.1	BACKGROUND OF THE AIR PERMEABILITY MEASUREMENT METHOD.....	132
6.1.2	AUTOMATION OF FAN PRESSURIZATION TESTS ON THE MODEL.....	133
6.1.3	EXPERIMENTAL DATA PRESENTATION.....	136
<b>6.2</b>	<b>IMPACT OF THE WIND ON THE ZERO-FLOW PRESSURE.....</b>	<b>136</b>
6.2.1	ZERO-FLOW PRESSURE DIFFERENCE DEPENDING ON WIND SPEED AND LEAK DISTRIBUTION.....	136
6.2.2	IMPACT OF THE ZERO-FLOW PRESSURE DIFFERENCE ON THE NUMBER OF PRESSURE STATIONS ACCORDING TO ISO 9972.....	138
<b>6.3</b>	<b>TESTS PERFORMED ACCORDING TO ISO 9972.....</b>	<b>139</b>
<b>6.4</b>	<b>ONE-POINT TESTS AND TWO-POINT TESTS.....</b>	<b>143</b>
6.4.1	ONE-POINT TEST RESULTS.....	144
6.4.2	TWO-POINT TEST RESULTS.....	147
<b>6.5</b>	<b>COMPARISON OF THE ERROR DUE TO WIND BETWEEN THREE TEST ANALYSIS METHODS.....</b>	<b>150</b>
<b>6.6</b>	<b>CONCLUSIONS.....</b>	<b>152</b>

<b>7. GENERAL CONCLUSIONS AND PERSPECTIVES .....</b>	<b>154</b>
<b>7.1 CHARACTERIZATION OF THE ERROR INDUCED BY THE WIND DURING PRESSURIZATION TESTS PERFORMED ON A REDUCED MODEL IN CONTROLLED LABORATORY CONDITIONS .....</b>	<b>ERREUR ! SIGNET NON DEFINI.</b>
<b>7.2 LIMITATIONS AND PERSPECTIVES .....</b>	<b>ERREUR ! SIGNET NON DEFINI.</b>
<b>REFERENCES .....</b>	<b>160</b>
<b>ANNEX A - EVALUATION OF THE ERROR DUE TO NEGLECTING THE GRAVITY TERM IN THE PRESSURE DIFFERENCE EVALUATION AT OPENINGS LEVEL .....</b>	<b>168</b>
<b>ANNEX B 1-POINT TEST RESULTS: <math>Q_4</math> VALUES .....</b>	<b>170</b>
<b>ANNEX C 1-POINT TEST RESULTS: <math>Q_{50}</math> VALUES .....</b>	<b>175</b>
<b>ANNEX D 2-POINT TESTS RESULT: <math>Q_4</math> VALUES .....</b>	<b>180</b>
<b>ANNEX E 2-POINT TEST RESULTS: <math>Q_{50}</math> VALUES .....</b>	<b>185</b>
<b>ANNEX F COMPARISON OF ERROR ON <math>Q_4</math> FOR DIFFERENT ANALYSIS METHODS.....</b>	<b>190</b>
<b>ANNEX G COMPARISON OF ERROR ON <math>Q_{50}</math> FOR DIFFERENT ANALYSIS METHODS.....</b>	<b>195</b>



## List of figures

Figure 1-1: Illustration of a fan pressurization test.....	33
Figure 1-2: Methodology developed to respond to the thesis problematic .....	36
Figure 2-1: Insulation types used in French buildings .....	42
Figure 2-2: Main materials for residential buildings .....	43
Figure 2-3: Number of building airtightness tests and their results according to the year of construction of the building .....	44
Figure 2-4: Impact of the main material on envelope airtightness for 170,028 single-family houses ( $q_{a4,med,sample} = 0.39 \text{ m}^3 \text{ h}^{-1} \text{ m}^{-2}$ ).....	45
Figure 2-5: Impact of the main material on envelope airtightness for 57,224 multi-family buildings ( $q_{a4,med,sample} = 0.57 \text{ m}^3 \text{ h}^{-1} \text{ m}^{-2}$ ).....	46
Figure 2-6: Impact of type of thermal insulation on envelope airtightness for single-family houses.....	47
Figure 2-7: Impact of type of ventilation system on envelope airtightness for single-family houses (left) and multi-family dwellings (right) .....	47
Figure 2-8: Variation of airleakage for wood structure houses according to climate and season ( $q_{a4,med,sample} = 0.43 \text{ m}^3 \text{ h}^{-1} \text{ m}^{-2}$ ).....	49
Figure 2-9: Variation of airleakage for heavy structure houses (with interior insulation) according to climate and season ( $q_{a4,med,sample} = 0.40 \text{ m}^3 \text{ h}^{-1} \text{ m}^{-2}$ ) .....	49
Figure 2-10: Distribution of flow exponent n for single-family houses.....	50
Figure 2-11: Distribution of flow exponent n for multi-family dwellings .....	51
Figure 2-12: Number of observations for 10 leaks identified on single-family houses with the highest median $q_{a4}$ value (from the sample of 121,478 measurements on houses).....	54
Figure 2-13: Airleakage test result distribution for multi-family dwellings (58,225 dwellings) .....	56
Figure 2-14: Airleakage test result distribution for single-family houses.....	56
Figure 3-1: Test bench used by Tamura in 1967-1968 to performed pressurization test [3] .....	62
Figure 3-2: Experimental measuring device used to evaluate an airleakage equivalent area [46].....	63
Figure 3-3: The exhaust fan apparatus developed by the National Research Council of Canada [47].....	64
Figure 3-4 : Representation of the sources of uncertainty during a fan pressurization test .....	91
Figure 4-1: Plan view of the idealized building with wind facing façade 1 .....	95
Figure 4-2: Closed system considered with the Boussinesq approximation and with $P_i \approx P_e$ (the air is assumed to enter the building through openings 1 and 2 and leave through the pressurization device). .....	98
Figure 5-1: Generic 2-storey house at full scale [m].....	106
Figure 5-2: Reduced model sizes [m].....	106
Figure 5-3: CFD calculations of wind velocity inside the testing chamber for a wind target equal to $7 \text{ m s}^{-1}$ .....	108
Figure 5-4: Design drawings of the model .....	109
Figure 5-5: Representation of CFD configurations in reduced scale - Case 2 and case 3tt .....	111
Figure 5-6: CFD simulations results for wind velocity and static pressure fields with an input wind speed of $12 \text{ m s}^{-1}$ .....	113

Figure 5-7: CFD simulations results for wind velocity and static pressure fields with an input wind speed of $4 \text{ m s}^{-1}$ .....	114
Figure 5-8: Different shapes tested for the contraction component .....	115
Figure 5-9: Wind velocity field inside the wind tunnel for different shapes of contraction component .....	116
Figure 5-10: Final dimension of wind tunnel [in mm] .....	117
Figure 5-11: Final reduced model .....	118
Figure 5-12: Pressurization device for reduced scale test .....	119
Figure 5-13: LabVIEW interface.....	119
Figure 5-14: VBA program interface for fan pressurization tests .....	120
Figure 5-15: Installed wind tunnel .....	120
Figure 5-16: Characterization of the airtightness of the model without deliberate leaks and with the smallest leak- Observation of the pressure decrease inside the model ....	121
Figure 5-17: Evaluation of the $C_p$ values on the opening site.....	124
Figure 5-18: Plan of measured points for the evaluation of the velocity field in the testing chamber (low direction from A to H) .....	124
Figure 5-19: Distribution of the wind velocities in the testing chamber for a mean wind velocity = $0.83 \text{ m s}^{-1}$ .....	125
Figure 5-20: Distribution of the wind velocities in the testing chamber for a mean wind velocity = $4.64 \text{ m s}^{-1}$ – Points A1 to E4.....	126
Figure 5-21: Distribution of the wind velocities in the testing chamber for a mean wind velocity = $4.23 \text{ m s}^{-1}$ – Points E1 to H4.....	126
Figure 5-22: Distribution of the wind velocities in the testing chamber WITH the model for a mean wind velocity = $4.22 \text{ m s}^{-1}$ .....	127
Figure 5-23: Representation of the mean wind velocities in the testing chamber for location A1 to I3, with model installed in the wind tunnel (mean velocity = $4.22 \text{ m s}^{-1}$ ) .....	128
Figure 5-24: Locations of some measured points for the pressure difference field evaluation in the testing chamber .....	128
Figure 5-25: Distribution of the pressure differences in the testing chamber WITH the model for a mean pressure difference = $-5.48 \text{ Pa}$ .....	130
Figure 6-1: Representation of the fan pressurization automation - Scheme of the VBA program that gives instructions to Labview apps .....	135
Figure 6-2: Location and nature of the external pressure tap .....	137
Figure 6-3: Location of the internal pressure tap .....	137
Figure 6-4: Zero-flow pressure difference for 9 configurations of leakage distribution depending on wind speed .....	138
Figure 6-5: Number of pressure stations for a fan pressurization test depending on the wind speed for nine on the leakage distributions .....	139
Figure 6-6: $q_{50}$ result for tests performed according to ISO 9972 .....	141
Figure 6-7: $q_4$ result for tests performed according to ISO 9972 .....	141
Figure 6-8: Error due to wind on $q_{50}$ for tests performed according to ISO 9972.....	143
Figure 6-9: Error due to wind on $q_4$ for tests performed according to ISO 9972.....	143
Figure 6-10: $q_4$ value for 1-point test scenarios for $r_{LD}=0.1$ depending on wind speed	145
Figure 6-11: $q_{50}$ value for 1-point test scenarios for $r_{LD}=0.1$ depending on wind speed .....	146
Figure 6-12: $q_4$ value for 1-point test scenarios for $r_{LD}=0.8$ depending on wind speed	146
Figure 6-13: $q_{50}$ value for 1-point test scenarios for $r_{LD}=0.8$ depending on wind speed .....	147
Figure 6-14: $q_4$ value for 2-point test scenarios for $r_{LD}=0.1$ depending on wind speed	148

Figure 6-15: $q_{50}$ value for 2-point test scenarios for $r_{LD}=0.1$ depending on wind speed	149
Figure 6-16: $q_4$ value for 2-point test scenarios for $r_{LD}=0.8$ depending on wind speed	149
Figure 6-17: $q_{50}$ value for 2-point test scenarios for $r_{LD}=0.8$ depending on wind speed	150
Figure 6-18: Comparison of the error on $q_4$ due to wind evaluated in 7 scenarios for $r_{LD}=0.4$	151
Figure 6-19: Comparison of the error on $q_4$ due to wind evaluated in 7 scenarios for $r_{LD}=0.8$	151
Figure 6-20: Comparison of the error on $q_{50}$ due to wind evaluated in 7 scenarios for $r_{LD}=0.7$	152



## List of tables

Table 2-1: Number of airtightness tests in the database according to the use of the building.....	41
Table 2-2: Number of airtightness tests in the database according to the construction phase .....	41
Table 2-3: Number of airtightness tests in the database depending on the type of ventilation system for residential and non-residential buildings.....	42
Table 2-4: Number of airtightness tests in the database according to the type of insulation for residential buildings .....	43
Table 2-5: Leak categories and occurrences.....	52
Table 3-1: Main Variations between the 4 standards regarding fan pressurization tests in 1984 [49] .....	65
Table 3-2: ASTM 779-10 and ISO 9972 requirements .....	67
Table 3-3: Studies analyzed in this chapter according to topics relevant for this review .....	71
Table 3-4: A summarized review of studies regarding fan pressurization test uncertainty .....	87
Table 4-1: Density and temperature equations at airflow paths .....	95
Table 4-2: Error due to gravity simplification for the evaluation of the pressure difference on a windward leak in pressurization .....	100
Table 4-3: Units of the independent variables of our model .....	101
Table 4-4: Definition of reference values and dimensionless variables .....	101
Table 5-1: Diameters of the reduced model openings for different leakage distribution ratios .....	107
Table 5-2: Evaluation of airflow provided by the pressurization device depending on the leak distribution ratio.....	110
Table 5-3: Evaluation of the real $q_4$ value of the model without wind with the same designed $q_4$ for all configurations.....	122
Table 5-4: Evaluation of the real $q_{50}$ value of the model without wind with the same designed $q_{50}$ for all configurations.....	122
Table 5-5: Measured characteristics of seven openings .....	123
Table 6-1: Reference values for $q_4$ and $q_{50}$ for wind impact evaluation.....	142

## **Abbreviations**

AIVC	Air Infiltration and Ventilation Centre
ATTMA	Air Tightness Testing & Measurement Association
BCCA	Belgian Construction Certification Association
CFD	Computational Fluid Dynamics
ELA	Effective Leakage Area
GUM	Guide to the Expression of Uncertainty in Measurement
IWLS	Iterative Weighted Least Square method
LBNL	Lawrence Berkeley National Laboratory
OLS	Ordinary Least Squares method
ResDB	Residential Diagnostics Database
RT2012	Régulation Thermique 2012 (French EP regulation)
WLOC	Weighted Line of Organic Correlation method

## Nomenclature

$A$	Area of opening ( $\text{m}^2$ )
$c_p$	Specific heat capacity at constant pressure ( $= 1\,004 \text{ J kg}^{-1} \text{ K}^{-1}$ )
$c_v$	Specific heat capacity at constant volume ( $= 1.4 c_p$ ) ( $\text{J kg}^{-1} \text{ K}^{-1}$ )
$C$	Leakage coefficient ( $\text{m}^3 \text{ h}^{-1} \text{ Pa}^{-n}$ )
$C_{pw}$	Wind pressure coefficients (-)
$C_z$	Discharge coefficients (-)
$ELA_4$	Equivalent leakage area at 4 Pa (according to ISO 9972) ( $\text{m}^2$ )
$EW_{\Delta p}$	Error due to the wind at the pressure difference $\Delta p$
$g$	Acceleration of gravity ( $= 9.81 \text{ m s}^{-2}$ )
$L$	Length (m)
$l_e$	Effective length of opening (m)
$m$	Mass (kg)
$n$	Flow exponent (-)
$p_i$	Pressure relative to external atmospheric pressure (Pa)
$q$	Volumetric airflow rate ( $\text{m}^3 \text{ s}^{-1}$ )
$q_m$	Mass airflow rate ( $\text{kg s}^{-1}$ )
$q_4$	Airleakage rate at 4 Pa ( $\text{m}^3 \text{ h}^{-1}$ )
$q_{50}$	Airleakage rate at 450 Pa ( $\text{m}^3 \text{ h}^{-1}$ )
$q_{a4}$	Airleakage rate at 4 Pa divided by the loss surface area excluding the basement floor ( $\text{m}^3 \text{ h}^{-1} \text{ m}^{-2}$ )
$r_{LD}$	Leakage distribution ratio (-)
$R$	Specific gas constant ( $= 287.058 \text{ J kg}^{-1} \text{ K}^{-1}$ )
$t$	Time (s)
$T$	Temperature (K)
$U$	Wind speed at the height of the building ( $\text{m s}^{-1}$ )
$V$	Internal building volume ( $\text{m}^3$ )
$X_{ref}$	Reference value for the variable X
$\bar{X}$	Scale ratio for the variable X

$z$	Altitude above ground level (m)
$\Phi$	Heat flux (W)
$\gamma$	Ratio of specific heats ( $\gamma = \frac{c_p}{c_v} = 1.4$ )
$\rho$	Air density ( $\text{kg m}^{-3}$ )
$\Delta p$	Pressure difference between the outside and the inside of the building or the model (Pa)
$i, e$	Pertaining to the inside (i) or the outside (e)
$1, 2$	Pertaining to opening number 1 (windward) or 2 (leeward)
$bd$	Pertaining to the pressurization device
$ref$	Pertaining to the reference conditions without wind
$w$	Pertaining to the wind
*	Non-dimensional quantity

# 1. Introduction

## 1.1 Thesis context

In the European Union, by the end of 2020, new buildings should comply with the European Directive 2010/31/EU and therefore reach the nearly zero energy building-level [1]. Thus, researchers, builders, manufacturers, and other stakeholders are gathering their forces to maintain good indoor quality and acceptable thermal comfort in buildings with the lowest energy and environmental cost, while taking the global warming phenomena into account. Within the framework of this alarming context, minimizing and controlling building envelope airleakage has become one of the major levers to reduce the energy use in buildings.

The Air Infiltration and Ventilation Glossary [2] defines the building air infiltration as “*the uncontrolled inward leakage of outdoor air through cracks, interstices, and other unintentional openings of a building, caused by the pressure effects of the wind and/or the stack effect*”. It is characterized by airleakage, which is “*the leakage of air in or out of a building or space driven by artificially induced pressures*”. The term airtightness is used to designate “*the leakage characteristics of a building. The smaller the airleakage rate at a given pressure difference across a building envelope, the greater the airtightness*”.

By 1975, Tamura had already estimated that heat loss due to envelope airleakage may represent 40% of the total heat loss from buildings [3]. More recent studies have estimated that infiltrations are responsible for up to 30% of heating demand [4], [5], [6], [7], [8], [9]. Poor building airtightness may also have a significant impact on indoor air quality and occupant comfort and maybe a significant source of noise transmission [10]. Therefore, improving buildings airtightness is a major issue for the next generation of buildings, both for new construction and rehabilitation programs. To do so, the first crucial step is to assess the performance of new and existing buildings. It will lead to the definition of action or levers research aiming to make the building envelope more airtight. In order to get a clear picture of the situation, we, therefore, need to measure the airleakage of building envelopes. The most common method used to perform this measurement is the fan pressurization test method, described in standards such as ISO 9972 [11] and ASTM E779-19 [12]. During this measurement, the heated volume of the building is put under pressurization (or depressurization) by a blowerdoor, after having switched-off the mechanical ventilation systems (or isolated intermittent or natural ventilation system) and sealed all components of the system. The airflow rate  $q$  provided by the blowerdoor to maintain a given pressure difference  $\Delta p$  between the indoor and the outdoor of the heating volume is measured. Then, for a reference pressure difference  $\Delta p_{\text{ref}}$ , the airflow rate through envelope leaks is evaluated (Figure 1-1) assuming that it corresponds the airflow rate provided by the blowerdoor.

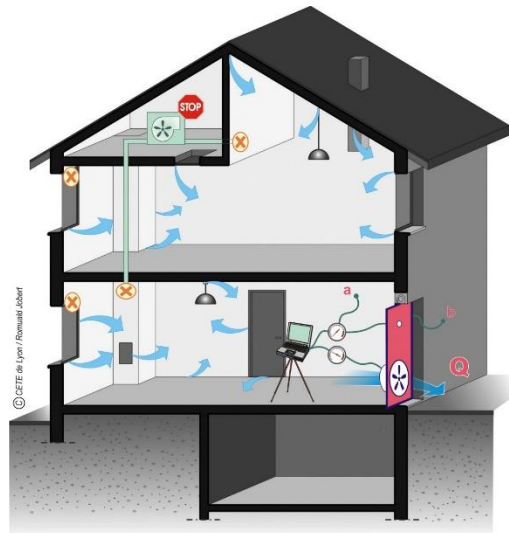


Figure 1-1: Illustration of a fan pressurization/depressurization test

In France, the Cerema has become a national reference regarding building airtightness thanks to field studies and research projects conducted for almost two decades on this topic. In 2008, the French Ministry in charge of the Construction created a national committee on building airtightness, called the “Club Permea”, led by the Cerema. It gathers professionals among builders, testers, and manufacturers to elaborate technical proposals for stakeholders regarding building airtightness. One of the major outcomes of this committee is the introduction of an airtightness requirement for new residential buildings with a mandatory justification in the current building energy regulation RT2012, and the creation of the national testers schemes for building air permeability measurement. Since joining the Cerema in 2011, I have been working on building airtightness by participating in the Club Permea, more especially in expert meetings for the review of international and national standards regarding airtightness measurement methods. In 2012, I created the national database that gathers data from all building airleakage tests that are performed by French authorized testers. Each year, this database is updated with dozens of thousands of measurements. I have presented the results of various analyses of this database in the Club Permea, during yearly national meetings of testers in France that gather 200 testers, in journal and conference papers, and in international conferences such as the Build’Air Symposium (Germany) and AIVC Conferences. The Air Infiltration and Ventilation Centre (AIVC), which is the oldest International Energy Agency (IEA) running annex under the Energy in Buildings and Communities (EBC) provides support to industry and research organizations regarding buildings airtightness and ventilation especially through conferences, webinars, guides, and technical notes. The existence and the active work of this center highlight that building airtightness is still a major issue for the quality of the construction, especially for energy savings and indoor air quality. Since 2012, I have presented papers each year at the AIVC conference, regarding airleakage measurement uncertainty, the French database of airleakage tests, the improvement of ventilation systems and indoor air quality

in dwellings, and the reliability of checks and measurements on ventilation systems. More recently, I have chaired topical sessions in the AIVC conference regarding airtightness measurements.

In the last few years, the number of fan pressurization tests has increased all over the world, as a result of regulation and energy program requirements. In this context, controlling and reducing the measurement uncertainty is essential to obtain reliable test results. Since 2018, I have been participating in the international Working Group of the TightVent Europe platform “Integrating uncertainties due to wind and stack in declared airtightness results”. With other members of this working group, I present my work during the topical sessions of AIVC conferences relating to the wind impact and participate in the writing of a collaborative paper on the review of current work regarding the impact of the wind during building airleakage measurement. In this working group and the AIVC Conferences, we observe that while the measurement uncertainty has been studied for several decades, there are still gaps in the knowledge of physics that occurs during a test, the variability of sources of errors, and the quantification of the uncertainty due to climatic conditions.

## **1.2 Research problematic**

In France, the current Energy Performance regulation RT2012 requires a justification of buildings airtightness for all new dwellings. For new non-residential buildings, measured good value for the airtightness indicator can be rewarded in the EP-calculation. This justification consists either of applying a certified quality framework (for a very small part of new buildings) or performing a building airtightness test [13]. Thus, every day, many tests are performed on new buildings in all regions of France. The RT2012 also requires that these tests are performed according to the international standard ISO 9972, which is applicable only under “calm” climatic conditions. Testers and building owners raise a technical problem: what is the solution in windy conditions? Many places in France are often, and for some always, under windy conditions. In these cases, how shall the test be performed? The requirements of the ISO 9972 can not be met, yet the test has to be done to meet the RT2012 requirement. To deal with these situations, we need either a measurement method that would be less impacted by the wind or a method that takes into account the error induced by the wind.

During an airleakage measurement, the wind strongly impacts the pressure differences around the building envelope, and thus the airflow rates through the leaks. It contradicts also the strong assumption of a unique pressure difference around the buildings assumed to be a unique zone in the measurement method. Depending on the nature and the location of the measurement device, the wind may also directly disrupt the measurement device. Existing studies have been dedicated to the evaluation of the error induced by the wind: they are either based on simplified numerical models or in-situ tests on very few buildings. However, the numerical models were not verified with experimental measurements in order to consolidate the results. Moreover, as field studies were

conducted on a small number of buildings, the results are not representative of all buildings (building geometry, quantity and distribution of leaks on building envelope) in the different situations (exposure to wind and environmental conditions). Collecting more data from field measurements performed in various buildings and various windy conditions can be very costly and time-consuming. One solution that may partially replace these measurements is to perform tests on a reduced model for which the airleakage would be carefully designed, controlled and quantified, in controlled laboratory conditions. Thus, the exact error induced by the wind on a measurement result can be precisely evaluated. Another advantage of a reduced scale experiment is the possibility to study various configurations of wind speed and leakage distribution in laboratory conditions.

This thesis aims to characterize the error induced by the wind during a building airleakage measurement with mainly two objectives:

- 1) To evaluate the error induced by the wind during tests performed according to the ISO 9972 method on a reduced model in controlled laboratory conditions.
- 2) To improve the test protocol either by reducing the error due to the wind or by improving the way the errors are taken into account in the test result.

### **1.3 Thesis methodology**

To evaluate the impact of the wind during an airleakage measurement using a reduced scale experiment, we will follow the methodology described in Figure 1-2. In the first step, we will use the French database of building airtightness to make statistical analysis of about 219,000 tests performed in France in order to precisely evaluate the real situation of the building stock. This analysis will lead to the identification of the geometrical and architectural configurations that we will integrate into our study. In a second step, we need to analyze the regulatory context and the existing testing protocols to identify the physical parameters that may have an impact on the uncertainty due to the wind. The outcomes of these two steps will lead to the development of the numerical model that describes a pressurization test on a single-zone building, and more especially the physics involved in the impact of the wind. The definition of this model representing a single-zone detached house should lead to 1) the design and the sizing of the experimental facility to reproduce pressurization tests on a reduced scale; 2) the identification of the sensors and actuators that we will need for our experimentation; 3) the selection of the experimental protocol that will lead to the evaluation of the impact of the wind. Then, we will be able to develop, install, and characterize our experimental facility that will include a model of a building, a pressurization device, and a wind tunnel. Once our facility will be working, we will perform numerous tests on the model with different wind conditions. All these tests will need to be performed with an automation system that will also ease the clustering and the analysis of the experimental data. All this process will lead to the evaluation of the wind impact through the analysis of measurements performed at a reduced scale in controlled laboratory conditions. This evaluation should lead to the

definition of specifications to improve tests performed in real buildings. It should also lead to the definition of recommendations to improve the ISO 9972 protocol.

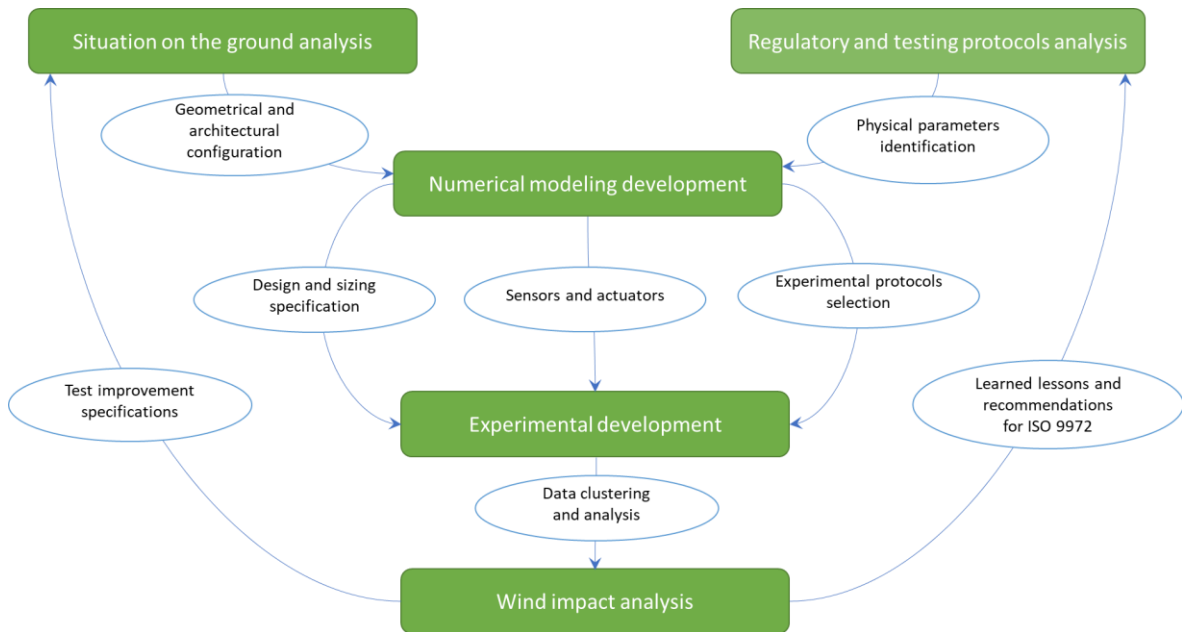


Figure 1-2: Methodology developed to respond to the thesis aim

Chapter 2 of this manuscript is dedicated to the evaluation of new French buildings' performance regarding envelope airtightness. The analysis of data collected from more than 219,000 tests is the first step to:

- 1) establish how tests are performed in France, on which buildings and under which conditions;
- 2) evaluate the range of airtightness value that is currently measured;
- 3) identify the limits of the test method from the in-situ point of view.

Thus, chapter 2 presents the evolution of building airtightness in France. We propose areas of improvement to reinforce building airtightness and then, we analyze the limits of current regulation and protocol regarding the test results.

Chapter 3 aims to list and analyze the factors that impact the uncertainty of the test result based on an extensive literature review. We first identify all sources of error during a fan pressurization test. Secondly, we collect and analyze studies dedicated to the evaluation of the uncertainty of the test result. From this analysis, we propose a map of all sources and how they induce uncertainties for each step of a test. Then, we identify research gaps and give some recommendations to develop future works in order to improve the knowledge regarding the uncertainty of the airtightness test result.

In Chapter 4, we propose a physical model that describes the governing physical phenomena during a fan pressurization test. We apply a dimensionless analysis to define similarity conditions in order to design a reduced scale experiment. Then, we define from this analysis the scale ratios between reduced scale and full scale.

Chapter 5 describes the process of design and characterization of the reduced scale experimental facility. We first apply the conclusions of Chapter 4 to define the sizes and characteristics of the different components of our facility: the model, the measurement device, and the wind tunnel. Secondly, we present the technical solutions we have developed and the final drawings of the facility. Finally, we analyze the results of measurements performed to characterize the facility performances.

Chapter 6 is dedicated to the evaluation of the impact of the wind during pressurization tests performed on our reduced model by our measurement device, under controlled conditions in our wind tunnel. We first describe the test protocol we apply, and the automation program we developed to perform numerous tests. Secondly, we focus on the impact of the wind on the zero-flow pressure measurement, which is a crucial step in the test protocol as it leads to the definition of validation criteria of the test. In the third section of this chapter, we evaluate the impact of the wind for tests performed according to the ISO 9972. Then, we test alternative protocols and evaluate the errors induced by the wind for these methods, and we compare them with the ISO 9972 results.

## 2. Improving building envelope knowledge from analysis of 219,000 certified on-site airleakage measurements in France

### 2.1 Integration of airtightness requirements in energy regulations and programs

In order to improve knowledge of existing envelope performance regarding airleakage, many experimental studies have been conducted from measurements performed on dwellings [14] (20 Italian residential buildings), [15] (9 Irish single-family houses), [16] (170 single-family houses and 56 apartments in Finland) and [17] (129 Spanish dwellings). Analyses of airleakage measurement results on these samples of buildings have made it possible to identify the most critical causes of envelope leakage, such as windows and chimneys without sealing [14], pipe and duct paths [17]. The first airleakage database to be developed and analyzed is the LBNL's residential diagnostics database (ResDB) including from 70,000 airleakage data across the United States in 2005 [18], to 134,000-175,000 data in 2013 [19] [20]. This database has been used to build a predictive model, even though the variability of measurement results and building characteristics makes this prediction very difficult and highly uncertain.

Nowadays, many countries include requirements for building airtightness in their current national regulations or energy-efficiency programmes, mainly to reduce building energy losses due to airleakage [21]. In some cases, the minimum requirement for building airtightness has to be justified by an airtightness test performed by accredited testers. In France, the current energy performance regulation RT2012 [22] requires that all new residential buildings must comply with a limit value for the French indicator  $q_{a4}$  ( $Q_{4Pa-surf}$  in French: airleakage rate at 4 Pa divided by the loss surface area excluding the basement floor):  $0.6 \text{ m}^3 \text{ h}^{-1} \text{ m}^{-2}$  for single-family houses (i.e. around  $n_{50}=2.3 \text{ h}^{-1}$ )<sup>1</sup> and  $1.0 \text{ m}^3 \text{ h}^{-1} \text{ m}^{-2}$  for multi-family buildings. Compliance is justified either by an airtightness test performed by a qualified tester or by applying a certified quality framework [13], which is detailed in the section 2.2. The same justification is required for non-residential buildings if the Energy Performance calculation takes into account a better-than-default value ( $1.7 \text{ m}^3 \text{ h}^{-1} \text{ m}^{-2}$  or  $3.0 \text{ m}^3 \text{ h}^{-1} \text{ m}^{-2}$  depending on the type of building). Moreover, the EP program Effinergie [23] imposes a more demanding limit for residential buildings and requires a measurement for small non-residential buildings (floor area below 3000 m<sup>2</sup>). As for the regulation, in the context of Effinergie, the test has to be performed by a qualified tester.

---

<sup>1</sup> The equivalence is calculated for a generic two-story house with an internal volume of 320 m<sup>3</sup> and a loss surface area excluding basement floor of 224 m<sup>2</sup>; and considering a flow exponent  $n=2/3$

In Flanders (Belgium), whereas the current regulation does not include a minimum requirement for building airtightness, the default value for airtightness used for the global performance of the building envelope implicitly imposes airtightness measurement for every new residential building since 2006, and the Flemish region introduced a qualified tester scheme in 2014 [24]. According to the Flanders' regulation, airtightness measurements have to be performed by a qualified tester. The Belgian Construction Certification Association (BCCA) proposes the main quality framework for airtightness testers approved by the Flemish government, which includes training, exam, onsite inspection, and desktop inspection. Information gathered through the qualification process is filled in the BCCA database.

In the UK, the 2006 building regulations include a limit value for new dwelling airtightness and mandatory measurement for a sampling of the new dwellings [25]. The Air Tightness Testing and Measurement Association (ATTMA) is approved by Governments in England, Northern Ireland, Scotland and Wales, and operates the main airtightness testers scheme in the UK. Its scheme includes an audit of the quality management system of the tester's company, an in-situ exam, and an administrative exam, especially regarding calibration of measurement device. Information gathered through the qualification process is filled in the ATTMA database which is currently the biggest airtightness test database in the world.

In Ireland, the new building regulation applying since 2019 introduces a backstop value for dwelling airtightness, which determined the type of ventilation system authorized in the dwelling. An airtightness test should be performed on every new dwelling by a certified tester [26]. In 2017, Leprince et al. summarized the EP requirements regarding building airtightness and competent tester scheme in 10 European countries [21]: 7 countries had a quality framework for building airtightness testers, and the number of qualified testers was increasing in these countries.

In addition to these competent tester schemes which have made it possible to collect hundreds of thousands of data from in-situ measurements, for example in the UK [25] (192,731 records in 2017) and in France [27] (219,000 measurements in 2019), this context has led to the development of instruments such as calibration rules, and testing guidelines [28]. In particular, standard ISO 9972 [11] requires periodic calibration of the measurement system and gives threshold values regarding the accuracy of the pressure-measuring device, the air flow rate measuring system, and the temperature-measuring device. Moreover, in France, the associated standard FD P50-784 [29] gives the calibration frequencies for each device.

## **2.2 French requirements and database development**

The French EP-regulation RT2012 requires that each airtightness test is performed by a qualified tester according to EN ISO 9972 and the French standard FD P50-784, as described by Leprince et al. [30]. The FD P50-784 requires that measurements are performed according to method 3 of EN ISO 9972 and specifies how the building must be prepared. More specifically, only the ventilation openings included in the EP-calculation are sealed, and all windows, doors, and trapdoors on the envelope are closed.

The French testers' scheme was developed in 2008. The certification body Qualibat annually assesses qualified testers. To be qualified, a tester has to:

- undergo state-approved training;
- pass the training examination (the theoretical part, with a state-approved multiple choice questionnaire; and the practical part, with a real test performed with a qualified tester);
- provide proof of sufficient testing experience with a minimum of 10 tests performed.

Once qualified, every tester is subjected to yearly follow-up checks, organized by the certification body. The follow-up checks include an analysis of some reports to verify their compliance with applicable standards and guidelines. The certification body can check the testers based on the documentation sent every year, but also on site, in particular, in case of complaints or doubts about their work. A committee involving stakeholders is in charge of delivering qualification, re-issuing qualification or handling complaints. The follow-up checks require provision of a professional standard form giving information on all airtightness measurements performed within the year (the professional measurement register). As of September 2020, 896 testers were qualified. Collected registers are annually compiled in a national database which is composed of 39 data fields as follows:

- general building information: owner, location, use (single-family for a building with one or two apartments, multi-family for a building with more than two apartments, several subcategories for non-residential buildings such as schools and office buildings), year of construction, year of rehabilitation;
- special requirements: label, certification;
- main building characteristics: main material, construction type (frame structure, bearing walls, combined or lightweight facade), insulation type, ventilation system, heating system;
- measurement protocol: operator, date of measurement, measurement device, time of measurement (construction phase of the building), method;
- measurement input data: envelope area (excluding low floors), floor area, volume;
- measurement results: airleakage coefficient  $C_L$ , flow exponent  $n$ ,  $q_{a4}$ ,  $n_{50}$ , uncertainties (the uncertainties are calculated according to Annex C of ISO 9972. FD P50-784 requires that the uncertainty on  $q_{a4}$  is below 15%);
- detected leakage locations: leakages being classified into 46 standardized categories.

Data are checked to ensure their accuracy, completeness, and reliability regarding the specifications of standards ISO 9972 and FD P50-784, in particular:

- the entries of multiple-choice data are consistent with the given lists of choices;
- the values for  $q_{a4}$  and for  $n_{50}$  are consistent with the values for  $C_L$  and  $n$ , and the values for the envelope area and internal volume;
- the value of the coefficient of determination  $r^2$  of the linear regression is between 0.98 and 1.00;
- the value for the flow exponent  $n$  is between 0.5 and 1.0;
- the uncertainty on  $q_{a4}$  is below 15%.

The database is fed annually with consolidated data from all collected registers, removing duplicates, irrelevant data, and incomplete recordings. Currently, more than 380,000 measurements performed between 2009 and 2018 have been recorded in the database. Data from around 63,000 tests are expected each year. Therefore, only analyses of data collected until December 2016 and published in 2019 by Mélois et al., in *Improving building envelope knowledge from analysis of 219,000 certified on-site airleakage measurements in France*, Building and Environment, [31] are presented in this manuscript.

## 2.3 French database analysis

### 2.3.1 Overview of new French building stock

Almost all measurements recorded in the database were performed on new buildings: 87% of buildings tested were built after 2008. Most of the measurements were performed on residential buildings, with 64% coming from single-family houses and 32% from multi-family dwellings (Table 2-1). The sample of non-residential buildings included in this database is not yet big enough to be representative of their diversity. All results presented in this analysis apply therefore only to residential buildings. 88% of these measurements were performed at the commissioning stage when all works that could alter building airtightness are carried out and 11% were performed during the construction stage (Table 2-2). However, in order to make relevant comparisons, all data and analyses presented in this manuscript concern only measurements performed at the commissioning stage.

Table 2-1: Number of airtightness tests in the database according to the use of the building

<b>Use of the building</b>	Single-family houses	Multi-family dwellings	Non-residential buildings	Total
<b>Number of tests</b>	140,542	70,632	8,023	219,197
<b>Distribution</b>	64.1%	32.2%	3.7%	100%

Table 2-2: Number of airtightness tests in the database according to the construction phase

<b>Construction step</b>	At commissioning	During construction	Before retrofitting	No information	Total
<b>Number of tests</b>	192,846	23,745	969	1,637	219,197
<b>Distribution</b>	88.0%	10.8%	0.4%	0.7%	100%

The database includes information regarding ventilation systems types that are described in Table 2-3. The context in France, regarding ventilation, has remained the same since

the 1982 regulation [32]: mandatory general and permanent ventilation of residential buildings with threshold values for exhaust airflows. Therefore, for more than 30 years, almost every building has been equipped with a mechanical ventilation system. These systems include exhaust air terminal devices in humid rooms, and either supply air terminal devices or air inlets in dry rooms. 90% of the buildings tested were equipped with a single-exhaust ventilation system and 6% with a balanced ventilation system. The “other” category includes ventilation “by window opening”, “on-off” systems and single-supply ventilation systems.

Table 2-3: Number of airtightness tests in the database depending on the type of ventilation system for residential and non-residential buildings

Type of ventilation system		Single-exhaust ventilation	Balanced ventilation	Other or none	Total
<b>Single-family houses</b>	<b>Number of tests</b>	116,847	6,736	3,257	126,840
	<b>Distribution</b>	92.1%	5.3%	2.6%	100%
<b>Multi-family dwellings</b>	<b>Number of tests</b>	57,049	1,142	630	58,821
	<b>Distribution</b>	97.0%	1.9%	1.1%	100%

The database includes data regarding insulation types that are described in Figure 2-1. gives the distribution of the insulation types depending on how the buildings are used. Traditionally, internal insulation walls are used in residential buildings (84% for multi-family dwellings and 64% for single-family houses). The category “distributed thermal insulation” includes wood-frame buildings with insulation between studs, lightweight insulating concrete, etc.

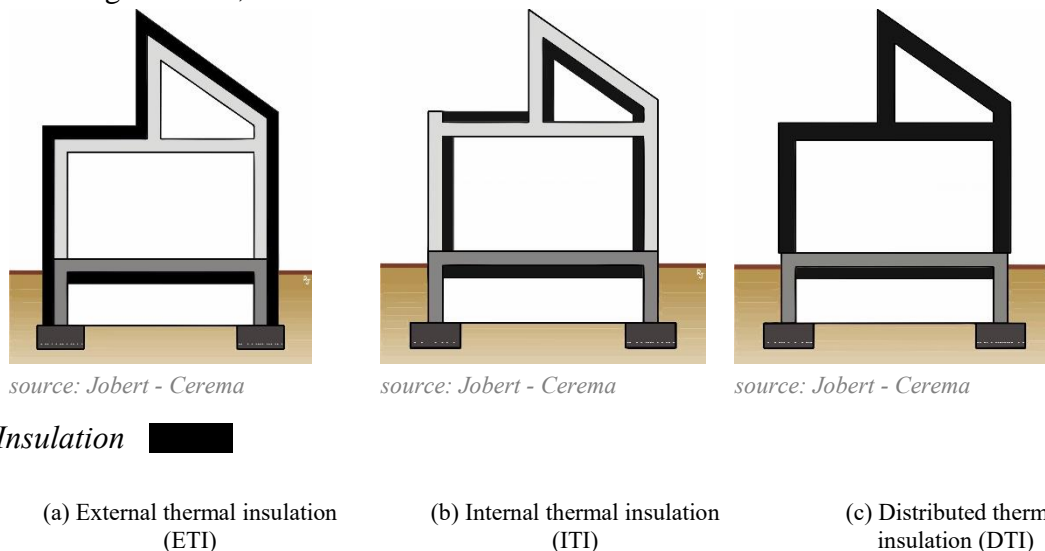


Figure 2-1: Insulation types used in French buildings

Table 2-4: Number of airtightness tests in the database according to the type of insulation for residential buildings

Type of insulation		Internal thermal insulation (ITI)	External thermal insulation (ETI)	Distributed thermal insulation (DTI)	Other or no information	Total
Single-family houses	Number of tests	107,544	2,975	6,171	10,150	126,840
	Distribution	84.8%	2.3%	4.9%	8.0%	100%
Multi-family dwellings	Number of tests	38,394	14,622	2,597	3,208	58,821
	Distribution	65.3%	24.9%	4.4%	5.5%	100%

Figure 2-2 shows the distribution of the main construction materials for residential buildings. Most single-family houses in the database are built of brick (46%), concrete (30%) and wood (9%). For multi-family dwellings, concrete is the main material (48%), followed by brick (27%) and wood (2%).

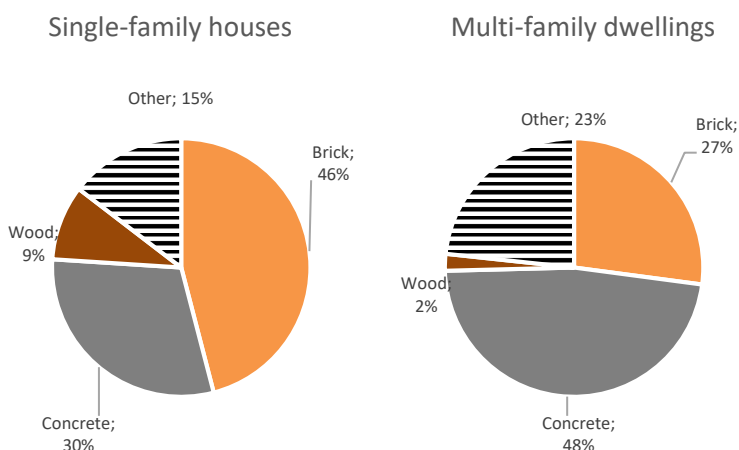


Figure 2-2: Main materials for residential buildings

### 2.3.2 Identification of factors impacting building airleakage and measurement results

#### 2.3.2.1 Changes over recent years

As two key issues, Figure 2-3 illustrates the number of tested buildings and the airleakage median value per year from 2000 to 2016. There are two major factors responsible for the changes shown in Figure 2-3: the EP label launched in 2007 and the current EP regulation (RT2012) applicable for residential buildings commissioned from 2014-2015. Therefore:

- before 2007: there are very few tests;
- between 2007 and 2013: the Effnergie label has led to a progressive increase in tests from fewer than 100 per year up to almost 20,000 per year in 2013;
- from 2014: the first RT2012 buildings were tested leading to more than 50,000 tests per year.

Regarding the airleakage median value, the implementation of the EP label requirements in 2007 clearly led to a significant decrease in the median value of  $q_{a4}$  for measured

residential buildings (mostly buildings applying for the label were tested). In 2011, half of the measured single-family houses had reached  $q_{a4}=0.42 \text{ m}^3 \text{ h}^{-1} \text{ m}^{-2}$  and half of the measured multi-family dwellings had reached  $q_{a4}=0.58 \text{ m}^3 \text{ h}^{-1} \text{ m}^{-2}$ . However, a small improvement was evident for houses with a median value of  $0.38 \text{ m}^3 \cdot \text{h}^{-1} \cdot \text{m}^{-2}$  in 2016 and no improvement for multi-family buildings. This may be due to the use of a new limit value of  $0.4 \text{ m}^3 \text{ h}^{-1} \text{ m}^{-2}$  in the EP label for single-family houses. From 2015 the median value becomes representative of all new residential buildings as the test has become mandatory for all new residential buildings.

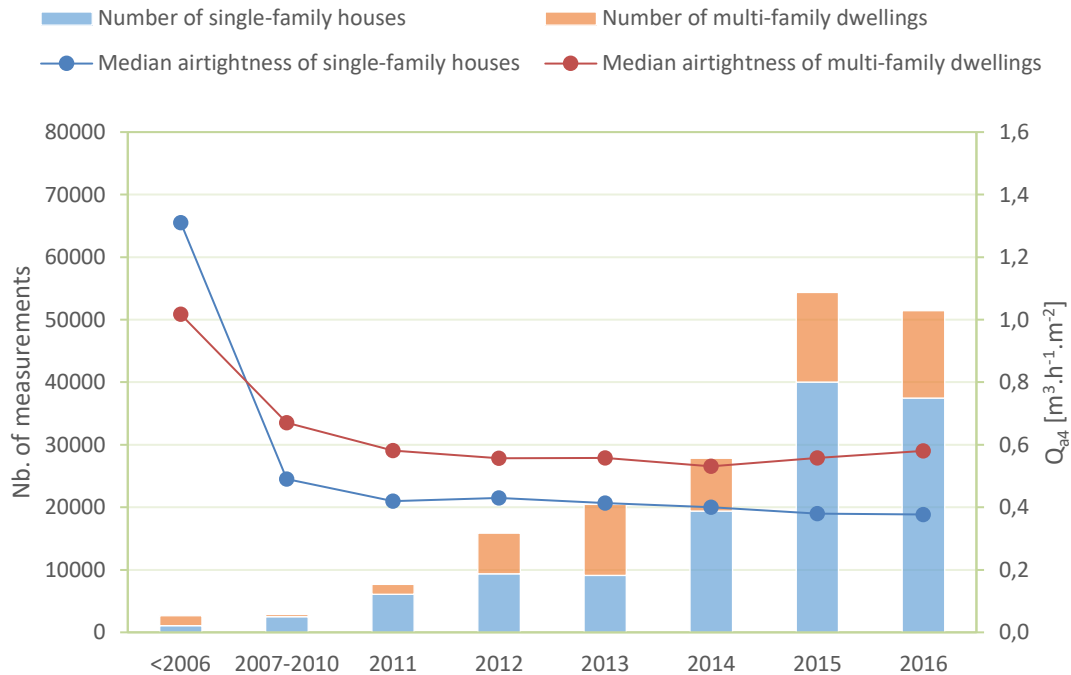


Figure 2-3: Number of building airtightness tests and their results according to the year of construction of the building

### 2.3.2.2 Impact of the construction method on airleakage

As the database includes various information regarding building characteristics, the following paragraphs provide an analysis of correlations between airleakage and:

- main material;
- insulation type;
- ventilation system.

In a previous analysis of this database [33], we had shown that there is no significant correlation between the volume and envelope airtightness. This manuscript does not therefore provide any further analysis regarding volume impact.

#### *Impact of main material on airleakage*

The database includes a large variety of main construction materials. This is due to the materials used in old buildings. In order to perform analysis on significant sub-samples, only data from residential buildings built since 2010 with brick, wood, and concrete are

detailed; all other types of material (steel, clay, stone, hemp, and straw) are grouped together in the “other” category. Figure 2-4 gives the distribution of  $q_{a4}$  results depending on the main material for measurements performed on single-family houses and Figure 2-5 on multi-family buildings. In this chapter, the box width represents the amount of material in the database, the median is represented by the central mark, the lower and upper edges of the box are the 25<sup>th</sup> (1st quartile) and 75<sup>th</sup> percentiles (3rd quartile) respectively. The whiskers extend to the most extreme data points not considering outliers ( $\pm 2.7$  times the standard deviation). The outliers are not plotted. The dashed line represents the median for the whole sample  $q_{a4,med,sample}$ . For single-family houses, the median airleakage varies from  $0.38 \text{ m}^3 \text{ h}^{-1} \text{ m}^{-2}$  for concrete-houses to  $0.44 \text{ m}^3 \text{ h}^{-1} \text{ m}^{-2}$  for wooden houses, through  $0.40 \text{ m}^3 \text{ h}^{-1} \text{ m}^{-2}$  for brick-houses (Figure 2-4). For multi-family dwellings, the median airleakage varies from  $0.54 \text{ m}^3 \text{ h}^{-1} \text{ m}^{-2}$  for concrete buildings to  $0.65 \text{ m}^3 \text{ h}^{-1} \text{ m}^{-2}$  for wooden buildings, through  $0.62 \text{ m}^3 \text{ h}^{-1} \text{ m}^{-2}$  for brick-buildings (Figure 2-5). According to these figures, wooden buildings are slightly less airtight than concrete and brick buildings; however, the difference is low. Field surveys have shown that wooden buildings can be very airtight if there is a vapor barrier and if it is properly fitted. Nevertheless, there is a lack of experience in France on wood construction that may lead to the vapor barrier being incorrectly fitted, thereby explaining the results for wooden buildings.

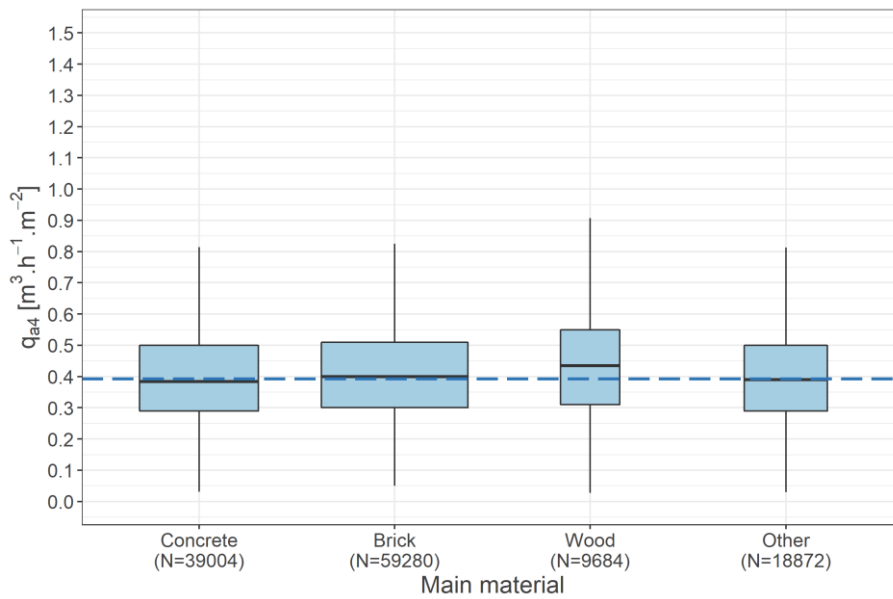


Figure 2-4: Impact of the main material on envelope airtightness for 170,028 single-family houses ( $q_{a4,med,sample} = 0.39 \text{ m}^3 \text{ h}^{-1} \text{ m}^{-2}$ )

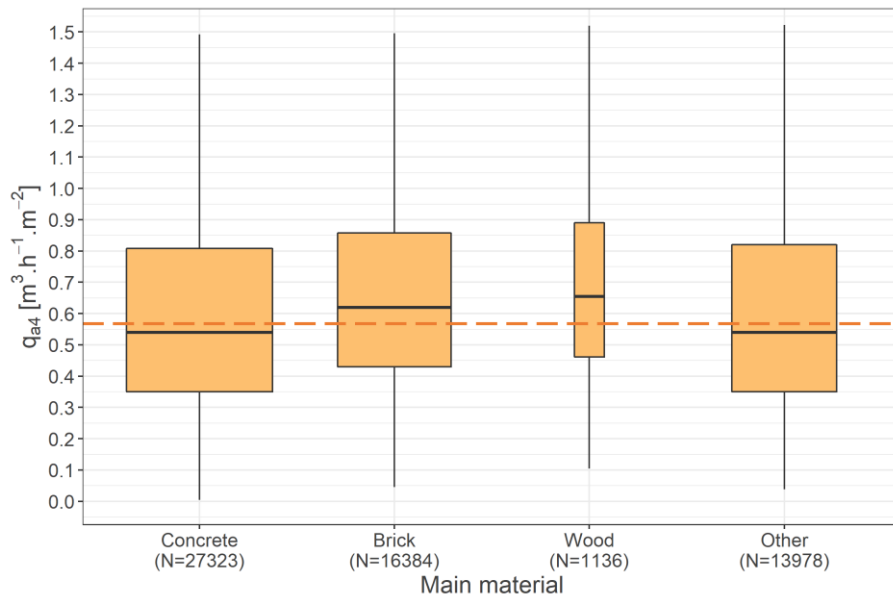


Figure 2-5: Impact of the main material on envelope airtightness for 57,224 multi-family buildings  
 $(q_{a4,med,sample} = 0.57 \text{ m}^3 \text{ h}^{-1} \text{ m}^{-2})$

#### *Impact of insulation method on airleakage*

Figure 2-6 provides the distribution of  $q_{a4}$  results according to insulation method (ITI= Internal thermal insulation, ETI=External thermal insulation, DTI= Distributed thermal insulation) for measurements performed on single-family houses and multi-family dwellings. For single-family houses, the airleakage seems to be slightly higher for the ETI. The ETI is not often used for single-family houses (only 2.3% of houses in the database) and requires a different technique to make the envelope airtight. The lack of experience of stakeholders with this type of building might explain the poorer result for ETI. Conversely, external insulated multi-family dwellings represent a significant percentage of the buildings in the database (24,9%) and are more airtight than internal insulated buildings. Probably because multi-family buildings are made with shuttered concrete which is naturally airtight, while single houses are mostly made with brick and concrete blocks that are not airtight. However, the distinction between shuttered concrete and concrete blocks is not made in the database so we cannot confirm this assumption. The results for DTI are similar to the result for ITI for both houses and multi-family dwellings.

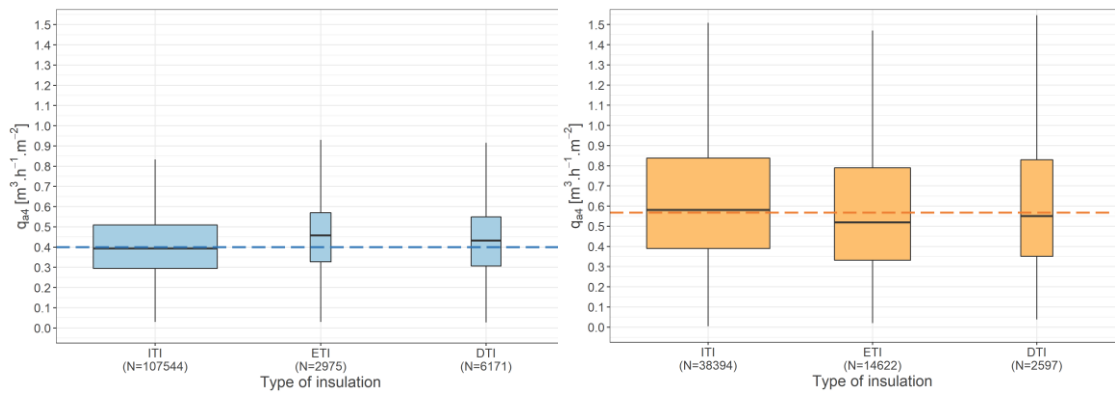


Figure 2-6: Impact of type of thermal insulation on envelope airtightness for single-family houses (left) and multi-family dwellings (right)

### *Impact of ventilation system on airleakage*

Figure 2-7 provides the distribution of  $q_{a4}$  results according to the ventilation system for measurements made on single-family houses and multi-family dwellings. For single-family houses, the variability of the results for balanced ventilation systems is higher than for exhaust ventilation systems and the median values are not significantly different, and so no conclusion can be drawn regarding the impact of the type of ventilation system on envelope airleakage. For multi-family dwellings, the balanced ventilation system shows lower airleakage. For this type of building, the use of balanced ventilation systems is very often part of a global quality approach to the building. The better results for balanced ventilation systems are probably therefore due to the awareness of the stakeholders.

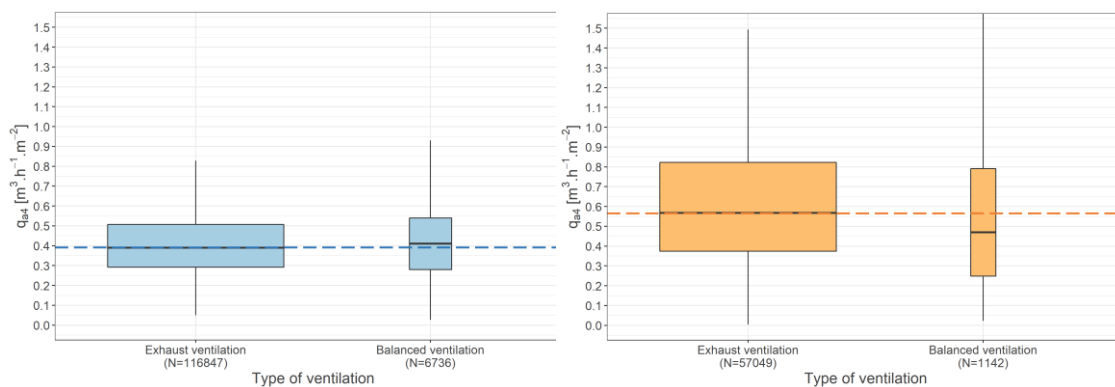


Figure 2-7: Impact of type of ventilation system on envelope airtightness for single-family houses (left) and multi-family dwellings (right)

### *2.3.2.3 Seasonal variation*

Several studies dealing with uncertainties in envelope airtightness measurements look at seasonal variations. ISO EN 9972 sets recommendations only on temperature difference

over the thermal envelope and on the wind speed limit. Nevertheless, the significant impact of seasonal change has been evaluated at between 5% and 120% [34], [35] and [36]. Analysis of the variation in the distribution of measurement results for each season makes it possible to detect a seasonal variation. Single-family houses measured in France have been therefore classified into categories according to the treatment of airtightness. The two main categories are:

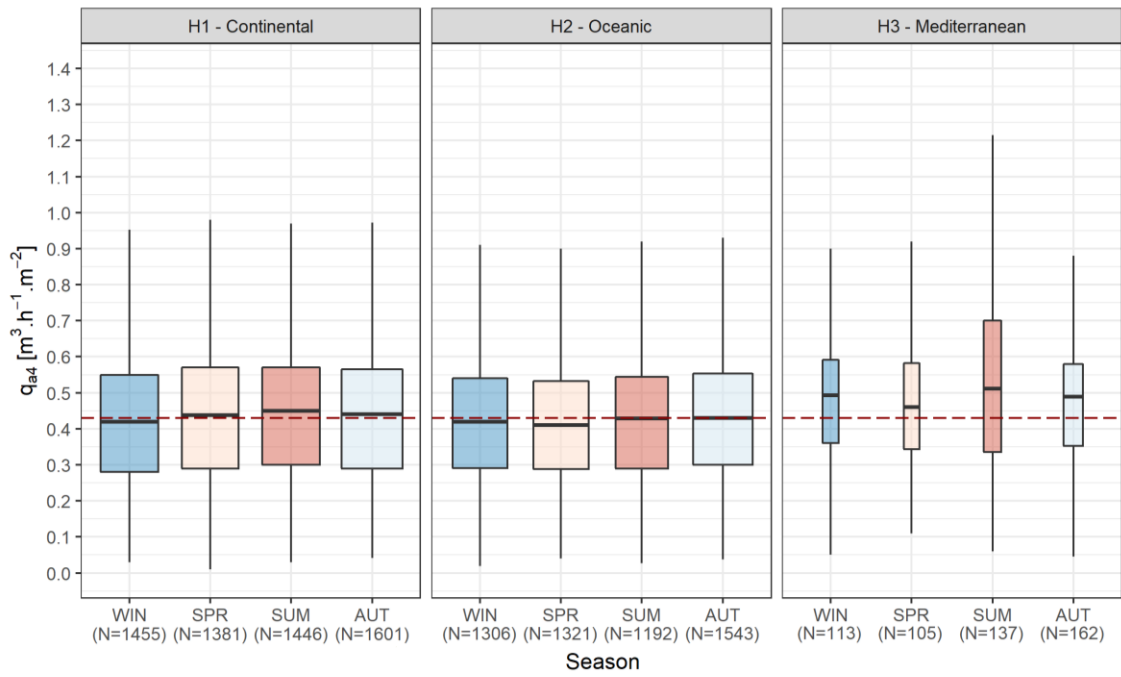
- wood structure houses where airtightness is provided by the vapour barrier;
- heavy structure with interior insulation where the air barrier is provided by plasterboard and mastic on the inside facing of the walls.

They were then classified regarding the climate of the region according to the three climatic zones of the French EP-regulation: continental climate (H1), oceanic climate (H2), and Mediterranean climate (H3). WIN=Winter; SPR=Spring; SUM=Summer; AUT=Autumn

Figure 2-8 and Figure 2-9 show the seasonal variations of airleakage in single-family dwellings for the two categories of airtightness treatments (WIN=Winter; SPR=Spring; SUM=Summer; AUT=Autumn). For wooden houses, Figure 2-8 shows no seasonal variation for continental and oceanic climates (less than 5%). These variations are higher for the Mediterranean climate but the samples are too small to enable any conclusions to be drawn. This result contradicts the findings of Walhgren [37] and Domhagen et al. [34] who found that in winter, Swedish wooden buildings were 8-10% leakier than in summer. For heavy structure houses with internal insulation (Figure 2-9), the results do not show seasonal variations as well (less than 3%).

Other results of this analysis concern the impact of the climate and the type of structure. For the Mediterranean climate, higher values for all seasons are observed with average values being between 7 and 19 % higher than all the wooden sample ones, and between 7% and 13% higher than all the heavy structure sample ones. Lower heating needs in this climate may induce less concern regarding airtightness and thus explain these differences. Nevertheless, further investigations need to be performed to confirm these results because the samples are quite small and the differences are not significant enough.

Finally, the comparison of Figure 2-8 and Figure 2-9 shows that wooden houses are leakier than heavy structure houses, which is consistent with previous analyses of Figure 2-4.



WIN=Winter; SPR=Spring; SUM=Summer; AUT=Autumn

Figure 2-8: Variation of airleakage for wood structure houses according to climate and season ( $q_{a4,med,sample} = 0.43 \text{ m}^3 \text{ h}^{-1} \text{ m}^{-2}$ )

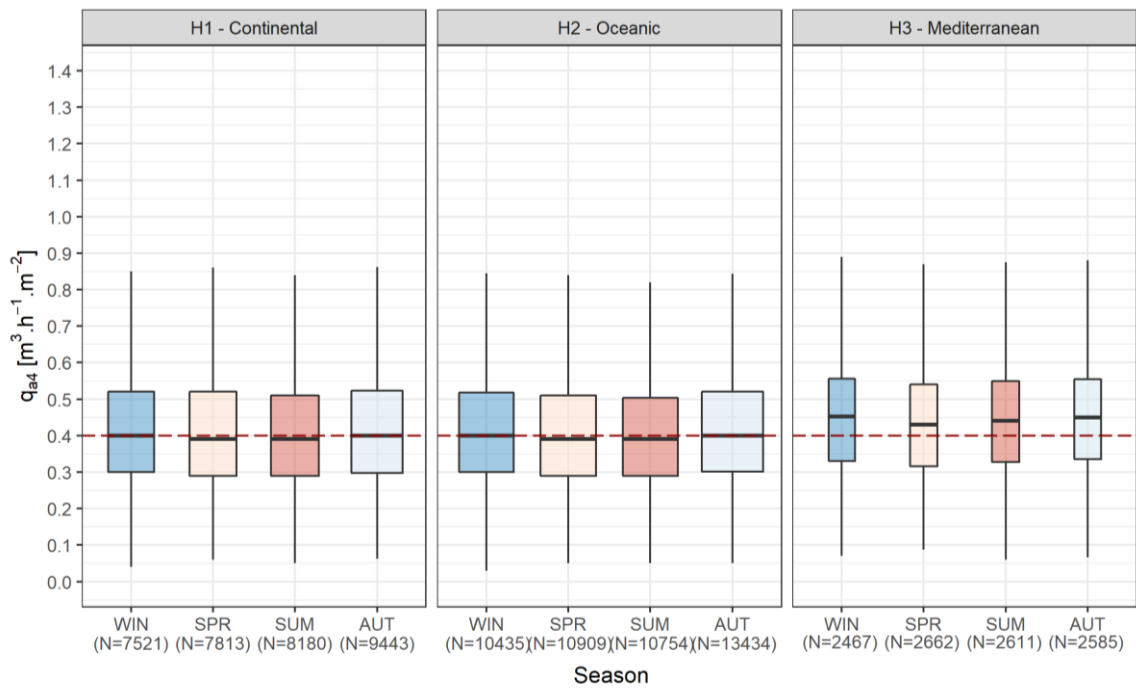


Figure 2-9: Variation of airleakage for heavy structure houses (with interior insulation) according to climate and season ( $q_{a4,med,sample} = 0.40 \text{ m}^3 \text{ h}^{-1} \text{ m}^{-2}$ )

#### 2.3.2.4 Distribution of the flow exponent $n$ values

The fan pressurization test method is based on a model (presented in chapter 3 of this manuscript) that introduces different parameters such as the flow exponent  $n$ . This exponent characterizes the flow regime through leaks: it varies from 0.5 for a completely turbulent flow to 1.0 for a completely laminar flow. As it may have a significant impact in the measurement result depending of the method used for the test, the analysis of the distribution of the  $n$  value from on-site data is very useful. Figure 2-10 and Figure 2-11 show the distribution of the flow exponent  $n$  for single-family houses and multi-family dwellings. For single family houses in the database, the average exponent is 0.668. This figure matches the commonly used default value ( $n=0.67$ ). It is also consistent with the mean value  $n=0.646$  for the houses included in the LBNL database [20]. The standard variation (0.051), which represents the variability of  $n$  values, is also consistent with the standard deviation of the LBNL database (0.057). As the regulatory French indicator is calculated from an extrapolated airflow at 4 Pa, the variability of  $n$  values confirms the relevance of the multi-point testing method compared to the one-point testing method which considers a default value for  $n$  and thus introduces error due to the gap between the default value and the real value of  $n$ . This conclusion also applies to multi-family dwellings, as the standard variation of  $n$  value is even higher (0.066).

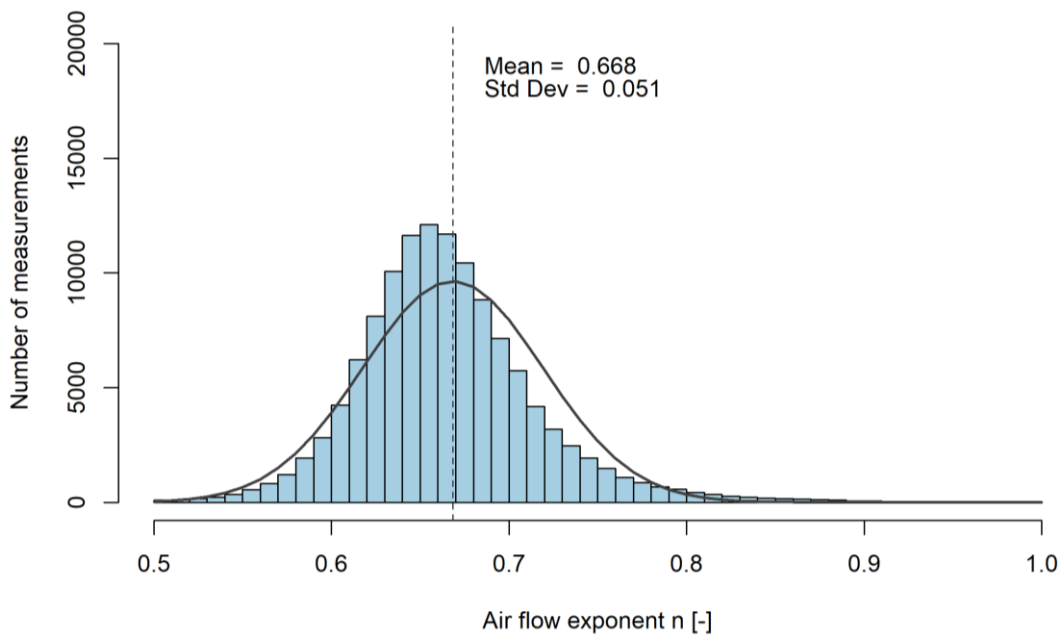


Figure 2-10: Distribution of flow exponent  $n$  for single-family houses

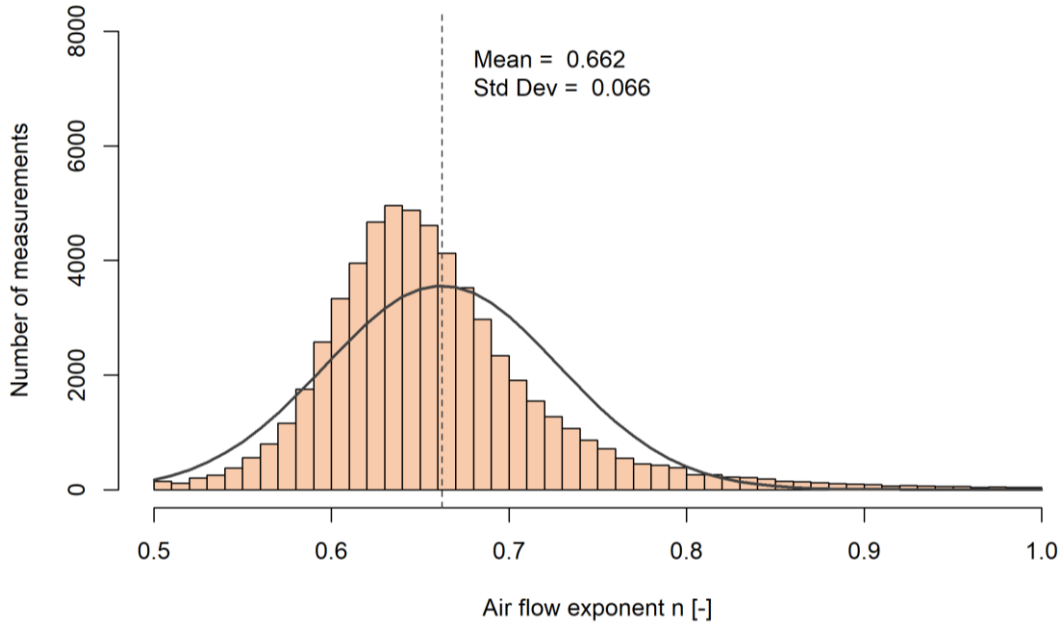


Figure 2-11: Distribution of flow exponent n for multi-family dwellings

### 2.3.3 *Identifying areas of improvement for building construction stakeholders and measurement testers*

#### 2.3.3.1 *Leaks distribution analyses*

According to the French standard FD P50-784 and the French tester's scheme, for each measurement, the tester has to detect major envelope leaks. Each identified leakage has to be described and located during the measurement and reported in the professional register according to the classification given in the FD P50-784. These categories include leaks detected on:

- main envelope area;
- wall, roof and floor junctions;
- doors and windows;
- building components penetrating the envelope;
- trapdoors;
- electrical components;
- door/wall and window/wall junctions;
- wood-burners, chimneys, elevators, cooker hoods, etc.

The leaks are identified according to ISO 9972 – Annex E using either an infrared thermo viewer, smoke or an air velocity meter. For each measurement recorded in the database, one or more leaks are declared according to the 46 subcategory classification. For each subcategory, Table 2-5 presents the occurrences in the database according to the building use. On average, 6 different leak locations per building are declared. For multi-family

dwellings, the three most frequently identified leak locations are “D3: Crossing floor and walls and/or partitions” (57% of dwellings), “C8: Rolling shutter casing” (55%), and “D4: Ventilation air terminal devices” (47%). For single-family houses, the three most frequently identified leak locations are “D3: Crossing floor and walls and/or partitions” (53% of houses), “F3: Electrical grids built on the external walls” (52%), and “C6: External sliding doors” (50%).

Table 2-5: Leak categories and occurrences

Categories	Subcategories	Occurrences	
		Multi-family dwellings 54,304 measurements	Single-family houses 109,224 measurements
<b>A: Main envelope area</b>	A1: Other leak on main envelope area	6%	9%
	A2: Vapour barrier membrane (or similar complex): adhesive junction between strips, puncture or tear	3%	4%
	A3: Liaisons mortar/glue between masonry blocks, panels between doublings	3%	4%
	A4: Opening (e.g.: wall plug) or not sealed junctions between panels	5%	8%
	A5: False ceiling slabs	3%	4%
<b>B: Wall, roof and floor junctions</b>	B1: Other leak on wall, roof and floor junctions	5%	7%
	B2: Junction between two vertical walls	4%	5%
	B3: Junction between wall base and floor	15%	22%
	B4: Junction between wall and high floor or pitched roof	4%	6%
	B5: Vapour barrier membrane (or similar complex): Attachment defective smooth with sill, intermediate floor, and top floor	3%	3%
<b>C: Doors and windows</b>	<b>C1: Other leaks on doors and windows</b>	<b>25%</b>	<b>28%</b>
	<b>C2: Window and French window: frames (no seals or compression default of seals)</b>	<b>30%</b>	<b>26%</b>
	C3: Window and French window: junction between glass and frame defective seal)	9%	8%
	C4: Landing door or fire door: poor compression of seals (excluding threshold bar)	4%	19%
	C5: Landing door or fire door: absent or ineffective threshold bar	4%	16%
	<b>C6: Sliding door: Excessive space between window portions of sliding frame, and/or top and bottom of frame</b>	<b>10%</b>	<b>50%</b>
	C7: Sliding door: Evacuation of condensates	4%	14%
	<b>C8: Rolling shutter casing</b>	<b>55%</b>	<b>17%</b>
<b>D: Building component penetrating the envelope</b>	D1: Another element through a wall	13%	15%
	D2: Vapour barrier membrane (or similar complex) through which duct, pipe, beams, hatches	4%	5%
	<b>D3: Crossing Floor and walls and/or partitions (any type of plumbing pipes and electrical conduits ...)</b>	<b>57%</b>	<b>53%</b>

	<b>D4: Ventilation air terminals: leaks at periphery of exhaust or supply air vents</b>	<b>47%</b>	<b>23%</b>
	D5: Beams: Linking beams or joist with walls	4%	6%
	D6: Beams: Liaison with ceiling beams or joists or floor	3%	5%
	D7: Stairs: Junction flooring / stairs or vertical walls / stairs	3%	8%
<b>E: Trapdoor</b>	E1: Another trapdoor	12%	10%
	E2: Trapdoor to attic (absent or ineffective seal)	5%	22%
	E3: Trapdoor to vertical technical duct (absent or ineffective seal)	18%	8%
<b>F: Electrical component</b>	F1: Another equipment	7%	11%
	<b>F2: Electrical board</b>	<b>45%</b>	<b>33%</b>
	<b>F3: Grids built on the exterior walls</b>	<b>36%</b>	<b>52%</b>
	F4: Grids built on the internal partition walls	24%	23%
	F5: Lighting components	7%	18%
<b>G: Door/wall and windows/wall junctions</b>	G1: Another leak on walls/doors and windows junction	4%	6%
	G2: Junction between walls and windows or French windows	12%	8%
	G3: Junction between walls and landing door or Fire door	4%	5%
	G4: Junction between internal panels and window and French window	20%	17%
	G5: Junction between internal panels and landing door or Fire door	5%	6%
	G6: Junction between vapor barrier membrane and door or window	3%	3%
<b>H: Wood-burner, chimney, elevator, cooker hood...</b>	H1: Another leak	10%	20%
	H2: Wood-burner, fireplace insert or boiler, or combustion-air air vent	7%	13%
	H3: Extractor hood with external evacuation	3%	7%
	H4: Trapdoor for smokes evacuation	3%	3%
	H5: Zenithal lighting roof lights	3%	3%
	H6: Elevator door (frame - connecting door ...)	3%	2%
	H7: Arrival air extraction or not described in the thermal calculation	3%	2%

The sample of single-family houses we analyze in this section is statistically significant: each leak has been identified in at least 2,000 houses. For each of the 46 subcategories, a subsample of all the houses where this particular leak has been identified was constituted. For each subsample, the median value for  $q_{a4}$  was then calculated from measurement results from all houses within this subsample. These 46 values of median  $q_{a4}$  are compared to the median value of the entire sample of houses (121,478 houses):  $q_{a4,med,sample} = 0.39 \text{ m}^3 \text{ h}^{-1} \text{ m}^{-2}$ . This comparison gives clues regarding the correlation between leak locations and airtightness levels in single-family houses. This is so because when the median value of the subsample is higher than the median value of the entire sample, the leak identified in the subsample can be considered as having a significant impact on house airleakage. Figure 2-12 shows the results for the 10 subcategories with the highest median value of  $q_{a4}$ . For each of these 10 subcategories, Figure 2-12 presents both the median value of  $q_{a4}$  for the subsample and the frequency of identification of the leak.

It should first be noted that the most frequent leak locations previously identified (F3, D3, and C6) do not appear in Figure 2-12. This result indicates that even if these leaks are the most frequently identified in houses, they are not significantly responsible for high

airleakage results. Secondly, we identified two leaks which seem to have a significant impact on house airleakage:

- houses with leaks due to lighting components (F5) have a median  $q_{a4}$  13% (+0.05  $\text{m}^3 \text{h}^{-1} \text{m}^{-2}$ ) higher than the  $q_{a4,med,sample}$ , and this leak is frequently identified: for 18% of the 109,224 houses of the sample;
- the leak due to the electrical board (F2) is both frequently identified and seems to have a significant impact on  $q_{a4}$ : the median  $q_{a4}$  is 8% higher than the  $q_{a4,med,sample}$  and has been identified in 33% of the houses of the sample;
- for the eight other leaks in the graph, impacts on  $q_{a4}$  are lower, between 6 and 8 %, with lower observation frequencies (7-22%).

Such information can be very useful to improve envelope airtightness, during both the design stage and on-site construction.

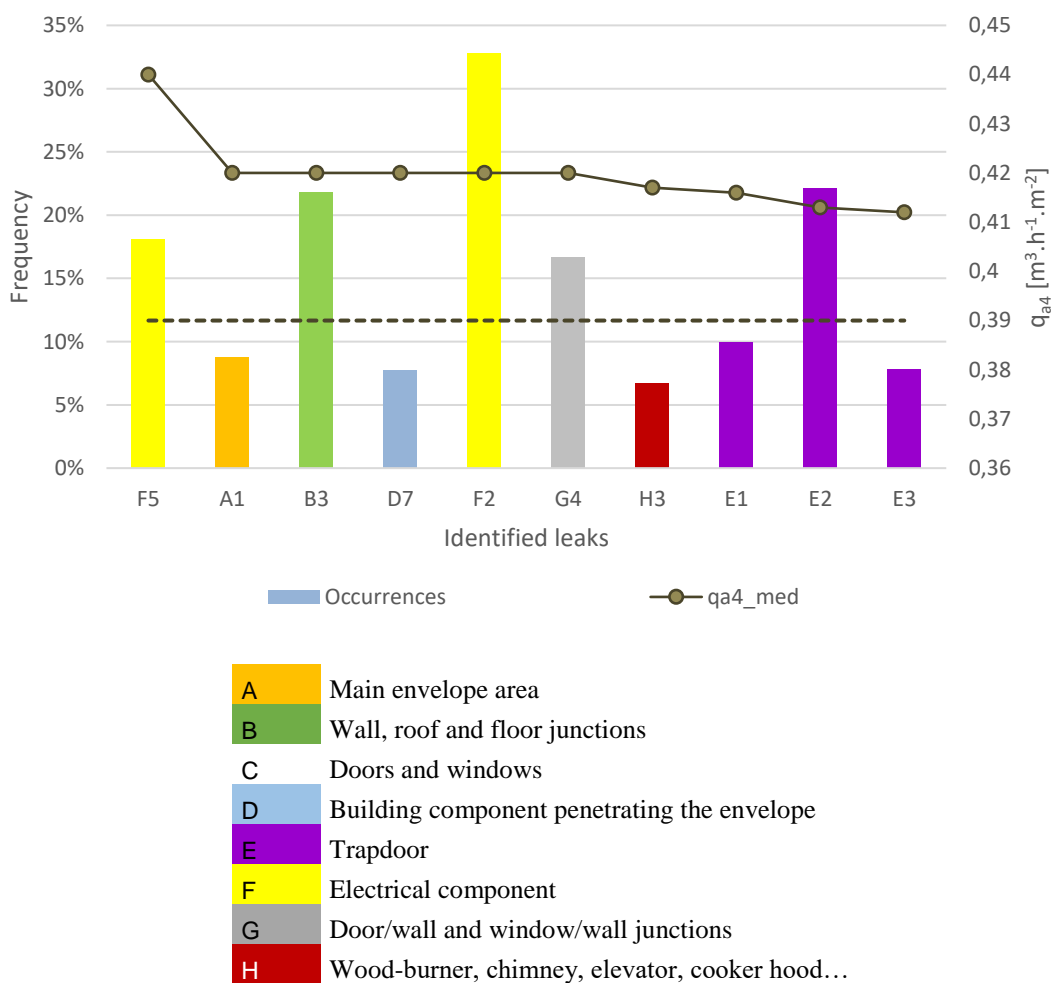


Figure 2-12: Number of observations for 10 leaks identified on single-family houses with the highest median  $q_{a4}$  value (from the sample of 121,478 measurements on houses)

Analysis based on leak location identification has, however, two limits. Firstly, the tester does not provide any information on the extent of the leakage. Secondly, not every leakage may be detected, especially when the targeted airtightness level is met, in which case the tester often does not perform any detailed leak location study. Nevertheless, the

average of 6 leak locations identified per building in this database indicates that testers perform this identification scrupulously.

#### 2.3.3.2 *Threshold effect in the distribution of test results due to regulatory limit values*

Figure 2-13 gives the number of measurements by airtightness level interval for multi-family dwellings and Figure 2-14 gives those for single-family houses in order to analyze the impact of the implementation of a threshold value in more detail. For multi-family buildings, the distribution is regular and is close to a skew-normal distribution. Figure 2-13 shows no threshold effect around the regulatory value of  $1.0 \text{ m}^3 \text{ h}^{-1} \text{ m}^{-2}$ . 86% of measurements are below this threshold, and 73% below the threshold of EP-label “Effinergie+”  $0.8 \text{ m}^3 \text{ h}^{-1} \text{ m}^{-2}$ . Note that most tests are performed by sampling, so in most cases, only dwellings are tested and not common parts. The test results we analyze here are the airleakage of the dwellings. In addition, the threshold value applies to the average value of the sample of dwellings and not to each dwelling in the sample. For single-family houses, Figure 2-14 clearly illustrates the threshold effect of the mandatory requirement of the EP-regulation for single-family dwellings ( $0.6 \text{ m}^3 \text{ h}^{-1} \text{ m}^{-2}$ ) which creates a discontinuity in the distribution of the measured values of the airleakage. This might be due to last-minute corrections on building envelopes during the commissioning test to force the measured airleakage below the regulatory threshold. Thus 93% of the measurements are below  $0.6 \text{ m}^3 \text{ h}^{-1} \text{ m}^{-2}$ . Also, more than half (53%) are below the threshold of EP-label “Effinergie+”  $0.4 \text{ m}^3 \text{ h}^{-1} \text{ m}^{-2}$ . Much field feedback indicates that mastic is used on the wall surface as a last-minute correction just after the first measurement in order to comply with the regulatory threshold. Moreover, these corrections are most of the time made without a backer rod. Wingfield et al. [38] have shown that after a few weeks of heating, mastics used without backer road may begin to shrink. This practice may therefore have an impact on the durability of envelope airtightness, and highlights the need for improvement in practices to comply with the airtightness threshold using durable solutions. This practice has also been identified in the UK. As a similar sharp peak is observed in their graphs, they suspect that the first measurements are performed but not recorded, and that refinement of air permeability is done before the recorded test. [25].

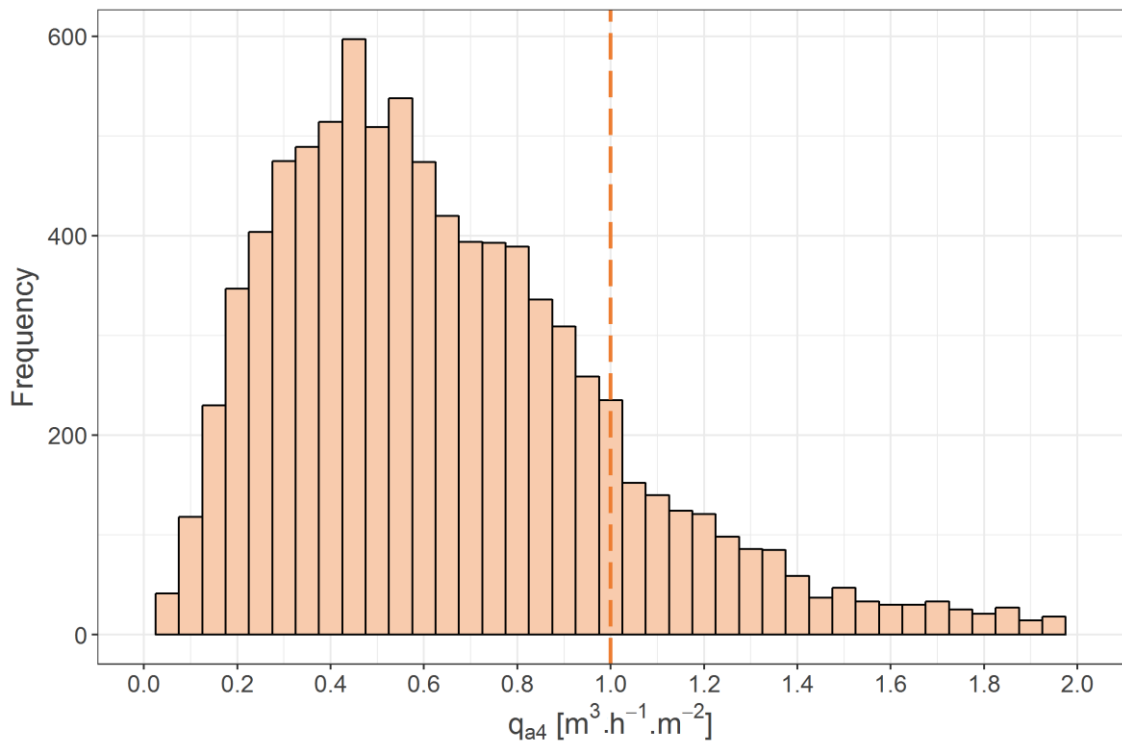


Figure 2-13: Airleakage test result distribution for multi-family dwellings (58,225 dwellings)

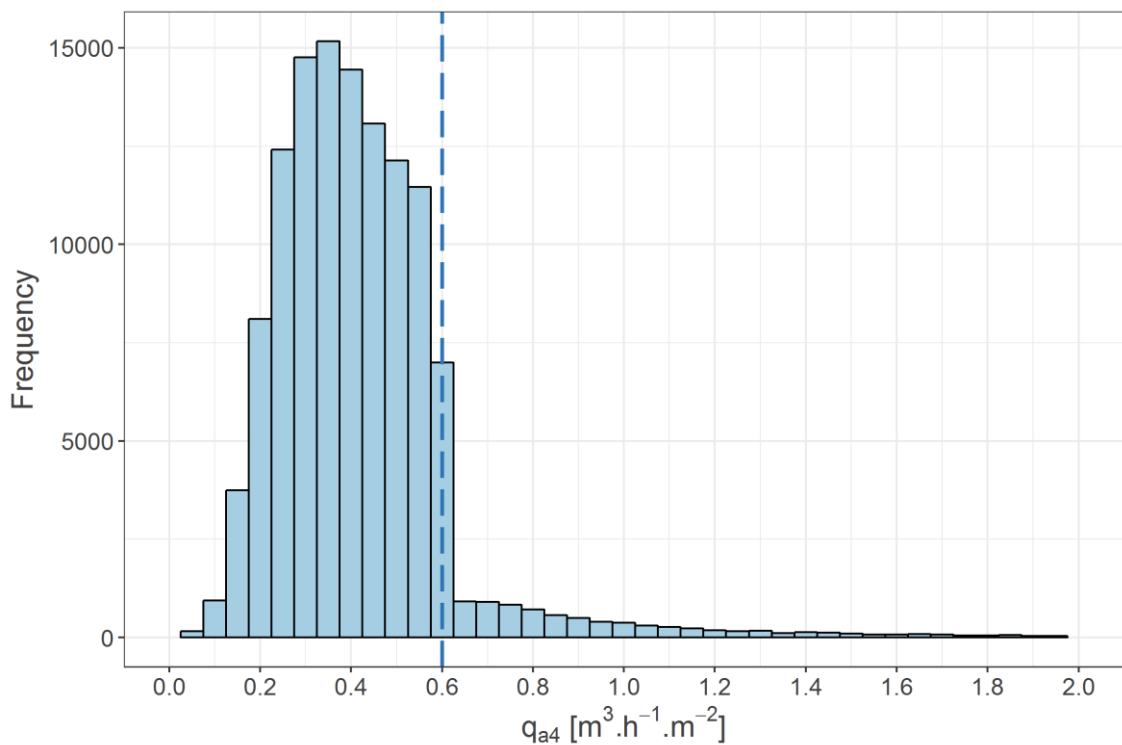


Figure 2-14: Airleakage test result distribution for single-family houses

## 2.4 Limits and applications of the database analysis

### 2.4.1 *Barriers in comparison with other databases*

This manuscript references two other very large databases. First, the LBNL database included in 2013 72% of detached houses, 6% of multi-family dwellings and 21% of mobile homes, and a large percentage of the dwellings in this database consist of existing and retrofitted (social) houses through weatherization programs [20]. Secondly, the UK database includes dwellings without distinction between houses and multi-family dwellings. The French database includes all types of buildings but essentially new buildings. Comparisons have been made regarding the flow exponent distribution and the threshold effect of limit values. Nevertheless, this manuscript does not provide further comparisons due to the following barriers:

- the airleakage measurements are made using different protocols, including different testing methods: either the one-point testing method or the multi-point method, different building preparations for the measurements: some envelope components are sealed in France and not in the UK or in the US, for example;
- the indicators are different:  $q_{a4}$ ,  $q_{50}$  and NL. It is not possible to calculate the equivalence between these indicators from the French database because it does not include information regarding the floor area, the building height or the total envelope area;
- the type of buildings included in the databases are different: the LBNL database includes only existing social houses before retrofitting; the UK database includes dwellings without distinction between houses and multi-family dwellings, and the French database includes all types of buildings but essentially new buildings.

### 2.4.2 *Feedback to testers and stakeholders*

The analyses presented in this manuscript and in previous publications have been presented in France both to testers and to stakeholders. Each year, during the national conference for testers organized by the qualification body, Cerema presents updated data analyses to over 200 testers. This presentation promotes the work of the testers and reminds them of the importance of providing reliable data. The discussions during this conference led to the sharing of feedback regarding field practices in order to improve and adapt the testers' scheme requirements. During this meeting, testers also provide valuable information to explain the results of the analysis. The stakeholders are also consulted, especially through the dissemination of these studies during national meetings regarding airtightness issues organized by the Ministry in charge of Construction. This is an important way to communicate these results and help them to improve the envelope airtightness of future buildings, especially through analysis of leak distribution.

### 2.4.3 *Improvement of databases in France and throughout the world*

The analyses performed on the database over the last few years regularly led to changes in the professional registers through feedback from the testers regarding the arrival of new heating, cooling and ventilation systems in buildings, or new constructional

techniques, and regarding the difficulties that they might have to complete certain fields in the register. Other fields are modified or added in order to perform more detailed analyses. Moreover, the experience shared with other people in charge of national databases has led to the definition of a framework in order to:

- share experience regarding the creation and management of building airtightness databases;
- consider some standardization method to enable cross-analysis between countries.

This last work was introduced during the TightVent Airtightness Associations Committee meetings and is still on-going.

## 2.5 Conclusions

The development of competent tester schemes provides a great opportunity to collect a number of reliable airleakage measurement results: up to 219,000 measurements in the French database. The analyses performed on the French database led to the identification of several factors that can significantly impact building airtightness. Firstly, wooden buildings have been found slightly less airtight than concrete and brick buildings, due to lack of field experience in France for this type of construction (from +15% for wooden single-family houses to +20% for wooden multi-family dwellings on the  $q_{a4}$  median value). Secondly, while there is no significant impact of the thermal isolation technique for single-family houses, external insulated multi-family buildings are generally more airtight. This observation may be explained by the use of naturally airtight shuttered concrete for this type of building. Similarly, the choice of ventilation system does not impact envelope airtightness for single family dwellings, whereas better results are observed for balanced ventilation (-17% on the  $q_{a4}$  median value) than for exhaust ventilation for multi-family buildings. This tendency may be due to a global quality approach for buildings where balanced ventilation systems are used.

Analysis of the French database has also led to the identification of levers to improve the practices of building construction stakeholders and testers. Firstly, the leakage location analyses have led to the identification of the most common leaks, both for single-family houses and multi-family houses. Moreover, influent leaks on envelope airtightness have been identified. These results can be very useful to improve envelope airtightness, during both the design stage and on-site construction. On the top of this classification, we identified that houses with leaks due to lighting components have a median  $q_{a4}$  13% higher than the  $q_{a4,med,sample}$ , and this leak is identified for 18% of the 109,224 houses of the sample. Secondly, the threshold effect of the mandatory requirement of the EP-regulation for single-family dwellings reflects the implementation of last-minute corrections. As this practice may have an impact on the durability of envelope airtightness, it highlights the need for practice improvements to comply with the airtightness threshold by using durable solutions.

Finally, some results presented in this paper confirm that the multi-point testing method can be used during all seasons in France. No significant seasonal variations have been identified, either for wooden buildings or for heavy structure buildings. Moreover, the

distribution of the n value for French buildings confirms the need for multi-point testing for an indicator extrapolated at 4 Pa.

This database will grow and change in the next few years, through feedback from the field and international sharing, which will lead to more analyses and comparisons in order to improve building performance.

The analysis of this database shows that numerous fan pressurization tests are performed in France, mostly on new residential buildings. These test results are used to justify that the building meets the EP regulation or an energy program requirement. It is also used to better understand what factors may influence building airtightness and thus, help to improve envelope performance. The reliability of these test results is therefore essential. However, the database includes very poor information regarding the uncertainty of the measurement result. The objective of this manuscript is to reinforce current knowledge regarding fan pressurization tests uncertainty, to better take this uncertainty into account in the analysis of the test result, and if possible, improve the current test method to reduce this uncertainty. The next chapter of this manuscript is dedicated to a literature review to evaluate the current knowledge regarding fan pressurization test uncertainty, and then identify research gaps that need to be fulfilled to lead to a quantification of this uncertainty.

## 3. Uncertainty sources in building pressurization tests: review and research gaps

### 3.1 Background

Within the 1950s and the 1960s, building airleakage evaluations were performed using a tracer gas measurement. This technique had some important disadvantages which were mainly the duration of the measurement, the influence of the weather conditions, and the cost of the test equipment [39]. Therefore, several experiments were conducted to develop a more appropriate method for determining building airleakage: the pressurization test method. With this method, the airflow rate through leaks is not directly measured. A similar method was first used to determine the airflow rate through a barrier in mines [40].

#### 3.1.1 Pressurization test principle

During a fan pressurization measurement, the “*building airtightness levels are measured by using a fan, temporarily installed in the building envelope (a blower door) to pressurize the building. Airflow through the fan creates an internal, uniform, static pressure within the building. The aim of this type of measurement is to relate the pressure differential across the envelope to the airflow rate required to produce it. Generally, the higher the flow rate required to produce a given pressure difference, the less airtight the building*” [2]. In the fan pressurization test method, the model considers that the airflows through the building envelope and building components can be represented by a single airflow rate through a single equivalent opening. In this model, the relation between this airflow through this equivalent opening and the indoor-outdoor pressure difference is simplified with the power-law relation given by equation (1) [41]:

$$q = C * \Delta p^n \quad (1)$$

where:

- $q$  is the volume flow rate [ $\text{m}^3 \text{h}^{-1}$ ]
- $\Delta p$  is the indoor-outdoor pressure difference [Pa]
- $C$  is the airleakage coefficient [ $\text{m}^3 \text{h}^{-1} \text{Pa}^{-n}$ ]
- $n$  is the flow exponent [-].

The flow exponent  $n$  varies from 0.5 for a completely turbulent flow (dominated by inertial forces) to 1.0 for a completely laminar flow (dominated by viscous forces) [42]. The objective of the pressurization test method is to measure an airflow rate for a given indoor-outdoor pressure difference  $\Delta p$ . To impose this pressure difference, a fan extracts air from the house or supplies air to it to maintain  $\Delta p$ . In stable conditions, the building envelope airleakage mass flow is considered equal to the mass airflow rate through the fan. Thus, for a given pressure difference  $\Delta p$ , measuring the airflow rate through the fan

leads to airleakage. To determine the airleakage for a specific pressure difference  $\Delta p$  there are three options:

1. impose  $\Delta p$  and obtain the airleakage directly (in reality, due to weather conditions and measuring device resolution, it is almost impossible to impose a given  $\Delta p$  exactly);
2. impose  $\Delta p$ , measure the associated airflow rates, and consider a fixed value for the flow exponent  $n$ . The value of  $C$  can be obtained for any pressure difference. This is known as the one-point measurement method;
3. impose several pressure differences and measure the associated airflow rates to determine values of  $C$  and  $n$  from a regression analysis applied to  $\ln(q)$  and  $\ln(\Delta p)$ . The airflow rate can be extrapolated to a reference pressure difference. This is known as the multi-point measurement method. This method, described in ISO 9972 and ASTM 779-19, is currently the most used.

Different indicators are mainly used:

- at 4 Pa: the effective leakage area  $ELA_4$ , mainly used in the US, is calculated from the leakage airflow rate extrapolated at 4 Pa. The specific leakage rate  $q_{a4}$  ( $Q_{4Pa-Surf}$  in French) used in France is also calculated from the leakage airflow rate extrapolated at 4 Pa. Both these indicators at 4 Pa are meant to characterize the airleakage of the building envelope under normal use conditions (4 Pa is considered consistent with a building indoor-outdoor pressure difference with no high wind speed or extreme temperature difference);
- at 9.8 Pa: in Japan, the airtightness requirement for residential buildings uses an indicator corresponding to an opening area calculated from an airflow rate extrapolated at 9.8 Pa (1 mmAq) [43];
- at 10 Pa: in the Netherlands, the specific leakage rate  $q_{10}$  is calculated from an airflow rate extrapolated at 10 Pa. It is also used in Canada to define the equivalent leakage area;
- at 50 Pa: the air change rate  $n_{50}$  and the specific leakage rate  $q_{50}$  are calculated from an airflow rate extrapolated at 50 Pa. They were introduced in the 1980s in the Swedish and Norwegian regulations. They are both currently used in most European countries and the US by the Residential Energy Services Network (RESNET);
- at 75 Pa: the US Army Corp of Engineers uses a specific airtightness requirement calculated from a leakage airflow rate at 75 Pa.

### 3.1.2 *Development of measuring device prototypes*

Tamura [3] described a series of pressurization tests performed in 1967-1968 on 6 houses in the Ottawa area with an experimental device (see Figure 3-1) including:

- a calibrated fan connected to a window through a metal duct;
- a damper to control air exhaust rate (from the fan);
- a pressure tap to measure the inside-to-outside pressure difference.

The objective of those tests was to determine airleakage rates through different envelope components. To evaluate those rates, many measurements were performed, all at 75 Pa (they were one-point measurements), with different sealed and unsealed components. All tests were performed with the interior doors open. This experiment took place in the summertime when the wind speed was lower than 5 mph ( $2.2 \text{ m s}^{-1}$ ).

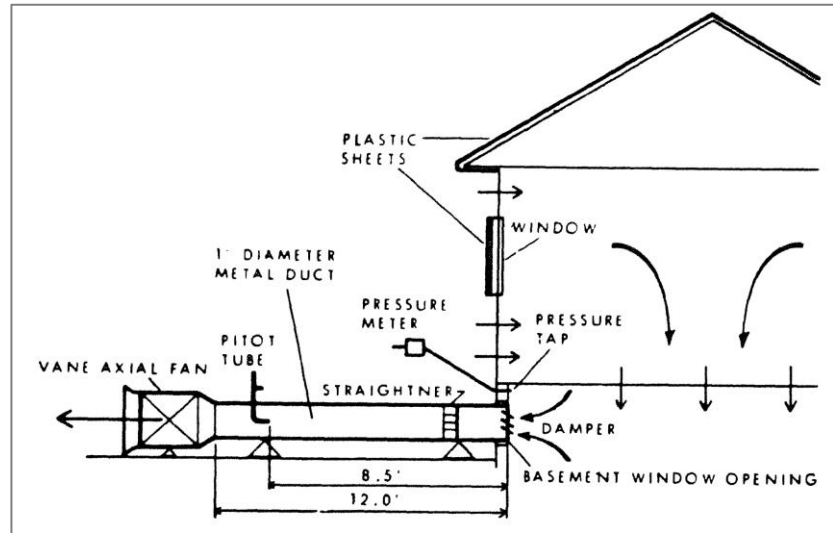


Figure 3-1: Test bench used by Tamura in 1967-1968 to performed pressurization test [3]

A readily portable version of this apparatus was developed in the UK and described by McIntyre and Newman [44]. It was placed on the exterior door of a house. They recommended not to perform tests in windy conditions to maintain a steady pressure difference.

Another similar prototype, called “the Super Sucker”, was used by Caffey to first evaluate the range of air infiltration of US houses, and then to identify leak locations and solutions to correct them in 50 homes in the US in 1974 [45]. The “Super Sucker” was calibrated using a laboratory wind tunnel, and its results were compared to the results of a gas tracer unit. This series of measurements led to the identification of 12 distinctive leakage areas in US houses (such as electrical components, exterior windows, and recessed spotlight) and an evaluation of the ranges of leakage airflow through them performing multiple measurements for different sealed components configurations.

In 1975, Stricker [46] used a fan mounted through a flexible plastic film placed in front of an opened window (see Figure 3-2) to exhaust air from houses to determine an airleakage equivalent area (ELA) directly from the measured indoor-outdoor pressure difference using a fan response curve.

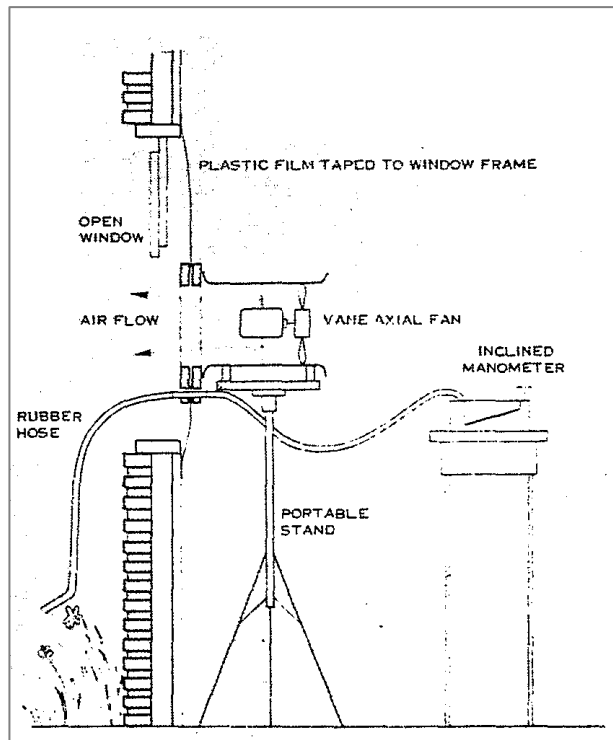


Figure 3-2: Experimental measuring device used to evaluate an airleakage equivalent area [46]

An easily portable apparatus was developed in Canada by the National Research Council of Canada [47] to perform airleakage measurement by pressurization test on small buildings in a short time (45 min). It was composed of a “*replacement plywood door section with a fan located in the center*” (Figure 3-3). The variable fan could ensure a 50 Pa pressure difference for all single-family houses. This apparatus was tested during a series of measurements performed in depressurization, in 1979. During all tests, interior doors remained open. Each test included different induced indoor-outdoor pressure differences. For each of them, the fan airflow rate was measured. The flow exponent  $n$  and the coefficient  $C$  were calculated from a regression analysis of the measurement data using equation (1).

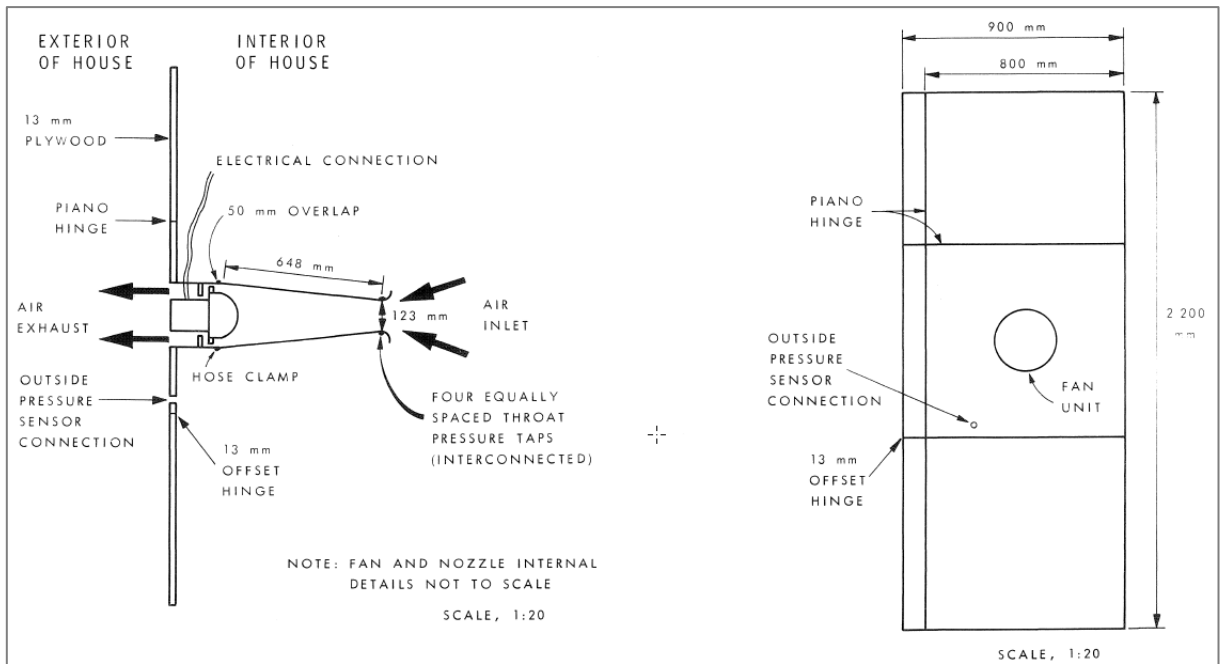


Figure 3-3: The exhaust fan apparatus developed by the National Research Council of Canada [47]

### 3.1.3 Pressurization test method at large scale testing

In 1978, Nevander and Kronvall reported that the pressurization test method “has a very dominating position in Sweden as method for testing whole houses for airleakage” [41]. This method included a series of imposed pressure differences and measured airflow rates at those points. The envelope preparation included the sealing of the voluntary opening such as ventilation air terminal devices, and the interior doors were open. The pressure difference points had to be between 20 and 55 Pa in absolute values, both in pressurization and depressurization. Measured airflow rates were corrected with the ratio between indoor temperature and outdoor temperature. The airleakage indicator was the airflow rate at 50 Pa as the average of the depressurization and the pressurization value. Requirements for measuring device uncertainty and airflow rate capacity or range existed, especially for manometers. An “upper limit for the error of the air flow measurement of  $\pm 6\%$ ” was suggested. The influence of the weather effects on the measurement had led to recommendations concerning the wind velocity (not higher than  $8 \text{ m}\cdot\text{s}^{-1}$ ) and indoor-outdoor temperature differences (not higher than  $30^\circ\text{C}$ ). In 1980, Sherman and Grimsrud from the Lawrence Berkeley Laboratory (US) stated that “Airleakage is usually measured by fan pressurization” [42]. This method leads to a graph relating the indoor-outdoor pressure difference and the airflow rate through the building envelope called the “leakage curve of building”. In 1984, Etheridge claimed that the fan pressurization method for measurements of a whole-house leakage was common practice in many countries [48].

### 3.1.4 Standards and methods

#### 3.1.4.1 Pressurization test standards in the 1980s

In 1984, four standards described a test pressurization method [49]:

- in 1980, the Swedish Standards Commission published the first standard for pressurization test: the SS 02 15 51 “Thermal insulation - determination of airtightness of buildings”;
- in 1981, the Norway standard NS 8200 “Airtightness of buildings. Test method” is published by the Norwegian Building Standard Council;
- In the US: in 1981, the standard ASTM E779-81 “Standard practice for measuring airleakage by the fan pressurization method” was published to ensure the uniformity of the pressurization test method, to be able to evaluate airleakage rates through buildings envelope. This standard was intended for one-story buildings [50];
- In 1983, the Canadian General Standard Board published the “Determination of the equivalent leakage area of building by the fan depressurization method” which applied to small detached buildings. This standard limited the method to depressurization tests.

Whereas each of these four standards described a method for a fan pressurization test, some significant differences existed [49]. Those differences are given in Table 3-1.

Table 3-1: Main differences between the 4 standards regarding fan pressurization tests in 1984 [49]

<b>Standard Requirements</b>	<b>Swedish standard SS 02 15 51 (1980)</b>	<b>Norway standard NS 8200 (1981)</b>	<b>American standard ASTM E779-81 (1981)</b>	<b>Canadian standard (1983)</b>
<i>External pressure measurement</i>	measured in a single-point placed 10 m from the building		no clear specification, but a single-point pressure tap in a door seemed sufficient	to be averaged from 4 taps pressure placed around the building
<i>Building preparation</i>	sealing of ventilation components	sealing of ventilation components and plumbing installations	-	very detailed sealing requirements
<i>Results: indicator</i>	airleakage at 50 Pa = average at -50 Pa (depressurization) and at +50 Pa (pressurization)	airleakage at 50 Pa = average at [-45 Pa; -50 Pa; -55 Pa] (depressurization) and at [+45 Pa; +50 Pa; +55 Pa] (pressurization)	-	method to calculate the equivalent leakage area at 10 Pa
<i>Flow rate precision</i>	± 6 %	± 6 %	± 6 %	± 5 %
<i>Pressure precision</i>	± 2.5 Pa	± 2 Pa	± 2.5 Pa	± 2 Pa

<i>Temperature precision</i>	-	-	$\pm 0.5\text{ }^{\circ}\text{C}$	$\pm 1\text{ }^{\circ}\text{C}$
<i>Overall precision</i>	$< \pm 8\%$	$\pm 8\%$	$< \pm 10\%$	-
<i>Pressure range</i>	0 to $\pm 55\text{ Pa}$	0 to $\pm 55\text{ Pa}$	0 to $\pm 75\text{ Pa}$	0 to $-50\text{ Pa}$
<i>Climatic limits: wind speed</i>	$< 10\text{ m.s}^{-1}$	$< 6\text{ m.s}^{-1}$	$< 4.4\text{ m.s}^{-1*}$	$< 5.5\text{ m.s}^{-1}$
<i>Climatic limits: indoor-outdoor temperature difference</i>	-	-	-	$< 11\text{ }^{\circ}\text{C}$

\*the US standard defined “ideal wind conditions” when the wind velocity is below 5 mph (2.2 m s<sup>-1</sup>), and recommended for measurements to be performed “with caution” if the wind velocity was from 5 mph to 10 mph (2.2, to 4.4 m s<sup>-1</sup>).

#### 3.1.4.2 Fan pressurization test methods in the 2010s

Three methods based on the pressurization test principle have been tested and studied in the 2010s [20,51,52]. For the three of them, the same power-law relation (given by equation (1)) is used:

- the one-point test method: this method consists in imposing a single pressure difference  $\Delta p$  and measuring the corresponding airflow rate  $q$ . In this method, we consider a default-value for the flow exponent  $n$ . Thus, we determine the  $C$  value according to equation (1). From this  $C$  value and the  $n$  default-value, we can calculate an airflow rate  $q$  for any pressure difference reference  $\Delta p_{\text{ref}}$ ;
- the two-point test method: this method consists in imposing a two pressure difference  $\Delta p_1$  and  $\Delta p_2$ : one at low pressure and the second one at high pressure, and measuring the corresponding airflow rates  $q_1$  and  $q_2$ . From those two points, we can draw the curve  $\ln(q) = C + n \cdot \ln(\Delta p)$  and thus determine  $C$  and  $n$  values. From those values, we can calculate an airflow rate  $q$  for any pressure difference reference  $\Delta p_{\text{ref}}$ ;
- the multi-point test method: this method consists in imposing several pressure differences (usually at least 5) and measuring the associated airflow rates. Then, we determine the values of  $C$  and  $n$  from a regression analysis applied to  $\ln(q)$  and  $\ln(\Delta p)$ . From those values, we can calculate an airflow rate  $Q$  for any pressure difference reference  $\Delta p_{\text{ref}}$ .

#### 3.1.4.3 Currently used fan pressurization standards and reference documents

In 2020, two major standards regarding fan pressurization method for determining building airleakage are commonly used:

- in the US: ASTM 779-19 “Standard test method for determining airleakage rate by fan pressurization” [12] which has replaced the ASTM E779-81;
- in Europe and Asia: ISO 9972 (2015) “Thermal performance building – Determination of air permeability of buildings – Fan pressurization method” [11].

Both of these standards describe a fan pressurization multi-point test method to characterize airleakage of building envelope. Table 3-2 compares these two methods.

Table 3-2: ASTM 779-10 and ISO 9972 requirements

	<b>ASTM 779-19</b>	<b>ISO 9972</b>
<b>Scope: buildings</b>	<ul style="list-style-type: none"> <li>- Single-zone buildings</li> <li>- Multi-zone buildings can be treated as single-zone buildings by opening interior doors or by inducing equal pressures in adjacent zones</li> </ul>	<ul style="list-style-type: none"> <li>- Buildings or part of buildings</li> <li>- Single-zone buildings</li> <li>- Multi-zone buildings can be treated as single-zone buildings by opening interior doors or by inducing equal pressures in adjacent zones</li> </ul>
<b>Weather conditions</b>	<p>Strong winds and large indoor-outdoor temperature differences shall be avoided</p> <ul style="list-style-type: none"> <li>- Temperature: product of the indoor/outdoor air temperature difference by the height of the building <math>\leq 200 \text{ m}^\circ\text{C}</math></li> </ul>	<p>Strong winds and large indoor-outdoor temperature differences are to be avoided</p> <ul style="list-style-type: none"> <li>- Temperature: <i>product of the indoor/outdoor air temperature difference by the height of the building <math>\leq 250 \text{ mK}</math></i></li> <li>- Wind: <ul style="list-style-type: none"> <li>- <i>wind speed near the ground <math>\leq 3 \text{ m}\cdot\text{s}^{-1}</math></i></li> <li>- <i>meteorological wind speed <math>\leq 6 \text{ m}\cdot\text{s}^{-1}</math> or <math>\leq 3</math> on the Beaufort scale</i></li> </ul> </li> </ul>
<b>Apparatus</b>	<ul style="list-style-type: none"> <li>- Pressure-measuring device: accuracy of <math>\pm 5\%</math> of the measured pressure or <math>0.25 \text{ Pa}</math>, whichever is greater</li> <li>- Airflow rate measuring device: accuracy of <math>\pm 5\%</math> of the measured flow</li> <li>- Temperature measuring device: accuracy of <math>\pm 1 \text{ }^\circ\text{C}</math></li> </ul>	<ul style="list-style-type: none"> <li>- Pressure-measuring device: accuracy of <math>\pm 1 \text{ Pa}</math> in the range of 0 to <math>100 \text{ Pa}</math></li> <li>- Airflow rate measuring device: accuracy of <math>\pm 7\%</math> of the reading</li> <li>- Temperature measuring device: accuracy of <math>\pm 0.5 \text{ K}</math></li> </ul> <p>Periodic calibration of the measurement system is required</p>
<b>Building preparation</b>	<ul style="list-style-type: none"> <li>- All interconnecting doors open + verification of the pressure homogeneity: pressure difference within the zone <math>\leq 10\%</math> of the measured indoor-outdoor pressure difference at the higher pressure used in the test (between highest ceiling elevation and lowest floor, and between the windward and leeward sides)</li> <li>- HVAC dampers and registers not adjusted, other dampers closed</li> </ul>	<ul style="list-style-type: none"> <li>- Completion of the envelope of the building or part of the building to be tested</li> <li>- All interconnecting doors open except if needed access doors to elevators or high-voltage cabins</li> <li>- 3 very detailed methods to described sealed/closed or open situation for: <ul style="list-style-type: none"> <li>- Ventilation openings</li> </ul> </li> </ul>

		<ul style="list-style-type: none"> <li>- Windows, doors, and trapdoors</li> <li>- Other openings</li> </ul>
<b>Method</b>	<ul style="list-style-type: none"> <li>- Pressurization and depressurization</li> <li>- Exterior pressure device across the building <i>at the bottom of the leeward side, average the pressures measured at multiple locations, avoiding exterior corners close to the middle of the exterior wall</i></li> </ul>	<ul style="list-style-type: none"> <li>- Pressurization or depressurization, <i>pressurization, and depressurization</i></li> <li>- <i>Indoor/outdoor pressure difference at the lowest floor level, one exterior pressure tap protected from the effects of dynamic pressure, some distance away from the building, not too close to other obstacle and not exposed to large temperature differences</i></li> </ul>
<b>Procedure</b>	<ul style="list-style-type: none"> <li>- Determine the elevation of the measurement site</li> <li>- Measure and record the indoor and outdoor temperatures at the beginning and the end of the test</li> <li>- Measure zero flow pressures with the fan openings blocked before and after the flow measurements, average at least a 10 s interval</li> <li>- Induced pressure from 10 to 60 Pa (if not possible substitute a partial range with at least 5 data points) with increments of 5 to 10 Pa, averaged over at least 10 s</li> </ul>	<ul style="list-style-type: none"> <li>- Measure and record the indoor and outdoor temperatures before, during and after the test</li> <li>- Measure zero flow pressures with the fan openings covered before and after the flow measurements, over at least a 30 s interval with minimum 10 values – Calculate the average of all values, average of positive values and average of negative values</li> <li>- Test not valid if one zero flow pressures average (in absolute) <math>\geq 5</math> Pa</li> <li>- Induced pressure from <math>\geq \max \{10 \text{ Pa}; 5 \cdot \Delta P_0\}</math> to at least 50 Pa, <i>100 Pa recommended</i> (if not possible reach at least 25 Pa) with increments of no more than 10 Pa</li> </ul>
<b>Data analysis</b>	<ul style="list-style-type: none"> <li>- Convert reading airflow rates to air flows through the building envelope  <math>Q = Q * \frac{\rho_{in}}{\rho_{out}}</math> or <math>Q = Q * \frac{\rho_{out}}{\rho_{in}}</math></li> <li>- Subtract zero flow pressures from the test pressures</li> <li>- Plot Q against the corresponding <math>\Delta P</math> on a log-log plot</li> <li>- Determine C and n using an unweighted log-linearized linear regression technique separately for pressurization and depressurization</li> <li>- Test not valid if <math>n &lt; 0.5</math> or <math>&gt; 1</math></li> <li>- Calculate C and n confidence intervals</li> <li>- Correct the C coefficient to standard conditions:  <math display="block">C_0 = C * \left(\frac{\mu}{\mu_0}\right)^{2n-1} * \left(\frac{\rho}{\rho_0}\right)^{1-n}</math></li> </ul>	<ul style="list-style-type: none"> <li>- Convert reading airflow rates to air flows through the building envelope  <math>Q = Q * \frac{\rho_{in}}{\rho_{out}} \approx Q * \frac{T_{out}}{T_{in}}</math> or <math>Q = Q * \frac{\rho_{out}}{\rho_{in}} \approx Q * \frac{T_{in}}{T_{out}}</math></li> <li>- Subtract zero flow pressures from the test pressures</li> <li>- Plot Q against the corresponding <math>\Delta P</math> on a log-log plot</li> <li>- Determine C and n using a least-squares technique separately for pressurization and depressurization, and calculate the coefficient of correlation <math>r^2</math></li> <li>- Test not valid if <math>n &lt; 0.5</math> or <math>&gt; 1</math> or if <math>r^2 &lt; 0.98</math></li> <li>- Calculate C and n confidence intervals,</li> <li>- Correct the C coefficient to standard conditions:  <math display="block">C_0 = C * \left(\frac{\rho}{\rho_0}\right)^{1-n} \approx C * \left(\frac{T_0}{T}\right)^{1-n}</math></li> </ul>

*in italic: recommendations*

Other methods exist and are used in some specific fields or some regions of different countries. The American standard ASTM E3158-18 provides a method to determine the airtightness of building envelopes or portions thereof by measuring the airleakage rate at specified reference pressure differentials for large and multi-family dwellings [53]. The US Army Corp of Engineers has its own test protocol since 2010 [54]. This standard is used to verify that all new Army buildings meet a specific airtightness requirement. The result of the test should be under 0.3 cfm/square foot at 75 Pa. To calculate this indicator, all 6 sides of the building are used to calculate the surface area in square feet, including floors that are in contact with the ground. This standard is used by other branches of the US military. The Air Barrier Association of America (ABAA) proposes a test method to assess that a building complies with a target airtightness level, and gives additional requirements and recommendations regarding large buildings. It is currently into a process to become an ASTM standard [55]. Finally, the International Code Council published in 2016 a standard [56]. This standard was designed mostly with single-family detached houses in mind but is also being used for multi-family buildings. A draft of recommended changes to be used for multifamily buildings is being worked. In Japan, measurements can be performed according to the JIS A2201-20003 standard [57].

### *3.1.5 Objectives and approach of the literature review analysis*

While alternative methods exist, such as the AC pressurization technique [58] and the pulse pressurization technique [59], this chapter focuses on fan pressurization methods, as they account for most of the airtightness measurements performed nowadays.

The purpose of this chapter is to identify and to quantify the key sources of uncertainty in a building fan pressurization test to prioritize research efforts to better understand and reduce uncertainties in such tests. This entails the following objectives:

- identify sources of uncertainties analyzed in the literature;
- identify methods to quantify their influence on the uncertainty in the pressurization test result;
- evaluate the barriers and gaps in research either to reduce or to characterize this uncertainty.

In addition, a specific desired outcome of this review is to clarify a map of uncertainty sources in building pressurization tests.

The approach to achieve this goal is mostly based on a literature review and interviews with experts. Over 39 papers dealing with uncertainties in building pressurization tests were selected and analyzed.

Table 3-3 categorizes these papers according to key topics addressed relevant to our review questions.

Table 3-3: Studies analyzed in this chapter according to topics relevant for this review

Topics of the study investigated in this paper	References
Regulations and Tester's scheme	[60,61]
Development of tests	[3,25,31,41,44–48]
Standards and guides	[2,11,12,29,62–64]
Alternative methods	[58,59]
Uncertainty of fan pressurization test	[20,28,31,48,49,51,52,65–96]

The international Guide to the Expression of Uncertainty in Measurement (GUM) [62] proposes definitions and methods relating to measurement uncertainty evaluation which are considered as references by metrology experts. According to the GUM, “*the measurement uncertainty, associated with the measurement result, characterizes the dispersion of the values that could reasonably be attributed to the measurand.*” A second concept explained by the GUM is the measurement error, which has two components: a systematic component, which can be reduced by the application of a correction, and a random component, which can be reduced with multiple measurements.

The GUM lists several sources of uncertainty in a measurement, including “*inadequate knowledge of the effects of environmental conditions on the measurement or imperfect measurement of environmental conditions*” and “*approximations and assumptions incorporated in the measurement method and procedure*”. In 1984, Persily and Grot [69] classified the sources of uncertainties for a fan pressurization test into two different families: the sources due to the test conditions (including the weather and the building’s leakages) and the sources related to the measurements performed to determine airflow rates and pressure differences (including device selection and calibration). Sherman and Palmiter [70] identified three categories of error that can impact the uncertainty of an airtightness measurement: precision errors, biases, and extrapolation errors. In 2012, Carrié and Wouters [71] proposed another classification with 5 families of sources: 1) building preparation; 2) reference values; 3) sampling assumptions; 4) device uncertainty and software errors; 5) wind and stack effect, reference pressure, data collection protocol, and analysis method. The literature provides neither an exhaustive list of errors nor a standard classification of these errors. Sections 3 and 4 below focus on multiple specific sources of uncertainty classified into two families: the uncertainties due to intrinsic model assumptions (paragraph 3.2) and uncertainties due to measuring equipment, protocol, and analysis (paragraph 3.3). Each section summarizes a review of the present knowledge, including how these sources affect the hypotheses of an ideal pressurization test, and the test results when available. Where knowledge was insufficient to quantify and deal efficiently with a specific issue, priority research efforts in specific areas are suggested.

### 3.2 Uncertainties due to intrinsic model assumptions

In this part, the impact of the model used when performing a fan pressurization measurement is discussed. First, paragraph 3.2.1 focuses on the variability of the indoor-outdoor pressure difference. In paragraph 3.2.2, the choice of the flow equation to

characterize the link between the airflow rate and the pressure difference is discussed. Finally, paragraph 3.2.3 is dedicated to the correction applied to measured pressure differences regarding the zero-flow pressure value as indicated by standards.

### 3.2.1 Variability of the indoor-outdoor pressure difference

The fan pressurization technique is based on the measurement of the indoor-outdoor pressure difference. Questions have been raised regarding the impact of the location and the nature of the taps used to perform this measurement, especially regarding the effects of wind for the external tap, and the homogeneity of the internal volume for the internal tap.

During an airtightness measurement, each measured airflow rate corresponds to one pressure difference between the inside and the outside, measured at a specific location. This location remains the same during the whole test. This pressure difference needs to be as stable as possible in order to apply equation (1) simply. The impact of the weather on the pressure difference measurement, namely the impact of wind and stack effects, therefore needs to be avoided.

For the internal tap, two requirements exist in standards ISO 9972 and ASTM 779-19. ISO 9972 requires that the tap shall not be influenced by the pressurization device. As for ASTM 779-19, it defines a single zone as “*a space in which the pressure differences between any two places differ by no more than 5% of the inside to outside pressure difference*”. Nevertheless, it specifies that for a pressurization test, “*all interconnecting doors in the conditioned space shall be open such that a uniform pressure shall be maintained within the conditioned space to within 10% of the measured inside/outside pressure difference*”. The ASTM requirement regarding pressure homogeneity is therefore less strict than its definition of a single zone. ISO 9972 is less demanding: it only mentions as a *good practice* for tall buildings to measure internal pressure on both the lowest floor and the top floor. However, none of the standards gives guidance to deal with stack effect due to tubing deployed at an uneven altitude between the tubing ends and the differential pressure sensors. Note that a difference of altitude between the external tap and the internal tap induces an additional pressure difference that is not corrected.

For the external tap, ISO 9972 recommends protecting the tap from the effects of dynamic pressure, especially in windy conditions. ASTM 779-19 recommends, when possible, locating the pressure tap at the bottom of the leeward wall. In 1990, Modera and Wilson [73] tested averaging the result given by 4 pressure probes on a single-family house on which continuous measurements were performed. The measurement results were estimated using the ELA (Effective Leakage Area) index. The scatter of ELA values at 4 Pa remained below 11% for wind speeds lower than 5 m.s<sup>-1</sup>. This measurement scatter was compared to measurement scatter from another campaign in which measurements were made according to the Canadian standard requirements without the spatial-averaging and time-averaging used by Modera and Wilson. The scatter obtained with the new technique was half the scatter obtained with the Canadian standard requirement. In contrast, in 2013, Brennan et al. [72] found from a repeatability campaign that any

location of the external tap on the leeward side of the building was the best configuration (better than averaging one tap on each facade). In 2019, Delmotte [93] proposed an explanation of the physics that apply on-field during a pressure measurement, particularly regarding the impact of the wind. He gives recommendations regarding the location (away from the building and any obstacle) and the nature of the pressure tap (T-pieces for example). In 2019 also, Novak [87] studied the impact of the location of the external pressure tap from 9 tests performed on the same building. He noticed no significant impact of the location but all tests were performed at low wind speed.

Overall, this review on this topic shows that there is no consensus on the location of the pressure taps to reduce the impact of wind and stack effects on the uncertainty of the measurement result. While avoiding the dynamic effect of the wind seems to be a common objective among professionals and scientists, no method has been clearly adopted. Some field studies put forward spatial averaging of different external taps, whereas other field data support a unique tap on the leeward side of the building. Note that the error due to dynamic pressure greatly depends on the building characteristics (especially the pressure coefficient of the facade depending on the exposure) and the wind conditions (speed, direction, and fluctuations). This could explain these diverging conclusions.

### 3.2.2 *Flow equation*

The pressurization test method is based on the assumption that the leakage airflow rate is a function of the pressure difference between inside and outside the envelope. This section discusses the impact of using the model regarding:

- the choice of a power-law equation versus a quadratic equation;
- the variation of the leakage coefficient C;
- the variation of the airflow exponent n.

#### 3.2.2.1 *Power-law versus quadratic*

In 1978, Nevander and Kronvall [41] presented the testing methods defined by a group in charge of coordinating research regarding building airtightness in Sweden. They described the relation between airflow through buildings and pressure differences as a power-law relation (equation (1)). In 1980, Sherman and Grimsrud [42] explained that:

- at very low pressure, as the flow is dominated by viscous forces, the flow is expected to be proportional to the pressure difference;
- at high pressure, as the flow is dominated by inertial forces, the flow is expected to be proportional to the square root of the pressure difference.

From field measurements on buildings, Sherman and Grimsrud observed that the leakage airflow behaves similarly to turbulent flow: they therefore used a square-root relation in their model. In 1984, Etheridge [48] questioned the power-law relation and introduced a quadratic relation (equation (2)), which was already used for the characterization of components such as doors and windows. The mathematical formulation of the quadratic law is as follows:

$$aq^2 + bq = \Delta p \quad (2)$$

where

- $a$  [ $\text{Pa h}^2 \text{ m}^{-6}$ ] and  $b$  [ $\text{Pa h m}^{-3}$ ] are constants
- $q$  is the volume flow rate [ $\text{m}^3 \text{ h}^{-1}$ ]
- $\Delta p$  is the indoor-outdoor pressure difference [Pa].

Etheridge demonstrated that the power-law equation was more appropriate when all leaks in the buildings followed a power-law relation; and on the contrary, that a quadratic relation was more appropriate when all leaks followed a quadratic relation. He also concluded that whereas both approaches gave similar results at high pressure, low-pressure results could be very different. He recommended that the coefficients of both relations should be calculated and quoted in pressurization test results.

In 1992, Sherman [79] demonstrated that the airflow through short circular pipes could be described using the power-law relation given in equation (1). He explained that the application of this relation for building airtightness characterization assumed that all envelope leaks could be described as one unique circular leak. In 1998, Walker et al. discussed the choice of a better representation of the flow through building envelopes from field and laboratory measurements [74]. They concluded that the power-law relation was better for all of the configurations they tested in the field (on one house) and in a laboratory: with small cracks only, with both small cracks and large holes and for furnace flues. At the same time, Etheridge [75] kept defending the quadratic equation that he considered no harder to use and more practically adapted for fan pressurization tests. Later, Chiu and Etheridge performed CFD calculations to compare both methods on two models of cracks [76]. They evaluated the errors in infiltration prediction for the cracks they considered were two to three times larger with the power-law relation than with the quadratic equation at low pressure (between 4 and 10 Pa). More recently, Baracu et al. proposed a new relation: an extended power-law relation [77]. This relation is meant to better take into account the regime and the nature of the flow. According to experimental tests they performed on a passive house and numerical calculations, the extended power-law seems to be more accurate, but is still not suitable on site for large scale tests.

In all, the debate between power-law equation supporters and quadratic equation defenders is still active. Nevertheless, the power-law equation remains the relation used by airtightness testers. For this reason, the following paragraphs focus only on power-law based methods.

### 3.2.2.2 Variation of the leakage coefficient $C$

From equation (1), it might be thought that the leakage coefficient  $C$  is a constant, but it is not.

First of all, the leakage coefficient  $C$  depends on the geometry of the orifices; more specifically the behavior of components such as valves or seals. The behavior of these components changes according to the magnitude and the direction of the pressure difference. While ISO 9972 recommends performing one set of measurements under depressurization and one set under pressurization, only one set is mandatory. This implicitly assumes that the behavior of the building envelope can be characterized by

measuring the airflow through leaks in only one direction, whereas the direction may change in real conditions depending on wind and temperature. Conversely, ASTM 779-19 requires that data should be collected both from pressurization and depressurization. This appears more relevant since from 10 tests performed in repeatability conditions on a test house, Delmotte and Laverge [52] observed a significant difference between pressurization results and depressurization results: for the particular house tested in this study, all leakage airflow rates measured under depressurization are lower than airflow rates under pressurization. This suggests that the ventilation behavior of the building they tested was different under pressurization and under depressurization.

Secondly, for a fan pressurization test performed according to standards, the airleakage coefficient  $C$  needs to be corrected to take into account the impact of real conditions. In 2014, Carrié [78] determined the corrections that should be applied to the power-law coefficient  $C$  to take into account temperature and pressure conditions. These corrections stem firstly from differences between the conditions at the measuring device and the conditions at the leak, and secondly from differences between the real conditions and the reference conditions. According to his analysis, the  $C$  value depends on air viscosity, air density, and the flow exponent  $n$ . The correction in ASTM 779-19 includes the impact due to viscosity and density variations, but the correction in ISO 9972 is incomplete: it does not include the viscosity correction. The impact of the correction greatly depends on atmospheric pressure. However, since it is easy to include in a measurement analysis, Carrié recommends applying this correction fully and systematically.

In all, the literature shows that the magnitude and direction of airflow, as well as temperature and pressure conditions can significantly affect the leakage flow coefficient. Information is also available to either reduce or correct the impacts of these parameters on the measurement result.

### *3.2.2.3 Variation of the airflow exponent $n$*

For the multi-point test method described in ISO 9972 and ASTM 779-19, the method consists in evaluating one value for the leakage coefficient  $C$  and one value for the flow exponent  $n$  from pressure steps from 10 to 100 Pa. The test method assumes that the leaks are stable over the measurement period and that the  $n$  value is constant for all pressure differences applied during the test.

As the result can be extrapolated at several pressure differences including 4 Pa, the test method assumes that the  $n$  value is constant at an extrapolated pressure difference much lower than the test pressure stations. In such cases, the flow exponent may be poorly determined because of the extrapolation itself. This topic is discussed in section 3.3.4.

Another source of error linked to the flow exponent  $n$  lies in its variations with pressure. This subject has been investigated by Sherman in the specific context of laminar flow in short pipes [79]. If  $n$  were constant, the power-law relation (equation (1)) would be absolute. Unfortunately,  $n$  depends on the pressure difference: therefore, this relation is a simplified model of the physical phenomena and may be responsible for errors.

This simplification was investigated in 2013 by Walker et al. [20] by evaluating the error due to a fixed exponent  $n$  for a one-point test method using a dataset of results of

pressurization tests performed on six test houses from the Alberta Home Heating Research Facility in Canada. The one-point test method involves performing only one airflow rate measurement around 50 Pa and considering a default value for the flow exponent  $n$ , here 0.65. The coefficient  $C$  is calculated from the one-point measurement results and a  $q_4$  or a  $q_{50}$  can be calculated from this  $C$ -value and the  $n$ -fixed-value. To evaluate the accuracy of this method and to compare it to the accuracy of the multi-point test technique, Walker et al. analyzed 6007 tests performed on the 6 test houses in 97 configurations regarding open and closed flues, windows, and passive vents, in pressurization and depressurization. They evaluated first the variability of the exponent  $n$  due only to envelope behavior: they considered only 301 tests for which the wind speed during the test was below  $1.5 \text{ m s}^{-1}$ . They evaluated that the standard deviation due to envelope behavior was 0.063. Then, they evaluated the global variability of the  $n$  due to wind and envelope behavior by analyzing all measurements: the standard deviation was then 0.073. They concluded that the majority of the standard deviation for all tests is due to changes in the envelope behavior. Secondly, they evaluated the error due to the variability of the exponent  $n$  for a one-point test with a fixed value of  $n$ . They estimated that fixing the  $n$ -value at 0.065 might induce an error between 15% and 21%. Nevertheless, note that the relative impact of the interpolation or extrapolation versus that of the pressure-dependence of the flow exponent is unclear in this study. A significant fraction of the standard deviation given by Walker and collaborators may stem from the statistical analysis beyond the pressure-dependence issue.

In summary of this topic, by construction equation (1) does not account for the variability of the flow exponent  $n$ , but several authors suggest that this approximation might induce a significant error.

### *3.2.3 Zero-flow pressure correction and measurement*

#### *3.2.3.1 A correction to eliminate the impact of wind*

During each step of the pressure difference sequence, the pressure difference between the inside of the envelope and the outside is measured. This pressure difference is due to the pressure applied by the pressurization device but also includes the natural pressure difference due to the wind and the stack effect. Wind and temperature conditions influence building airtightness measurement results because they affect the pressure difference seen by the leaks of the building envelope. As the duration of a pressurization test is around 10 minutes, the temporal variation of the temperature is most of the time too slow to have an impact on the result. On the contrary, the temporal variations of the wind may be fast enough to generate errors.

The pressurization test method requires that the pressure differences used to calculate leakage airflow rates are corrected by subtracting the natural pressure difference. This natural pressure difference is evaluated from two zero-flow pressure measurements: one performed before the pressure difference sequence and another after the sequence. ISO 9972 requires that the zero-flow pressure is measured for at least 30 seconds (with a minimum of 10 values) and ASTM 779-19 requires a 10-second interval. The average of

the results of these two measurements is used to correct the pressure difference measured during the sequence. Equation (1) is then corrected as indicated in equation (3), where  $\Delta p_0$  is the average indoor-outdoor pressure difference before and after the pressure sequence [Pa].

$$q = C * (\Delta p - \Delta p_0)^n \quad (3)$$

Etheridge and Sandberg [80] introduced this correction in 1996: they compared 2 theoretical curves of airflow rate depending on the pressure difference: one with neither wind nor temperature difference, and another with these two quantities non-zero. They calculated that the displacement due to weather conditions is constant: it should therefore be included in the equation to correct the result and eliminate the impact of the weather. It can be shown that the zero-flow pressure correction using equation (3) is strictly true for a network of parallel leaks, each with a flow exponent of 1. Nevertheless, this is only an approximation when the flow exponent differs from 1. Using equation (3) as per ISO 9972 or ASTM 779-19 also implicitly assumes that the two series of 30 seconds – or 10 seconds – are representative of the natural pressure fluctuations during the test that lasts around 10 min.

The relevance of this correction with equation (3) has been studied by Carrié and Leprince [51] in steady wind and isothermal conditions. They applied the zero-flow pressure correction and obtained significant errors due to wind: 12% for wind speeds up to  $10 \text{ m s}^{-1}$  at 50 Pa and 60% at 10 Pa. In other words, the zero-flow correction did not eliminate the impact of the wind. Later, Carrié and Mélois [94] modelled fan pressurization tests with a periodic wind. They also applied the zero-flow pressure correction, but they confirmed that this correction did not eliminate the impact of the wind on the measurement result. The pressure differences induced by wind and stack vary spatially because of the variability of the spatial distribution of the wind pressures on facades; they also vary with time because of the time-dependence of the wind speed and direction as well as air temperatures. However, by construction equation (1) does not account for these effects of spatial and time variations on the pressure seen by the leaks: it assumes that the effect of the pressures seen by the leaks on the leakage airflow rate can be viewed as a single pressure difference exerted on all leaks. Carrié and Mélois [94] suggested further research to contain the uncertainty due to fluctuations of the pressure signals. They mentioned using signal processing techniques to cross-analyze the wind spectrum and the measured values during the zero-flow pressure measurement to identify possible indicators that may determine the optimal duration of the measurement.

Overall, correcting equation (1) to account for the zero-flow pressure as done in equation (3) is convenient because it is simple and consistent when the flow measured through the blower door is zero; however, two uncertainty components stem from the zero-flow pressure correction: 1) the component due to the correction model itself, and 2) the component due to the estimation of the zero-flow pressure. The literature appears insufficient to be able to quantify these components in a practical manner for a general case.

### 3.2.3.2 Evaluation of the zero-flow pressure

In addition to the accuracy of the zero-flow pressure correction, the measurement of the zero-flow pressure itself has been investigated. In 2017, Delmotte [81] studied the impact of the assumption of a constant zero-flow pressure difference on test uncertainty. He proposed a method to take into account the variability of the zero-flow pressure into the evaluation of the combined standard uncertainty of the induced pressure difference. He demonstrated that incorrect values for zero-flow pressure difference could lead to an error in the C and n values. Prignon et al. [82] went further on the quantification of the uncertainties in zero-flow and envelope pressures, using the experimental data from 31 tests performed on one building. They showed that the uncertainty on the zero-flow pressure measurement could significantly increase the uncertainty in pressure measurements, and thus questioned the use of an ordinary least-square method. Nevertheless, this study did not confirm the better results obtained by Delmotte [81] with a bi-linear distribution of the zero-flow pressure values to correct the pressure measurements.

Prignon et al. reinforced their study with tests performed on 30 different buildings [95]. They conducted a statistical analysis to find variables with the most significant impact on the uncertainty on the pressure measurement due to the uncertainty of the zero-flow pressure. This analysis showed that increasing the duration of the zero-flow pressure measurement lead to reducing the uncertainty due to zero-flow pressure approximation. The authors gave the limitations of their work, mainly due to the size of their building sample and the need for field data to validate the model they created.

Based on numerical analyses on an idealized building, Carrié and Mélois [94] have shown that wind frequency was an important parameter to be considered in order to correctly assess the zero-flow pressure. This seems logical because if the sampling time is smaller than the period of the variations, the measurement will capture only one part of the change in the signal.

## 3.3 Uncertainties due to measuring protocol, equipment, and analysis

### 3.3.1 Building preparation

Performing a fan pressurization test requires specific work to prepare the building that includes installing the pressurization devices and closing and/or sealing components such as ventilation openings, fire-guards, smoke-guards, and letter boxes. How the building is prepared depends on the purpose of the test. For example, if the test aims at characterizing the envelope with its unintentional openings only, intentional natural ventilation inlets/outlets have to be sealed. Conversely, they would not be closed if the intention is to characterize the permeability due to all openings. This is the reason why three methods of preparation are defined in ISO 9972.

Leprince and Carrié compared the building preparation rules for 11 European countries from a questionnaire addressed to national representatives of airtightness testers [28]. They showed that most of the countries included specific requirements that might have a

significant impact on the measurement result. Any comparison from one country to another should therefore be performed with caution.

In 2010, Rolfsmeier et al. [83] studied the difference between tests performed by 17 testers on the same building. The error on the test result varied from 7% to 63% when there was no specific attention to prepare the building, whereas it stayed below 6% when the building was correctly prepared. Of course, for a specific measurement, the error is probably strongly dependent on building characteristics and applicable rules. Nevertheless, this study demonstrates that significant errors can be attributed to building preparation even when the testers apply the same rules.

### *3.3.2 Sampling procedure*

For large buildings such as multi-family dwellings, ISO 9972 offers the possibility to evaluate building airtightness by performing a pressurization test on only a part of the building. In Europe, different sampling methods are based on the total number of apartments or the total envelope area [84]. Performing a test by sampling implicitly means that the results obtained on the building parts are representative of the building as a whole and can be used to assign an airtightness rating for the whole building. Nevertheless, three parameters will impact the representativeness of the building parts. First of all, when the sampling procedure concerns a group of apartments with identical design, there are often differences from one apartment to another during the construction phase. These may be due, for example, to a change of construction companies, a change of workers, a change of material, or a change of internal partitioning required by the owner. All these changes may have an impact on the envelope airtightness. Secondly, a group of apartments may be considered as being similar but not identically designed: the number of rooms, the surface area of the windows and the wall surface area may change from one apartment to another. Representative sampling might therefore be difficult to achieve in this case. In turn, this might generate uncertainties on the results attributed to all apartments. Thirdly, when the sampling represents a part of one building, isolating this part completely might not be possible and the resulting ventilation behavior might not be representative of the whole building.

Moujalled et al. evaluated the impact of different sampling methods for 10 multi-family dwellings [85]. They measured the airtightness of each apartment. They also performed a measurement of the common areas and a global measurement of the whole building. They tested 3 different sampling methods. Their analyses showed that the sampling method gave results similar to the whole building measurement result only when all apartments presented uniform airtightness performance. They also showed that a leakage in the common areas could have a significant impact on air permeability of the whole building when they included the lift shaft and basement parking. Novak [86] conducted a similar study to test the sampling rules applying in the Czech Republic on one multi-family building. He showed that measuring only apartments could not lead to a correct estimation of the airtightness of the whole building because of the leakages between apartments and in the common parts of the building.

In turn, it appears that a sampling method to estimate the overall airtightness of a large building is often necessary for practical and financial reasons. However, none of the studies quoted above gives any guidance to help estimate the uncertainty induced by the sampling method, although their results show that this may be very significant.

### 3.3.3 *Pressure measurement and airflow measurement uncertainties*

During a fan pressurization test, two measurements are performed at the same time: an internal-external pressure difference measurement and an airflow measurement through the pressurization device (the fan). The uncertainties due to these measuring instruments must obviously be considered.

In 1984, Persily focused on errors due to calibration [88]. To ensure sufficient fan capacity, most blower doors measure airflow rates using a calibration formula to relate airflow rates to fan speed and pressure difference. The calibration formula depends on air density, which varies with pressure difference, temperature, and humidity. He calculated that the difference between the calibration conditions and the test conditions regarding temperature and pressure difference could induce differences of up to 10% on air density. In 1991, Murphy et al. investigated the reproducibility and the repeatability of pressurization measurement from a series of measurements performed on four houses according to the method described in the ASTM standard [65]. Three operators performed 144 tests with four blower doors. Before each test, the blower door was completely disassembled. To maintain repeatable conditions, wind velocity and direction were measured and tests were performed only for wind velocity lower than  $2.24 \text{ m s}^{-1}$  (5 mph). To evaluate the repeatability of the tests, Murphy et al. compared the airflow-pressure curves obtained on the same house by the same operator. For each operator, the curves intersected a nearly identical point at high-pressure, but they differed by 20% at 4 Pa. The same tendency was observed for reproducibility: 7.5% at 50 Pa and 23.5% at 4 Pa. The bulk of these errors was attributed to the measuring devices.

In 1994, Sherman and Palmiter [70] estimated the global uncertainty of an airtightness measurement from calculations considering different sources. They first considered a systematic error equal to 2.5 Pa for pressure measurement that may be due to non-linearities in the gauge, calibration errors, hysteresis, and sticking problems. They also considered a bias error of 5%. For the airflow estimations, as these are usually performed from pressure drop measurements across a calibrated plate, they considered both bias error and precision error equal to 5%, to take into account the error relating to the determination of the plate properties. With this, they evaluated the overall uncertainty of an airtightness measurement by performing an error propagation analysis. At 50 Pa, the uncertainty due to measuring device uncertainties was estimated to be around 7%, whereas it reached 40% at 4 Pa. Carrié and Leprince [51] also considered bias and precision errors for both airflow measurement (95% confidence interval = 2% for precision error and 4% for bias error) and pressure measurement (95% confidence interval = 0.5% for precision error and 0.15% for bias error). For both a one-point test and a 2-point test, the combined uncertainty for no wind at 50 Pa was around 5%. This estimate included only uncertainties due to measuring instruments.

Therefore, although measurement techniques and data acquisition techniques have developed considerably between 1984 and 2016, the drop in the uncertainty contribution of the measurement devices appears modest on the strength of the studies mentioned above. Clearly, this cannot be neglected in an uncertainty analysis. Fortunately, this contribution can be assessed using standard uncertainty analysis techniques extensively described in the GUM [62].

To contain those instrument errors, note that both ISO 9972 and ASTM 779-19 include requirements regarding measuring device uncertainty. For pressure difference instruments, standard ISO 9972 requires an accuracy of 1 Pa on the range [0-100 Pa] while ASTM 779-19 requires an accuracy of 5% or 0.25 Pa, whichever is the greater. Regarding airflow measurement, ISO 9972 requires an accuracy of 7% while ASTM 779-19 requires an accuracy of 5%.

Nevertheless, another subject of concern is the quality of the calibration. It seems that this is hardly ever analyzed and yet it might induce significant uncertainty. In 2019, Leprince et al. [92] analyzed the quality of the calibration performed on fans of various blower doors. They found that some laboratories had a low measurement capability index, which could give a large degree of uncertainty for the calibration result. Requirements regarding measurement calibration should therefore include requirements regarding either the quality of the calibration or the method used to include the uncertainty of the calibration itself in the total uncertainty estimation. Otherwise, the calibration might lead to significant errors due to the measuring device.

#### *3.3.4 Regression analysis methods*

When all data from measurements are collected, the airtightness of the building envelope is determined from a mathematical model. While ASTM requires the use of an unweighted linear regression technique to estimate the leakage coefficient  $C$  and the airflow exponent  $n$ , ISO 9972 requires only a least squares method. In addition, ISO 9972 includes an informative annex that recommends using an ordinary (unweighted) least squares method and provides all the equations for estimating  $C$ ,  $n$ , and uncertainties. This technique is therefore widely used in practice.

In 2011, Delmotte and Laverge conducted a pressurization test campaign to evaluate the repeatability and the reproducibility of the test protocol with the currently used manufactured blower doors under low wind speed conditions [52]. They first performed 10 tests on one house under repeatability conditions, in terms of both pressurization and depressurization, with 10 pressure stations from 10 to 100 Pa. They calculated the standard deviations of three extrapolated airflow rates at 4, 50, and 100 Pa. For both depressurization and pressurization, the scatter was greatest at 4 Pa, with a standard deviation of 5.2% and 5.1% respectively. It decreased at higher pressure: 2.0% and 1.2% at 50 Pa, and 1.7% and 1.4% at 100 Pa. Delmotte and Laverge identified two main causes: variations due to weather at low pressure, and errors due to the non-weighted regression which were maximal at the lowest and the highest pressures.

Delmotte and Laverge proposed new calculations using weighted regression. These calculations led to lower standard deviations at low pressure and no significant change at

high pressure. Ten other pressurization tests were performed on the same house by 10 different laboratories, under reproducibility conditions. Similar tendencies were observed. For both depressurization and pressurization, the scatter was greatest at 4 Pa, with a standard deviation respectively 7.9% and 11.1%. It decreased at higher pressure: 2.5% and 2.9% at 50 Pa; 2.9% and 3.2% at 100 Pa.

Note that in 1994, Sherman and Palmiter [70] already questioned the use of an unweighted regression analysis highlighting the fact that this method assumes that uncertainties on pressure difference are negligible, which is not correct. At that time, they already recommended performing a weighted analysis.

In 2012, Okuyama and Onishi [96] explained that a weighted method should be used to take into account possible sudden changes from one measurement point to another, and so attribute a small weighting to measured values with a large error. They compared the results obtained from two different weighted methods (by residuals and by measurement uncertainty) to the results obtained from the unweighted method in different scenarios that included varying C value and wind turbulence. They concluded that the weighted method by residuals was more appropriate for airtightness measurement. In 2013, Delmotte [89] pointed out that the ordinary least squares method (OLS) is applicable only when the values of airflow rates are equally uncertain and the uncertainties on pressure differences are negligible. When the first assumption regarding airflow rates is not met (which may be the case in practice), he explained that a weighted least squares method should be used. When the second assumption is not met either, another method is needed. In 2017 [81], he analyzed the suitability of a third method for airtightness measurement: the weighted line of organic correlation (WLOC), which considers both pressure difference and airflow rate uncertainties. Including also an evaluation of the uncertainty on the zero-flow pressure difference, he obtained a better repeatability standard deviation for the low-pressure stations than with the method described in the standards. In 2018 and 2019, Prignon et al. [82,90,95] performed a new zero-flow pressure uncertainty evaluation from field data and confirmed that the uncertainty of the zero-flow pressure was not negligible. They confirmed that OLS was inadequate for airtightness measurement; only methods considering the zero-flow pressure uncertainty shall be used. This includes the WLOC method or iterative weighted least square (IWLS) method. More recently, Prignon et al. studied [91] the impact of the linear regression technique regarding the uncertainty of airtightness measurement results. They used data from the field to evaluate the impact of changing the linear regression technique, both on the airtightness results and on the uncertainties evaluation. They compared OLS, WLOC, and IWLS methods. They found that whereas the three methods give similar results regarding the average value of the airflow rate (for all pressure difference) and standard deviation (for pressure difference close to the centroid of the pressure sequence, here 50 Pa), IWLS and WLOC compared to OLS led to: 1) reduce the standard deviation of both in pressurization and depressurization, 2) reduce the uncertainty for the airflow rate for pressure differences away of the centroid of the pressure sequence, and 3) better estimate the uncertainty of the measurement result. Consequently, they suggest using WLOC or IWLS instead of OLS.

### 3.3.5 Reference values for derived quantities

The last step in the process of an airtightness measurement is the calculation of derived quantities, i.e., the final measurement results. The most commonly used derived quantities include the air change rate at 50 Pa ( $n_{50}$  used for example in Germany), the specific leakage rate at 50 Pa ( $q_{E50}$  used for example in the UK), or the specific leakage area at 4 Pa ( $ELA_{E4}$  used for example in the US). They involve three key reference values: the internal volume, the envelope area, and the floor area. Errors on these reference values are sources of uncertainties on the measurement results. To contain deviations, ISO 9972 gives recommendations to calculate these reference values, including the following simplifications:

- the internal volume is calculated without subtracting the internal walls and floors, and the volume of the furniture;
- the floor area is calculated according to national regulations;
- the envelope area is calculated using internal dimensions, without subtracting the area at the junction of internal walls, floors and ceilings with exterior components.

Clearly, the underlying assumptions behind these simplifications should be assessed in the light of the context and purpose of the measurement to be performed.

In addition, evaluating the reference values brings in another component of uncertainty. Mathematically, this component is straightforward to include in an uncertainty analysis; however, the difficulty lies in assessing the uncertainty of the reference value itself. We are only aware of the French approach to this problem.

In this country [29], when the reference value is given by national regulations, the uncertainty of this value is considered equal to zero; when the reference value is calculated by the tester, the uncertainty associated with this value is from 3% to 10%, depending on the reliability of the drawings and the feasibility of the on-site measurements. It is a rough approach based on expert-statements which was found necessary because of the significant contribution made by this component of uncertainty.

## 3.4 Mapping of the current knowledge regarding the sources of errors characterization

The previous sections of this chapter show that there are a number of aspects that can influence the results of an airtightness test by fan pressurization, although the key principles behind this method might seem simple and clear at first sight. There exists a significant body of literature addressing uncertainty in these tests. To give a quick overview of the literature analyzed in this paper, Table 3-4 classifies the papers into three families and gives the major findings of the authors. Overall, there are a number of exploratory studies looking at specific cases and conditions and showing the significant influence of several parameters. Nevertheless, in general, the literature provides little guidance on how to deal with the contribution of these parameters in uncertainty analyses. None of the papers analyzed address uncertainty in pressurization tests as part of a holistic approach.

The representation of the sources of uncertainty during a fan pressurization test shown in Figure 3-4 is an attempt to help fill this gap. It summarizes the different sources of uncertainties for all variables used to calculate the result of a fan pressurization test. Figure 3-4 lists all sources due to the test procedure at each step of the measurement on the left, and the external sources due to weather on the top. There are several sources of uncertainty that seem sufficiently documented to be readily included in uncertainty analyses. These sources include:

- measuring device accuracy and calibration quality. Both aspects are covered in the GUM [62], but our review shows issues with the calibration quality in particular. One reason lies in the large range of airflow rates covered by standard pressurization devices to avoid switching devices in the field. Note that these sources of errors may require additional research work to be dealt with in an uncertainty analysis. If so, it would be mostly to match existing knowledge to the specific features of building airtightness tests;
- temperature and pressure corrections to be applied to the airflow rate and the leakage coefficient. The corrections are well documented. It is unclear why they are only partially applied in ISO 9972. Note that these do not concern stack effect issues, which are discussed below.

As for the reference values, these carry an uncertainty component that is mathematically straightforward to address; however, the failure to properly include this component in uncertainty analysis seems to be due to the lack of statistical data relevant to specific types of measurements in specific contexts.

Similarly, it seems that the availability of field data relevant to specific contexts is often the major barrier to giving guidance to quantify the uncertainty originating from preparing the building. This uncertainty entails uncertainty components due to sampling and preparation of the part of the building to be measured (e.g., sealing unintentional openings). This issue seems to be properly understood now, although dissemination is always welcome to consolidate good practice. In any case, it is clear that given the significant errors found in the literature with the sampling procedures, an estimation of the uncertainty due to sampling should be included in the uncertainty analysis of a pressurization test. Nevertheless, we are aware neither of guidance on this subject, nor of methods or data that could be used to derive this guidance. Note also that additional work on the sampling issue could be inspired by European standard EN 14134 [63] on performance measurement and checks for ventilation systems. This standard provides the sampling error associated with the size of the sample, depending on the total number of apartments or houses.

It may be relevant to pursue research work on regression methods. The ordinary (unweighted) least squares method has been widely used for decades; however, because fundamental assumptions are violated in its application to pressurization tests, a more appropriate mathematical analysis should apply. Methods such as WLOC and IWLS seem promising. With today's available computing power, it is unclear to us why these methods are not in use, since they would involve only a modest or no additional burden on the tester if included in software analysis tools for these tests.

The power-law model is another potential research subject because two components that are often seen as constants, namely the flow coefficient and the flow exponent, are in fact parameters that can vary during a pressurization test. As each opening airleakage coefficient depends a) on the magnitude and the direction of the pressure difference, and b) on the density and viscosity of the air, the airleakage coefficient considered in Equation 1 also depends on these variables. In practice, this can be partially overcome by: 1) using a correction that includes the air density and viscosity; 2) using measurements performed in depressurization and in pressurization. The first point is documented as mentioned above. As for the second point, it is difficult to infer general conclusions from pre-existing work because the cases investigated remain limited compared to the variety of cases that can be encountered in the field. Note also that bi-directional measurements are not mandatory in ISO 9972 because some building designs prevent testing in pressurization and depressurization modes. To give just one example, this may be the case with a stretched ceiling where the ceiling bows down significantly when depressurizing the building.

As for the flow exponent, it remains unclear to the authors whether its pressure dependence can lead to a significant uncertainty component. This remark extends to the choice of the power law versus the quadratic law where there remain active debates amongst the scientific community. Unfortunately, the discussions we are aware of do not always make clear the influence of the purpose of the measurement on the possible outcomes. In fact, different conclusions may be reached depending on whether the test is performed to verify if the envelope meets a requirement, or whether it primarily aims to estimate the infiltration airflow rate. In the first case, the chosen method for the test needs only to be consistent with the requirement. In the second case, it is preferable to choose a method that is most accurate near the operating pressures. This may appear to be favourable to the quadratic law which should be more accurate at low pressures; however, its cost-benefit over the power law remains unclear.

This review also shows that the reasons and limitations of the zero-flow pressure approximation are very poorly understood among both professionals and scientists. In fact, because the relation between the airflow rate and the pressure difference is not linear (except if  $n=1$ ), the zero-flow pressure correction is only an approximation. Therefore, two uncertainty components stem from the zero-flow flow pressure correction: 1) the component due to the correction model itself; 2) the component due to the estimation of the zero-flow pressure. If these components were known, there would be little difficulty in propagating their influence in an uncertainty analysis; our review shows, however, that there is a clear need for further research for proper characterization of these components. This is linked to the spatial and temporal fluctuations of the differential pressure across the leaks during the measurement.

In fact, looking back at Figure 3-4, temporal fluctuations and spatial variations of differential pressures remain in a group of uncertainty sources that have not yet been mentioned in this discussion, together with the duration of the measurement.

Concerning spatial variations, wind is clearly identified as a major problem, with different views on ways to minimize its effect, namely on the location of the pressure taps (average over the four walls, positioned to the leeward). Also, in addition to the temperature effect

on the leakage flow coefficient and airflow rate which can be corrected, temperature differences may drive significant changes in pressure differentials across the envelope. ISO 9972 and ASTM 779-19 attempt to solve this issue by restricting the range of validity of the measurements with criteria on the homogeneity of the pressure difference across the leaks or between spaces in the part of the building to be measured. Furthermore, the zero-flow pressure requirement in ISO 9972 is also meant to restrict changes in pressure differences across the leaks. In practice, these criteria disqualify many buildings from being tested according to these standards, in particular, high-rise buildings or buildings tested in windy conditions. Unfortunately, we have not found relevant literature addressing the uncertainty component associated with these spatial variations in a global uncertainty assessment.

On temporal fluctuations, there is also a clear need for research linked to signal processing techniques. With the uptake of relatively low-cost sensors and high-frequency data acquisition systems, analysing the pressure signal together with the wind spectrum could be helpful in deriving methods to better characterize the differential pressures, including the zero-flow pressure.

Finally, this review mentions the existence of testers' schemes that help to reduce errors due to tester practices. The use of software to perform the measurement, both to drive the blower door and to perform the mathematical analysis, can obviously eliminate many errors. Errors may still arise due to involuntary software errors, but these can be reduced by means of a validation process for the software. For instance, in France, Cerema provides a tool [64] to help editors verify that their software meets the requirements of ISO 9972 and the French standard FD P50-784 [29]. Other voluntary errors might occur which can be partially contained in a testers' scheme with appropriate controls. Nevertheless, all of the aspects mentioned in this last paragraph do not seem relevant for an uncertainty evaluation of an airtightness test.

Table 3-4: A summarized review of studies regarding fan pressurization test uncertainty

Authors	Ref	Family of uncertainty source	Sub-family	Detailed sub-family	Type of study					Conclusion related to this review
					Review	Theoretical	Calculation	Laboratory tests	Field tests	
A. K. Persily	[66]	O-U	-	-					X	- evaluated a 15% error on airflow rate for wind speed above 2.5 m s <sup>-1</sup>
A. K. Persily, R. A. Grot	[69]	O-U	-	-					X	- evaluated that uncertainties are largest outside of the range of the measured data and smallest around the middle of the measured pressure differences - evaluated that a combination of pressurization and depressurization data reduced the uncertainties
M. H. Sherman, L. Palmiter	[70]	O-U	-	-			X			- recommended performing a weighted analysis
F. R. Carrié, P. Wouters	[71]	O-U	-	-	X					- identified sources of uncertainty
T. Brennan et al.	[72]	IMA-U	Variability of $\Delta p$	-					X	- estimated that an external tap on the leeward side of the building is the best configuration - evaluated a scatter for $ELA_4 \leq 11\%$ for wind speed $\leq 5 \text{ m s}^{-1}$ with time-averaged and space-averaged pressure measurement
M. P. Modera, D. J. Wilson	[73]	IMA-U	Variability of $\Delta p$	-					X	- evaluated a scatter with average technique = half scatter with the conventional method
P. duPont	[67]	IMA-U	Variability of $\Delta p$	-					X	- estimated that the error due to wind is from 24% to 74% with wind velocity from 2.24 m s <sup>-1</sup> to 4.47 m s <sup>-1</sup> (5 mph to 10 mph) in depressurization tests
J. Novak	[87]	IMA-U	Variability of $\Delta p$	-					X	- identified no significant impact of the tap location
C. Delmotte	[81]	IMA-U	Variability of $\Delta p$	-			X			- estimated that the location of the external pressure tap may induce a significant overestimation of the induced pressure (up to 13%)
M. H. Sherman, D. T. Grimsrud	[68]	IMA-U	Flow equation	<i>Power-law vs quadratic</i>					X	- observed that the leakage airflow behaves similarly to turbulent flow: for this reason, they used a square-root relation in their model.
D.W. Etheridge	[48]	IMA-U	Flow equation	<i>Power-law vs quadratic</i>			X			- questioned the power-law relation and introduced a quadratic relation - concluded that when both approaches give similar results at high pressure, low-pressure results can be very different. He recommended that the coefficients of both relations should be calculated and quoted in pressurization test results.

I.S. Walker et al.	[74]	IMA-U	Flow equation	Power-law vs quadratic			X	X	- concluded that the power-law relation is better for all configurations that they tested on the field (on one house) and in a laboratory
D.W. Etheridge	[75]	IMA-U	Flow equation	Power-law vs quadratic	X	X			- defended the quadratic equation that he has considered no harder to use and more practically suited to fan pressurization tests
Y.H. Chiu, D.W. Etheridge	[76]	IMA-U	Flow equation	Power-law vs quadratic			X		- calculated that errors in infiltration prediction are two to three times larger with the power-law relation than with the quadratic equation
T. Baracu et al.	[77]	IMA-U	Flow equation	Power-law vs quadratic			X	X	- proposed a new relation: an extended power-law relation that takes into account the regime and the nature of the flow.
M. H. Sherman	[79]	IMA-U	Flow equation	Power-law vs quadratic			X		- demonstrated that the airflow through short circular pipes can be described using the power-law relation
C. Delmotte, J. Laverge	[52]	IMA-U	Flow equation	C variation				X	- observed that all leakage airflow rates measured under depressurization are significantly lower than airflow rates under pressurization
P. duPont	[67]	IMA-U	Flow equation	C variation				X	- observed that errors fell from 1% to 10% with an average result of combined pressurization and depressurization tests
F. R. Carrié	[78]	IMA-U	Flow equation	C variation			X		- justified that the impact of the incomplete correction depends on the atmospheric pressure and leads to a few percent difference in the airflow rate
I. S. Walker et al.	[20]	IMA-U	Flow equation	n variation				X	- evaluated that an error of 0.1 on the n-value may induce an error of 29% on q <sub>4</sub>
M. H. Sherman	[79]	IMA-U	Flow equation	n variation			X		- explained that as n depends on the pressure difference, the power-law relation is a simplified model and thus may be responsible for errors
D.W. Etheridge, M. Sandberg	[80]	IMA-U	$\Delta p_0$	wind impact			X		- observed that the displacement due to weather conditions on the airflow rate curve is constant: it should therefore be included in the equation to correct the result and eliminate the weather impact.
F. R. Carrié, V. Leprince	[51]	IMA-U	$\Delta p_0$	wind impact				X	- evaluated the error due to wind when the zero-flow pressure correction is applied: 12% at 10 m s <sup>-1</sup> at 50 Pa and 60 % at 10 Pa
F.R. Carrié, A.B. Mélois	[94]	IMA-U	$\Delta p_0$	wind impact				X	- observed that the error due to the wind is not eliminated by the zero-flow pressure correction
C. Delmotte	[81]	IMA-U	$\Delta p_0$	$\Delta p_0$ evaluation			X	X	- proposed a method to take into account the variability of the zero-flow pressure in the evaluation of the combined standard uncertainty of the induced pressure difference
M. Prignon et al.	[82]	IMA-U	$\Delta p_0$	$\Delta p_0$ evaluation				X	- estimated that the uncertainty on the zero-flow pressure measurement can significantly increase the uncertainty in pressure measurements
M. Prignon et al.	[95]	IMA-U	$\Delta p_0$	$\Delta p_0$ evaluation			X	X	- estimated that measuring the zero-flow pressure difference for more than 30 seconds leads to a small reduction of the zero-flow pressure measurement uncertainty

V. Leprince, F.R. Carrié	[28]	PEA-U	Building preparation	-	X		- observed that building preparation varies from one country to another
S. Rolfmeier et al.	[83]	PEA-U	Building preparation	-		X	- estimated that the error on the test result varies from 7% to 63% depending on building preparation, and stays below 6% when specific attention to building preparation is given
W. Walther, B. Rosenthal	[84]	PEA-U	Sampling procedure	-	X		- observed different sampling methods in Europe based on the total number of apartments or the total envelope area
B. Moujalled et al.	[85]	PEA-U	Sampling procedure	-		X	- observed that samples give a similar result to overall building tests only when apartments present uniform airtightness performance
J. Novak	[86]	PEA-U	Sampling procedure	-		X	- observed that leakage in common areas may have an important impact on the air permeability of the whole building
W. E. Murphy et al.	[65]	PEA-U	$\Delta p$ and Q	-		X	- observed that measuring only apartments cannot lead to a correct estimation of the airtightness of the whole building
M. H. Sherman, L. Palmiter	[70]	PEA-U	$\Delta p$ and Q	-		X	- estimated repeatability: for each operator, the airflow-pressure curves differ by 20% at 4 Pa whereas they intersect at a high-pressure difference
F. R. Carrié, V. Leprince	[51]	PEA-U	$\Delta p$ and Q	-		X	- estimated reproducibility: 7.5% at 50 Pa and 23.5% at 4 Pa
A. K. Persily	[88]	PEA-U	$\Delta p$ and Q	-		X	- estimated uncertainty due to measuring device uncertainties = 7% at 50 Pa, 40% 4 Pa
V. Leprince et al.	[92]	PEA-U	$\Delta p$ and Q	Calibration		X	- estimated uncertainty due to measuring device uncertainties = 5% at 50 Pa
C. Delmotte, J. Laverge	[52]	PEA-U	Regression methods	-		X	- estimated that the difference between calibration conditions and test conditions could lead to differences of up to 10% on air density
C. Delmotte	[81]	PEA-U	Regression methods	-		X	- observed that low calibration quality induces high uncertainty for the calibration result
M. Prignon et al.	[82]	PEA-U	Regression methods	-		X	- estimated that weighted regression leads to low standard deviation of the result at low-pressure reference
C. Delmotte	[89]	PEA-U	Regression methods	-		X	- observed better repeatability for low pressure using a WLOC
M. Prignon et al.	[90]	PEA-U	Regression methods	-		X	- explained that as the uncertainty on the zero-flow pressure measurement is not negligible the OLS is not appropriate
M. Prignon et al.	[91]	PEA-U	Regression methods	-		X	- explained that as the uncertainty on the zero-flow pressure measurement is not negligible the OLS is not appropriate
						X	- estimated that WLOC and IWLS show lower standard deviation and better uncertainty evaluation than OLS
						X	- observed that WLOC and IWLS lead to lower standard deviation of n and of C than OLS
						X	- observed that WLOC and IWLS lead to lower uncertainty of airflow rate at a pressure remote from the centroid of the pressure sequence

M. Prignon et al.	[95]	PEA-U	Regression methods	-	X	X	- observed that WLOC and IWLS lead to a better estimate of measurement uncertainty
H. Okuyama, Y. Onishi	[96]	PEA-U	Regression methods	-	X	X	- explained that WLOC and IWLS should be considered instead of OLS - estimated that a weighted method by residuals is more appropriate than un-weighted uncertainty methods and uncertainty methods weighted by measurement

Key: O-U: Overall Uncertainty

IMA-U: Intrinsic Model Assumption Uncertainties

PEA-U: Protocol, Equipment and Analysis Uncertainties

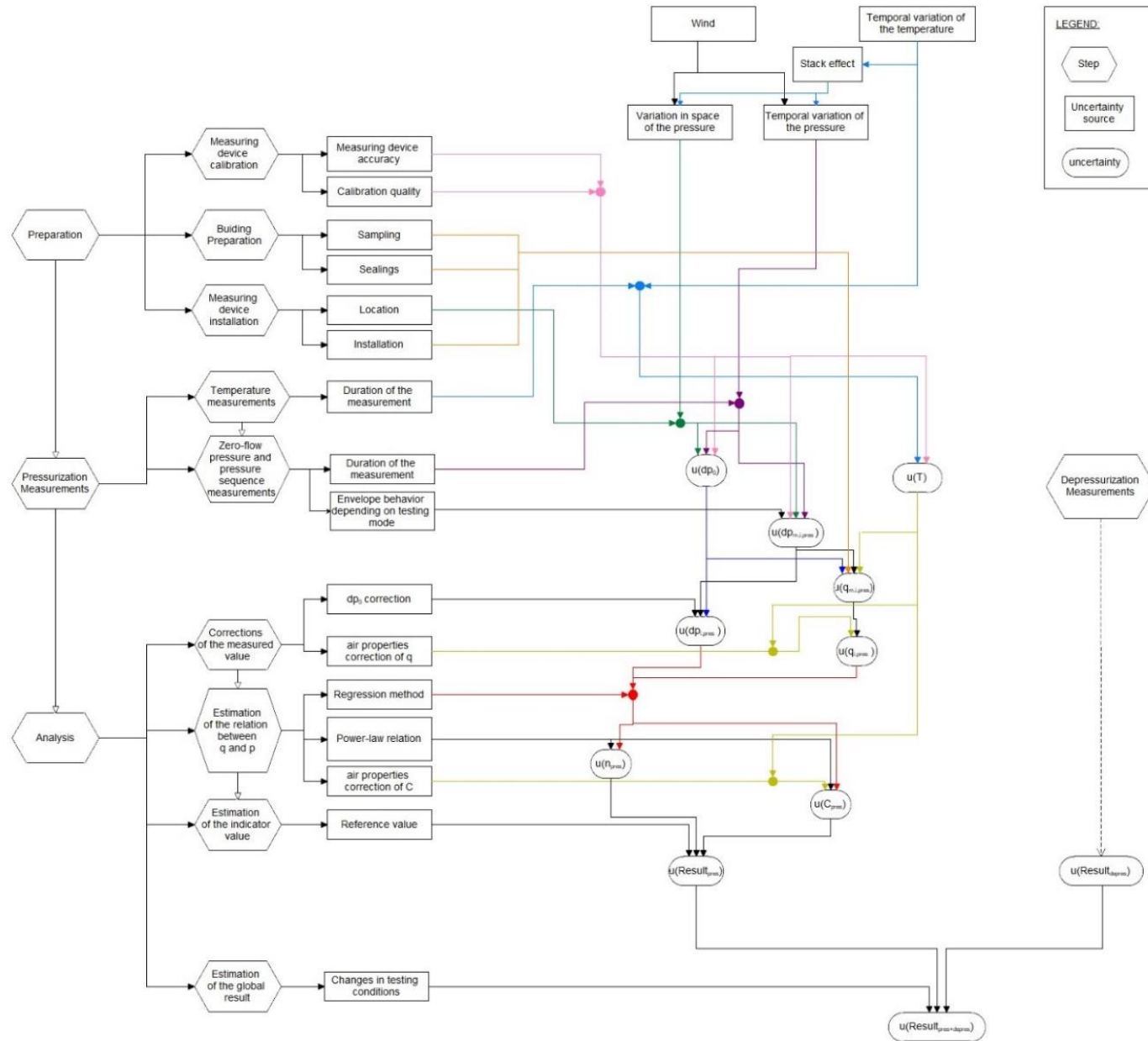


Figure 3-4 : Representation of the sources of uncertainty during a fan pressurization test

### 3.5 Conclusion

The building fan pressurization test method aims to characterize the permeability of a building envelope by matching the parameters of a power-law relationship to a series of measurements of leakage air flow rates and differential pressures. Several sources of error lie in the measurement itself, i.e., the uncertainty of the measurement devices and the actions undertaken by the tester. Existing methods can deal with these sources either with schemes to contain them when possible and justify neglecting them; or by quantifying them as part of a global uncertainty analysis. These methods include state-of-the-art guidance on measurement uncertainty evaluation or requirements and recommendations in standards or testers' schemes.

There are also a number of sources linked to the flow model. In fact, the model assumes that the leakage airflow rate through all leakage paths can be viewed as that flowing through a single opening according to a power law. Although the test method gives corrections to account for the heterogeneity of the differential pressures across the leaks or the temperature and pressure dependence of the power-law model, there remain errors. This literature review shows that these model errors can dominate the uncertainty in the results when wind or stack effects compromise the assumed homogeneity of the differential pressures across the leaks. Although this problem is well-identified, there remains a considerable need for research both to reduce its impact with modified protocols and to quantify the corresponding uncertainties as part of a holistic approach to uncertainty assessment. This work may entail exploratory theoretical and experimental work in order to better understand the heterogeneity in space and time of the differential pressures, and to correct them more effectively than with the present zero-flow correction.

Therefore, there remain a need for further investigations to better understand the physics during airtightness tests. More specifically, it is necessary to understand how the wind affects pressurization tests in order to characterize the error induced by the wind on the test results. This would imply controlling the wind speed, direction, and fluctuations to study all configurations. This also would require to know precisely the airtightness of the building, to be able to vary the leakage distribution, and to use a very precise measurement device. A feasible solution, very less expensive and more technically feasible, is to perform pressurization tests using reduced scale experiments. Indeed, this method allows to perform tests on a model for which the exact envelope airtightness is known under controlled wind conditions. Thus, the exact error induced by the wind on a measurement result can be evaluated. Another advantage of a reduced scale experiment is the possibility to study various configurations of wind speed and airleakage distribution in laboratory conditions. To reproduce a fan pressurization test on a reduced scale to study wind impact requires to define the physics that will be studied, in order to define the similarity conditions. Thus, the results will be transposable from reduced scale to full scale. This work is presented in the next chapter of this manuscript.

## 4. Definition of the similarity conditions and the scale ratios for the reduced scale experimental facility

The reproduction of physics on a reduced model requires to respect similarity conditions between a full scale and a reduced scale. Indeed, the results obtained on a reduced scale are true on a full scale only when the similarity conditions are met. To define these conditions, we need first to describe the physics we want to observe. Thus, the first objective of this chapter is to describe what happens during an airleakage measurement performed on a real building during windy conditions. Many characteristics of the studied building such as its geometry, the number, and the nature of the floors and walls, the equipment, etc. may have an impact on the behavior of the building during a fan pressurization measurement. To understand and interpret the results of reduced scale experiments, we decide to focus only on single-family houses. Moreover, during a building airleakage measurement, the internal volume is considered as a single-zone. According to the ISO 9972 [11], a multi-zone building can be treated as a single-zone building by opening interior doors. For this study, we thus only focus on the flows through openings on the envelope. We do not consider flows through internal partitions, neither the motion of the air inside the space: we consider a generic single-house as a single zone building.

The second objective of this chapter is to define the similarity conditions between full scale tests and reduced scale experiments. This includes a dimensional analysis of the equations that describe the physics during a fan pressurization test. This analysis leads to bringing out non-dimensional numbers: the conservation of the values of these numbers between the scales will guarantee the similarity.

The last section of this chapter is dedicated to the definition of scale ratios, which will lead to the design of the experimental facility.

This chapter includes results presented in two papers:

- Carrié and Mélois (2019) in *Modelling building airtightness pressurisation tests with periodic wind and sharp-edged openings*, in Energy and Buildings [94];
- Mélois et al. in *Model scale reproduction of building airleakage measurements in a wind tunnel: design and characterization of a new experimental facility*, submitted in Building and Environment (September 2020).

## 4.1 Modeling building airtightness pressurization tests with sharp-edged openings

### 4.1.1 Introduction

as we want to design our experimental facility for future studies, we will consider the relations between scale ratios as defined in the general situation. In two papers [97,98], Etheridge focused on fluctuating wind pressures in a naturally ventilated enclosure with two openings. He laid down fundamental equations of four models to address his problem. The flow equations of the most rigorous model—the “Quasi-steady/Temporal inertia model”—are of interest to model other problems involving fluctuating wind pressures, including pressurization tests with unsteady wind. Note also that in his book ([80], pp. 96-99), Etheridge explained how the quasi-steady assumption and time-averaging can influence the error in the airflow rate. He detailed the case of an orifice plate meter in a pipe and gives the error in the airflow rate as a function of the Strouhal number in that specific case. However, the natural ventilation and orifice plate meter problems tackled by Etheridge [97,98] are clearly different from that of a pressurization test involving air forced into or out of an enclosure by a pressurization device and multiple openings subjected to different pressures because of wind and stack effects. For our study, we describe only a quasi-steady temporal inertia model for a fan pressurization test. We derive two other models: a quasi-steady compressible and isothermal models. They are described and analyzed in [94].

### 4.1.2 Idealized building

In accordance with Carrié and Leprince [51], we assume that the building can be represented by a single zone separated from the outside by two types of walls: walls on the windward side of the building which are subject to the same upwind pressure; and walls on the leeward side which are subject to the same downwind pressure (Figure 4-1). We further assume that all leaks on the windward (respectively, leeward) side can be represented as a single opening at a given height—e.g.,  $z_1$  if opening 1 is on the windward side (respectively, leeward) —subjected to the same pressure difference.

In the field, the roof, the sides (façades n°3 and n°4 in Figure 4-1), and the leeward façade (n° 2 in Figure 4-1) have negative pressure coefficients on average; the windward façade (n°1) has a positive pressure coefficient on average. In our idealized building, only one average pressure coefficient is considered for all leaks on the windward (resp. leeward) façades. Similarly, only one average height is considered for all leaks on the windward (resp. leeward) façades. This is of course a crude representation of the complexity of real airflow paths. Nevertheless, it has the advantage of remaining relatively simple while allowing us to describe the airflow rates in leaks subjected to different pressures during a pressurization test, which is the key problem in presence of wind. The system of interest can be represented as shown in Figure 4-1.

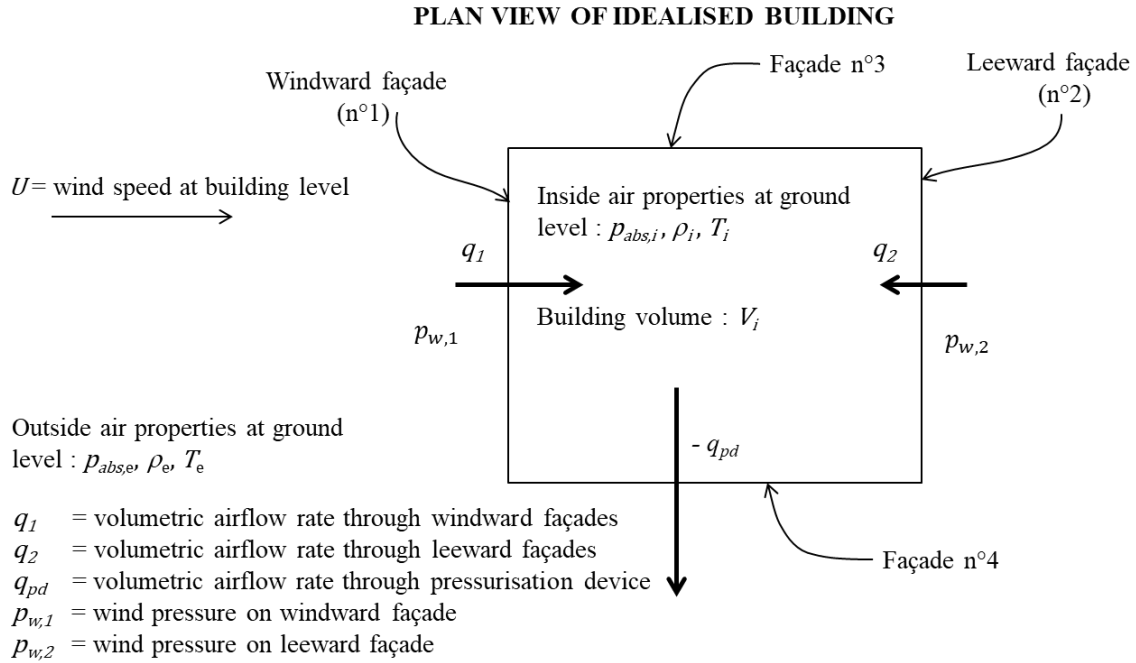


Figure 4-1: Plan view of the idealized building with wind facing façade 1

#### 4.1.3 Temperature and density of airflows entering and leaving the building

To remain consistent with the complexity level of our idealized building, we assign a density and temperature to the airflow paths entering or leaving the space as if the air was directly transferred in or out of the enclosure, without interaction with the building fabric or pressurization equipment. This leads to the equations detailed in Table 4-1 when the subscripts “e” pertains to the external conditions and “i” to internal conditions..

Table 4-1: Density and temperature equations at airflow paths (positive signs correspond to inward flows)

Density	Eq. n°	Temperature	Eq. n°
$\rho_{pd} = \begin{cases} \rho_e & \text{if } \text{sign}(q_{pd}) \geq 0 \\ \rho_i & \text{if } \text{sign}(q_{pd}) < 0 \end{cases}$	(4)	$T_{pd} = \begin{cases} T_e & \text{if } \text{sign}(q_{pd}) \geq 0 \\ T_i & \text{if } \text{sign}(q_{pd}) < 0 \end{cases}$	(5)
$\rho_1 = \begin{cases} \rho_e & \text{if } \text{sign}(q_1) \geq 0 \\ \rho_i & \text{if } \text{sign}(q_1) < 0 \end{cases}$	(6)	$T_1 = \begin{cases} T_e & \text{if } \text{sign}(q_1) \geq 0 \\ T_i & \text{if } \text{sign}(q_1) < 0 \end{cases}$	(7)
$\rho_2 = \begin{cases} \rho_e & \text{if } \text{sign}(q_2) \geq 0 \\ \rho_i & \text{if } \text{sign}(q_2) < 0 \end{cases}$	(8)	$T_2 = \begin{cases} T_e & \text{if } \text{sign}(q_2) \geq 0 \\ T_i & \text{if } \text{sign}(q_2) < 0 \end{cases}$	(9)

#### 4.1.4 Pressure difference at leakage sites

The pressure difference at the windward opening  $\Delta p_1$  is:

$$\Delta p_1(t) = p_{w,1}(t) - (\rho_e(t) - \rho_i(t))gz_1 - p_i(t) \quad (10)$$

with:

- $p_{w,1}$  the pressure induced by the wind on the windward façade;

- $z_1$  the height of the windward opening from the ground;
- $p_i$  the pressure inside the building relative to external atmospheric pressure.

Similarly, at the leeward opening:

$$\Delta p_2(t) = p_{w,2}(t) - (\rho_e(t) - \rho_i(t))gz_2 - p_i(t) \quad (11)$$

with:

- $p_{w,2}$  the pressure induced by the wind on the leeward façade;
- $z_2$  the height of the windward opening from the ground.

#### 4.1.5 Flow through leakage sites

In his analysis of unsteady flow effects due to fluctuating wind pressures, Etheridge [97,98] proposes to use a so-called “Quasi-steady/Temporal inertia model” (or QT model) to describe the flow through the leaks. Applying the same approach in our case leads to the following flow equations through the leaks:

$$2C_{z,1}A_1l_{e,1}\frac{dq_1(t)}{dt} = -q_1^2(t) \text{sign}(q_1(t)) + 2C_{z,1}^2A_1^2\frac{\Delta p_1(t)}{\rho_1} \quad (12)$$

$$2C_{z,2}A_2l_{e,2}\frac{dq_2(t)}{dt} = -q_2^2(t) \text{sign}(q_2(t)) + 2C_{z,2}^2A_2^2\frac{\Delta p_2(t)}{\rho_2} \quad (13)$$

with:

- $C_{z,j}$  the discharge coefficient of the orifice j, j=1 on windward and j=2 on leeward façade;
- $A_j$  the area of the orifice j;
- $l_{e,j}$  the entry length of the orifice j;
- $q_j$  the volumetric airflow rate through the orifice j.

Regarding the entry length, Etheridge used Modera’s experimental data [99] to show that the opening diameter was a reasonable estimate of this parameter. Therefore, we write:

$$l_{e,1} = \sqrt{\frac{4A_1}{\pi}}; l_{e,2} = \sqrt{\frac{4A_2}{\pi}} \quad (14)$$

#### 4.1.6 Equation of state

We assume that the air behaves like a perfect gas, therefore:

$$p_{abs,0} = \rho_0 R T_0 \quad (15)$$

$$p_{abs,e} = \rho_e R T_e \quad (16)$$

$$p_{abs,i} = p_{abs,e} + p_i = \rho_i R T_i \quad (17)$$

with:

- $p_{abs}$  the absolute pressure in standard conditions;
- $p_{abs,e}$  the absolute external pressure;
- $T$  the temperature.

#### 4.1.7 Continuity equation

The mass air flow rates through the leakage sites and the pressurization device are:

$$q_{m,pd} = \rho_{pd} q_{pd} \quad (18)$$

$$q_{m,1} = \rho_1 q_1 \quad (19)$$

$$q_{m,2} = \rho_2 q_2 \quad (20)$$

with:

- $q_m$  the massive airflow rate;
- the subscript “ $pd$ ” pertains to the pressurization device.

Writing the mass balance of the internal volume gives:

$$\frac{dm_i(t)}{dt} = V_i \frac{d\rho_i(t)}{dt} = q_{m,pd}(t) + q_{m,1}(t) + q_{m,2}(t) \quad (21)$$

with:

- $m_i$  the mass of the air inside the building;
- $V_i$  the internal volume.

#### 4.1.8 Energy conservation equation

Etheridge [97,98] assumes that the bulk behavior of the internal volume follows a polytropic process, yielding:

$$\frac{p_i(t)}{\rho_i(t)^{n_p}} = K \quad (22)$$

where  $K$  is a constant. For a perfect gas, if the process is adiabatic,  $n_p = \gamma$ ; whereas, if the process is isothermal,  $n_p = 1$ . In the adiabatic case, this relationship stems from applying the state equation and the first principle of thermodynamics to a closed system with homogeneous state variables. This assumption is convenient because it reduces the energy conservation equation to a simple mathematical form (equation (22)). Although

the air pressure and temperature inside values differ from outside values, this assumption can be justified with the Boussinesq approximation—i.e., the density variations are considered only in the buoyancy terms, in other words, in the terms where gravity appears in equations (10)(4) and (11) (6)— and since the absolute pressure is nearly identical inside and outside the building (see Figure 4-2).

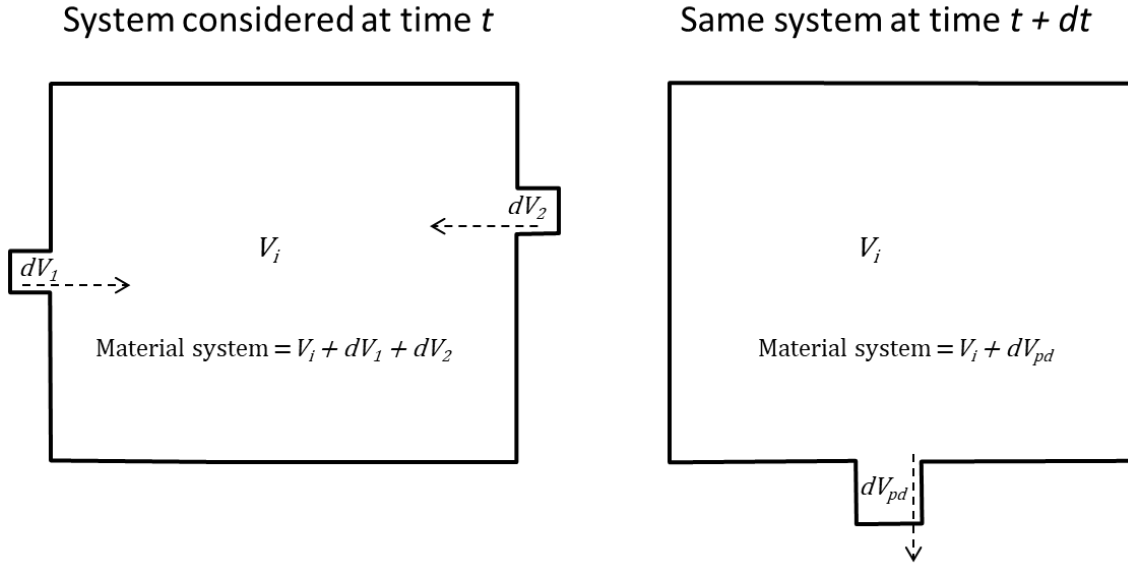


Figure 4-2: Closed system considered with the Boussinesq approximation and with  $P_i \approx P_e$  (the air is assumed to enter the building through openings 1 and 2 and leave through the pressurization device).

However, in the more general case, the internal volume is an open system and air at different temperatures flows in and out of this volume. When we apply the energy conservation principle to the internal volume, accounting for energy exchanges due to the air entering and leaving the building, but neglecting other energy transfer through the walls, mechanical stress, or internal sources, we obtain:

$$V_i c_v \frac{d(\rho_i(t) T_i(t))}{dt} = \Phi_{pd}(t) + \Phi_1(t) + \Phi_2(t) \quad (23)$$

Where:

$$\Phi_{pd} = \rho_{pd} c_p q_{pd} T_{pd} \quad (24)$$

$$\Phi_1 = \rho_1 c_p q_1 T_1 \quad (25)$$

$$\Phi_2 = \rho_2 c_p q_2 T_2 \quad (26)$$

We solved the system of equations to obtain the dynamic behavior of the airflow rates and state variables in the enclosure and the leaks, making it possible to numerically estimate the uncertainty of the airleakage coefficient in one-point pressurization tests with a periodic wind. These results are presented in [94]. Our analyses showed the significant impact of the wind frequency on the results and have confirmed that ignoring the zero-

flow pressure uncertainty is inappropriate because of its significant contribution to the uncertainty of the leakage airflow rate error. We have also shown that the wind fluctuations can yield much larger uncertainties than the average wind alone. Nevertheless, in this manuscript, we only focus on the evaluation of error due to steady wind with experimental tests due to technical and financial limit for our experimental facility. Thus, the next section is dedicated to the definition of similarity conditions from the analysis of the model we have defined.

## 4.2 Definition of similarity conditions

### 4.2.1 Simplification of the model

To study only the impact of the wind, we consider initial isothermal conditions that we will impose in our laboratory. In laboratory conditions, we also expect that the temperatures, and thus the air densities, will not significantly vary during each test. Equations (10) and (11) can therefore be simplified by neglecting the “gravity term”  $(\rho_0 - \rho_i)gz$ . We have evaluated the impact of this simplification on the variation of the pressure difference at the openings in this study for:

- wind speeds from 0 to 12 m s<sup>-1</sup>;
- pressure differences between indoor and outdoor imposed by the pressurization measurement device from 10 to 70 Pa (pressurization) and from -70 to -10 Pa (depressurization);
- leak heights from 0.1 m to 2.5 m;
- windward leak and leeward leak.

We calculated for different situation the value of the pressure difference due to the “gravity term”  $(\rho_0 - \rho_i)gz$ : this component seems to be negligible compared to the wind part  $C_{pw,1} \frac{\rho_0 U(t)^2}{2}$  and the blowerdoor part  $p_i(t)$ . In order to confirm this observation, we evaluate the error we make if we evaluate the pressure difference without the gravity part both in pressurization and depressurization, for a windward leak and a leeward leak for two pressure differences induced by a blowerdoor and three different leak heights. Table 4-2 presents the error in pressurization on a windward leak. The errors evaluated for the other configurations are presented in Annex A. For all configurations, we have calculated the theoretical maximum error of this simplification on the evaluation of the pressure difference at the leak level: the maximal error is 0.35%. Therefore, we decide to neglect the gravity term to define the similarity conditions of the experimental facility. Equations (10) and (11) become equations (27) and (28).

$$\Delta p_1(t) = C_{pw,1} \frac{\rho_0 U(t)^2}{2} - p_i(t) \quad (27)$$

$$\Delta p_2(t) = C_{pw,2} \frac{\rho_0 U(t)^2}{2} - p_i(t) \quad (28)$$

Table 4-2: Error due to gravity simplification for the evaluation of the pressure difference on a windward leak in pressurization

U (m s <sup>-1</sup> )	p <sub>i</sub> = 10 Pa			p <sub>i</sub> = 70 Pa		
	z=0,1 m	z=1 m	z=2,5 m	z=0,1 m	z=1 m	z=2,5 m
0	0,001%	0,012%	0,029%	0,001%	0,012%	0,029%
1	0,001%	0,012%	0,030%	0,001%	0,012%	0,029%
2	0,001%	0,013%	0,033%	0,001%	0,012%	0,030%
3	0,002%	0,016%	0,040%	0,001%	0,012%	0,030%
4	0,002%	0,023%	0,056%	0,001%	0,013%	0,031%
5	0,005%	0,047%	0,118%	0,001%	0,013%	0,033%
6	-0,014%	-0,138%	<b>-0,345%</b>	0,001%	0,014%	0,035%
7	-0,002%	-0,025%	-0,061%	0,001%	0,015%	0,037%
8	-0,001%	-0,013%	-0,031%	0,002%	0,016%	0,040%
9	-0,001%	-0,008%	-0,020%	0,002%	0,018%	0,045%
10	-0,001%	-0,006%	-0,014%	0,002%	0,020%	0,051%
11	0,000%	-0,004%	-0,011%	0,002%	0,024%	0,061%
12	0,000%	-0,003%	-0,009%	0,003%	0,031%	0,077%

#### 4.2.2 Definition of dimensionless numbers

##### 4.2.2.1 Application of the Vaschy-Buckingham theorem

To ensure that the results we will obtain on the reduced scale tests are consistent with the physics that occur on a full scale, we have to respect the similarity conditions. We aim to evaluate the error induced by the wind during a fan pressurization measurement. We define this error for a fixed pressure difference  $\Delta p$  as the relative gap between the real leakage rate  $q_{\Delta p,ref}$ , which is the reference value measured without wind, and the leakage rate measured under windy conditions  $q_{\Delta p,m}$  according to equation (29).

$$E_{W_{\Delta p}} = \frac{q_{\Delta p,m} - q_{\Delta p,ref}}{q_{\Delta p,ref}} \quad (29)$$

According to equations we defined previously in this chapter, the error  $E_{W_{\Delta p}}$  depends on numerous variables. The Vaschy-Buckingham theorem provides a method for computing sets of dimensionless numbers from the model variables to define the similarity conditions. We apply this method by first determining 8 independent variables that are involved in our model (for example, as the internal temperature  $T_i$  depends on the external temperature  $T_e$ , we consider only the temperature  $T$  as an independent variable of our model). Table 4-4 lists these variables. These variables are expressed in 4 fundamental units: kilogram (kg), meter (m), second (s), and degree Kelvin (K). Our model is defined by 8 independent variables expressed in 4 units. According to the Vaschy-Buckingham method, we need to define 4 dimensionless numbers (8 minus 4) to establish similarity conditions.

Table 4-3: Units of the independent variables of our model

Variable		Unit exponent			
		kg	m	s	K
p	Pressure	1	-1	-2	0
$\rho$	Air density	1	-3	0	0
U	Wind speed at the height of the building	0	1	-1	0
t	time	0	0	1	0
A	Area of opening	0	2	0	0
q	Volumetric airflow rate	0	3	-1	0
$c_v$	Specific heat capacity at constant volume	0	2	2	-1
T	Temperature	0	0	0	1

#### 4.2.2.2 Dimensionless numbers

To respect similarity conditions between full scale tests and reduced scale experiments, we perform a dimensional analysis that brings out our 4 dimensionless numbers. The conservation of the values of these numbers between the scales will guarantee the similarity. To identify these numbers, we introduce a reference value  $X_{ref}$  for each dimensional variable X of our model equations, according to the method described by N. Le Roux [100]. Table 4-4 defines this  $X_{ref}$  reference value for every variable of our equations.

Table 4-4: Definition of reference values and dimensionless variables

Variable		$X_{ref}$ Reference values	Dimensionless variable
p	Pressure	$p_{ref}$	$p^* = \frac{p}{p_{ref}}$
$\rho$	Air density	$\rho_{ref}$	$\rho^* = \frac{\rho}{\rho_{ref}}$
U	Wind speed at the height of the building	$U_{ref}$	$U^* = \frac{U}{U_{ref}}$
z	Half-height of the building	$z_{ref}$	$z^* = \frac{z}{z_{ref}}$
A	Area of opening	$A_{ref}$	$A^* = \frac{A}{A_{ref}}$
L	Length	$L_{ref}$	$L^* = \frac{L}{L_{ref}}$
$V_i$	Internal building volume	$V_{i,ref}$	$V_i^* = \frac{V_i}{V_{i,ref}}$
q	Volumetric airflow rate	$q_{ref}$	$q^* = \frac{q}{q_{ref}}$
T	Temperature	$T_{ref}$	$T^* = \frac{T}{T_{ref}}$
t	Time	$t_{ref}$	$t^* = \frac{t}{t_{ref}}$

As the purpose of this analysis is to define the sizes of the experiment respecting similarity conditions, we consider a specific configuration with two identical openings

(same size and same height) in isothermal initial conditions and with a steady wind. Equations (27) and (28) are similar, one for each opening. We introduce dimensionless variables in a generic equivalent equation (equation (30)).

$$\Delta p(t) = C_{pw} \frac{\rho U(t)^2}{2} - p_i(t) \quad (30)$$

The first dimensionless number appears in bold in equation (31).

$$\Delta p^* = \left( \frac{\rho_{ref} \cdot U_{ref}^2}{p_{ref}} \right) \cdot C_{pw} \frac{\rho^* \cdot U^{*2}}{2} - p_i^* \quad (31)$$

Equations (12) and (13) are also “similar” for both openings. We introduce dimensionless variables in one generic equivalent equation (equation (32)).

$$\frac{4C_z A^{3/2} dq(t)}{\sqrt{\pi}} = -q^2(t) \text{sign}(q(t)) + 2C_z^2 A^2 \frac{\Delta p(t)}{\rho_0} \quad (32)$$

We define the reference time as follow:  $t_{ref} = \frac{L_{ref}}{U_{ref}}$  with  $L_{ref}$  a characteristic length. The second and third dimensionless numbers are obtained in bold in equation (33).

$$\frac{\sqrt{A_{ref}}}{L_{ref}} \cdot \sqrt{\frac{p_{ref} \cdot A_{ref}^2}{\rho_{ref} \cdot q_{ref}^2}} \cdot \sqrt{\frac{\rho_{ref} \cdot U_{ref}^2}{p_{ref}}} \cdot \frac{4 \cdot C_z \cdot A^{3/2}}{\sqrt{\pi}} \cdot \frac{dq^*}{dt^*} = -q^{*2} \text{sign}(q^*) + \frac{p_{ref} \cdot A_{ref}^2}{\rho_{ref} \cdot q_{ref}^2} 2C_z^2 \cdot A^{*2} \frac{\Delta p^*}{\rho^*} \quad (33)$$

The fourth dimensionless number is obtained in bold in equation (34) using similarly the mass balance (equation (21)).

$$\left( \frac{V_{ref} \cdot U_{ref}}{L_{ref} \cdot q_{ref}} \right) V_i^* \frac{d\rho^*}{dt^*} = \sum \rho^* \cdot q^* \quad (34)$$

The introduction of the dimensionless variables into energy conservation does not reveal any new dimensionless number (equation (35)).

$$\left( \frac{V_{ref} \cdot U_{ref}}{L_{ref} \cdot q_{ref}} \right) V_i^* c_v \frac{dp^*}{dt^*} = \sum \rho^* \cdot c_p \cdot q^* \cdot T^* \quad (35)$$

As a result, we have identified our four dimensionless numbers presented in equations (36) to (39).

$$\Pi_1 = \frac{\rho_{ref} \cdot U_{ref}^2}{p_{ref}} \quad (36)$$

$$\Pi_2 = \frac{p_{ref} \cdot A_{ref}^2}{\rho_{ref} \cdot q_{ref}^2} \quad (37)$$

$$\Pi_3 = \frac{\sqrt{A_{ref}}}{L_{ref}} \quad (38)$$

$$\Pi_4 = \frac{V_{ref} \cdot U_{ref}}{L_{ref} \cdot q_{ref}} \quad (39)$$

## 4.3 Definition of the scale ratios

### 4.3.1 General configuration

To reach similarity conditions, the values of the dimensionless numbers  $\Pi_1$  to  $\Pi_4$  have to be identical both at reduced scale and full scale. For each variable, we defined the scale ratio  $\bar{X}$  as follow:

$$\bar{X} = \frac{X_{ref\ model}}{X_{ref\ real}}$$

We assume that the air has the same properties on the reduced scale and the full scale: the scale ratio of air densities is equal to 1. The conservation of  $\Pi_1$  to  $\Pi_4$  therefore leads to the four relations between scale ratios: equation (40) to equation (43).

$$\bar{U}^2 = \bar{p} \tag{40}$$

$$\bar{p} \cdot \bar{A}^2 = \bar{q}^2 \tag{41}$$

$$\bar{A}^{0,5} = \bar{L} \tag{42}$$

$$\bar{V} \cdot \bar{U} = \bar{L} \cdot \bar{q} \tag{43}$$

For our study, we already know that we will need to impose a scale ratio for lengths to design a model that can fit into a wind tunnel, which sizes have to be adapted to our laboratory. Thus, we will have a fixed ratio for length  $k = \bar{L}$ . That defined directly the scale ratios for areas according to the relation (42). Then, we have the liberty to define another scale ratio. By considering a scale ratio for wind speed  $\bar{U} = 1$ , we obtain the scale ratio for pressure  $\bar{p} = 1$ . That means that we can design our experimental facility considering wind speeds and pressure differences similar to the full scale. We will consider this configuration in chapter 5 to design our facility.

### 4.3.2 Simplification for steady conditions

As we have first considered studying the impact of the wind both in steady and unsteady conditions, we have defined the scale ratios for all situations. Nevertheless, due to time and technical reasons, we will only consider steady wind in the next parts of this manuscript.

In steady conditions, the equations of our model are simpler: all variables do not depend on time. Thus, equation (33) becomes (44), equation (34) becomes (45), and equation (35) becomes (46).

$$-q^{*2} \text{sign}(q^*) + \frac{p_{ref} \cdot A_{ref}^2}{\rho_{ref} \cdot q_{ref}^2} 2C_z^2 \cdot A^{*2} \frac{\Delta p^*}{\rho^*} = 0 \tag{44}$$

$$\sum \rho^* \cdot q^* = 0 \quad (45)$$

$$\sum \rho^* \cdot c_p \cdot q^* \cdot T^* = 0 \quad (46)$$

Therefore, we only have to conserve dimensionless numbers  $\Pi_1$  and  $\Pi_2$  to satisfy similarity conditions for steady winds. We then do not have a relation between length, surface, and volume scale ratios. It means that in steady conditions, surface and volumetric distortion are authorized. However, as we want to design our experimental facility for future studies, we will consider the relations between scale ratios as defined in the general situation.

#### 4.4 Conclusions

We first proposed a physical model that describes the governing physical phenomena during an air leakage measurement performed on a full scale simplified building (a single-zone building with 2 leaks: one on the windward façade and one on the leeward façade) during windy conditions. This model includes 2 equations defining the pressure difference at leakage sites, 2 equations defining airflow through leaks, one continuity equation and one energy conservation equation. From these equations, we performed a dimensional analysis to define the similarity conditions between full scale tests and reduced scale experiments. This analysis leads to bring out four non-dimensional numbers which values have to be conserved between scales to guarantee the similarity. This conservation led to the definition of relations between scale ratios regarding:

- the wind speed;
- the pressure differences;
- the lengths;
- the areas;
- the volumes
- the airflows.

The analysis of these relations show that it will be possible to impose a scale ratio of 1 for the wind speed and pressure differences. It means that we can design our experimental facility considering wind speeds and pressure differences similar to the full scale. The design of the facility will be described in the next chapter of this manuscript.

## **5. Reduced scale reproduction of building pressurization tests in a wind tunnel: design and characterization of a new experiment facility**

The goal of this part is to provide an experimental facility to evaluate the impact of the wind on building airtightness measurements and to test solutions to reduce the uncertainty of the test results intrinsic to the wind effect. This entails the following objectives:

- carry out pressurization tests in reduced scale;
- generate steady wind conditions at different wind speeds;
- accurately measure pressure differences, wind speeds, and airflow rates.

To meet these objectives, the experimental facility will include:

- a model of a single-zone building in reduced scale;
- a pressurization measurement device which will replace a blower door in reduced scale;
- the wind tunnel that will create steady wind conditions;
- the necessary sensors and actuators.

We first define the sizes of the model and the wind tunnel section from the scale ratios we defined in the previous chapter, including CFD simulations to optimize the wind tunnel design. We present the technical solutions for each component of the experimental facility that will be scalable for future studies. That includes the model, the wind tunnel, and our own pressurization device that fits the model size.

Then, we present the characterization of the experimental facility. More especially, we perform various measurements to validate the characteristics of the model and to evaluate pressure and wind velocity fields in the testing chamber of the wind tunnel.

### **5.1 Design and sizing of the experiment**

#### *5.1.1 Definition of the reference full scale building*

The full scale studied building is a generic 2-story house, as illustrated in Figure 5-1. The limit value required for the new houses in the current French EP-regulation (RT2012) is expressed using the  $q_{a4}$  indicator and can be converted using the effective leakage area:  $ELA_4 = 0.0142 \text{ m}^2$ . This value is also used for the full scale building.

#### *5.1.2 Design of the reduced building model*

##### *5.1.2.1 Definition of the scale ratio*

Because the wind tunnel has to fit the laboratory, the maximum cross-section of its testing chamber has to be  $1.0 \times 1.0 \text{ m}^2$ . To avoid the need for blockage analysis and correction, the cross-section of the building model has to be below 5% of the testing chamber (the

part of the tunnel in which the target wind speed is achieved and stable) cross-section: 0.05 m<sup>2</sup>. This limit is defined by the ASCE as indicated by Choi and Kwon (1998) [101]. The cross-section of the real house is 6.0x5.0=30.0 m<sup>2</sup>. The model is therefore designed from the real house sizes implementing a scale ratio of 1/25<sup>th</sup>. The sizes of the model are presented in Figure 5-2. The cross-section of the model is 0.20x0.24=0.048 m<sup>2</sup>, which respects the 5% limit.

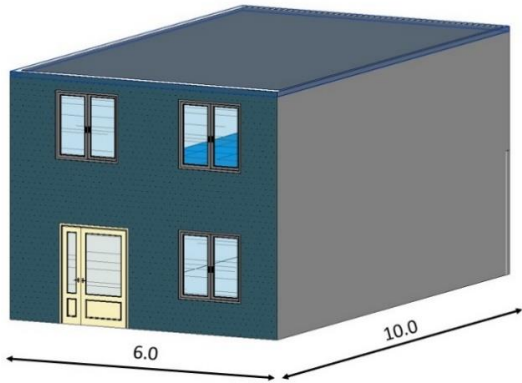


Figure 5-1: Generic full scale 2-storey house [m]

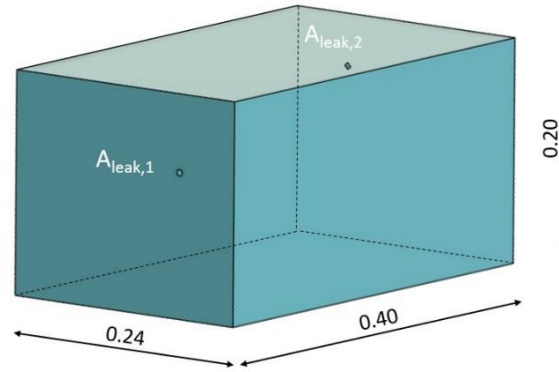


Figure 5-2: Reduced model sizes [m]

#### 5.1.2.2 Definition of the sizes of the leaks

In real houses, the diameter of the leaks might vary from less than 1.0 mm to more than 10 cm [102]. Applying the 1/25<sup>th</sup> scale ratio to leaks would lead to very small leaks with diameters less than 0.04 mm. The airflow through an opening with this size will be completely laminar and will not reproduce the behavior of the airflow through real leaks. To reproduce the behavior of a real airflow, the model will therefore include only two openings, as already described in chapter 4. The total leakage area of the model remains consistent with the real house characteristics (equation (47))

$$A_{1,model} + A_{2,model} = \left(\frac{1}{25}\right)^2 * ELA_{4,real} = 2.27 * 10^{-5} m^2 \quad (47)$$

with:

- $A_{1,model}$  the area of the windward opening of the reduced model;
- $A_{2,model}$  the area of the leeward opening of the reduced model;
- $ELA_{4,real}$  the equivalent leakage area at 4 Pa of the full scale house.

Each opening will be perfectly circular. Even if this case does not completely represent common leaks of building envelopes, this first design shape has the crucial advantage of making it possible to better characterize the airflow behavior. In future work, further designs with different shapes and materials for the openings will be able to provide other types of airflow.

Carrie and Leprince [51] have shown that whereas the total leakage area is not an influential parameter in the evaluation of the impact of the wind, the distribution of the leaks between the windward and leeward facades has a large impact on the error due to

the wind. The model will therefore include different leak sizes to study different leak distributions. A leakage distribution ratio  $r_{LD}$  is defined according to equation (48).

$$r_{LD} = \frac{A_1}{A_1 + A_2} \quad (48)$$

As the leakage distribution in real buildings is extremely variable [103], we consider 9 configurations: from  $r_{LD} = 10\%$  to  $r_{LD} = 90\%$ . Table 5-1 describes the diameter of these configurations.

Table 5-1: Diameters of the reduced model openings for different leakage distribution ratios

<b>r<sub>LD</sub></b>	<b>0.1</b>	<b>0.2</b>	<b>0.3</b>	<b>0.4</b>	<b>0.5</b>	<b>0.6</b>	<b>0.7</b>	<b>0.8</b>	<b>0.9</b>
Windward leak size [% of ELA <sub>4</sub> ]	10	20	30	40	50	60	70	80	90
Windward leak diameter [mm]	1.7	2.4	2.9	3.4	3.8	4.2	4.5	4.8	5.1
Leeward leak size [% of ELA <sub>4</sub> ]	90	80	70	60	50	40	30	20	10
Leeward leak size diameter [mm]	5.1	4.8	4.5	4.2	3.8	3.4	2.9	2.4	1.7

### 5.1.2.3 Definition of the location of the leaks

The location of the openings has to be carefully defined to avoid turbulence in the boundary layer. We first conducted a preliminary experiment with a cubic model made of wood (200\*200\*200 mm<sup>3</sup>) and we tested six locations of the openings (three on the lower half and three on the upper half of the façade), both for the windward and the leeward facades. The wind was provided by a small fan placed about 1.5 m in front of the wooden model. For each location, the ratio between the pressure coefficients was evaluated from pressure difference measurements. For the three high openings, the ratio  $C_{p, windward} / C_{p, leeward}$  is evaluated from -1.6 to -5.8, which is consistent with values in the literature (-3.5 for a low-rise building, with a square low floor, exposed to the wind [104]). In contrast, for the three low openings, the  $C_p$  ratio varies from -78.8 to 187.3. These values might indicate that the low openings are disturbed by the turbulence in the boundary layer.

Secondly, to accurately evaluate the height of the boundary layer in the real wind tunnel and with the final design of the model placed in the testing chamber (TC), we performed a numerical simulation using the CFD with K-Omega SST for turbulence model assumptions. The CFD model calculates the height of the boundary layer for the locations of the windward façade (0.77 m from the TC entrance) and the leeward facade (1.17 m from the TC entrance). At the windward facade location, the height of the boundary layer is 17 mm at 1 m.s<sup>-1</sup> and 12 mm at 7 m.s<sup>-1</sup>. At the leeward facade location, the height of the boundary layer is 10 mm at 1 m s<sup>-1</sup> and 7 mm at 7 m s<sup>-1</sup>, as illustrated in Figure 5-3. The openings have to be located above 17 mm from the bottom of the façades.

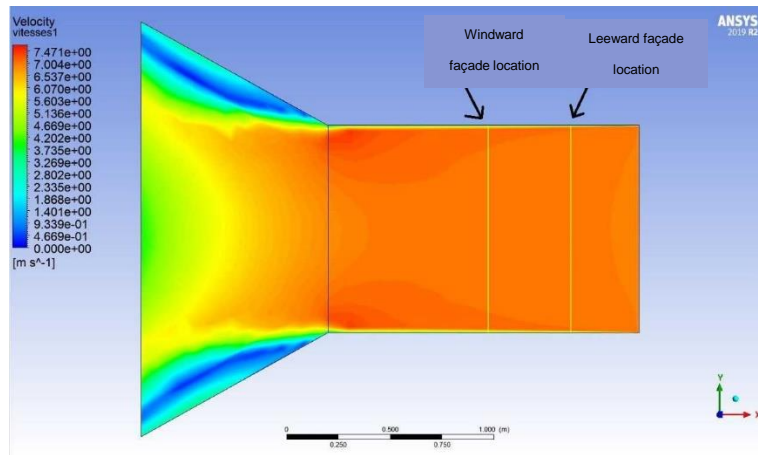


Figure 5-3: CFD calculations of wind velocity inside the testing chamber for a wind target equal to  $7 \text{ m s}^{-1}$

The last verification concerns the mutual impact of the openings. In a real building, external walls are several meters away from each other, whereas in the model, there are only several dozen centimeters between the windward and the leeward facades: the airflow due to one opening might influence the airflow through another opening. To prevent this influence, the openings are not in front of each other.

To avoid boundary layer turbulence and impact of one opening on the other one, both openings are therefore located  $0.13 \text{ m}$  away from the bottom of the model,  $0.07 \text{ m}$  away from the right-hand side of each facade.

#### 5.1.2.4 Technical solutions for the reduced model

To build the model, we chose a metallic frame with removable Plexiglas® facades fixed to the frame with screws and seals. This solution will make it possible in the future to test new facades with more openings, for example. Two opposite facades include a large circular opening. We designed several metallic disks: each of them is drilled to one of the diameters defined in Table 5-1. These cylinders are plugged onto the large circular opening like corks (Figure 5-4a). This solution enables us in the future to design as many different opening sizes and shapes as possible.

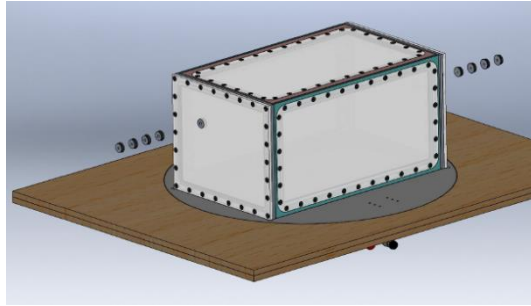
To fix the model into the tunnel, the floor of the model (Figure 5-4c and d) is made up of a large circular plane which includes:

- one block, making it possible to place the model always at the same location, with a defined angle from  $0^\circ$  to  $360^\circ$  in relation to the axis of the tunnel;
- two clamps to fix the model into the wind tunnel and prevent it from moving during a test.

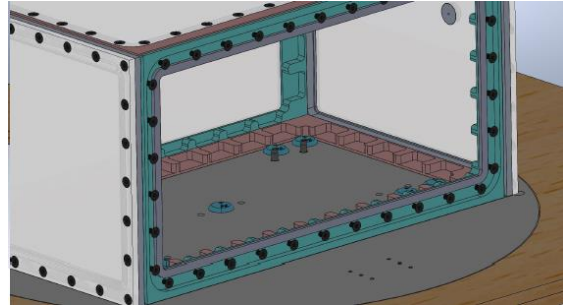
To allow accurate measurement of physical parameters inside the model, the floor of the model includes:

- 2 taps (Figure 5-4b) to which we can connect flexible tubes to measure pressure differences or to supply air to pressurize the model and

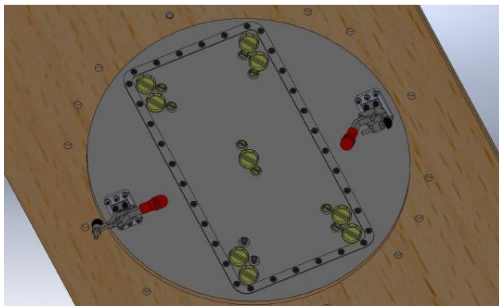
- 7 other circular (Figure 5-4d) airtight openings to insert a thermometer, for example. For each of the openings, a sealing system is used to ensure perfect airtightness when the opening is not used.



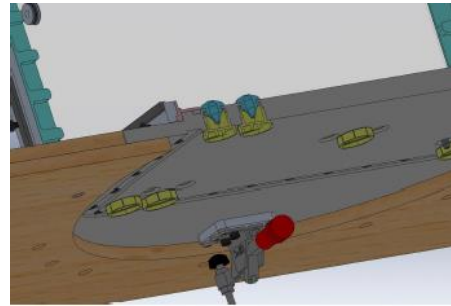
(a) Cylinders to be plugged



(b) 2 taps to connect flexible tubes



(c) Model floor



(d) Airtight openings on the model floor

Figure 5-4: Design drawings of the model

### 5.1.3 Specifications for the pressurization device

According to ISO 9972 [11], the lowest pressure difference is 10 Pa and the maximum required is 50 Pa; a pressure difference up to 100 Pa is recommended. In order to investigate the wind impact in various conditions, the pressurization device must therefore be able to:

- 1) Impose pressure differences from 10 to 100 Pa for all configurations of leak distributions and wind speeds of up to  $7 \text{ m s}^{-1}$ ;
- 2) Accurately measure the airflow rate that it will provide;
- 3) Fit into the reduced model.

The pressurization device should make it possible to perform a pressurization test in a similar way to a blower door. We evaluate the airflow rate that has to be provided by the pressurization device for different wind speeds at each of the pressure differences of the test sequence, for all configurations of leak distribution. In this study, we consider only steady wind. Equations (12) and (13) then become equations (49) and (50).

$$q_1 = C_{z,1} A_1 \sqrt{2 \frac{|\Delta p_1|}{\rho_0}} \quad (49)$$

$$q_2 = C_{z,2} A_2 \sqrt{2 \frac{|\Delta p_2|}{\rho_0}} \quad (50)$$

As the leaks are circular openings, we assume that the values of the discharge coefficients are  $C_{z,1} = C_{z,2} = 1.0$ . Regarding pressure difference evaluation, we consider the following wind pressure coefficients:  $C_{p,1} = 0.5$  and  $C_{p,2} = -0.7$  [105]. In steady conditions, the mass balance equation becomes equation (51).

$$q_{m,bd} + q_{m,1} + q_{m,2} = 0 \quad (51)$$

For each leak distribution configuration, each wind speed, and each pressure difference imposed by the pressurization device, we calculate the theoretical airflow provided by the pressurization device using successively:

- 1) equations (27) and (28) to determine the pressure differences at each opening;
- 2) equations (49) and (50) to determine the airflow through each opening;
- 3) equation (51) to determine the airflow rate provided by the pressurization device.

Table 5-2 gives the maximum and the minimum airflow rates that the pressurization device should provide corresponding to 100 Pa and 10 Pa pressure difference, respectively, depending on the leak distribution. The range of this airflow is also set to  $[3.0 \cdot 10^{-5}; 3.0 \cdot 10^{-4} \text{ m}^3 \text{ s}^{-1}]$ .

Table 5-2: Theoretical evaluation of airflow provided by the pressurization device depending on the leak distribution ratio

Leak distribution configuration*	90/10	80/20	70/30	60/40	50/50	40/60	30/70	20/80	10/90
$q_{bd,max} [\text{m}^3 \text{ s}^{-1}]$	$2.5 \cdot 10^{-4}$	$2.5 \cdot 10^{-4}$	$2.5 \cdot 10^{-4}$	$2.5 \cdot 10^{-4}$	$2.5 \cdot 10^{-4}$	$2.5 \cdot 10^{-4}$	$2.6 \cdot 10^{-4}$	$2.6 \cdot 10^{-4}$	<b><math>2.7 \cdot 10^{-4}</math></b>
$q_{bd,min} [\text{m}^3 \text{ s}^{-1}]$	<b><math>3.8 \cdot 10^{-5}</math></b>	$5.0 \cdot 10^{-5}$	$6.1 \cdot 10^{-5}$	$7.2 \cdot 10^{-5}$	$8.4 \cdot 10^{-5}$	$9.3 \cdot 10^{-5}$	$9.3 \cdot 10^{-5}$	$9.3 \cdot 10^{-5}$	$9.3 \cdot 10^{-5}$

\*windward leak area / leeward leak area [% total area]

#### 5.1.4 Design of the wind tunnel

Standard ISO 9972 indicates that for a meteorological wind speed above  $6 \text{ m s}^{-1}$  the zero-flow pressure difference requirement (one of the requirements defined in this standard for performing such a test) is unlikely to be respected. To evaluate the relevance of this requirement, the wind speed will vary from 0 to at least  $7 \text{ m s}^{-1}$ . The wind tunnel has therefore been sized to provide a steady wind from 0 to at least  $7 \text{ m s}^{-1}$  in the test chamber. With this range of wind speed, the wind tunnel is a “Low-speed wind tunnel” [106]. The wind tunnel is then designed according to the methodology explained by Stefano et al. [107]. It includes five components which will be described in this section:

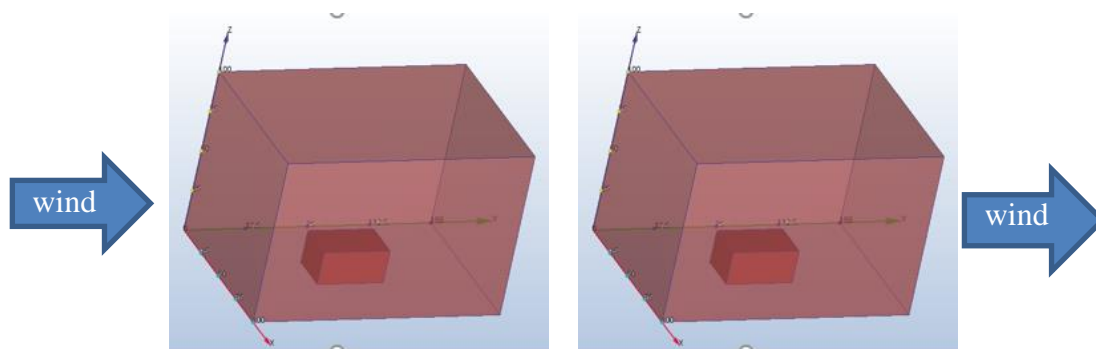
- 1) a settling chamber with a honeycomb and 2 screens;
- 2) a contraction component;

- 3) a test chamber;
- 4) a diffuser;
- 5) a fan.

#### 5.1.4.1 Testing chamber (TC) design

The area of the cross-section of the testing chamber is  $1.0 \times 1.0 \text{ m}^2$  to fit into the laboratory. To easily install the model and different sensors, we set the length of the TC to 1.5 m. This respects the condition given by Stefano et al.: the length should be between 0.5 and 3 times the hydraulic diameter of the TC (1 m). To validate the size of the testing chamber, we carried out a simplified CFD simulation to compare the wind velocity fields and the pressure fields for a real scale house and for the model in the TC. For these simulations, the air is provided into the wind tunnel at the velocity of  $4 \text{ m s}^{-1}$  and  $12 \text{ m s}^{-1}$ . We studied three different situations:

- Case 1: represents a house on a full scale, away from any obstacle. This case is the reference case (only at  $12 \text{ m s}^{-1}$ );
- Case 2: represents the model inside the testing chamber of the wind tunnel. Air is blown into the testing room, which corresponds to wind blowing on a house (Figure 5-5 (a));
- Case 3: represents the model inside the testing chamber of the wind tunnel. Air is attracted into the testing room, which corresponds to the wind direction in our wind tunnel (the fan will be installed at the end of the testing chamber) (Figure 5-5 (b)).



(a) Wind source in case 2

(b) Wind source in case 3

Figure 5-5: Representation of CFD configurations in reduced scale - Case 2 and case 3

The results of the CFD simulations given in Figure 5-7 ( $12 \text{ m s}^{-1}$ ) and Figure 5-6 ( $4 \text{ m s}^{-1}$ ) are the wind velocity and static pressure values for a horizontal plane with a height of 20 cm.

Both for static pressure and wind velocity fields, the CFD simulations show no significant difference between the full scale house without nearby obstacles and the model installed in the wind tunnel. The walls of the wind tunnel should therefore not induce significant perturbations on the wind velocity and static pressure around the model. We also observe

that when the wind is attracted at the end of the tunnel, the drop of speed after the model is less important than when the wind is blown at the entrance of the wind tunnel. Therefore, we will need to verify with experimental measurements that the wind velocity field after the model is not too disrupted by the position of the fan at the end of the wind tunnel.

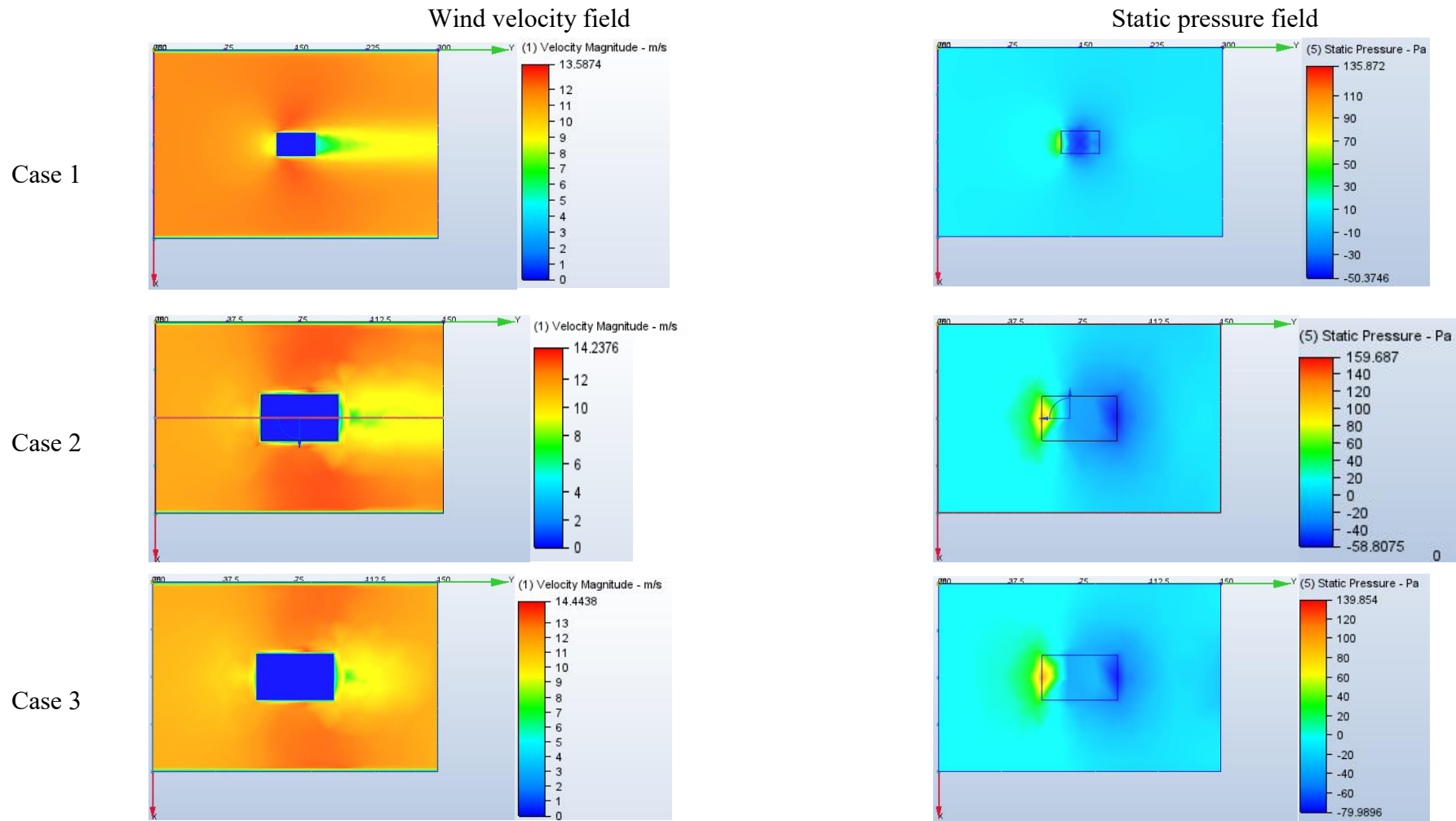


Figure 5-6: CFD simulations results for wind velocity and static pressure fields with an input wind speed of  $12 \text{ m s}^{-1}$

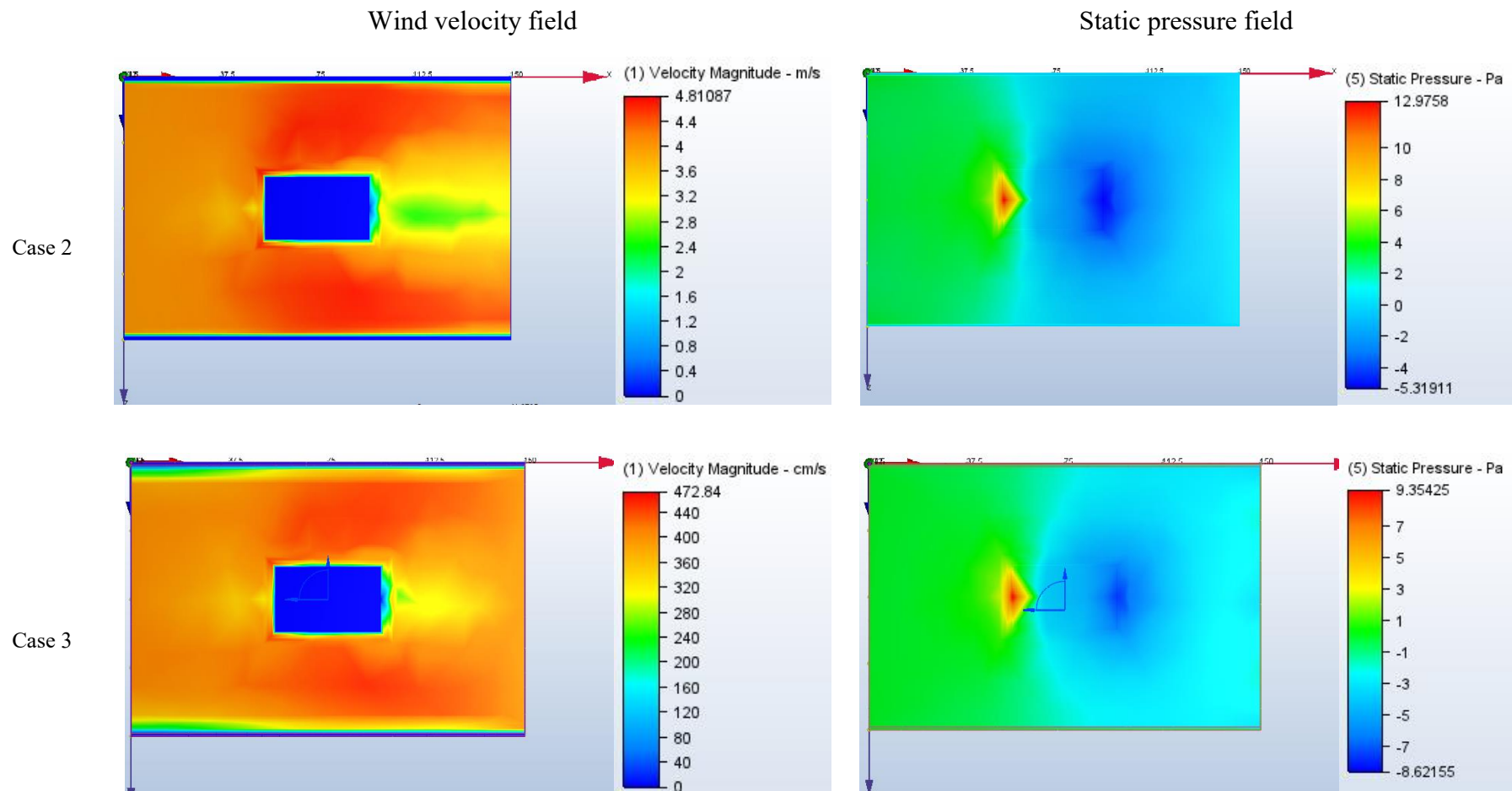


Figure 5-7: CFD simulations results for wind velocity and static pressure fields with an input wind speed of  $4 \text{ m s}^{-1}$

### 5.1.4.2 Contraction design

The contraction component serves to 1) accelerate the flow in the TC and 2) provide a flow inside the TC with a uniform velocity profile. Firstly, the ratio between the cross-section areas of the contraction component should be in the range 4-6 [108] for a TC whose cross-section is greater than 0.5 m. For considerations of space, we designed a contraction component with a ratio of 4; this leads to an upstream cross-section of 2.0\*2.0 m<sup>2</sup>. The theoretical shape of the contraction component is given by the Bell-Metha fifth-order polynomials [109]. However, due to the difficulties of fabricating a curved shape, we need to simplify the contraction by using inclined planes. We tested several slopes with CFD calculations, from 25° to 45° (Figure 5-8(b) to (f)), to compare the velocity profiles of the airflow in the TC cross-section between the Bell-Metha form and the simplified shapes. Figure 5-9 shows the dispersion of the estimated velocity values in the flow direction at 8 points of the test section depending on the form of the contraction component. We selected the 30° simplified contraction component because it offers an acceptable compromise between a small deviation in the velocity field in the flow direction (less than 3% discrepancy from the Bell-Mehta form) and because it is not difficult to fabricate.

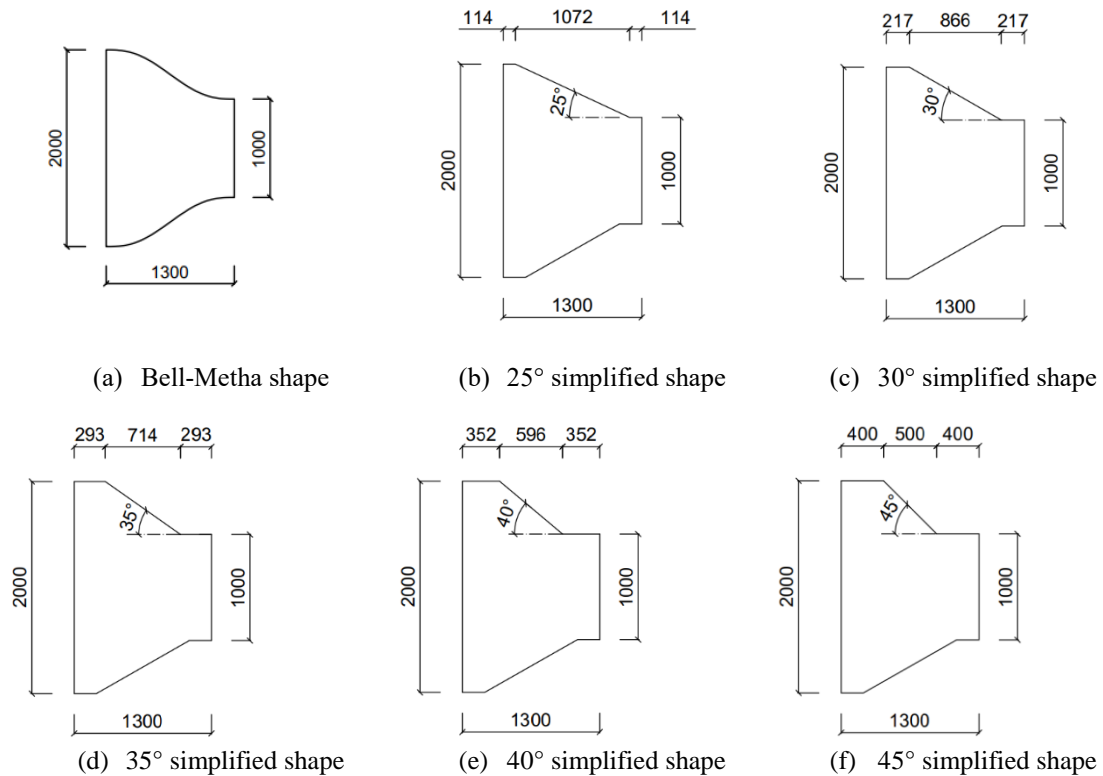


Figure 5-8: Different shapes tested for the contraction component

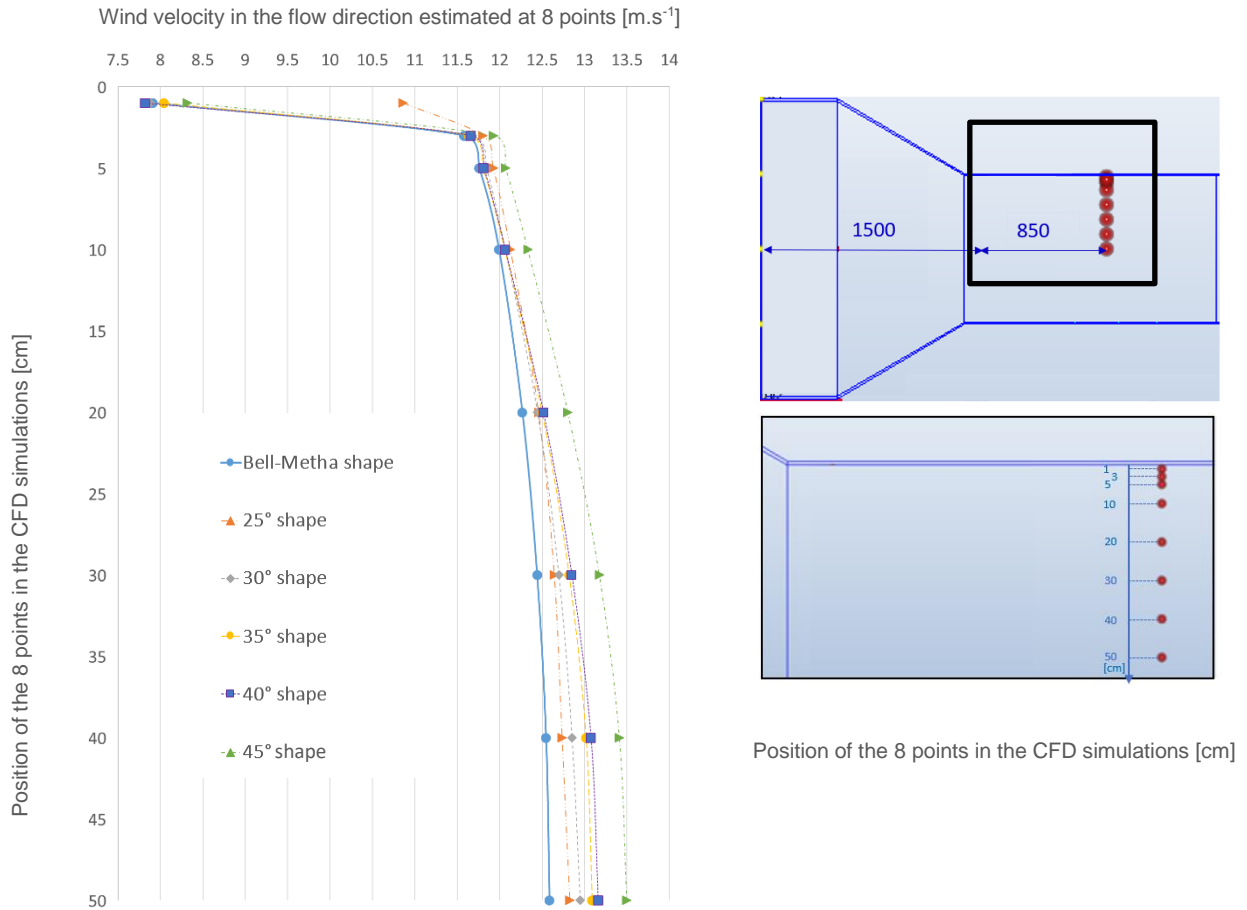


Figure 5-9: Wind velocity field inside the wind tunnel for different shapes of contraction component

#### 5.1.4.3 Settling chamber design

The cross-section of the settling chamber is equal to the maximal cross-section of the contraction  $2.0 \times 2.0 \text{ m}^2$ . The settling chamber includes a honeycomb and two screens; each of these components is  $2.0 \times 2.0 \text{ m}^2$ . The wind tunnel includes a honeycomb made of aluminium with the following characteristics:

- 1) honeycomb diameter = 6 mm;
- 2) sheet thickness = 0.7 mm;
- 3) length = 45 mm;
- 4) cross-section =  $2.0 \times 2.0 \text{ m}^2$ .

The porosity of the honeycomb is 0.8 (minimum value = 0.8 [107]) and the ratio between length and hydraulic diameter is 7.5, complying with the range of 6-8 as recommended by [107].

According to Prandtl [110], it is more efficient to have a series of screens with different porosities. Their porosity has to be between 0.58 and 0.8. This wind tunnel includes two types of perforated plates: one made of galvanized steel with a porosity of 0.64 and one made of steel with a porosity of 0.74.

#### 5.1.4.4 Diffuser and fan design

To produce wind speeds up to  $7 \text{ m s}^{-1}$  in the testing chamber, the fan will need to provide a maximum airflow rate equal to  $25,200 \text{ m}^3 \text{ h}^{-1}$ . The wind tunnel includes an axial fan with a maximum airflow rate which can reach around  $43,000 \text{ m}^3 \text{ h}^{-1}$ , depending on the pressure drop. This fan can be controlled with a frequency converter. Its diameter is equal to 1.0 m. As the diameter of the fan corresponds to the size of the testing chamber, there is no minimum length for the diffuser.

#### 5.1.4.5 Final design of the wind tunnel

Figure 5-10 shows the key components of the wind tunnel which is 4.11 m long with a maximal cross-sectional area of  $4.0 \text{ m}^2$  for the settling chamber and  $1 \text{ m}^2$  for the test chamber.

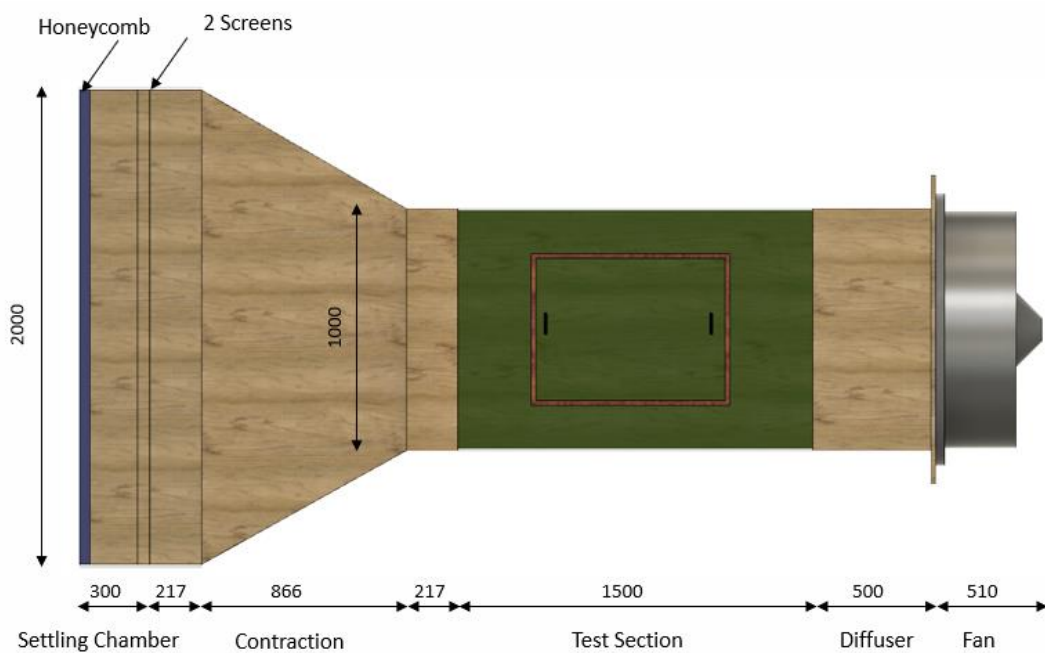
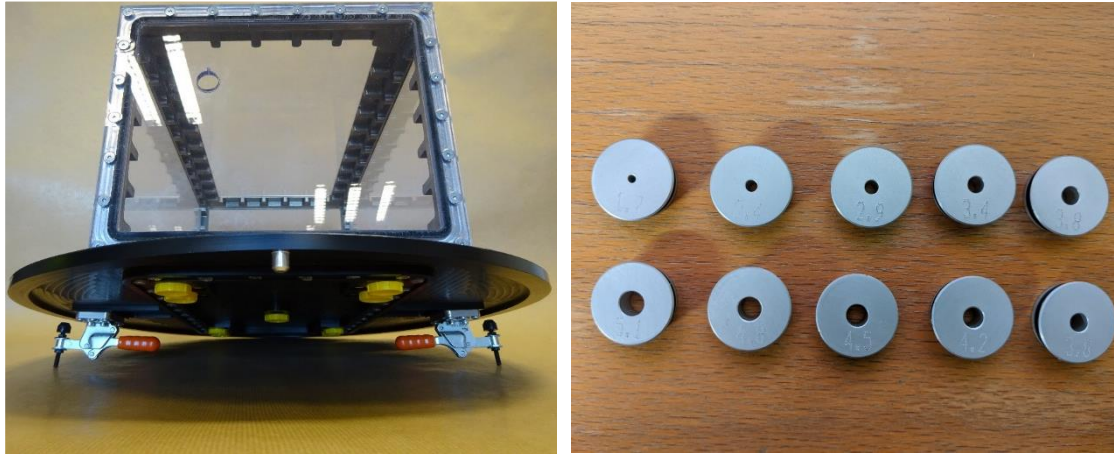


Figure 5-10: Final dimension of wind tunnel [in mm]

## 5.2 Results: experiment facility Installation, validation, and lessons for ISO 9972 protocol implementation

### 5.2.1 Installation of the experiment facility

Figure 5-11 shows the final model (a) with some of the metallic openings (b).



(a) Final reduced model

(b) Metallic openings

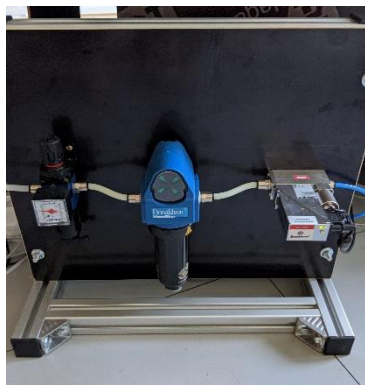
Figure 5-11: Final reduced model

The pressurization device includes a flow controller (Figure 5-12a) that meets the design requirements: it provides airflow rates from  $0.4 \text{ l min}^{-1}$  to  $100 \text{ l min}^{-1}$  ( $6.7 \cdot 10^{-6} \text{ m}^3 \text{ s}^{-1}$  to  $1.7 \cdot 10^{-3} \text{ m}^3 \text{ s}^{-1}$ ) and its uncertainty is  $\pm 5\%$  of the measured value  $\pm 0.096 \text{ l min}^{-1}$  ( $1.6 \cdot 10^{-6} \text{ m}^3 \text{ s}^{-1}$ ). As the flow controller can only supply air and not exhaust air, our experimentation will only include pressurization tests. For a real building, there is often a significant difference between pressurization results and depressurization results, especially due to the existence of valve effect in the walls. Due to the nature of the walls of our model, we do not expect any difference. Performing tests only on pressurization should not induce a significant bias in our results.

Another difference between our pressurization device and a blowerdoor is that our device will not be placed on the envelope on the model. For real building, the blowerdoor is placed either on the entrance door or another external door. Thus, the wind impacts not only the envelope including the leaks but also the fan of the pressurization device. This impact depends on the characteristic of each fan pressurization device, and the quantification of this impact comes under the responsibility of the manufacturer. Our pressurization device will be connected directly on the model floor: in this way, the wind will not have any impact on it and the error we will evaluate will only be due to the impact of the wind on the model envelope.

The flow controller is connected to a compressor (Figure 5-12b) that provides air at  $3.0 \times 10^5 \text{ Pa}$ . The flow controller is managed using the LabVIEW environment (Figure 5-13). The application we developed defines the target airflow supplied in the model

depending on the pressure difference measured by a manometer (Figure 5-12c). The LabVIEW interface is connected to the flow controller, the manometer, the frequency driver of the wind tunnel ventilator, anemometers, and temperature sensors. The LabVIEW application is called by a VBA program (Figure 5-14) to reproduce pressurization tests in repeatability conditions for different wind speeds. Figure 5-15 shows the wind tunnel. The wind tunnel is installed in a 4,60x6,75 m<sup>2</sup> dedicated room. The wall behind the settling chamber of the wind tunnel is more than 1 m away from the honeycomb, which respects a half diameter limit to provide his impact on the flow inside the wind tunnel.



(a) Airflow controller



(b) Compressor



(c) Manometer

Figure 5-12: Pressurization device for reduced scale test

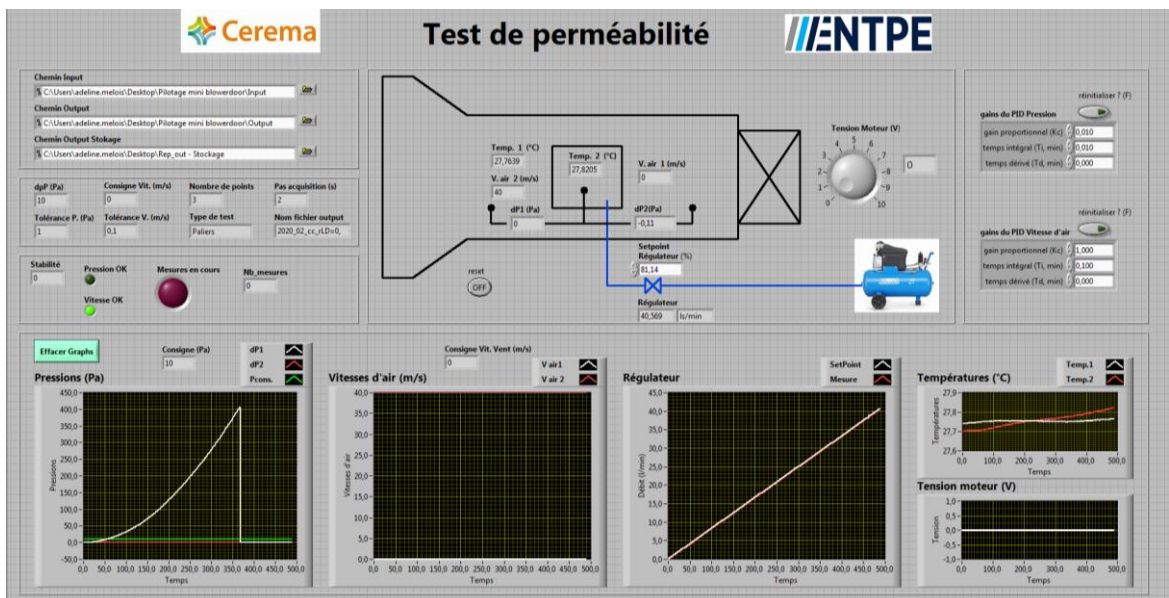


Figure 5-13: LabVIEW interface

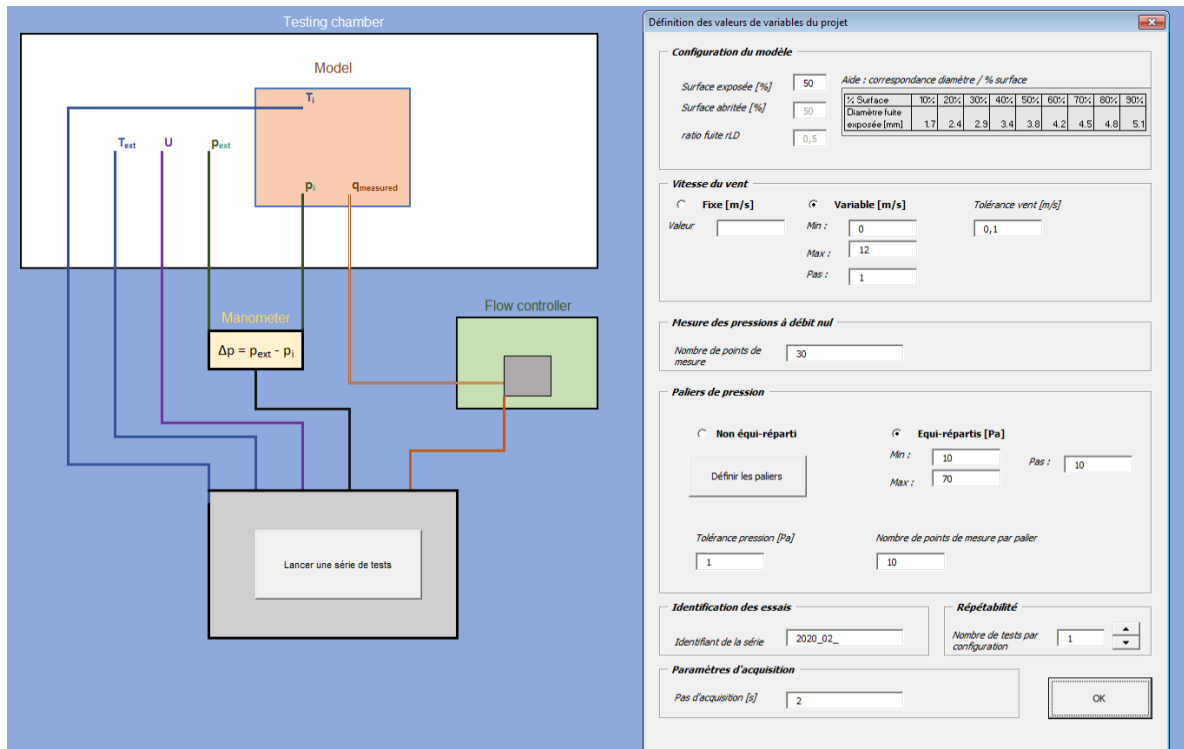


Figure 5-14: VBA program interface for fan pressurization tests

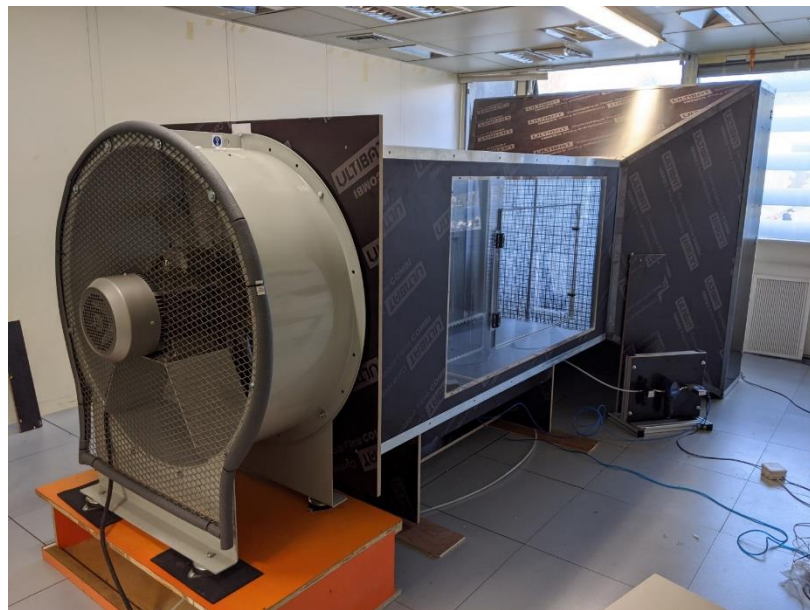


Figure 5-15: Installed wind tunnel

### 5.2.2 Validation of the model characteristics

The model has to behave like a real building during a pressurization test. This section presents the results of the characterization of the following parameters:

- 1) the airtightness of the model for all leakage distributions;

- 2) the airflow through each opening;
- 3) the pressure coefficient on both the windward and the leeward facades at the opening sites.

#### 5.2.2.1 Airtightness of the model for all leakage distributions

We first evaluate the airtightness of the model without deliberate leaks by subjecting the model to a pressure difference  $\Delta p=200$  Pa, then analyzing the changes in pressure inside the model when pressurization stops. Figure 5-16 compares the decrease of the pressure inside the model without deliberate leaks to the decrease with the smallest deliberate leak: a 1.7 mm diameter leak. With only the smallest leak, the pressure inside the building drops from 200 Pa to 0 Pa in less than 4 seconds. Without any deliberate leak, it takes around 12 minutes to drop from 200 Pa to 10 Pa. This test shows that the model frame is extremely airtight.

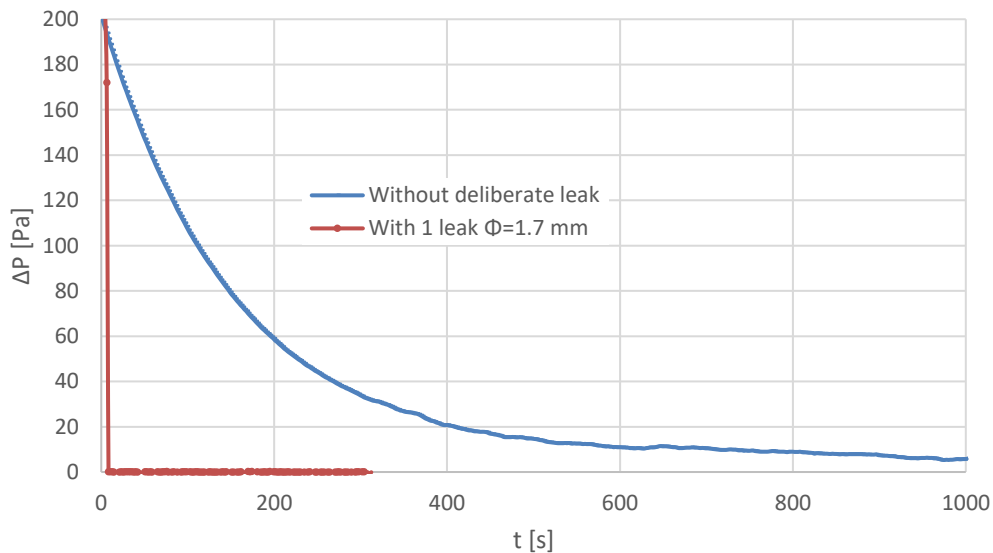


Figure 5-16: Characterization of the airtightness of the model without deliberate leaks and with the smallest leak- Observation of the pressure decrease inside the model

We then evaluate the airtightness of the model with the two openings for the nine configurations of leakage distributions using two methods. First of all, we perform tests without wind according to ISO 9972 with pressure sequences from 10 to 100 Pa. For each test, we calculate the  $q_4$  of the model (Table 5-4). These values will be used as the reference airleakage of the model: the error due to wind will be evaluated from these references. The evaluation of these references therefore has to be as accurate as possible. However, the pressurization method used in the ISO 9972 induces some uncertainties, even with no wind in controlled laboratory conditions. To assess these reference values, we then perform another series of measurements directly at 4 Pa. As we perform the tests in laboratory conditions, the environmental conditions were controlled and it was therefore possible to impose 4 Pa exactly, which is not possible in real conditions. For

each configuration, we therefore directly measured a second value for  $q_4$  by imposing a difference of 4 Pa between the inside and the outside of the model, and measured the airflow rate provided by the pressurization device to maintain the 4 Pa difference (Table 5-4). We also evaluate  $q_{50}$  of the model from both methods (Table 5-4): tests performed according to ISO 9972 and tests performed directly at 50 Pa. For all configurations, the  $q_4$  values obtained with both methods are similar: the maximum difference is  $0.007 \text{ m}^3 \text{ h}^{-1}$  which represents 4%. For all configurations, the average value for  $q_4$  is  $0.168 \text{ m}^3 \text{ h}^{-1}$  with ISO 9972 and  $0.167 \text{ m}^3 \text{ h}^{-1}$  with the direct measurement at 4 Pa. For all configurations, the  $q_{50}$  values obtained with both methods are also similar: the maximum difference is  $0.003 \text{ m}^3 \text{ h}^{-1}$  which represents 0.5%. For all configurations, the average value for  $q_{50}$  is  $0.631 \text{ m}^3 \text{ h}^{-1}$  with ISO 9972 and  $0.632 \text{ m}^3 \text{ h}^{-1}$  with the direct measurement at 50 Pa. These values correspond to an effective leakage area  $\text{ELA}_4 = 1.8 \cdot 10^{-5} \text{ m}^2$ . This is significantly smaller than the value used to design the model ( $2.27 \cdot 10^{-5} \text{ m}^2$ ). This may be due to the limit of accuracy during the manufacturing of the leaks or to the lower discharge coefficient than assumed in the design calculation.. The model is therefore more airtight. As the airtightness level does not significantly influence the impact of the wind during measurements, this difference between designed airtightness and real airtightness of the model will not have an impact on future experiments, but the real value will be used in calculations.

Table 5-3: Evaluation of the real  $q_4$  value of the model without wind with the same designed  $q_4$  for all configurations

<b>r<sub>LD</sub></b>	<b>q<sub>4</sub> (ISO 9972 test)</b> [m <sup>3</sup> h <sup>-1</sup> ]	<b>q<sub>4</sub> (direct measurement @4Pa)</b> [m <sup>3</sup> h <sup>-1</sup> ]	<b>Difference between results from both methods</b> [m <sup>3</sup> h <sup>-1</sup> ]
<b>0.1</b>	0.175	0.170	0.005
<b>0.2</b>	0.167	0.167	0
<b>0.3</b>	0.163	0.163	0
<b>0.4</b>	0.166	0.167	-0.001
<b>0.5</b>	0.172	0.165	0.007
<b>0.6</b>	0.166	0.167	-0.001
<b>0.7</b>	0.163	0.163	0
<b>0.8</b>	0.167	0.167	0
<b>0.9</b>	0.175	0.170	0.005
<b>average</b>	0.168	0.167	0.001

Table 5-4: Evaluation of the real  $q_{50}$  value of the model without wind with the same designed  $q_{50}$  for all configurations

<b>r<sub>LD</sub></b>	<b>q<sub>50</sub> (ISO 9972 test)</b> [m <sup>3</sup> h <sup>-1</sup> ]	<b>q<sub>50</sub> (direct measurement @50Pa)</b> [m <sup>3</sup> h <sup>-1</sup> ]	<b>Difference between results from both methods</b> [m <sup>3</sup> h <sup>-1</sup> ]
<b>0.1</b>	0.631	0.629	0.002
<b>0.2</b>	0.632	0.635	-0.002
<b>0.3</b>	0.627	0.629	-0.002
<b>0.4</b>	0.636	0.638	-0.002
<b>0.5</b>	0.622	0.623	-0.001
<b>0.6</b>	0.638	0.640	-0.002
<b>0.7</b>	0.627	0.627	-0.001
<b>0.8</b>	0.632	0.635	-0.003
<b>0.9</b>	0.632	0.631	0.001
<b>average</b>	0.631	0.632	0.001

### 5.2.2.2 Airflow through each opening

To characterize the flow through each of the openings, we performed pressurization tests on the model with only one opening, without wind. With the two smallest openings, the model was too airtight: it was not possible to induce pressure differences of less than 200 Pa which is the saturation point of the manometer. For each of the other openings, we performed a pressurization test according to ISO 9972 on the model with only one opening. We then characterized the flow coefficient C and the flow exponent of each of these openings. For each opening, Table 5-5 gives the designed values for the diameter, C and n, and the experimental values (the experimental value for the diameter is evaluated from experimental values of C and n, that are used to calculate the leakage area and therefore the opening diameter assuming  $C_{z,1}=C_{z,2}=1$ ).

Table 5-5: Measured characteristics of seven openings

Designed values			Experimental values		
Diameter [10 <sup>-3</sup> m]	Flow exponent n [-]	Flow coefficient C [m <sup>3</sup> s <sup>-1</sup> Pa <sup>-n</sup> ]	Diameter [10 <sup>-3</sup> m]	Flow exponent n [-]	Flow coefficient C [m <sup>3</sup> s <sup>-1</sup> Pa <sup>-n</sup> ]
2.4	0.50	5.8 10 <sup>-6</sup>	2.5	0.54	5.6 10 <sup>-6</sup>
2.9	0.50	8.5 10 <sup>-6</sup>	3.0	0.53	8.3 10 <sup>-6</sup>
3.4	0.50	1.2 10 <sup>-5</sup>	3.4	0.53	1.1 10 <sup>-5</sup>
3.8	0.50	1.5 10 <sup>-5</sup>	3.8	0.52	1.4 10 <sup>-5</sup>
4.2	0.50	1.8 10 <sup>-5</sup>	4.1	0.51	1.7 10 <sup>-5</sup>
4.5	0.50	2.0 10 <sup>-5</sup>	4.4	0.50	1.9 10 <sup>-5</sup>
5.1	0.50	2.6 10 <sup>-5</sup>	5.0	0.49	2.5 10 <sup>-5</sup>

### 5.2.2.3 Pressure coefficients on both the windward and the leeward facades

At one point of an external facade, the pressure coefficient depends on the wind speed, the reference pressure, and the pressure at this point according to equation (52).

$$C_p = \frac{2(p_i - p_{ref})}{\rho_0 U^2} \quad (52)$$

To evaluate the  $C_p$  value for both openings of the model, the pressure difference between inside the model and an external reference located in the TC has been measured for all wind speeds in the following configurations:

- a single 5.1 mm leak on the windward facade;
- a single 10 mm leak on the windward facade;
- a single 5.1 mm leak on the leeward facade;
- a single 10 mm leak on the leeward facade.

For each configuration, Figure 5-17 presents the  $C_p$  values evaluated according to equation (52). The mean value for the  $C_p$  at the windward (respectively leeward) opening site is 0.42 (respectively -0.57). The order of magnitude of this  $C_p$  values is consistent with the values given by Liddament [104]: +0.4 for the average value on the windward façade and -0.3 for the average value on the leeward façade.

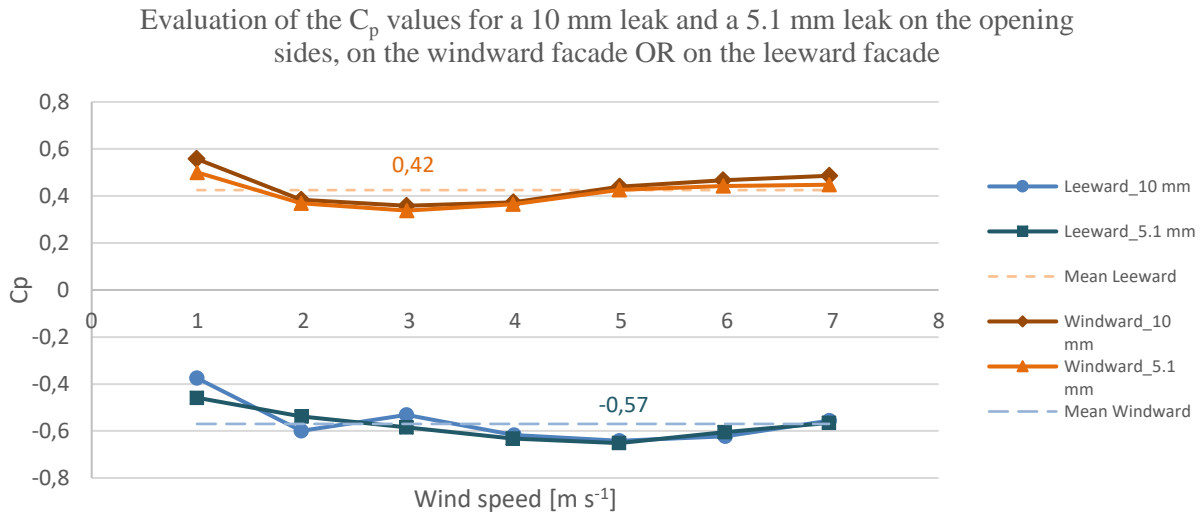


Figure 5-17: Evaluation of the  $C_p$  values on the opening site

### 5.2.3 Wind speed field in the testing chamber

The wind speed can be stabilized below  $1 \text{ m s}^{-1}$  in the testing chamber and the maximum stabilized speed is  $7.5 \text{ m s}^{-1}$ . We performed velocity measurements at 32 equally spaced locations covering the whole testing chamber (one point every  $0.20 \text{ m}$ ) to assess the homogeneity of the wind speed inside the testing chamber of the wind tunnel. We measured the wind velocity at  $0.25 \text{ m}$  from the ground of the testing chamber, for different wind speed configurations, for  $1 \text{ min}$  with  $1 \text{ point per second}$ , with a directional hot wire anemometer.

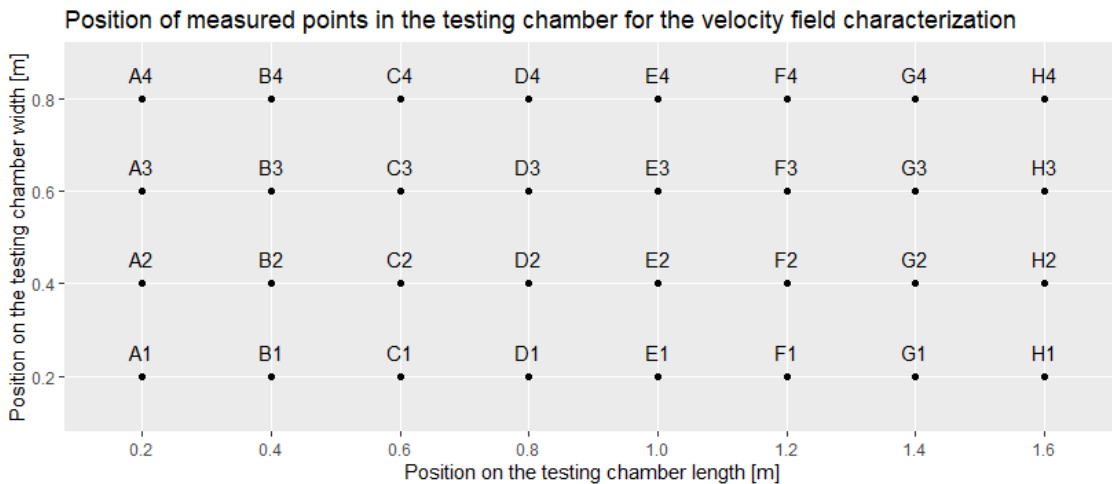


Figure 5-18: Plan of measured points for the evaluation of the velocity field in the testing chamber (low direction from A to H)

We first collect data for a low speed configuration: the mean wind velocity was  $0.83 \text{ m s}^{-1}$ . Figure 5-19 shows the distribution of the measured velocity for points A1 to E4 (for this first series of measurements, no data was collected for F1 to H4). The maximum standard deviation for the 20 locations during a one-minute measurement is  $0.008 \text{ m s}^{-1}$ : this result confirms the temporal stability of the wind speed for each location. Regarding

the 20 averaged values of wind speed, the minimum wind speed measured is  $0.82 \text{ m s}^{-1}$  and the maximal wind speed is  $0.84 \text{ m s}^{-1}$ : the maximal deviation of wind speeds in the test chamber is 3%.

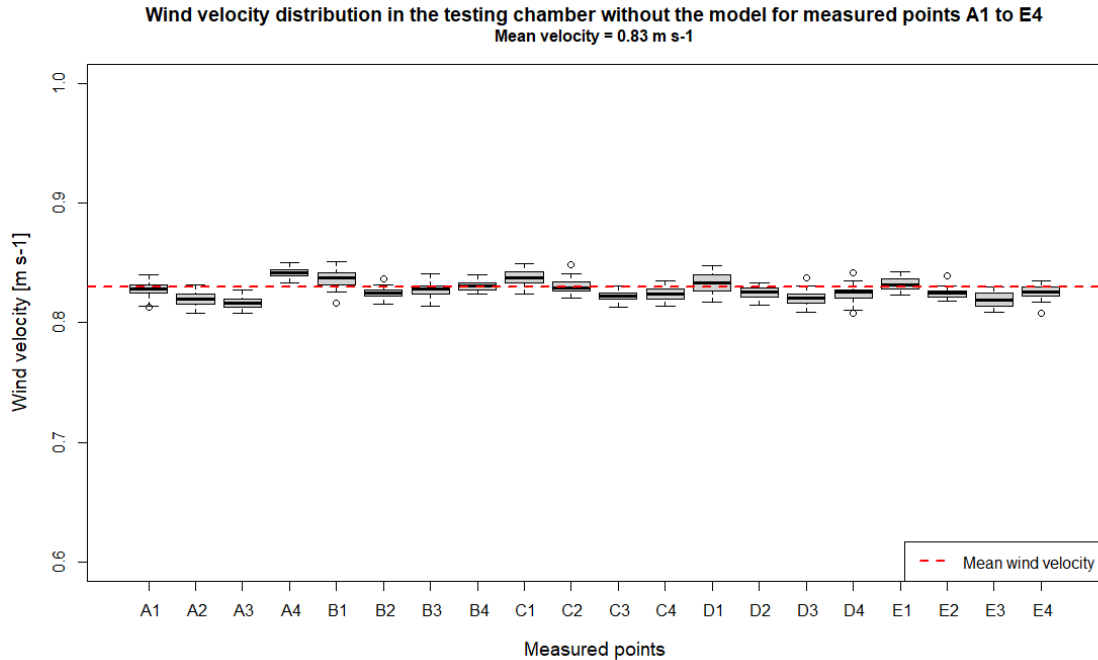


Figure 5-19: Distribution of the wind velocities in the testing chamber for a mean wind velocity =  $0.83 \text{ m s}^{-1}$

We then collect data for a higher speed configuration: the mean wind velocity was around  $4.5 \text{ m s}^{-1}$ . Because the measurements were performed in two days, the fan has been shut down in the middle of the series, the data has to be analyzed separately.

Figure 5-20 shows the distribution of the measured velocity for points A1 to E4, with a mean velocity =  $4.64 \text{ m s}^{-1}$ , and Figure 5-21 shows the distribution of the measured velocity for points E1 to H4, with a mean velocity =  $4.23 \text{ m s}^{-1}$ . The maximum standard deviation for the 28 locations during a one-minute measurement is  $0.09 \text{ m s}^{-1}$ : this result confirms the temporal stability of the wind speed for each location. Regarding the 28 averaged values of wind speed, the minimum wind speed measured is  $4.51 \text{ m s}^{-1}$  and the maximal wind speed is  $4.90 \text{ m s}^{-1}$  for the first serie (A1 to E4) and the minimum wind speed measured is  $4.08 \text{ m s}^{-1}$  and the maximal wind speed is  $4.44 \text{ m s}^{-1}$  for the second serie (E1 to H4). The maximal distribution of wind speeds in the test chamber is less than 9%.

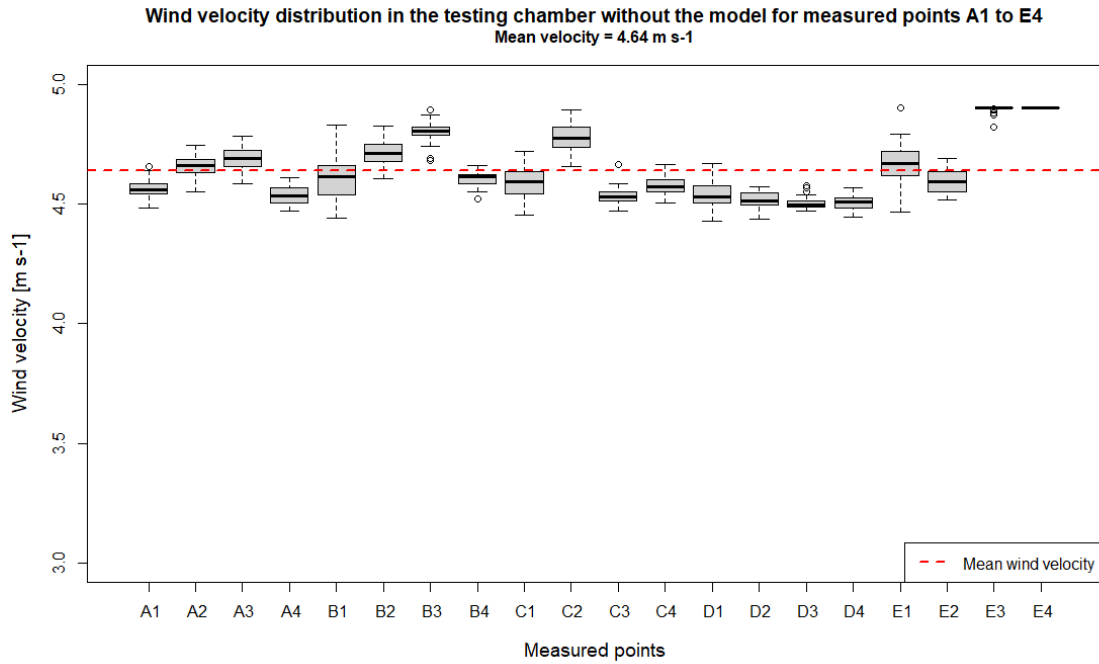


Figure 5-20: Distribution of the wind velocities in the testing chamber for a mean wind velocity = 4.64 m s<sup>-1</sup> – Points A1 to E4

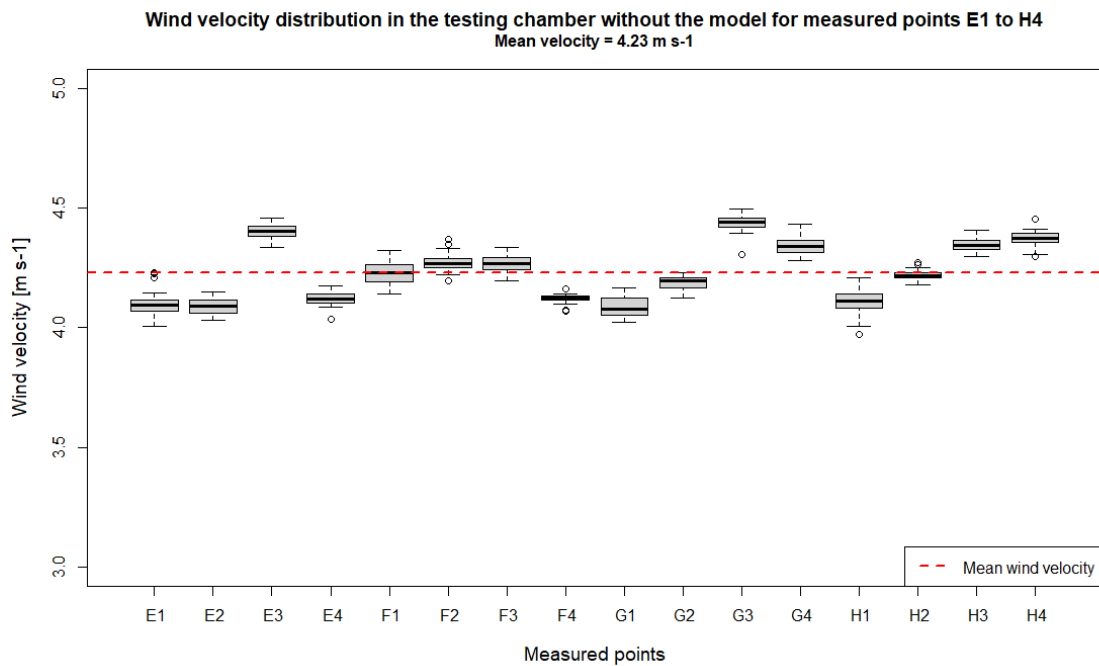


Figure 5-21: Distribution of the wind velocities in the testing chamber for a mean wind velocity = 4.23 m s<sup>-1</sup> – Points E1 to H4

We also analyze the wind velocity field in the testing chamber when the model is installed in the wind tunnel. Indeed, in section 5.1.4.1, we have evaluated the velocity speed with the model using CFD simulations to assess the similarity between a building in full scale and the model in the wind tunnel. We perform velocity measurements in 27 locations of the testing chamber (the model is installed on points D2, D3, E2 and E3), with 1 min per

location and 1 measurement per second. Figure 5-22 gives the measurements results for the 27 locations and Figure 5-23 proposes a representation of the mean wind velocities in the testing chamber. The maximum standard deviation for the 27 locations during a one-minute measurement is  $0.17 \text{ m s}^{-1}$ : the model does not impact the temporal stability of the wind speed for each location. On the contrary, the model affects significantly the homogeneity of the wind speed inside the testing chamber: we observe a minimal velocity of  $3.19 \text{ m s}^{-1}$  just before the windward facade and a maximal velocity of  $4.80 \text{ m s}^{-1}$  at the end of the testing chamber. The CFD simulations (section 5.1.4.1) showed inverse results, with lower downstream wind speeds. This difference may be due to the CFD simplification: the CFD model did not include the screens and the honeycomb of the wind tunnel. As CFD simulations include limits, we can not conclude regarding the perfect similarity between full scale velocity field and the velocity field in our tunnel. This will require experimental measurements on real buildings that are not included yet in our study.

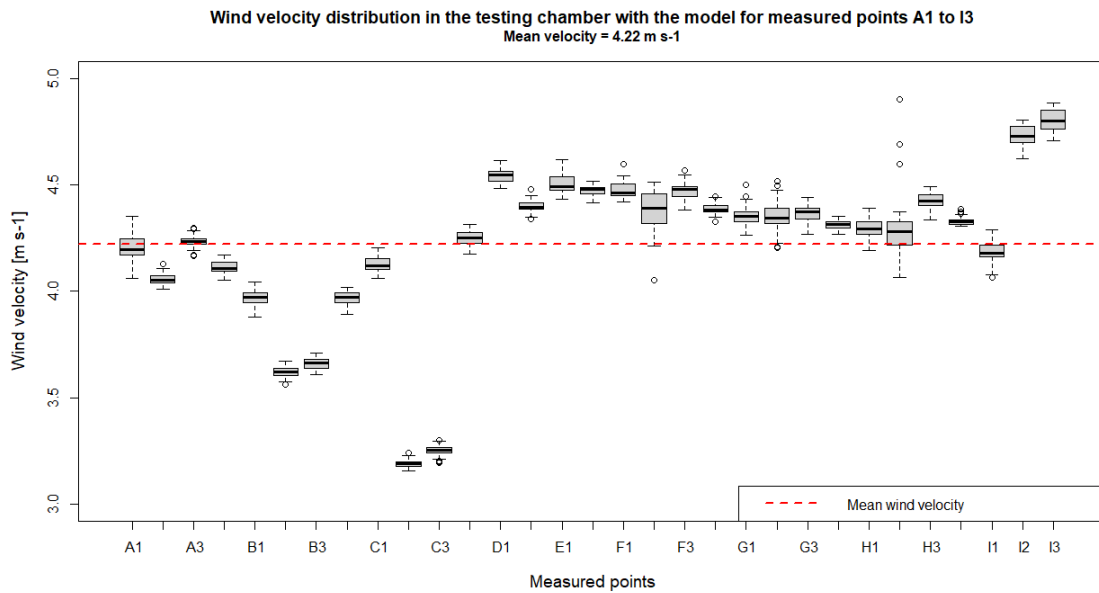


Figure 5-22: Distribution of the wind velocities in the testing chamber WITH the model for a mean wind velocity =  $4.22 \text{ m s}^{-1}$

Representation of mean wind velocities in the testing chamber (mean value =  $4.22 \text{ m s}^{-1}$ )  
 $[\text{m s}^{-1}]$

A1	B1	C1	D1	E1	F1	G1	H1	I1
4.21	3.97	4.13	4.54	4.51	4.48	4.36	4.30	4.18
A2	B2	C2	Model		F2	G2	H2	I2
4.06	3.62	3.19			4.38	4.35	4.30	4.73
A3	B3	C3			F3	G3	H3	I3
4.23	3.66	3.25			4.47	4.31	4.42	4.80
A4	B4	C4	D4	E4	F4	G4	H4	
4.11	3.97	4.25	4.40	4.47	4.39	4.31	4.33	

= Mean value     
   $\leq 90\%$  Mean value     
   $\geq 110\%$  Mean value

Figure 5-23: Representation of the mean wind velocities in the testing chamber for location A1 to I3, with model installed in the wind tunnel (mean velocity =  $4.22 \text{ m s}^{-1}$ )

#### 5.2.4 Pressure difference field in the testing chamber

During the design phase, we have also evaluated the pressure difference field in the testing chamber using CFD simulations (section 5.1.4.1). To study the pressure difference distribution around the model, we performed similar measurements as for velocity field: we measured the pressure difference between inside the testing chamber and a reference point outside the wind tunnel (inside the laboratory, i.e. protected of external environment) for 64 measured points distributed all around the model. Figure 5-24 shows the locations of the measured points in front of the leeward face (on the left of the picture), and along one lateral facade (on the bottom of the picture).

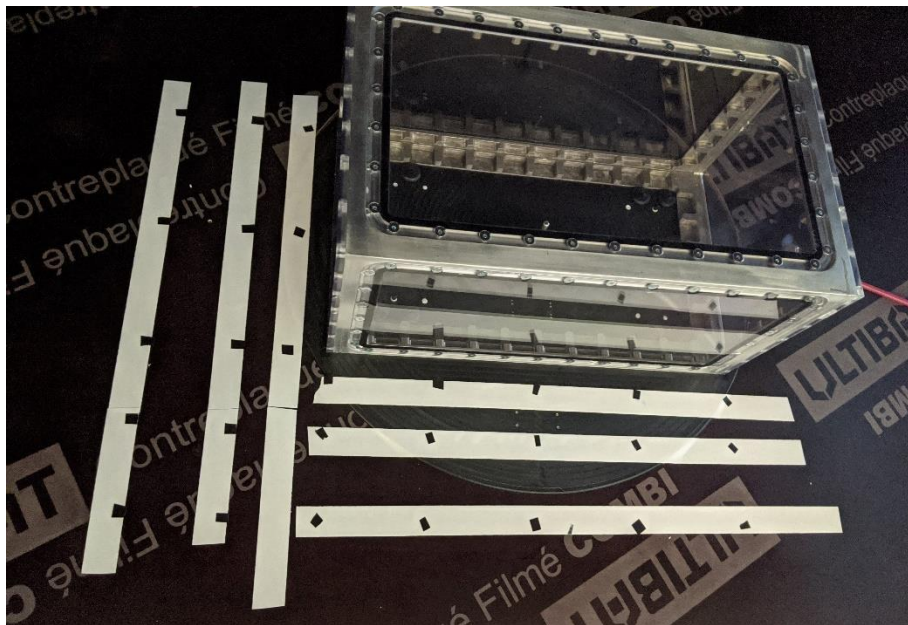


Figure 5-24: Locations of some measured points for the pressure difference field evaluation in the testing chamber

Figure 5-25 shows the distribution of the measured pressure differences for points A1 (upstream points) to Z6 (downstream points) for a mean pressure difference of  $-5.48 \text{ Pa}$ , which corresponds to a mean wind speed of  $4.0 \text{ m s}^{-1}$  in the testing chamber. The

maximum standard deviation for the 64 locations during a one-minute measurement is 0.63 Pa, and the maximal range for one point is less than 2 Pa: this result shows that pressure field in the testing chamber is not completely stable in time and thus the location of the reference and the duration of the measurement may have an influence on the test result.

Pressure difference distribution in the testing chamber with the model  
Mean pressure difference = -5.48 Pa

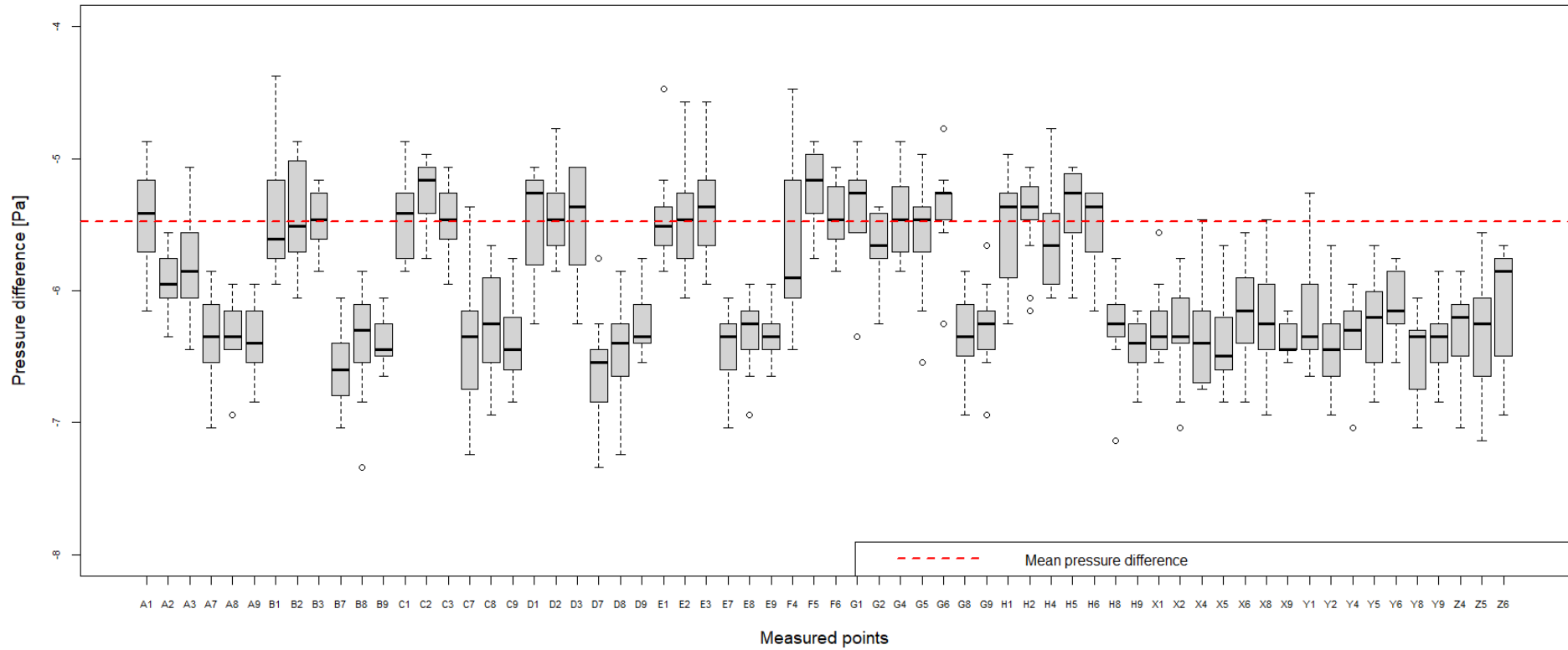


Figure 5-25: Distribution of the pressure differences in the testing chamber WITH the model  
for a mean pressure difference = -5.48 Pa

### 5.3 Conclusions

To evaluate the impact of the wind on building airtightness measurement, we have designed an experimental facility to reproduce pressurization tests on a reduced scale level. This facility includes a model that reproduces a single-zone building, a pressurization device that replaces a blower door, and a wind tunnel that reproduces steady wind conditions. The design phase was performed according to the similarity conditions that ensure that the experimental results on the reduced scale will be consistent with physics that occurs on a full scale.

The model is scalable and provides nine configurations of leakage distribution between windward and leeward façades, with the same averaged total airtightness for all configurations  $q_4=0.17 \text{ m}^3 \text{ h}^{-1}$ . The airflow through each leak has been characterized and corresponds to turbulent airflows ( $n=0.5$ ). The model includes movable façades and openings: the model can be developed to include more openings and openings with different shapes and materials. The values of the pressure coefficient evaluated on the windward and leeward façade correspond to the orders of magnitude given in the literature.

Our pressurization device includes a flow controller connected to a compressor that provides air at 3 bar. The flow controller is controlled by a LabVIEW program that defines the target airflow supplied in the model depending on the pressure difference measured by a manometer. The LabVIEW interface is connected to the flow controller, the manometer, the frequency driver of the wind tunnel ventilator, anemometers, and temperature sensors. The LabVIEW program is called by a VBA program to reproduce fan pressurization tests in repeatability conditions for different wind speeds.

The wind tunnel is 4.11 m long and includes a  $1.0*1.0*1.5 \text{ m}^3$  testing chamber. The wind speed inside the testing chamber is homogeneous and can be stabilized from less than  $1 \text{ m s}^{-1}$  to  $7.5 \text{ m s}^{-1}$ . The wind velocity inside the testing chamber are very stable in time and stable in space. Regarding the pressure differences, we observed significant variations through time depending of the location.

Therefore, we can reproduce pressurization tests according to ISO 9972 using our experiment facility, including pressure sequences from 10 to 100 Pa for different steady wind conditions and with 9 leakage distributions. We will first use our experimental facility to evaluate the uncertainty of the ISO 9972 protocol regarding the wind impact. We will then use it to test different developments of the protocol to reduce the impact of the wind. The facility can be used for other studies: the wind tunnel is already used to evaluate the impact of wind on water evaporation in new building components. Other applications regarding building measurements and ventilation device characterization are under development.

## 6. Evaluation of the impact of the wind during a pressurization measurement

In this section, we analyze the impact of the wind for nine configurations corresponding to the nine leakage distributions of our model. All results concern only steady wind conditions. All tests involve the same wind speeds and pressure differences we meet on full scale measurements, as we apply a scale ratio equal to 1 for these physical variables. Our model represents a simplified (2 leaks) single-zone detached house with a scale ratio equal to 1/25.

In this chapter, we first explain the ISO 9972 protocol we follow to reproduce pressurization tests including two requirements supposing limiting errors due to the wind: the zero-flow pressure difference and the pressure sequence range. In the second part, we analyze the impact of the wind on these two requirements. In the third part, we present the evaluation of the impact of the wind on test results according to ISO 9972 and we evaluate and compare the error due to wind for alternative analysis methods without any requirements such as the zero-flow pressure difference and the pressure sequence range. We focus in this chapter on three sources on uncertainty: the zero-flow pressure correction, the regression method and the variation in space of the pressure (see Figure 3-4).

### 6.1 Reproduction of pressurization tests

#### 6.1.1 Background of the air permeability measurement method

This part deals with airleakage measurement using the pressurization method as described in ISO 9972 [11]. All tests are performed in pressurization, with the same temperature inside and outside the model. They include the following steps complying with the ISO 9972:

- 1) A zero-flow pressure measurement is performed before and after the pressure sequence. Each measurement lasts 60 seconds (ISO 9972 requires at least 30 s) and includes at least 30 points (10 points minimum in the ISO 9972). The test is considered valid only if both the absolute zero-flow pressure differences measured before ( $|\Delta p_{0,1}|$ ) and after ( $|\Delta p_{0,2}|$ ) the pressure sequence are below 5 Pa as required in the ISO 9972. More specifically, the average of the positive values and the absolute average of the negative values must be below 5 Pa.
- 2) For the pressure sequence:
  - (a) the lowest pressure difference is at least 10 Pa or  $5\Delta p_0$ , whichever is the greater, with an allowance of  $\pm 3$  Pa;
  - (b) the highest pressure difference is 100 Pa;
  - (c) the increment is approximately 10 Pa;
  - (d) the sequence includes at least 5 approximately equally spaced stations;
  - (e) for each station, 10 measurements are performed;

- (f) each point of the pressure sequence lasts 20 seconds and includes 10 points (one point every 2 seconds). Recording starts when three successive measurements meet the pressure target  $\pm 1$  Pa and the wind speed target  $\pm 0.1$  m s<sup>-1</sup>.

Each pressure difference imposed during the pressure sequence is called “station”.

- 3) The pressure differences  $\Delta p_m$  measured during the pressure sequence are corrected using the zero-flow pressure difference according to equation (53).

$$\Delta p = \Delta p_m - \frac{\Delta p_{0,1} + \Delta p_{0,2}}{2} \quad (53)$$

with  $\Delta p_{0,1}$  (respectively  $\Delta p_{0,2}$ ) the average zero-flow pressure measured before (respectively after) the pressure sequence;

- 4) The airleakage coefficient  $C$  and the flow exponent  $n$  are calculated from a regression analysis applied to  $\ln(q)$  and  $\ln(\Delta p)$ , with  $q$  the corrected airflow rates during the pressure sequence.
- 5) The reference airflow rate is extrapolated at 4 Pa ( $q_4$ ) and 50 Pa ( $q_{50}$ ), using these  $\{C,n\}$  calculated values and the power law equation.

### 6.1.2 Automation of fan pressurization tests on the model

Pressurization tests on our model are performed with our measurement device including an airflow controller, a compressor and a manometer. We developed an automatic program that includes Labview applications and a VBA program to control our measurement device. The VBA program reproduces all steps of an airleakage measurement as described in section 6.1.1, but also controls the wind speed in the wind tunnel. The VBA program:

- defines the wind speed target;
- defines the number of tests per configuration of leakage distribution;
- for each configuration of leakage distribution, for each test:
  - o defines the input for the initial zero-flow pressure measurement, such as the number of measured points and the duration of the measurement, and runs the Labview application;
  - o reads the output from Labview, including 30 measurements for pressure difference and wind speed;
  - o for each pressure difference of the sequence:
    - defines the input for the measurement, including the pressure difference target and runs the Labview application;
    - reads the output from Labview, including 10 measurements for pressure difference, wind speed, and airflow measured by the flow controller;
  - o defines the input for the final zero-flow pressure measurement and runs the Labview application;
  - o reads the output from Labview, including 30 measurements for pressure difference and wind speed;
- record all output files.

Every time an input file is created, the Labview application performs a new measurement: it controls the manometer, the airflow controller, and the frequency driver of the wind tunnel ventilator according to the instruction it received by the VBA program, and records data from these sensors, the anemometer, and thermometers. Then it generates an output file that is recorded and read by the VBA program. The whole process is described in Figure 6-1.

When all steps are performed, output files are analyzed using an R program to evaluate the airleakage indicators  $q_4$  and  $q_{50}$ , according to either Annex C of ISO 9972 (ordinary least square method) or alternative methods described in part 6.4.

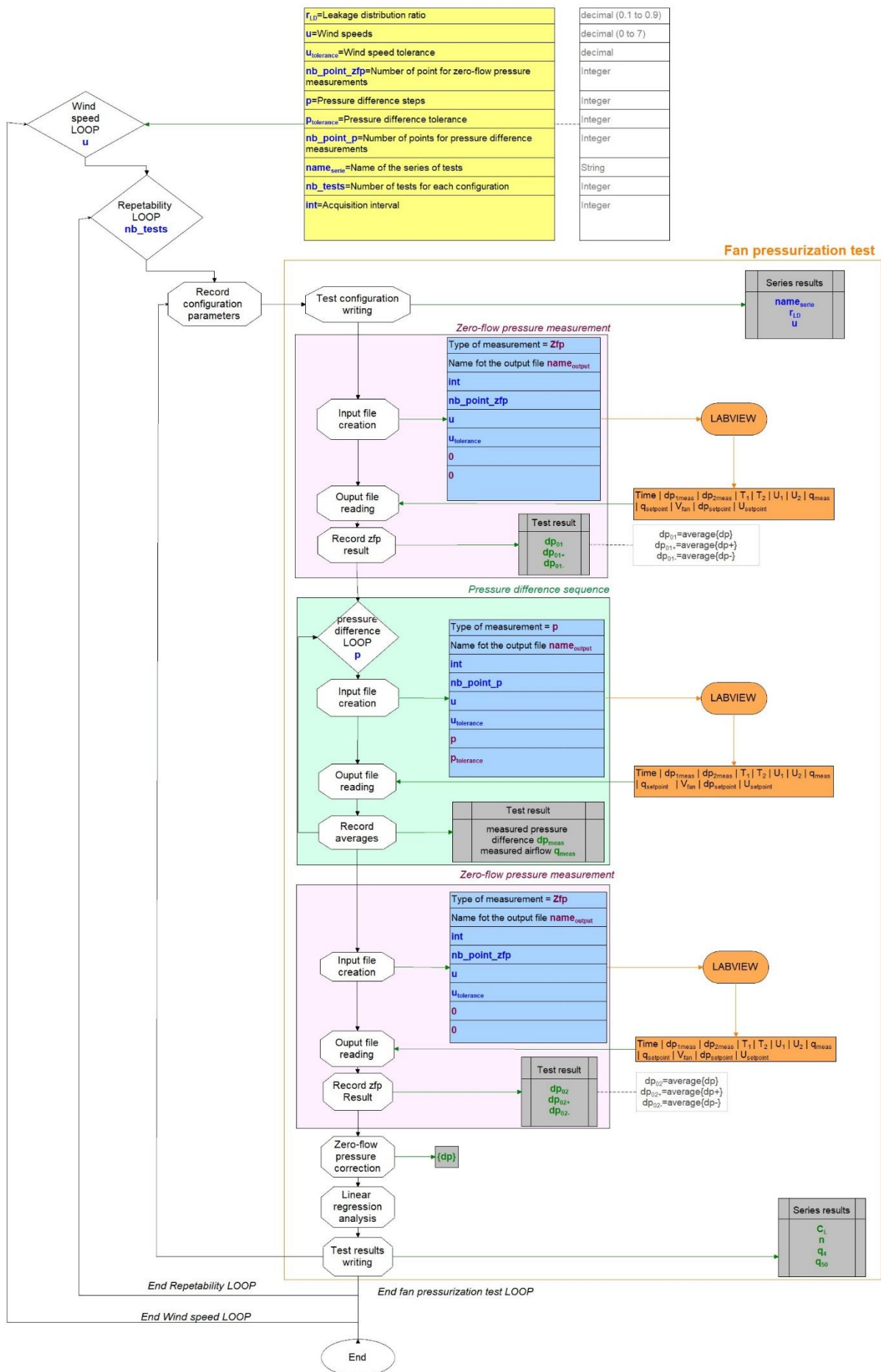


Figure 6-1: Representation of the fan pressurization automation - Scheme of the VBA program that gives instructions to Labview apps

### 6.1.3 *Experimental data presentation*

For the nine leakage distributions and for eight wind speeds (from 0 to 7 m s<sup>-1</sup>), we performed a pressurization test which includes:

- 2 zero-flow pressure measurements;
- up to 10 airflow-pressure measurements (from 10 to 100 Pa).

It corresponds to 96 measurements per configuration of leakage distribution. Thus, 864 measurements are performed and results are recorded in 864 files. Each file includes experimental data regarding:

- the target pressure difference;
- the target wind speed;
- the temperature inside the model;
- the temperature inside the wind tunnel (corresponding to outside the model);
- the wind speed inside the wind tunnel at the model height;
- the pressure difference between inside the model and inside the wind tunnel (corresponding to outside the model);
- The measured airflow rates provided by the airflow controller.

The next sections are dedicated to the analysis of these 864 files.

## **6.2 Impact of the wind on the zero-flow pressure**

### 6.2.1 *Zero-flow pressure difference depending on wind speed and leak distribution*

The zero-flow pressure difference is the indicator related to environmental conditions that validates the test. In our study, only the wind impacts the zero-flow pressure difference, depending also on the leak distribution. For each of the nine configurations of leakage distributions of the model, we measured the zero-flow pressure difference for wind speed from 0 to 7 m s<sup>-1</sup>. The external pressure tap is equipped with a T connector (Figure 6-2) to measure only static pressure. It is placed at the beginning of the testing chamber, on the floor, upstream the model. The internal pressure tap is located on the floor inside the model, away from the pressure device connector and the openings (Figure 6-3).



Figure 6-2: Location and nature of the external pressure tap

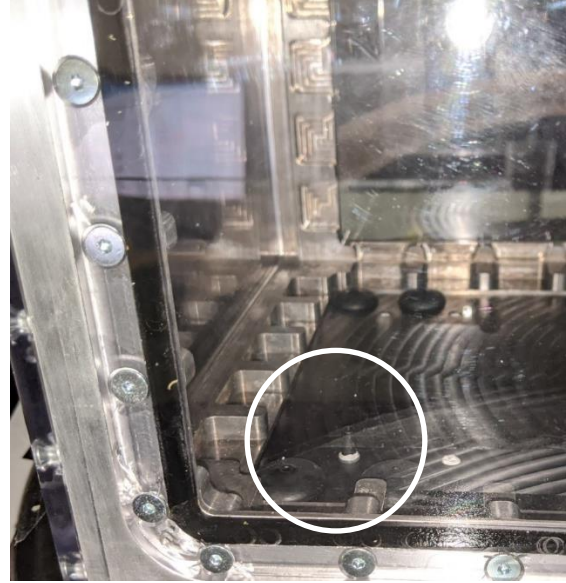


Figure 6-3: Location of the internal pressure tap

For each fan pressurization test, we measured an initial ( $\Delta p_{0,1}$ ) and a final ( $\Delta p_{0,2}$ ) zero-flow pressure differences, each lasts 60 seconds and includes 30 measurements. The zero-flow pressure difference ( $\Delta p_0$ ) is equal to the average of these measurements, according to equation (54).

$$\Delta p_0 = \frac{\Delta p_{0,1} + \Delta p_{0,2}}{2} \quad (54)$$

Figure 6-4 presents the zero-flow pressure differences for the 9 nine configurations of leakage distributions (with the leakage distribution  $r_{LD}=0.1$  to  $0.9$ ), for wind speeds up to  $7 \text{ m s}^{-1}$ . First of all, we see that for all configurations, the zero-flow pressure difference increases when the wind speed increases, which is consistent with physics laws. Secondly, when leaks are mostly located on the leeward side ( $r_{LD}=0.1$  to  $0.5$ ), the zero-flow pressure is negative whereas it becomes positive when most leaks are located on the wind facade ( $r_{LD}=0.6$  to  $0.9$ ). The ISO 9972 constraints concern the absolute value  $|\Delta p_0|$ , which must not exceed 5 Pa. We observe that:

- $|\Delta p_0|$  can be very high when the leakage is mostly located on the leeward façade. For  $r_{LD}=0.1$  and  $r_{LD}=0.2$ ,  $|\Delta p_0|$  is higher than 16 Pa at  $7 \text{ m s}^{-1}$ , which is more than three times the ISO 9972 threshold value 5 Pa. For these configurations, only tests performed with wind speeds less than  $3 \text{ m s}^{-1}$  meet this ISO 9972 requirement. This is consistent with the ISO 9972 which notes that a wind speed near the ground above  $3 \text{ m s}^{-1}$  will unlikely lead to a zero-flow pressure below 5 Pa;
- $|\Delta p_0|$  is lower when the leakage is mostly located on the windward façade: from  $r_{LD}=0.7$  to  $r_{LD}=0.9$ ,  $|\Delta p_0|$  is higher than 5 Pa only when the wind speed exceeds  $5 \text{ m s}^{-1}$ ;
- we observe a specific configuration for  $r_{LD}=0.6$ :  $|\Delta p_0|$  is extremely low and stable, with a maximum value of 1 Pa at  $7 \text{ m s}^{-1}$ . For this configuration, we can perform tests according to ISO 9972 in all windy conditions. This seems to correspond to a specific situation for which the pressure due to the wind is compensated by the

specific leakage distribution and the specific wind pressure coefficients on our model. This point should be further investigated. Indeed, we could wonder if such an equilibrium state could often be reached in a real building or if it is just a laboratory case due to laboratory mastered and simplified conditions.

From this analysis, we show that the zero-flow pressure difference is not a direct indicator for environmental conditions. Indeed, for the same wind speed, its value varies very significantly from one leakage distribution to another one. We will analyze the link between the zero-flow pressure difference value and the error induced by the wind in section 6.3.

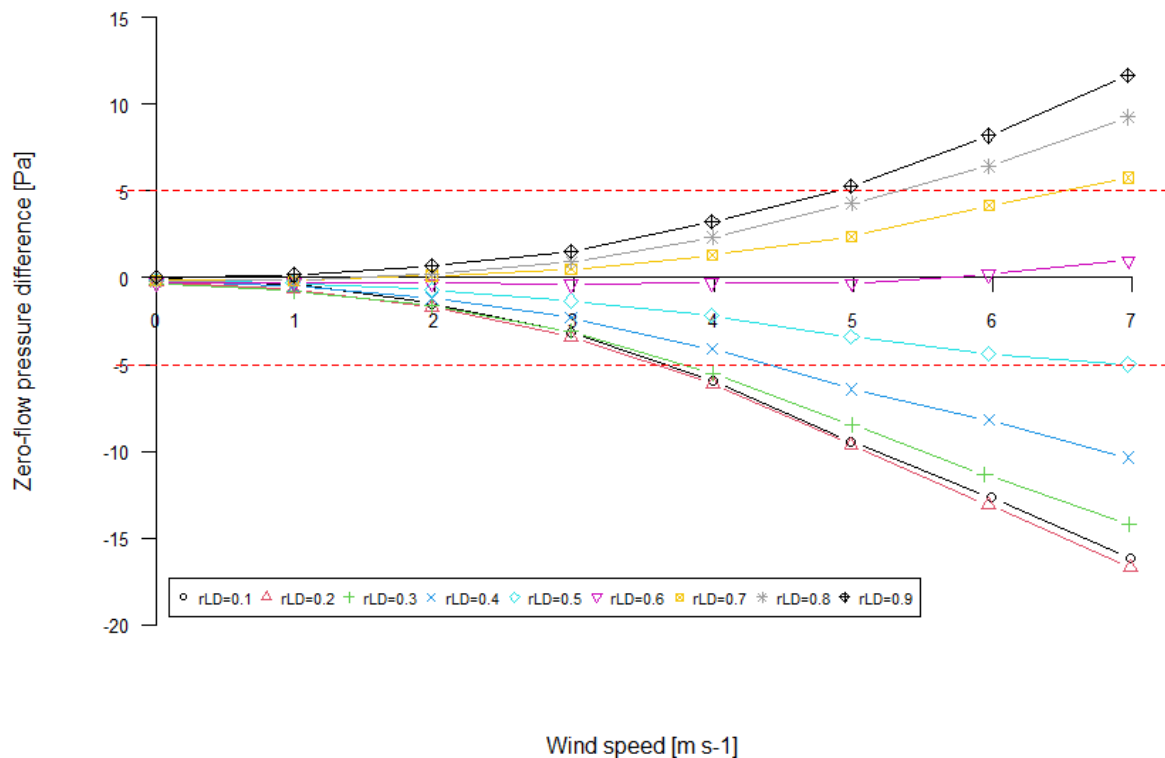


Figure 6-4: Zero-flow pressure difference for 9 configurations of leakage distribution depending on wind speed

### 6.2.2 Impact of the zero-flow pressure difference on the number of pressure stations according to ISO 9972

ISO 9972 requires a minimum of 5 pressure stations for the pressure sequence, with a first station which must be the maximum between 10 Pa and 5 times the zero-flow pressure difference ( $(5\Delta p_0)$ ). We looked at the possible stations without taking into account the 5 Pa limit for the zero-flow pressure difference: we do not eliminate tests with zero-flow pressure difference absolute value higher than 5 Pa. As the first station has to be at least equal to 5 times the absolute zero-flow pressure value  $\pm 3$  Pa, the maximum value for the first station is 60 Pa, which leads to a higher station value of 100 Pa, considering an increment of 10 Pa. This corresponds to a maximum zero-flow pressure of 12.6 Pa. Figure 6-5 represents the number of stations for each leakage distribution depending on the wind speed. When the leakage is mostly on the leeward

side ( $r_{LD}=0.1$  to  $0.3$ ), it is not possible to perform pressurization tests for wind speeds higher than  $5 \text{ m s}^{-1}$ : as the zero-flow pressure can be higher than  $12.6 \text{ Pa}$ , the pressure sequence does not include the minimum 5 stations. On the contrary, for  $r_{LD}=0.6$ , all tests include 10 stations, for all wind speeds.

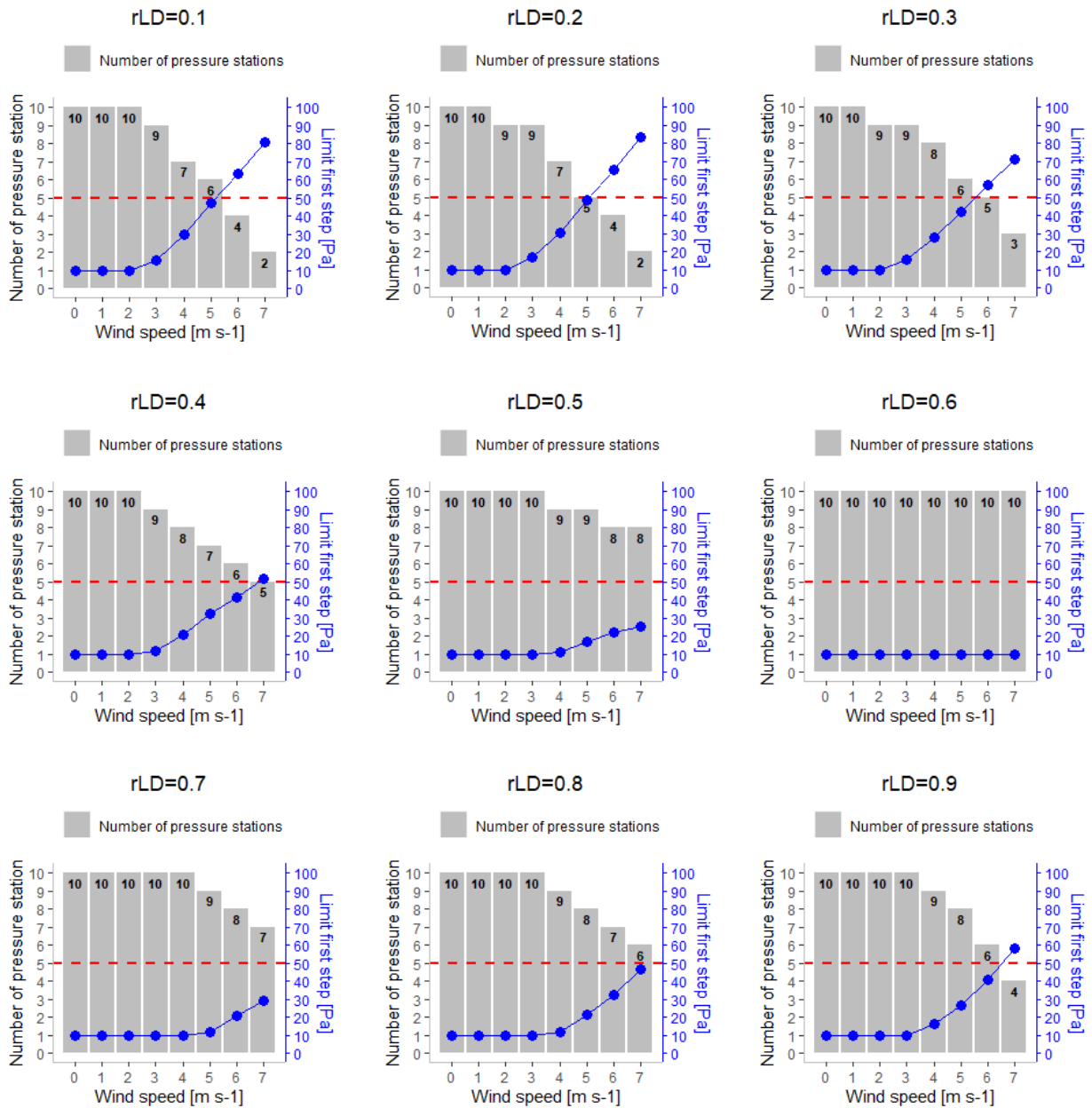


Figure 6-5: Number of pressure stations for a fan pressurization test depending on the wind speed for nine on the leakage distributions

### 6.3 Tests performed according to ISO 9972

In this part, we consider tests performed according to ISO 9972 method as described in part 6.1.1 (only tests with a zero-flow pressure difference less than  $5 \text{ Pa}$  and at least 5 stations). This means that depending on the leakage distribution, maximal wind speed varies from  $3$  to  $7 \text{ m s}^{-1}$ . For all of the nine configurations of leakage distribution and all

wind speeds, we calculate the airleakage airflow rates  $q_4$  and  $q_{50}$  according to equations (55) and (56), in compliance with ISO 9972 (with  $C$  and  $n$  evaluated from an ordinary least square analysis). In many countries, the airtightness indicator is calculated at a reference of 50 Pa (especially  $n_{50}$ ), and thus uses the  $q_{50}$  value. In France, the regulatory threshold value and the airtightness indicator used in the energy performance calculation is calculated at 4 Pa, and thus used the  $q_4$  value.

Figure 6-6 presents  $q_{50}$  values and Figure 6-7 presents  $q_4$  values.

$$q_4 = C * 4^n \quad (55)$$

$$q_{50} = C * 50^n \quad (56)$$

We observe significant variations for  $q_4$  values when the wind speed increases. Further analyzing these data, these variations strongly depend on the  $\Delta p_0$  threshold requirement, which depends on the leakage distribution:

- For  $r_{LD}=0.1$  to  $0.4$ : the limit regarding  $\Delta p_0$  validates tests only up to  $3 \text{ m s}^{-1}$  and  $4 \text{ m s}^{-1}$ . We do not observe a significant impact of the wind for these configurations with this limit;
- For  $r_{LD}=0.5$ : the limit regarding  $\Delta p_0$  validates tests up to  $6 \text{ m s}^{-1}$ . The wind does not induce significant impact for this configuration for low and medium wind speed, whereas we observe a significant decrease of the  $q_4$  value at  $6 \text{ m s}^{-1}$ ;
- For  $r_{LD}=0.6$ : all tests are validated, as the  $\Delta p_0$  stays very low for all wind speeds. We observe a very significant variation of the  $q_4$  value: for wind speeds from  $4 \text{ m s}^{-1}$ , the value of  $q_4$  strongly decreases when the wind speed increases;
- For  $r_{LD}=0.7$  to  $0.9$ : the limit regarding  $\Delta p_0$  validates tests up to  $6 \text{ m s}^{-1}$  ( $r_{LD}=0.7$ ),  $5 \text{ m s}^{-1}$  ( $r_{LD}=0.8$ ) and  $4 \text{ m s}^{-1}$  ( $r_{LD}=0.9$ ). For these configurations, we observe a significant variation of the  $q_4$  value:  $q_4$  value increases with the wind speed.

These results show also that the relevance of the  $\Delta p_0$  limit requirement depends on the leakage distribution:

- when leakage is mostly on the leeward façade ( $r_{LD}=0.1$  to  $0.4$ ), the  $\Delta p_0$  limit validates tests only below  $4 \text{ m s}^{-1}$ . For these wind speeds, we do not observe a significant impact on the wind;
- when the leakage is mostly located on the windward facade ( $r_{LD}=0.7$  to  $0.9$ ), the wind will induce a significant overestimation of the  $q_4$  value for wind speeds above  $3 \text{ m s}^{-1}$ , whereas the  $\Delta p_0$  limit validates tests with winds up to  $6 \text{ m s}^{-1}$ ;
- for the specific configurations  $r_{LD}=0.6$ : the  $\Delta p_0$  limit validates all tests whereas this is the configuration for which the variations of  $q_4$  due to wind are the most significant.

Therefore, the  $\Delta p_0$  limit does not eliminate all significant errors due to wind for all configurations.

Variation of  $q_{50}$  measured according to ISO9972 depending on wind speed and leak distribution rLD

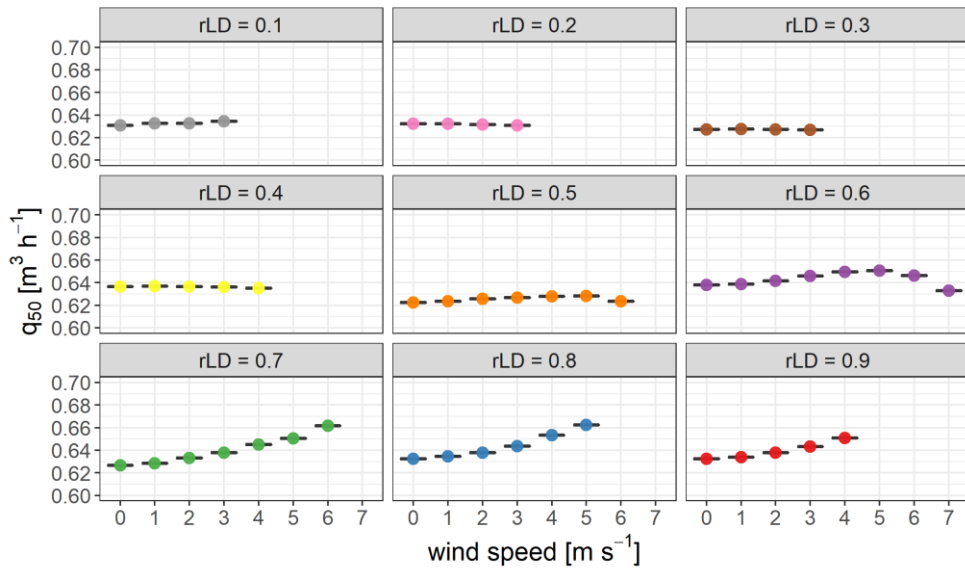


Figure 6-6:  $q_{50}$  result for tests performed according to ISO 9972

Variation of  $q_4$  measured according to ISO9972 depending on wind speed and leak distribution rLD

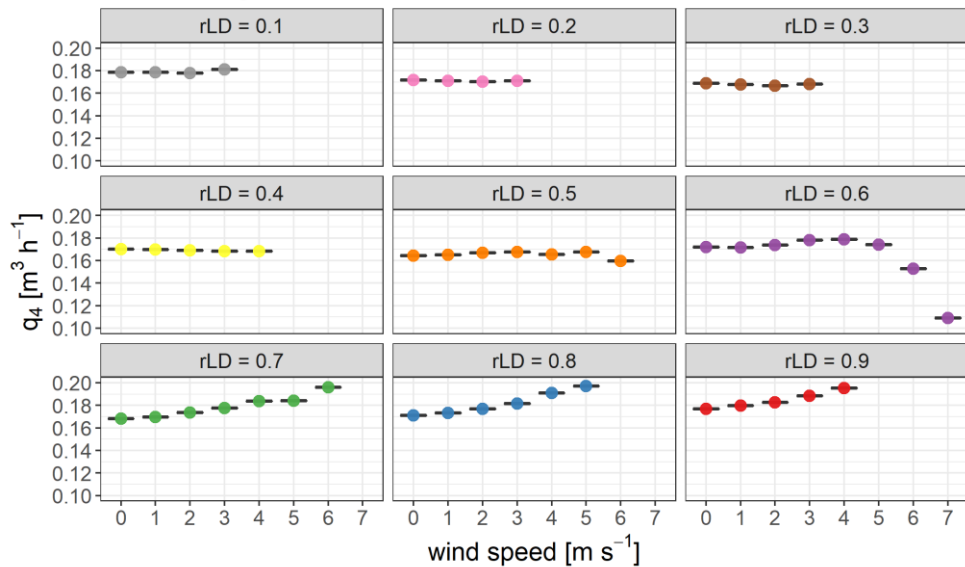


Figure 6-7:  $q_4$  result for tests performed according to ISO 9972

To evaluate the error due to wind, we need to define the real airleakage of our model, or more exactly the reference value we consider as the real value. In section 5.2.2.1, we presented two methods to evaluate the reference airleakage value with no wind: either a calculated value from a test performed according to ISO 9972 or from a direct measurement at 4 Pa for  $q_4$  and at 50 Pa for  $q_{50}$ . For all configurations, the maximal absolute gap between these two methods results is very low:  $0.007 \text{ m}^3 \text{ h}^{-1}$  at 4 Pa and  $0.003 \text{ m}^3 \text{ h}^{-1}$  at 50 Pa. We chose to consider the directly measured  $q_4$  and  $q_{50}$  as the reference value in our wind impact evaluation (Table 6-1).

Table 6-1: Reference values for  $q_4$  and  $q_{50}$  for wind impact evaluation

$r_{LD}$	<b><math>q_4</math> (direct measurement @4Pa) [<math>m^3 h^{-1}</math>]</b>	<b><math>q_{50}</math> (direct measurement @50Pa) [<math>m^3 h^{-1}</math>]</b>
<b>0.1</b>	0.170	0.629
<b>0.2</b>	0.167	0.635
<b>0.3</b>	0.163	0.629
<b>0.4</b>	0.167	0.638
<b>0.5</b>	0.165	0.623
<b>0.6</b>	0.167	0.640
<b>0.7</b>	0.163	0.627
<b>0.8</b>	0.167	0.635
<b>0.9</b>	0.170	0.631

Then, for each test, we evaluate the relative error due to wind  $E_{w_{\Delta p}}$  for a pressure difference  $\Delta p$  comparing the reference value  $q_{\Delta p, ref}$  and the test result  $q_{\Delta p, m}$  according to equation (57).

$$E_{w_{\Delta p}} = \frac{q_{\Delta p, m} - q_{\Delta p, ref}}{q_{\Delta p, ref}} \quad (57)$$

Figure 6-8 presents the calculated errors on  $q_{50}$  and Figure 6-9 presents the calculated errors on  $q_4$  for all leak distributions and for different wind speeds. For tests performed according to ISO 9972, the error due to wind on the  $q_{50}$  stays below 6% ( $3.5 \cdot 10^{-2} m^3 h^{-1}$ ) for all wind speeds and all leakage distributions. There is no significant impact of the leakage distribution. As we observed previously, the error due to wind on  $q_4$  strongly depends on leakage distribution:

- for configurations with less leakage on the windward facade ( $r_{LD} \leq 0.4$ ), the wind error is evaluated only for small wind speed because tests under strong wind are not validated, due to the  $\Delta p_0$  limit. For these configurations, the error due to wind stays below 7% ( $1.1 \cdot 10^{-2} m^3 h^{-1}$ ) for wind speed up to  $4 m s^{-1}$  and stays below 2% when the leaks are equally distributed for wind speed up to  $6 m s^{-1}$ ;
- on the contrary, the error due to wind reaches 20% when 70% of the leakage area is located on the windward facade ( $r_{LD}=0.7$ ), and 35% ( $5.8 \cdot 10^{-2} m^3 h^{-1}$ ) when 60% of the leakage area is located on the windward facade ( $r_{LD}=0.6$ ). For configurations where most of the leakage is located on the windward facade, the constraint regarding the zero-flow pressure does not prevent significant error due to wind on the result.

This evaluation of the wind impact for tests performed according to ISO 9972 shows first that wind may thus induce strong error on  $q_4$  whereas it does not significantly impact  $q_{50}$ . Secondly, the leakage distribution impacts the error due to the wind on  $q_4$ . Then, it calls the ISO 9972 zero-flow pressure difference constraint into question to ensure the reliability of the test result. These conclusions are consistent with the numerical evaluation performed by Carrié and Leprince [51]. As they analyzed only simulations for a 1-point test and 2-point test, we can not compare the error values they have obtained with the error values we have evaluated in this part. In the next part, we analyze the same experimental data using different methods to evaluate the impact of wind with alternative analysis protocols.

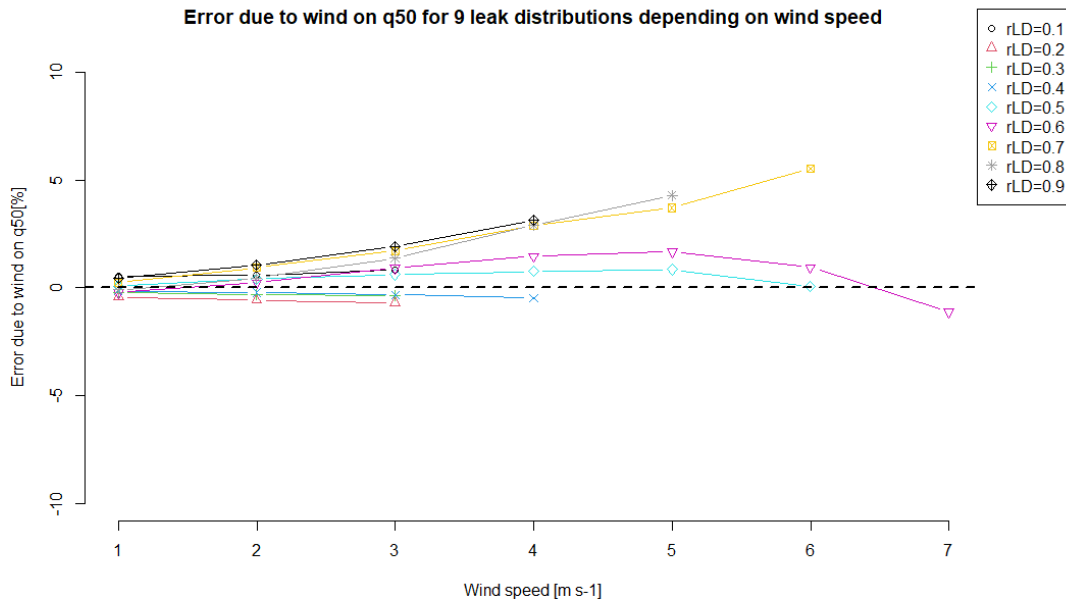


Figure 6-8: Error due to wind on q<sub>50</sub> for tests performed according to ISO 9972

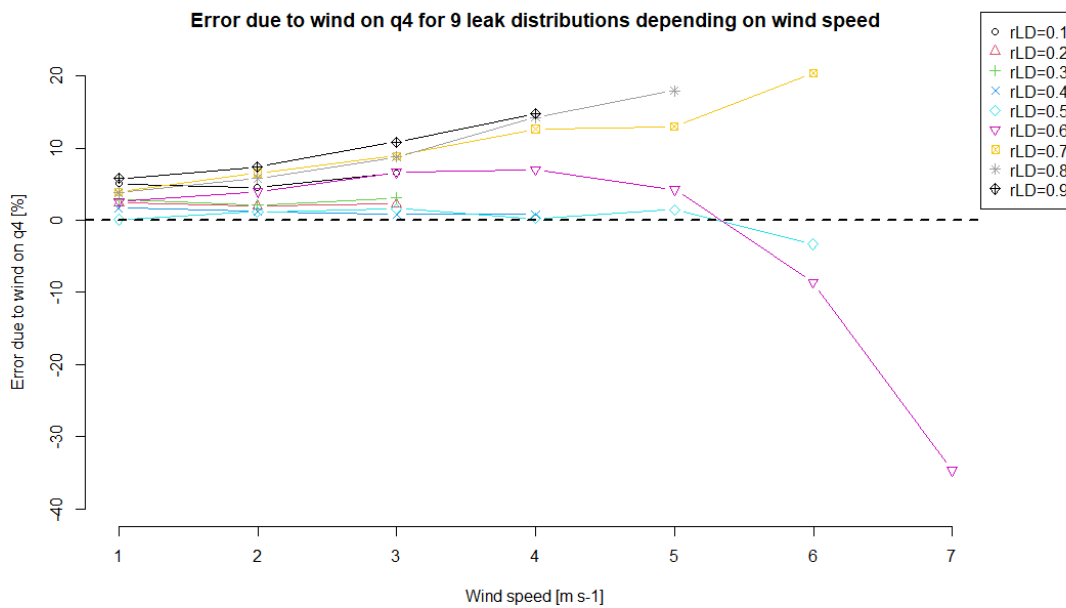


Figure 6-9: Error due to wind on q<sub>4</sub> for tests performed according to ISO 9972

## 6.4 One-point tests and two-point tests

In chapter 3, we presented different types of airleakage test that differ from the ISO 9972 one, and especially one-point tests with a fixed pressure difference value, and two-point tests. As we observed strong errors with the ISO 9972 method, these methods could be alternative analysis methods to reduce the impact of the wind on a test result.

In their numerical study, Carrié and Leprince have evaluated the impact of the wind on these two types of tests. To compare their results with experimental data, we now consider these methods of test according to the following scenario on the pressure stations and the airflow exponent:

- Scenario 1A: one-point test at 10 Pa + n=0.5;
- Scenario 1B: one-point test at 50 Pa + n=0.5;
- Scenario 1C: one-point test at 100 Pa + n=0.5;
- Scenario 2A: two-point test at 10 and 50 Pa;
- Scenario 2B: two-point test at 10 and 100 Pa;
- Scenario 2C: two-point test at 50 and 100 Pa.

For all configurations, we evaluate  $q_4$  and  $q_{50}$  for each scenario depending on wind speed. For scenario 1A, 1B, and 1C, the flow exponent  $n$  is equal to 0.5 (that corresponds to the  $n$  value we evaluated in chapter 5, section 5.2.2.2) and the leakage coefficient  $C$  is calculated according to equation (58):

$$C = \frac{q_{\Delta p}}{\Delta p^{0.5}} \quad (58)$$

$q_{\Delta p}$  and  $\Delta p$  are the airflow and corrected pressure difference for a target pressure difference equal to 10 Pa (scenario 1A), 50 Pa (scenario 1B), and 100 Pa (scenario 1C).

For scenario 2A, 2B, and 2C, the flow exponent  $n$  is calculated according to equation (59) and the leakage coefficient  $C$  is calculated according to equation (60):

$$n = \frac{\ln(q_{\Delta p,2}) - \ln(q_{\Delta p,1})}{\ln(\Delta p_2) - \ln(\Delta p_1)} \quad (59)$$

$$C = \frac{q_{\Delta p,1}}{\Delta p_1^n} \quad (60)$$

with  $q_{\Delta p,1}$  and  $\Delta p_1$  are airflow and the corrected pressure difference for a target pressure difference equal to 10 Pa (scenario 2A and 2B), and 50 Pa (scenario 2C), and  $q_{\Delta p,2}$  and  $\Delta p_2$  are airflow and the corrected pressure difference for a target pressure difference equal to 50 Pa (scenario 2A), and 100 Pa (scenario 2B and 2C).

#### 6.4.1 One-point test results

Figure 6-10 and Figure 6-11 give  $q_4$  and  $q_{50}$  values for the three scenarios of 1-point test when leakage is mostly located on the leeward facade ( $r_{LD}=0.1$ ). Figure 6-12 and Figure 6-13 give  $q_4$  and  $q_{50}$  values for the three scenarios of 1-point test when leakage is mostly located on the windward facade ( $r_{LD}=0.8$ ). All results for  $q_4$  and  $q_{50}$  values are presented in Annex B and Annex C.

- for  $r_{LD}=0.1$ , the strong winds induce significant error on the  $q_4$  value and the  $q_{50}$  value: we observe that scenario 1A gives the maximal errors with  $1.3 \cdot 10^{-2} \text{ m}^3 \text{ h}^{-1}$  (corresponds to a relative error of 8%) on  $q_4$  and  $2.8 \cdot 10^{-2} \text{ m}^3 \text{ h}^{-1}$  (corresponds to a relative error of -4%) on  $q_{50}$ . We also observe that results for scenario 1A are more impacted by the wind when the wind speed increases.
- for  $r_{LD}=0.8$ , the wind induces very significant error, more especially for scenario 1A: we observe a maximal error of  $6.2 \cdot 10^{-2} \text{ m}^3 \text{ h}^{-1}$  (corresponds to a relative error of -37%) on  $q_4$  and  $26.5 \cdot 10^{-2} \text{ m}^3 \text{ h}^{-1}$  (corresponds to a relative error of -42%) on  $q_{50}$ . The order of magnitude of these errors is consistent with the maximal error

due to wind evaluated by Carrié and Leprince [51], which was around 40% at  $6 \text{ m s}^{-1}$  for a 1-point analysis at 10 Pa. For scenario 1B and 1C, the error due to wind increases with wind speed but is less important:  $2.6 \cdot 10^{-2} \text{ m}^3 \text{ h}^{-1}$  (15%) on  $q_4$  and  $4.7 \cdot 10^{-2} \text{ m}^3 \text{ h}^{-1}$  (7%) on  $q_{50}$ . Carrié and Leprince only evaluated the maximal error for scenario 1B, which was 3%.

The analysis of all results presented in Annex B and Annex C leads to the following conclusions:

- the impact of the wind on  $q_4$  and  $q_{50}$  increases when the part of leakage on the windward facade increases;
- the impact of the wind on  $q_4$  and  $q_{50}$  for a 1-point test method increases when the pressure difference of the measured point decreases;
- for  $q_4$ :
  - for scenario 1B and 1C (50 Pa and 100 Pa), the wind induces an overestimation of the  $q_4$  value;
  - for scenario A1 (10 Pa), the wind induces first an overestimation for wind speed up to  $4 \text{ m s}^{-1}$ . Then, for stronger winds, we observe an underestimation of  $q_4$  which is more important when the leakage is mostly on the windward side (when  $r_{LD}$  is increasing);
- regarding  $q_{50}$ , we observe essentially an impact of the wind for scenario 1A (10 Pa): the wind induces an increasing underestimation of the  $q_{50}$  when the wind speed increases, except when leakage is mostly on the windward side ( $r_{LD} \geq 0.8$ ) for which there is an overestimation of  $q_{50}$  for medium wind speeds and then an important underestimation for strong winds.

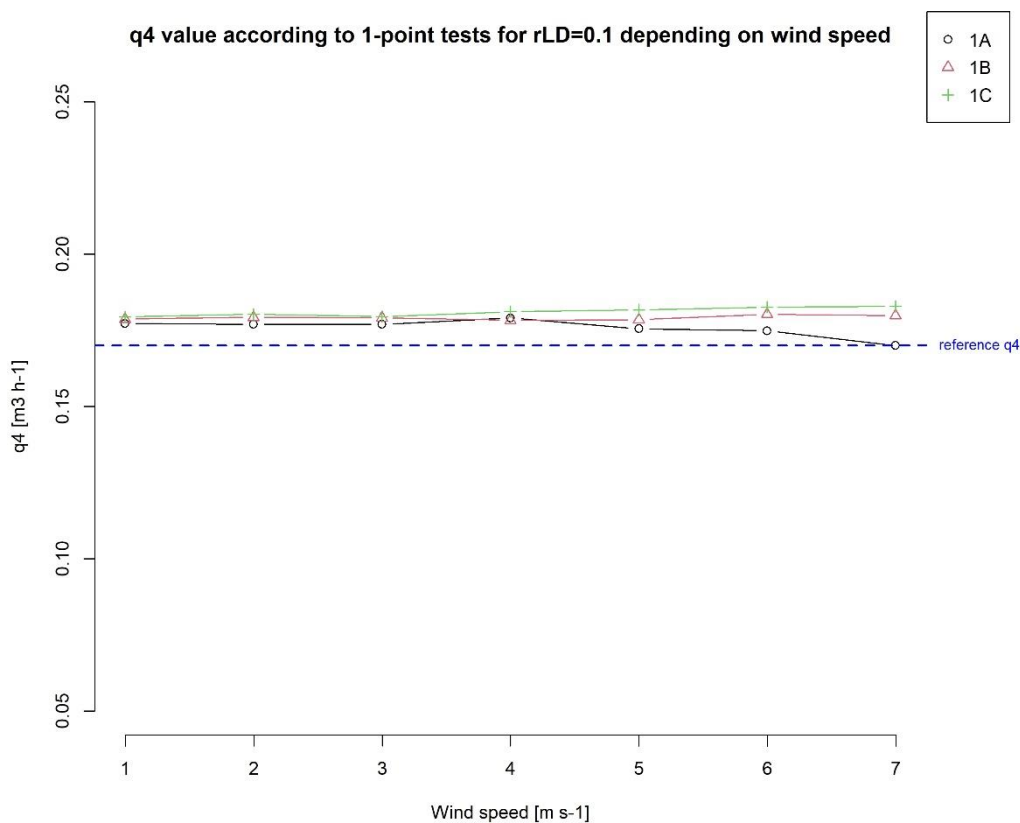


Figure 6-10:  $q_4$  value for 1-point test scenarios for  $r_{LD}=0.1$  depending on wind speed

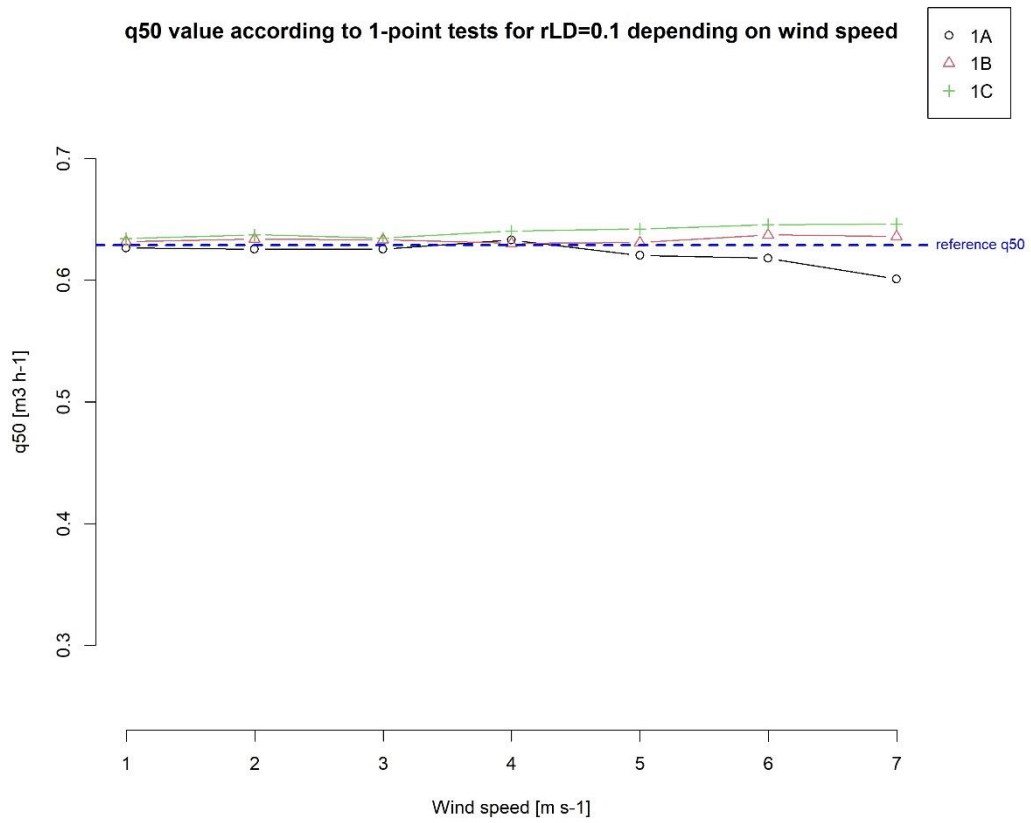


Figure 6-11:  $q_{50}$  value for 1-point test scenarios for  $r_{LD}=0.1$  depending on wind speed

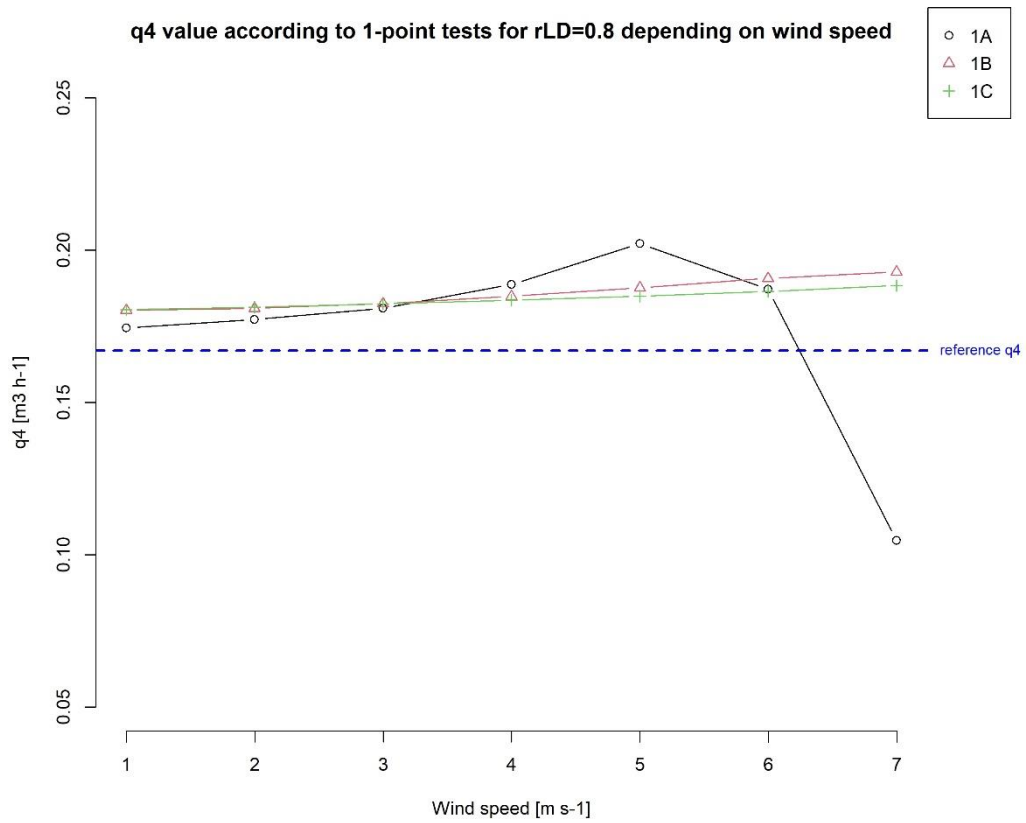


Figure 6-12:  $q_4$  value for 1-point test scenarios for  $r_{LD}=0.8$  depending on wind speed

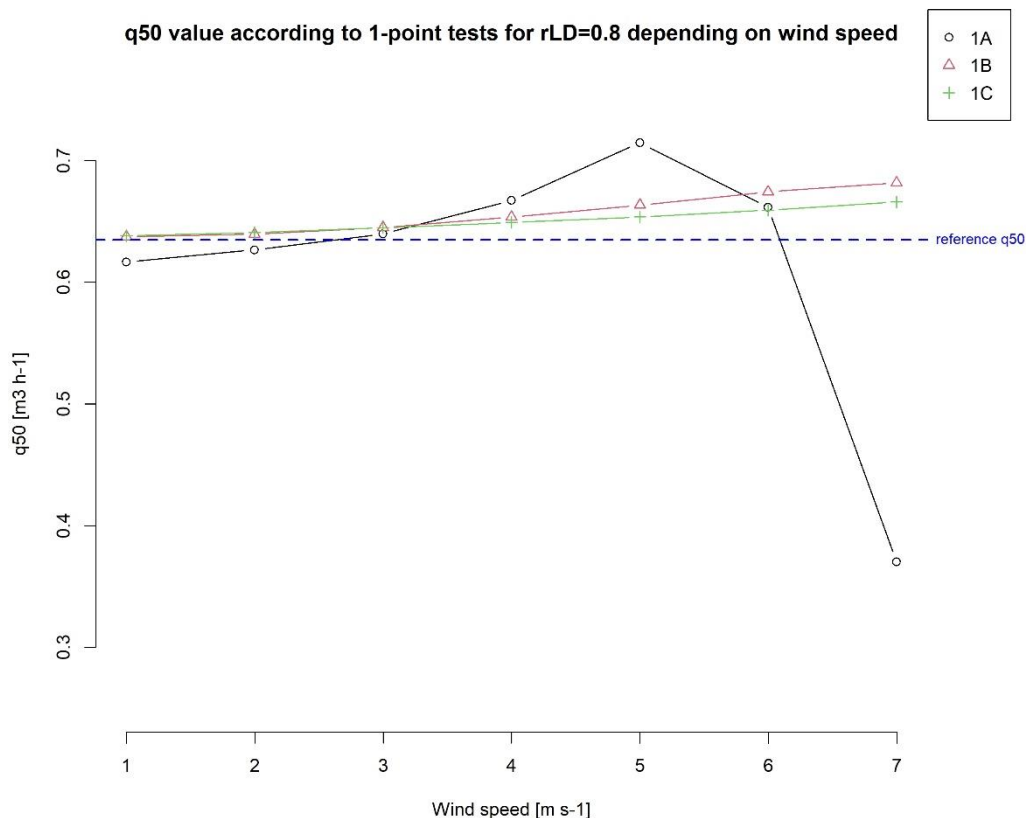


Figure 6-13: q<sub>50</sub> value for 1-point test scenarios for r<sub>LD</sub>=0.8 depending on wind speed

#### 6.4.2 Two-point test results

Figure 6-14 and Figure 6-15 give q<sub>4</sub> and q<sub>50</sub> values for the three scenarios of 2-point test when leakage is mostly located on the leeward facade (r<sub>LD</sub>=0.1).

Figure 6-16 and Figure 6-17 give q<sub>4</sub> and q<sub>50</sub> values for the three scenarios of 2-point test when leakage is mostly located on the windward facade (r<sub>LD</sub>=0.8). All results for q<sub>4</sub> and q<sub>50</sub> values are presented in Annex D and Annex E.

- For r<sub>LD</sub>=0.1, the wind induces a significant error on the q<sub>4</sub> value but not on the q<sub>50</sub> value: we observe a maximal error for scenario 2A of 1.3 10<sup>-2</sup> m<sup>3</sup> h<sup>-1</sup> (corresponds to a relative error of -11%) on q<sub>4</sub> against 2.8 10<sup>-2</sup> m<sup>3</sup> h<sup>-1</sup> (corresponds to a relative error of -1%) on q<sub>50</sub>. We also observe that results for scenarios 2A and 2B are more impacted by the wind when the wind speed increase;
- for r<sub>LD</sub>=0.8, the wind induces a very significant error. Indeed, for all scenarios: we observe a maximal error of 4.4 10<sup>-2</sup> m<sup>3</sup> h<sup>-1</sup> for scenario 2B (corresponds to a relative error of -26%) on q<sub>4</sub> and 26.5 10<sup>-2</sup> m<sup>3</sup> h<sup>-1</sup> for scenario 2A (corresponds to a relative error of 11%) on q<sub>50</sub>. Carrié and Leprince evaluated the maximal error due to wind for a scenario similar to 2A: the maximal error was around 25% for a wind speed of 5 m s<sup>-1</sup>. They also observed that the error is very significantly reduced when most of the leaks are on the leeward facade, which is consistent with our results.

The analysis of all results presented in Annex D and Annex E leads to the following conclusions:

- the impact of the wind on  $q_4$  and  $q_{50}$  increases when the part of leakage on the windward facade increases;
- the impact of the wind on  $q_4$  and  $q_{50}$  for a 2-point test method increases when the pressure difference of the measured points decreases;
- when leakage is mostly on the leeward facade ( $r_{LD} \leq 0.4$ ), the wind induces an underestimating of  $q_4$  and  $q_{50}$ ;
- when leakage is mostly on the windward facade ( $r_{LD} \geq 0.6$ ), the sign of the error induced by the wind varies depending on the scenario, the airtightness indicator, and the wind speed. There is no clear tendency.

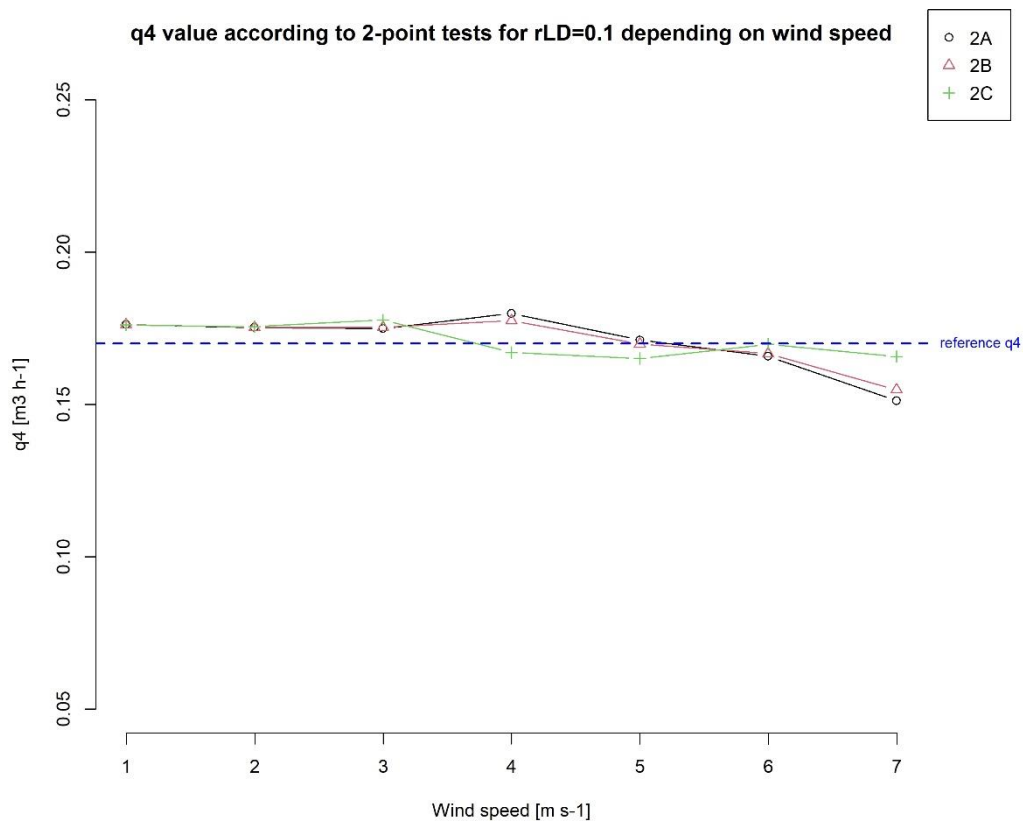


Figure 6-14:  $q_4$  value for 2-point test scenarios for  $r_{LD}=0.1$  depending on wind speed

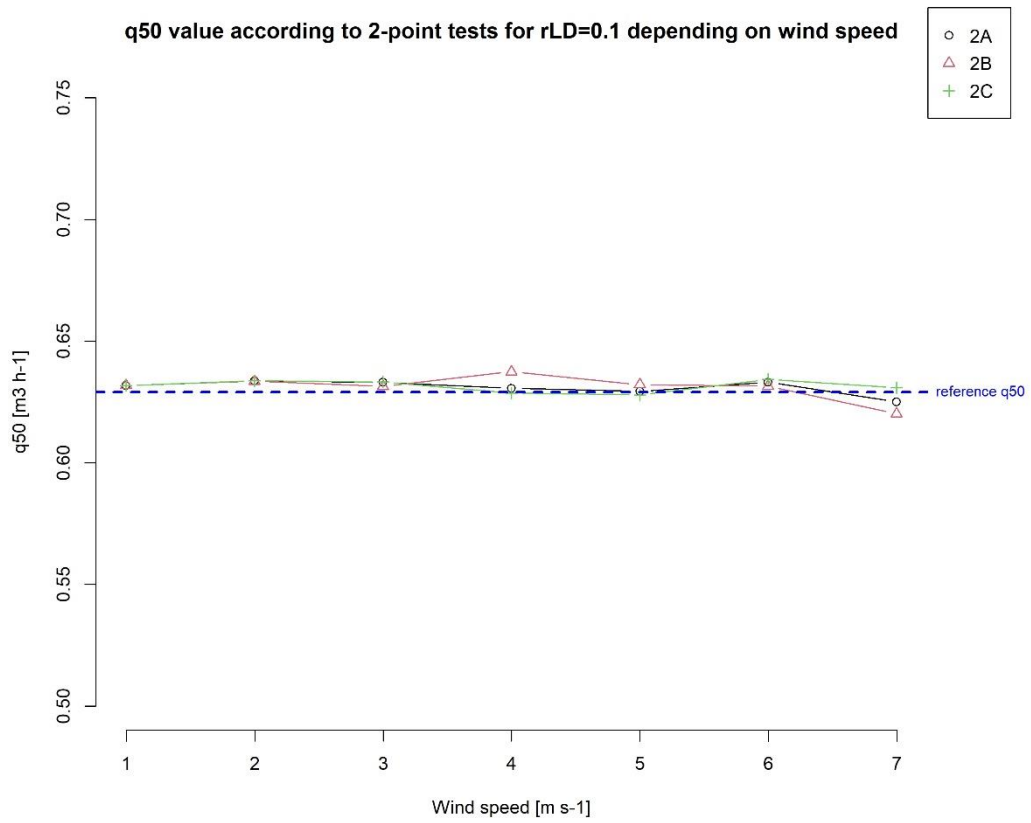


Figure 6-15: q<sub>50</sub> value for 2-point test scenarios for r<sub>LD</sub>=0.1 depending on wind speed

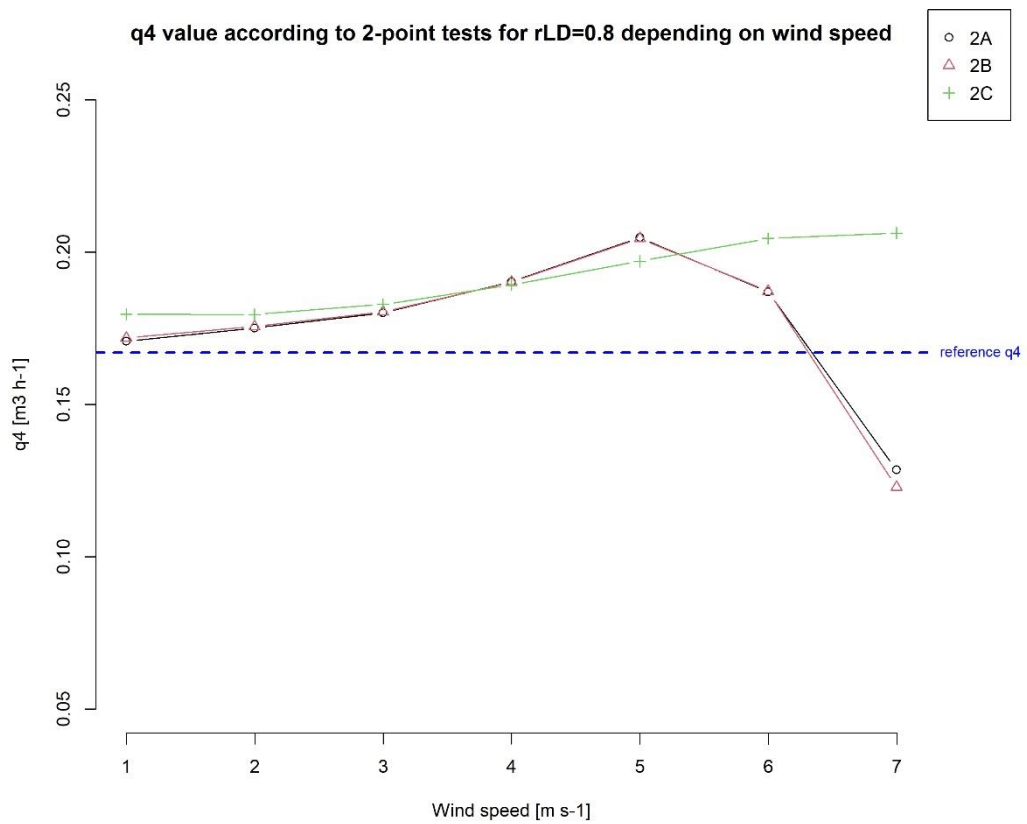


Figure 6-16: q<sub>4</sub> value for 2-point test scenarios for r<sub>LD</sub>=0.8 depending on wind speed

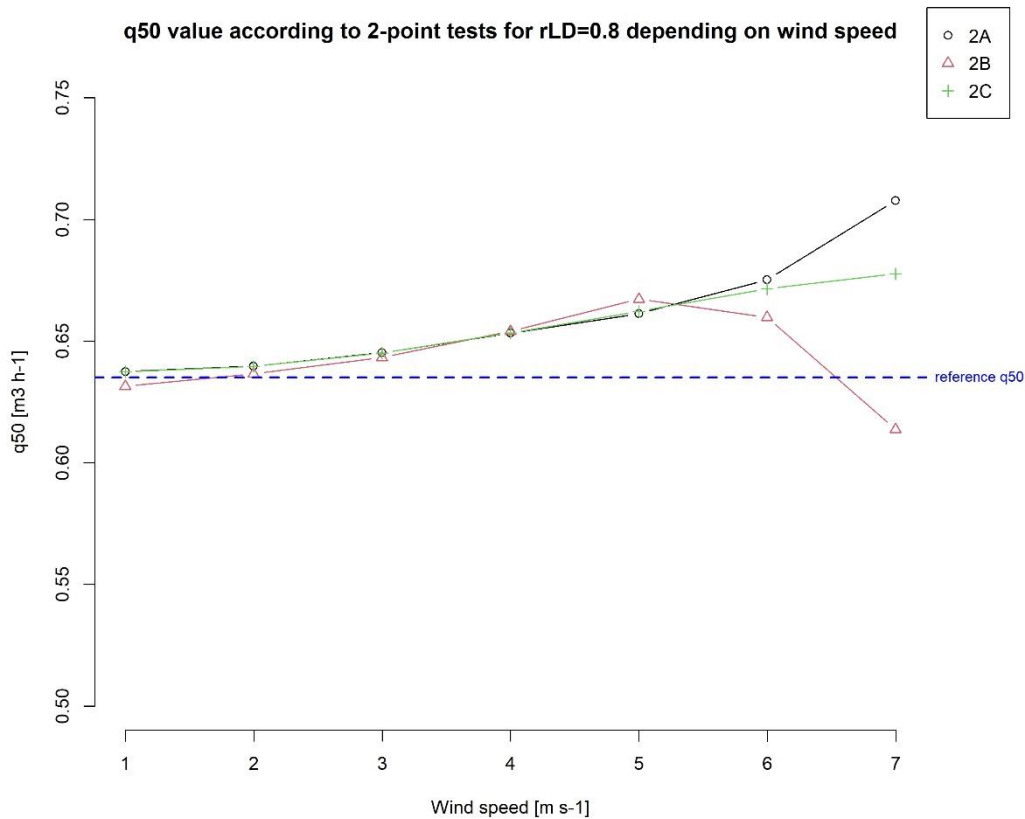


Figure 6-17:  $q_{50}$  value for 2-point test scenarios for  $r_{LD}=0.8$  depending on wind speed

## 6.5 Comparison of the error due to wind between three test analysis methods

In the two previous sections, we presented the  $q_4$  and  $q_{50}$  value evaluated for different wind speeds according to three analysis methods: ISO 9972 method, 1-point test method (with three variants), and 2-point test method (with three variants). For each leakage distribution, the three methods have been applied to the same experimental data: the comparison of these test results exactly leads to assess the impact of the wind due to the choice of the method. In this section, we compare the error due to the wind to first identify the method that leads to the most reliable results. As we have seen previously that the ISO 9972 requirement regarding the limit value of the zero-flow pressure difference is not always relevant, we recalculated ISO 9972 results without applying this constraint. All results are presented in Annex F for  $q_4$  and Annex G for  $q_{50}$ .

Figure 6-18 presents the error on  $q_4$  for  $r_{LD}=0.4$  and Figure 6-19 for  $r_{LD}=0.8$ . We observe that:

- when leakage is mostly on the leeward side, the error obtained with the ISO 9972 analysis is one of the smallest, for all wind speed.;
- when leakage is mostly on the windward facade, the error obtained with the ISO 9972 analysis is also the smallest for wind speed below  $4 \text{ m s}^{-1}$ . Then, when the wind speed increases, this ISO 9972 error significantly increases too whereas the errors obtained with scenarios 1B and 1C become the smallest.

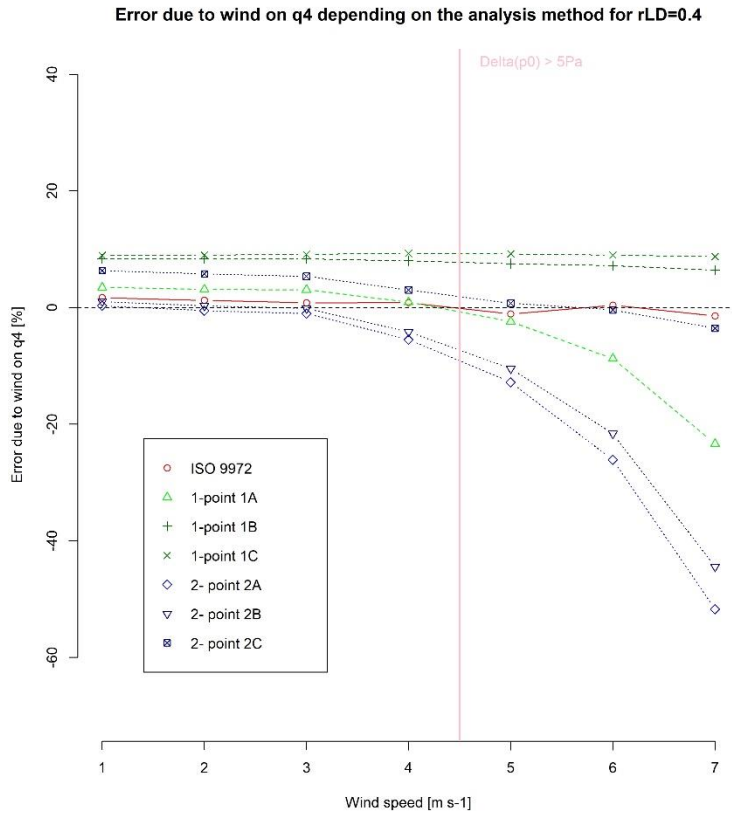


Figure 6-18: Comparison of the error on  $q_4$  due to wind evaluated in 7 scenarios for  $r_{LD}=0.4$

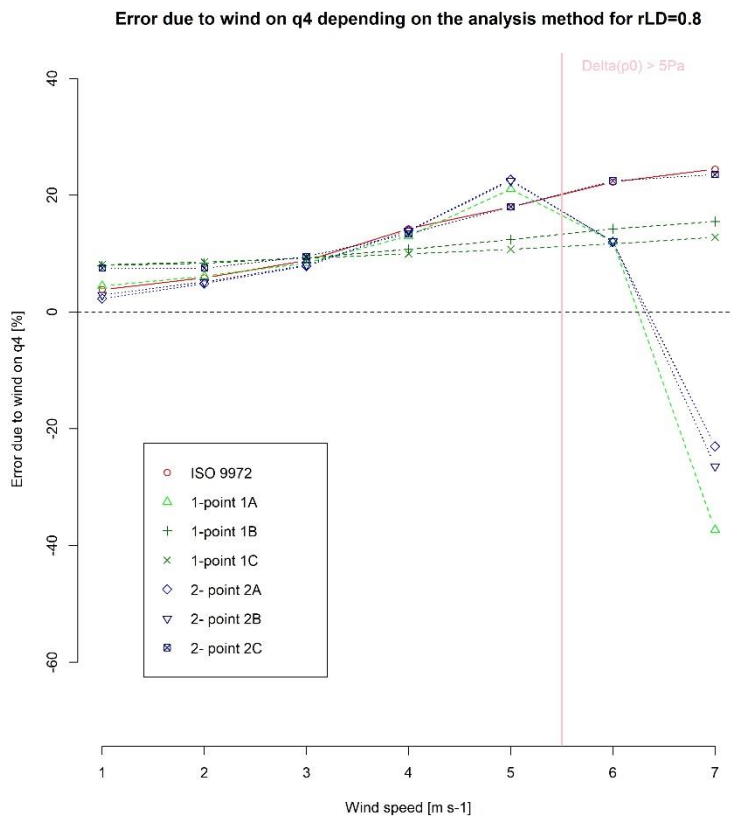


Figure 6-19: Comparison of the error on  $q_4$  due to wind evaluated in 7 scenarios for  $r_{LD}=0.8$

Figure 6-20 presents the error on  $q_{50}$  for  $r_{LD} = 0.7$ . For all leakage distributions, the error obtained with the ISO 9972 on  $q_{50}$  stays one of the smallest for all wind speeds.

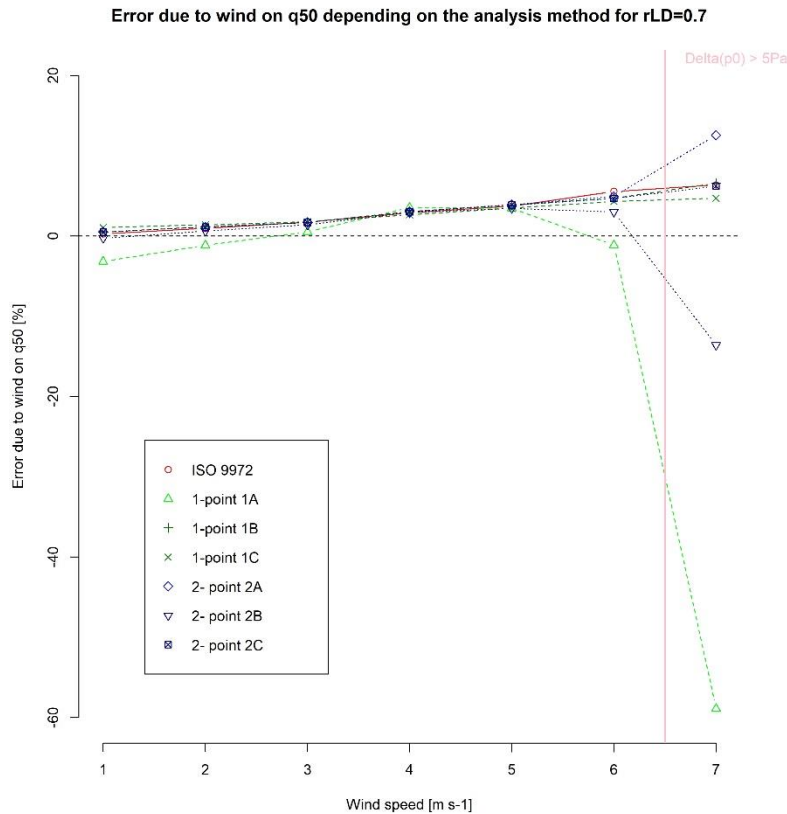


Figure 6-20: Comparison of the error on  $q_{50}$  due to wind evaluated in 7 scenarios for  $r_{LD}=0.7$

From these comparisons, we can conclude that in our reduced scale experiment, with steady wind conditions, the ISO 9972 analysis is more appropriate than a 1-point method and a 2-point method for an airtightness indicator at 50 Pa. This conclusion concerns all wind speeds and all leakage distributions. When we use an indicator at 4 Pa like in France, the conclusion depends on the leakage distributions:

- When leakage is mostly on the leeward side, the ISO 9972 analysis is also more reliable than a 1-point method and a 2-point method, for all wind speeds;
- When leakage is mostly on the windward side, a 1-point analysis with a pressure station at 50 Pa or 100 Pa gives lower error when the wind is above 4 m s<sup>-1</sup>.

## 6.6 Conclusions

We performed measurements for the nine leakage distributions of our model, under eight different wind speeds. That represents 96 pressurizations tests and 864 measurements. All these measurements were performed using Labview applications and a VBA program developed in this thesis to control the experimental facility and record all output files.

We first analyzed the zero-flow pressure differences as it is considered as an indicator of the environmental conditions. More important, it is one of the major criteria to validate a test according to the ISO9972 standard. We observed that the variation of the zero-flow pressure difference induced by the wind strongly depends on the leakage distribution. Moreover, we showed that we can obtain very low zero-flow pressure differences for

strong winds, which indicates that the zero-flow pressure difference is not always a relevant indicator of the windy conditions.

We then evaluated the error due to wind for tests performed according to ISO 9972, by comparing the test results to the real value of  $q_4$  and  $q_{50}$  of the model that we measured directly at 4 Pa and 50 Pa. Depending on the leakage distribution, we performed tests for maximal wind speed from 3 to 7 m s<sup>-1</sup>, due to the zero-flow pressure difference limit at 5 Pa. We first observed that the error induced by the wind strongly depends on the leakage distribution and the airleakage indicator. For  $q_{50}$ , the error induced by the wind stays below 6% for all configurations. For  $q_4$ , the maximal error varies from 2% (leaks equally distributed, wind speed = 6 m s<sup>-1</sup>) to 35% (60% of the leakage on the windward facade). These results call the ISO 9972 zero-flow pressure difference constraint into question to ensure the reliability of the test result.

As we observed strong errors with the ISO 9972 method due to wind impact, we looked for an alternative analysis method to reduce the impact of the impact on a test result. Thus, we evaluated  $q_4$  and  $q_{50}$  using three different 1-point test method and 2-point test methods. We compare the error induced by the wind for these methods to the error obtained by the test performed according to ISO 9972. For our reduced scale experiment, under steady wind conditions, the ISO 9972 analysis is more appropriate than a 1-point method and a 2-point method for an airtightness indicator at 50 Pa. This conclusion concerns all wind speeds and all leakage distributions. When we use an indicator at 4 Pa, the conclusion depends on the leakage distributions:

- When leakage is mostly on the leeward side, the ISO 9972 measurement method is also more reliable than a 1-point method and a 2-point method, for all wind speeds;
- When leakage is mostly on the windward side, a 1-point analysis with a pressure station at 50 Pa or 100 Pa gives lower error when the wind is above 4 m s<sup>-1</sup>.

These results showed that none of the six tested methods lead to a strong reduction of the impact of the wind. Nevertheless, it showed that an alternative method might lead to fewer errors due to wind for some configurations. More tests, more configurations, and more alternative methods should be tested to result in different protocols, each of them might be the most appropriate for some specific configurations and wind conditions.

## 7. General conclusions and perspectives

### 7.1 Conclusions

Nowadays airleakage measurements are widely performed in several countries to assess the as-built performance of dwellings in order to comply with energy performance regulation requirements (around 65,000 tests per year in France). These measurements must be performed according to the international standard ISO 9972, which is applicable only under calm climatic conditions (a maximum wind speed of  $6 \text{ m s}^{-1}$  is recommended). However, in many situations, wind conditions can be higher depending on the building location and the climatic conditions. Therefore, the requirements of the ISO 9972 cannot be met, yet the test has to be done to meet the mandatory requirement. Several studies have tried in the past to evaluate the error induced by the wind during an airleakage measurement but there is still a lack of knowledge to qualify and quantify the impact of the wind on the airleakage measurement.

This thesis aimed to characterize the error induced by the wind during a building airleakage measurement through laboratory experiments on reduced scale model in wind tunnel. The main objectives of this research were to:

- 1) evaluate the error induced by the wind during tests performed according to the ISO 9972;
- 2) improve the test protocol either by reducing the error due to the wind or by improving the way the errors are taken into account in the test result.

In the first step, we evaluated the real situation of buildings airtightness in France thanks to statistical analysis of the national airtightness database, that represents 219,000 onsite tests performed on French buildings. The analysis of the tests performed on residential buildings first led to the identification of different factors that can significantly impact building airtightness:

- the nature of the main construction material: wooden buildings are slightly less airtight than concrete and brick buildings, from +15% for wooden single-family houses to +20% for wooden multi-family dwellings on the median value of the airflow rate  $q_{a4}$ ;
- for multi-family buildings the technique of thermal insulation implementation: external insulated multi-family dwellings are more airtight than internal insulated buildings;
- for multi-family buildings the ventilation system: the balanced ventilation system shows lower airleakage, -17% on the  $q_{a4}$  median value.

The analysis of the leakage location led to the identification of the most common leaks and influent leaks on envelope airtightness results, as levers to improve envelope airtightness, during both the design stage and on-site construction. On the top of this classification, we identified that houses with leaks due to lighting components have a median  $q_{a4}$  13% higher than the global sample and this leak is identified for 18% of the 109,224 houses of the sample. We also observed no significant seasonal variations of the test results. Finally, we noticed that the database includes very poor information regarding the uncertainty of the measurement results.

Second, we evaluated the current knowledge regarding the uncertainty of fan pressurization test results through the analysis of standards, guides, papers dealing with early measurements in the 1970s and 1980s in addition to 39 studies dedicated to uncertainties in building pressurization tests. We identified two categories of sources:

- several sources of error are related to the measurement itself, especially due to the measurement devices and the actions undertaken by the tester;
- other sources are linked to the flow model. We highlighted that although the test method gives corrections to account for the heterogeneity of the differential pressures across the leaks or the temperature and pressure dependence of the power-law model, there remains errors that can dominate the uncertainty in the test results. Although this problem is well-identified, there remains a considerable need for research both to reduce its impact with modified protocols and to quantify the corresponding uncertainties as part of a holistic approach to uncertainty assessment. This work should include exploratory theoretical and experimental research in order to better understand the heterogeneity in space and time of the differential pressures, and to correct them more effectively than with the present zero-flow correction.

Then, according to the state of the art and the analysis of the situation on the ground we performed, we developed a methodology to design and build an experimental facility to characterize the impact of the wind on pressurization test on a reduced model. To do so, we first proposed a physical model that describes the governing physical phenomena during an airleakage measurement performed on a full scale simplified building during windy conditions. From the dimensional analysis of this model, we defined the similarity conditions between full scale tests and reduced scale experiments. Indeed, this analysis led to establish four new non-dimensional numbers, which values have to be conserved between scales to guarantee the similarity. Consequently, we defined four relations between scale ratios regarding the wind speed, the pressure differences, the lengths, the areas, the volumes, and the airflows. The analysis of these relations showed that it was possible to impose a scale ratio of 1 for the wind speed and pressure differences, which was the solution we applied for our experimental facility.

The experimental facility we designed and constructed includes a model (scale 1/25<sup>th</sup>) that represents a single-zone building, a pressurization device that replaces a blowerdoor, and a wind tunnel that reproduces steady wind conditions. The model is scalable and provides nine configurations of leakage distribution between windward and leeward façades, with the same averaged total airtightness for all configurations  $q_4=0.17 \text{ m}^3 \text{ h}^{-1}$ . Our pressurization device includes a flow controller connected to a compressor. The wind tunnel is 4.11 m long and includes a  $1.0*1.0*1.5 \text{ m}^3$  testing chamber. The wind speed inside the testing chamber is homogeneous and can be stabilized from less than  $1 \text{ m s}^{-1}$  to  $7.5 \text{ m s}^{-1}$ . Our experimental facility is controlled by a VBA program coupled to Labview applications we have developed, to control all components and collect all experimental data.

Thanks to our new experimental facility, we performed 96 pressurizations tests that include 864 measurements under steady conditions: for the nine configurations of leakage distribution of our model and under eight different wind speeds (from 0 to 7 m s<sup>-1</sup>). We first analyzed the zero-flow pressure differences as it is considered as an indicator of the environmental conditions. More important, it is one of the major criteria to validate a test according to the ISO 9972 standard. We observed that the variation of the zero-flow pressure difference induced by the wind strongly depends on the leakage distribution: from less than 1 Pa to more than 16 Pa. Moreover, we showed that we can obtain very low zero-flow pressure differences (1 Pa) for strong winds (7 m s<sup>-1</sup>), which indicates that the zero-flow pressure difference is not always a relevant indicator of the windy conditions.

Then, we evaluated the error due to wind for tests performed according to ISO 9972. We observed that the error induced by the wind strongly depends on the leakage distribution, especially for q<sub>4</sub>, with a maximal error varying from 2% (leaks equally distributed) to 35% (60% of the leakage on the windward facade). We also evaluated q<sub>4</sub> and q<sub>50</sub> using 1-point and 2-point test methods according to three different scenarios (depending on the values of the pressure differences). For our reduced scale experiment, under steady wind conditions, the ISO 9972 method is more appropriate than both 1-point and 2-point test methods for an airtightness indicator at 50 Pa. This conclusion concerns all wind speeds and all leakage distributions. When we use an indicator at 4 Pa, as it is the case in France, the conclusion depends on the leakage distributions:

- when leakage is mostly on the leeward side, the ISO 9972 measurement method is also more reliable than both 1-point and 2-point test methods, for all wind speeds;
- when leakage is mostly on the windward side, 1-point test method with a pressure station at 50 Pa or 100 Pa gives lower error when the wind is above 4 m s<sup>-1</sup>.

These results showed that none of the six tested methods led to a strong reduction of the impact of the wind. Nevertheless, it showed that an alternative method might lead to fewer errors due to wind for some configurations.

## 7.2 Perspectives

Our experimental study relies on measurements performed:

- on reduced scale;
- in laboratory conditions;
- during steady windy conditions for a maximum wind speed equal to 7 m s<sup>-1</sup>;
- without stack effect;
- on a single-zone model with two circular leaks;
- in pressurization.

For cost and technical reasons, we have chosen to analyze the wind impact from reduced scale experiments. Although we have respected the similarity conditions, due especially to the size and the shape of the model leaks, the behavior of the air through our leaks might differ from real building leaks. Moreover, the nature of the walls of our model did

not reproduce any valve effect that can happen on full scale buildings. We did not also take into account the impact of internal partitions, that may induce disturbance on the air moving inside the building during a test. We tested nine configurations of leakage distributions, whereas an infinite number of distributions exists for real buildings. As we have shown that this factor very significantly influences the error due to wind, the results of our experimental evaluation do not provide a maximal error that can occur on full scale buildings.

We only reproduced steady wind conditions. We have shown that wind fluctuations may induce larger errors than the mean speed value. Thus, for this reason also, the errors we evaluated are not maximum values.

Because our tests are performed with these conditions, our evaluation of the impact of the wind during pressurization tests performed according to ISO9972 did not lead to the definition of corrections that can be applied for real tests. Nevertheless, it first gives an order of magnitude of the error that be induced by steady wind. As this error can be very high, this study highlights the need to improve the measurement protocol. Whereas the alternative analysis methods we studied did not give more reliable results than the ISO 9972 method, they showed that depending on the wind speed and the leakage distributions, other analysis methods need to be tested.

In order to have an other added value of the developed experimental facility and give it a second life, we advice to continue the work with other reduced scale experiments and full scale experiments.

First, in order to consolidate our results, we need to perform the same measurements under repeatability conditions. Then, with the same experimental data, different analysis methods can be tested, including multi-points methods with non-equally-distributed stations. Analysis methods that take into account the uncertainty of the zero-flow pressure measurement also need to be tested from our experimental data.

As our model is scalable, we also plan to perform new tests with:

- different types of leaks: different shapes, different sizes and different n values (with the integration of insulation material for example);
- adding more leaks: this will require to perform a new similarity analysis and might lead to the modification of the experimental facility.

Another evolution of our experimentation would be to reproduce unsteady conditions. We do not know yet if it will be feasible in our wind tunnel, or if we will need to use an existing atmospheric wind tunnel, which may induce the need to integrate corrections due to a high blocking ratio. We can also consider including stack effect, with the installation of heating system and insulation material on our model.

Secondly, we propose to confront our results to full scale measurements performed on a full scale single-zone experimental building. This step will require a long period of measurements to be able to consider various windy conditions.

As an example of other uses of our experimental facility, a new collaboration between ENTPE-Cerema and Nottingham University has been initiated to test another airtightness

measurement method (the Pulse method). In another field of research, the experimental facility is currently used to study the evaporation of water in insulation material. Many other applications are being discussed with insulation and ventilation industrials.



## References

- [1] European Parliament and Council, Directive 2010/31/EU of 19 May 2010 on the energy performance of buildings, 2010.
- [2] M. Limb, Air infiltration and ventilation glossary, AIVC. (1992) 47.
- [3] G.T. Tamura, Measurement of air leakage characteristics of house enclosures, ASHRAE Trans. (1975) 202–211.
- [4] F.R. Carrié, B. Rosenthal, An overview of national trends in envelope and ductwork airtightness, AIVC Ventilation Information paper. (2008).
- [5] V. Leprince, A. Bailly, F.R. Carrié, M. Olivier, State of the Art of Non-Residential Buildings Air-tightness and Impact on the Energy Consumption, in: Proceedings of the 32nd AIVC Conference, 12-13 October 2011, Brussels, Belgium, 2011: pp. 12–13. <http://www.aivc.org/sites/default/files/7b2.pdf>.
- [6] J.M. Logue, M.H. Sherman, I.S. Walker, B.C. Singer, Energy impacts of envelope tightening and mechanical ventilation for the U.S. residential sector, Energy and Buildings. 65 (2013) 281–291. <https://doi.org/10.1016/j.enbuild.2013.06.008>.
- [7] J. Jokisalo, J. Kurnitski, M. Korpi, T. Kalamees, J. Vinha, Building leakage, infiltration, and energy performance analyses for Finnish detached houses, Building and Environment. 44 (2009) 377–387. <https://doi.org/10.1016/j.buildenv.2008.03.014>.
- [8] T. Kalamees, Air tightness and air leakages of new lightweight single-family detached houses in Estonia, Building and Environment. 42 (2007) 2369–2377. <https://doi.org/10.1016/j.buildenv.2006.06.001>.
- [9] F. Richieri, B. Moujalled, S. Salem, M. Bourdassol, F.R. Carrié, Numerical evaluation of the airtightness impact on energy needs in mechanically ventilated dwellings, in: 8th International BUILDAIR Symposium on Building and Ductwork Airtightness, Hannover, Germany, 2013: p. 11 p. [http://www.aivc.org/sites/default/files/52\\_0.pdf](http://www.aivc.org/sites/default/files/52_0.pdf) (accessed March 18, 2016).
- [10] M.H. Sherman, W.R. Chan, Building Airtightness: Research and Practice. Building Ventilation: The State of the Art Review, LBNL Report. (2004).
- [11] ISO, EN ISO 9972: Thermal performance of buildings - Determination of air permeability of buildings - Fan pressurization method, (2015).
- [12] ASTM, E779-19 Standard Test Method for Determining Air Leakage Rate by Fan Pressurization, ASTM International. (2019). <https://doi.org/10.1520/E0779-19>.
- [13] S. Charrier, A.B. Mélois, F.R. Carrié, Building airtightness in France: regulatory context, control, procedures, results, QUALICHeCK. (2015). <http://qualicheck-platform.eu/wp-content/uploads/2016/12/QUALICHeCK-Factsheet-37.pdf>.
- [14] F.R. d'Ambrosio Alfano, M. Dell'Isola, G. Ficco, F. Tassini, Experimental analysis of air tightness in Mediterranean buildings using the fan pressurization method, Building and Environment. 53 (2012) 16–25. <https://doi.org/10.1016/j.buildenv.2011.12.017>.
- [15] D. Sinnott, Dwelling airtightness: A socio-technical evaluation in an Irish context, Building and Environment. 95 (2016) 264–271. <https://doi.org/10.1016/j.buildenv.2015.08.022>.
- [16] J. Vinha, E. Manelius, M. Korpi, K. Salminen, J. Kurnitski, M. Kiviste, A. Laukkarinen, Airtightness of residential buildings in Finland, Building and Environment. 93 (2015) 128–140. <https://doi.org/10.1016/j.buildenv.2015.06.011>.
- [17] J. Feijó-Muñoz, R.A. González-Lezcano, I. Poza-Casado, M.Á. Padilla-Marcos, A. Meiss, Airtightness of residential buildings in the Continental area of Spain, Building and Environment. (2018). <https://doi.org/10.1016/j.buildenv.2018.11.010>.

- [18] W.R. Chan, W.W. Nazaroff, P.N. Price, M.D. Sohn, A.J. Gadgil, Analyzing a database of residential air leakage in the United States, *Atmospheric Environment*. 39 (2005) 3445–3455. <https://doi.org/10.1016/j.atmosenv.2005.01.062>.
- [19] W.R. Chan, J. Joh, M.H. Sherman, Analysis of air leakage measurements of US houses, *Energy and Buildings*. 66 (2013) 616–625. <https://doi.org/10.1016/j.enbuild.2013.07.047>.
- [20] I.S. Walker, M.H. Sherman, J. Joh, W.R. Chan, Applying Large Datasets to Developing a Better Understanding of Air Leakage Measurement in Homes, *International Journal of Ventilation*. 11 (2013). <https://www.tandfonline.com/doi/abs/10.1080/14733315.2013.11683991>.
- [21] V. Leprince, F.R. Carrié, M. Kapsalaki, Building and ductwork airtightness requirements in Europe – Comparison of 10 European countries, in: *Proceedings of 38th AIVC Conference, 13-14 September 2017, Nottingham, UK, 2017*.
- [22] JO, Méthode de calcul Th-BCE 2012 - ANNEXE A l'arrêté portant approbation de la méthode de calcul Th-BCE 2012, (2011).
- [23] Effinergie, Règles techniques Labels Effinergie + - Version 7, (2017).
- [24] M. De Strycker, L. Van Gelder, V. Leprince, Quality framework for airtightness testing in the Flemish Region of Belgium – feedback after three years of experience, in: *In Proceedings of the 39th AIVC Conference “Smart Ventilation for Buildings,” Antibes Juan-Les-Pins, France, 2018*. <https://www.aivc.org/resource/quality-framework-airtightness-testing-flemish-region-belgium-feedback-after-three-years>.
- [25] J. Love, J. Wingfield, A.Z.P. Smith, P. Biddulph, T. Oreszczyn, R. Lowe, C.A. Elwell, ‘Hitting the target and missing the point’: Analysis of air permeability data for new UK dwellings and what it reveals about the testing procedure, *Energy and Buildings*. 155 (2017) 88–97. <https://doi.org/10.1016/j.enbuild.2017.09.013>.
- [26] Government of Ireland, Technical Guidance Document L- Conservation of Fuel and Energy – Dwellings, 2019.
- [27] B. Moujalled, V. Leprince, A.B. Mélois, French database of building airtightness, statistical analyses of about 215,000 measurements: impacts of buildings characteristics and seasonal variations, in: *Antibes, 2018*.
- [28] V. Leprince, F.R. Carrié, Comparison of building preparation rules for airtightness testing in 11 European countries, in: *Poznań, Poland, 2014*. <https://www.aivc.org/resource/comparison-building-preparation-rules-airtightness-testing-11-european-countries> (accessed December 5, 2018).
- [29] FD P50-784 Juillet 2016 Performance thermique des bâtiments - Guide d'application de la norme NF EN ISO 9972, (2016).
- [30] V. Leprince, R. Carrié, M. Olivier, The quality framework for Air-tightness measurers in France: assessment after 3 years of operation., in: *Proceedings 32nd AIVC Conference “Towards Optimal Airtightness Performance,” Brussels, Belgium, 2011: p. 6 p.* <http://www.aivc.org/sites/default/files/4b2.pdf> (accessed October 26, 2016).
- [31] A.B. Mélois, B. Moujalled, G. Guyot, V. Leprince, Improving building envelope knowledge from analysis of 219,000 certified on-site air leakage measurements in France, *Building and Environment*. (2019). <https://doi.org/10.1016/j.buildenv.2019.05.023>.
- [32] JO, Arrêté du 24 mars 1982 consolidée relatif à l'aération des logements : aération générale ou permanente, (n.d.).
- [33] V. Leprince, A. Bailly, F.R. Carrié, M. Olivier, State of the Art of Non-Residential Buildings Air-tightness and Impact on the Energy Consumption, in: *Proceedings*

- of the 32nd AIVC Conference “Towards Optimal Airtightness Performance,” Brussels, Belgium, 2011: pp. 12–13.  
<http://www.aivc.org/sites/default/files/7b2.pdf> (accessed October 26, 2016).
- [34] F. Domhagen, P. Wahlgren, Consequences of Varying Airtightness in Wooden Buildings, *Energy Procedia*. 132 (2017) 873–878.  
<https://doi.org/10.1016/j.egypro.2017.09.688>.
- [35] H. Yoshino, System for ensuring reliable airtightness level in Japan, in: Brussels, Belgium, 2012.
- [36] W. Borsboom, W. de Gids, Seasonal variation of facade airtightness: field observations and potential impact in NZEB, in: Brussels, Belgium, 2012.
- [37] P. Wahlgren, SEASONAL VARIATION IN AIRTIGHTNESS, (n.d.) 8.
- [38] V. Leprince, B. Moujalled, A. Litvak, Durability of building airtightness, review and analysis of existing studies, (n.d.) 14.
- [39] J. Kronvall, Testing of houses for air leakage using a pressure method, *ASHRAE Trans.* (1978) 72–79.
- [40] E.D. Thimons, R.P. Vinson, F.N. Kissell, A. Tall, Window method for measuring leakage, 4,055,074, 1977.
- [41] L.E. Nevander, J. Kronvall, Air tightness of buildings - Research in Sweden, in: Paris, France, 1978.
- [42] M.H. Sherman, D.T. Grimsrud, Measurement of infiltration using fan pressurization and weather data, NASA STI/Recon Technical Report N. 81 (1980).  
<http://adsabs.harvard.edu/abs/1980STIN...8132332S> (accessed June 6, 2018).
- [43] H. Yoshino, The current of air-tightness and ventilation system in houses of Japan, in: Kyoto, 2008: pp. 341–347.
- [44] I.S. McIntyre, C.J. Newman, The testing of whole houses for air leakage, Princes Risborough Laboratory, 1975.
- [45] G.E. Caffey, Residential air infiltration, *ASHRAE Trans.* (1979).
- [46] S. Stricker, Measurement of air leakage of houses, Ontario hydro research quarterly. 4th quarter (1974) 11–18.
- [47] Orr H. W, Figley D. A., An exhaust fan apparatus for assessing the air leakage characteristics of houses, (1980).
- [48] D.W. Etheridge, Air leakage characteristics of houses—a new approach, *Building Services Engineering Research and Technology*. 5 (1984) 32–36.
- [49] P.J. Jackman, Review of building airtightness and ventilation standards, in: Nevada, 1984.
- [50] K.J. Gadsby, D.T. Harrje, Fan pressurization of buildings: Standards, calibration, and field experience, *ASHRAE Trans.*; (United States). 91:2B (1985).  
<https://www.osti.gov/biblio/5552192>.
- [51] F.R. Carrié, V. Leprince, Uncertainties in building pressurisation tests due to steady wind, *Energy and Buildings*. 116 (2016) 656–665.  
<https://doi.org/10.1016/j.enbuild.2016.01.029>.
- [52] C. Delmotte, J. Laverge, Interlaboratory tests for the determination of repeatability and reproducibility of buildings airtightness measurements, in: Proceedings of the 32nd AIVC Conference, 12-13 October 2011, Brussels, Belgium, 2011.
- [53] ASTM - E06 Committee, ASTM E3158 - 18: Standard Test Method for Measuring the Air Leakage Rate of a Large or Multizone Building, (2018).  
<https://doi.org/10.1520/E3158-18>.
- [54] A. Zhivov, D. Bailey, D. Herron, U.S. Army Corps of Engineers Air Leakage Test Protocol for Building Envelopes - Version 3, (2015).

- [55] ABAA, ABAA Standard Method for Building Enclosure Airtightness Compliance Testing, (2016).
- [56] ANSI/RESNET/ICC, ANSI/RESNET/ICC 380-2016: Standard for Testing Airtightness of Building Enclosures, Airtightness of Heating and Cooling Air Distribution Systems, and Airflow of Mechanical Ventilation Systems, (2016).
- [57] JIS, JSA - JIS A 2201 - Test method for performance of building airtightness by fan pressurization, (n.d.).
- [58] M.P. Modera, M.H. Sherman, AC pressurization: a technique for measuring leakage area in residential buildings, in: In Proceedings of American Society of Heating, Refrigerating and Air-Conditioning Engineers' Semiannual Meeting, 23 Jun 1985, Honolulu, HI, USA, 1985.
- [59] E. Cooper, X. Zheng, C. Wood, M. Gillot, D. Tetlow, S. Riffat, L.D. Simon, Field trialling of a pulse airtightness tester in a range of UK homes, *International Journal of Ventilation*. 18 (2016) 1–18. <https://doi.org/10.1080/14733315.2016.1252155>.
- [60] C. Mees, X. Loncour, Quality framework for reliable fan pressurisation tests, Qualicheck. (2016).
- [61] V. Leprince, F.R. Carrié, Reasons behind and lessons learnt with the development of airtightness testers schemes in 11 European countries, in: Proceedings of the AIVC International Workshop, 18-19 March 2014, Brussels, Belgium, 2014.
- [62] BIPM, JCGM 100:2008 - Evaluation of measurement data - Guide to the expression of uncertainty in measurement, (2008).
- [63] CEN, EN 14134: Ventilation for buildings - Performance measurement and checks for residential ventilation systems, (2019).
- [64] Cerema, Outil\_verification\_calculs\_perméa\_enveloppe, Cerema, 2017. [http://www.rt-batiment.fr/IMG/xlsx/outil\\_verification\\_calculs\\_perméa\\_enveloppe\\_iso\\_v4.xlsx](http://www.rt-batiment.fr/IMG/xlsx/outil_verification_calculs_perméa_enveloppe_iso_v4.xlsx).
- [65] W.E. Murphy, D.G. Colliver, L.R. Piercy, Repeatability and reproducibility of fan pressurization devices in measuring building airleakage, *ASHRAE Trans.* (1991) 885–895.
- [66] A.K. Persily, Repeatability and accuracy of pressurization testing, in: Proceedings of ASHRAE-DOE Conference, Dec 6-9 1982, USA, 1982: pp. 380–390.
- [67] P. duPont, Blower doors: variation in leakage measurements, *Energy Auditor & Retrofitter*. (1986) 7–10.
- [68] M.H. Sherman, D.T. Grimsrud, Infiltration-pressurization correlation: Simplified physical modeling, *ASHRAE Trans.* (1980).
- [69] A.K. Persily, R.A. Grot, Accuracy in Pressurization Data Analysis, *ASHRAE Trans.* (1984).
- [70] M. Sherman, L. Palmiter, Uncertainties in Fan Pressurization Measurements, *Airflow Performance of Building Envelopes, Components, and Systems*. (1994). <https://doi.org/10.1520/STP14701S>.
- [71] F.R. Carrié, P. Wouters, Building airtightness: a critical review of testing, reporting and quality schemes in 10 countries, *AIVC Technical note*. 67 (2012).
- [72] T. Brennan, G. Nelson, C. Olson, Repeatability of Whole-Building Airtightness Measurements: Midrise Residential Case Study, in: In Proceedings of AIVC International Workshop, April 18-19, 2013, Washington D.C, 2013.
- [73] M.P. Modera, D.J. Wilson, The Effects of Wind on Residential Building Leakage Measurements, Air Change Rate and Airtightness in Buildings -. *ASTMSTP 1067* (1990). <https://doi.org/10.1520/STP17210S>.

- [74] I.S. Walker, D.J. Wilson, M.H. Sherman, A comparison of the power law to quadratic formulations for air infiltration calculations, *Energy and Buildings*. 27 (1998) 293–299. [https://doi.org/10.1016/S0378-7788\(97\)00047-9](https://doi.org/10.1016/S0378-7788(97)00047-9).
- [75] D.W. Etheridge, A note on crack flow equations for ventilation modelling, *Building and Environment*. 33 (1998) 325–328. [https://doi.org/10.1016/S0360-1323\(97\)00072-3](https://doi.org/10.1016/S0360-1323(97)00072-3).
- [76] Y.H. Chiu, D.W. Etheridge, Calculations and Notes on the Quadratic and Power Law Equations for Modelling Infiltration, *International Journal of Ventilation*. 1 (2002) 65–77. <https://doi.org/10.1080/14733315.2002.11683623>.
- [77] T. Baracu, V. Badescu, C. Teodosiu, M. Degeratu, M. Patrascu, C. Streche, Consideration of a new extended power law of air infiltration through the building's envelope providing estimations of the leakage area, *Energy and Buildings*. 149 (2017) 400–423. <https://doi.org/10.1016/j.enbuild.2017.04.055>.
- [78] F.R. Carrié, Temperature and pressure corrections for power-law coefficients of airflow through ventilation system components and leaks, in: in proceedings of 35th AIVC Conference, 24-25 September 2014, Poznań, Poland, 2014.
- [79] M. Sherman, A Power-Law Formulation of Laminar Flow in Short Pipes, *J. Fluids Eng*. 114 (1992) 601–605. <https://doi.org/10.1115/1.2910073>.
- [80] D.W. Etheridge, M. Sandberg, *Building Ventilation: Theory and Measurement*, JOHN WILEY & SONS, JOHN WILEY & SONS, 1996. <https://www.wiley.com/en-us/Building+Ventilation%3A+Theory+and+Measurement-p-9780471960874> (accessed November 12, 2018).
- [81] C. Delmotte, Airtightness of Buildings—Considerations regarding the Zero-Flow Pressure and the Weighted Line of Organic Correlation, in: In Proceedings of 38th AIVC Conference, 13-14 September 2017, Nottingham, UK, 2017.
- [82] M. Prignon, A. Dawans, S. Altomonte, G. Van Moeseke, A method to quantify uncertainties in airtightness measurements: Zero-flow and envelope pressure, *Energy and Buildings*. 188–189 (2019) 12–24. <https://doi.org/10.1016/j.enbuild.2019.02.006>.
- [83] S. Rolfsmeier, K. Vogel, T. Bolender, Ringversuche zu Luftdurchlässigkeitsmessungen vom Fachverband Luftdichtheit im Bauwesen e.V., in: In Proceedings of 6th Build'air Symposium, May 6, 2011, Berlin-Adlershof, 2011.
- [84] W. Walther, B. Rosenthal, Airtightness testing of large and multi-family buildings in an energy performance regulation context, *ASIEPI Information Papers P165*. (2009).
- [85] B. Moujalled, F. Richieri, F.R. Carrié, A. Litvak, Comparison of sampling methods for air tightness measurements in new French residential buildings, in: In Proceedings of CISBAT 2011 - International Conference, Lausanne, Switzerland, 2011.
- [86] J. Novak, The use of a sampling method for airtightness measurement of multifamily residential buildings - An example, in: In the Proceedings of 32nd AIVC Conference, Brussels, Belgium, 2011. <https://www.aivc.org/resource/use-sampling-method-airtightness-measurement-multifamily-residential-buildings-example> (accessed February 20, 2020).
- [87] J. Novak, Influence of the external pressure tap position on the airtightness test result, in: In Proceedings of 40th AIVC Conference, 15-16 October 2019, Ghent, Belgium, 2019. <https://www.aivc.org/resource/influence-external-pressure-tap-position-airtightness-test-result> (accessed February 17, 2020).

- [88] A.K. Persily, Air flow calibration of buildings pressurization devices, NBS Report. NBSIR 84-2849 (1984).
- [89] C. Delmotte, Airtightness of buildings—Calculation of combined standard uncertainty, in: In Proceedings of 34th AIVC Conference, 24-25 September 2014, 2014.
- [90] M. Prignon, A. Dawans, G. Van Moeseke, Uncertainties in airtightness measurements: regression methods and pressure sequences, in: In Proceedings of the 39th AIVC Conference “Smart Ventilation for Buildings,” Antibes Juan-Les-Pins, France, 2018. <https://www.aivc.org/resource/uncertainties-airtightness-measurements-regression-methods-and-pressure-sequences>.
- [91] M. Prignon, C. Delmotte, A. Dawans, S. Altomonte, G. van Moeseke, On the impact of regression technique to airtightness measurements uncertainties, *Energy and Buildings*. 215 (2020) 109919. <https://doi.org/10.1016/j.enbuild.2020.109919>.
- [92] V. Leprince, C. Delmotte, I. Caré, Deviation of blower-door fans over years through the analysis of fan calibration certificates, in: In Proceedings of the 40th AIVC Conference “From Energy Crisis to Sustainable Indoor Climate – 40 Years of AIVC,” Ghent, Belgium, 2019. <https://www.aivc.org/resource/deviation-blower-door-fans-over-years-through-analysis-fan-calibration-certificates> (accessed June 3, 2020).
- [93] C. Delmotte, Airtightness of buildings – Considerations regarding place and nature of pressure taps, in: In Proceedings of 40th AIVC Conference, 15-16 October 2019, Ghent, Belgium, 2019. <https://www.aivc.org/resource/airtightness-buildings-considerations-regarding-place-and-nature-pressure-taps> (accessed February 17, 2020).
- [94] F.R. Carrié, A.B. Mélois, Modelling building airtightness pressurisation tests with periodic wind and sharp-edged openings, *Energy and Buildings*. (2019). <https://doi.org/10.1016/j.enbuild.2019.109642>.
- [95] M. Prignon, A. Dawans, G. Van Moeseke, Quantification of uncertainty in zero-flow pressure approximation, in: In Proceedings of 40th AIVC Conference, 15-16 October 2019, Ghent, Belgium, 2019. <https://www.aivc.org/resource/quantification-uncertainty-zero-flow-pressure-approximation> (accessed February 13, 2020).
- [96] H. Okuyama, Y. Onishi, Reconsideration of parameter estimation and reliability evaluation methods for building airtightness measurement using fan pressurization, *Building and Environment*. 47 (2012) 373–384. <https://doi.org/10.1016/j.buildenv.2011.06.027>.
- [97] D.W. Etheridge, Unsteady flow effects due to fluctuating wind pressures in natural ventilation design—mean flow rates, *Building and Environment*. 35 (2000) 111–133.
- [98] D.W. Etheridge, Unsteady flow effects due to fluctuating wind pressures in natural ventilation design—instantaneous flow rates, *Building and Environment*. 35 (2000) 321-337 111–133.
- [99] M.P. Modera, Periodic flow through thin-plate slots., Doctoral Dissertation, Dept. of heating and Ventilating, Royal institute of Tehcnology of Stockholm, 1989.
- [100] N. Le Roux, Etude par similitude de l’influence du vent sur les transferts de masse dans les bâtiments complexes, Université de La Rochelle, 2011.
- [101] C.-K. Choi, D.K. Kwon, Wind tunnel blockage effects on aerodynamic behavior of bluff body, *Wind and Structures An International Journal*. (1998).
- [102] M. Orme, M.W. Liddament, A. Wilson, Numerical data for air infiltration and natural ventilation calculations, n.d.

- [103] G. Guyot, J. Ferlay, E. Gonze, M. Woloszyn, P. Planet, T. Bello, Multizone air leakage measurements and interactions with ventilation flows in low-energy homes, *Building and Environment*. 107 (2016) 52–63.  
<https://doi.org/10.1016/j.buildenv.2016.07.014>.
- [104] M.W. Liddament, *A Guide to Energy Efficient Ventilation - AIC-TN-VENTGUIDE-1996*, (1996) 254 pp.
- [105] ASHRAE, *2009 ASHRAE Handbook - Fundamentals*, SI Edition, 2009.
- [106] C. Ge, *Design, construction and characterization of a wind tunnel*, New Jersey Institute of Technology, 2015.
- [107] S. Mauro, S. Brusca, R. Lanzafame, F. Famoso, A. Galvagno, M. Messina, Small-Scale Open-Circuit Wind Tunnel: Design Criteria, Construction and Calibration, *International Journal of Applied Engineering Research*. 12 (2017) 13649–13662.
- [108] M.A. Gonzalez Hernandez, A.I. Moreno Lopez, A. A., J.M. Perales Perales, Y. Wu, S. Xiaoxiao, Design Methodology for a Quick and Low-Cost Wind Tunnel, in: N. Ahmed (Ed.), *Wind Tunnel Designs and Their Diverse Engineering Applications*, InTech, 2013. <https://doi.org/10.5772/54169>.
- [109] J.H. Bell, R.D. Mehta, *Contraction design for small low-speed wind tunnels*, 1988. <https://ntrs.nasa.gov/search.jsp?R=19890004382>.
- [110] L. Prandtl, *Attaining a steady air stream in wind tunnels*, (1933).  
<http://ntrs.nasa.gov/search.jsp?R=19930094691> (accessed November 26, 2019).



## Annex A - Evaluation of the error due to neglecting the gravity term in the pressure difference evaluation at openings level

Error due to gravity simplification for the evaluation of the pressure difference on a leeward leak in  
depressurization

U (m s <sup>-1</sup> )	p <sub>i</sub> = -10 Pa			p <sub>i</sub> = -70 Pa		
	z=0,1 m	z=1 m	z=2,5 m	z=0,1 m	z=1 m	z=2,5 m
0	0,001%	0,012%	0,029%	0,001%	0,012%	0,029%
1	0,001%	0,012%	0,030%	0,001%	0,012%	0,029%
2	0,001%	0,014%	0,034%	0,001%	0,012%	0,030%
3	0,002%	0,017%	0,043%	0,001%	0,012%	0,031%
4	0,003%	0,028%	0,069%	0,001%	0,013%	0,032%
5	0,012%	0,121%	<b>0,303%</b>	0,001%	0,013%	0,033%
6	-0,004%	-0,039%	-0,097%	0,001%	0,014%	0,036%
7	-0,002%	-0,015%	-0,038%	0,002%	0,016%	0,039%
8	-0,001%	-0,009%	-0,022%	0,002%	0,017%	0,044%
9	-0,001%	-0,006%	-0,015%	0,002%	0,020%	0,050%
10	0,000%	-0,004%	-0,011%	0,002%	0,024%	0,060%
11	0,000%	-0,003%	-0,009%	0,003%	0,031%	0,078%
12	0,000%	-0,003%	-0,007%	0,005%	0,045%	0,114%

Error due to gravity simplification for the evaluation of the pressure difference on a leeward leak in  
pressurization

U (m s <sup>-1</sup> )	p <sub>i</sub> = 10 Pa			p <sub>i</sub> = 70 Pa		
	z=0,1 m	z=1 m	z=2,5 m	z=0,1 m	z=1 m	z=2,5 m
0	0,001%	0,012%	0,029%	0,001%	0,012%	0,029%
1	0,001%	0,011%	0,028%	0,001%	0,012%	0,029%
2	0,001%	0,010%	0,025%	0,001%	0,011%	0,029%
3	0,001%	0,009%	0,022%	0,001%	0,011%	0,028%
4	0,001%	0,007%	0,018%	0,001%	0,011%	0,027%
5	0,001%	0,006%	0,015%	0,001%	0,010%	0,026%
6	0,001%	0,005%	0,013%	0,001%	0,010%	0,025%
7	0,000%	0,004%	0,011%	0,001%	0,009%	0,023%
8	0,000%	0,004%	0,009%	0,001%	0,009%	0,022%
9	0,000%	0,003%	0,007%	0,001%	0,008%	0,021%
10	0,000%	0,003%	0,006%	0,001%	0,008%	0,019%
11	0,000%	0,002%	0,005%	0,001%	0,007%	0,018%
12	0,000%	0,002%	0,005%	0,001%	0,007%	0,017%

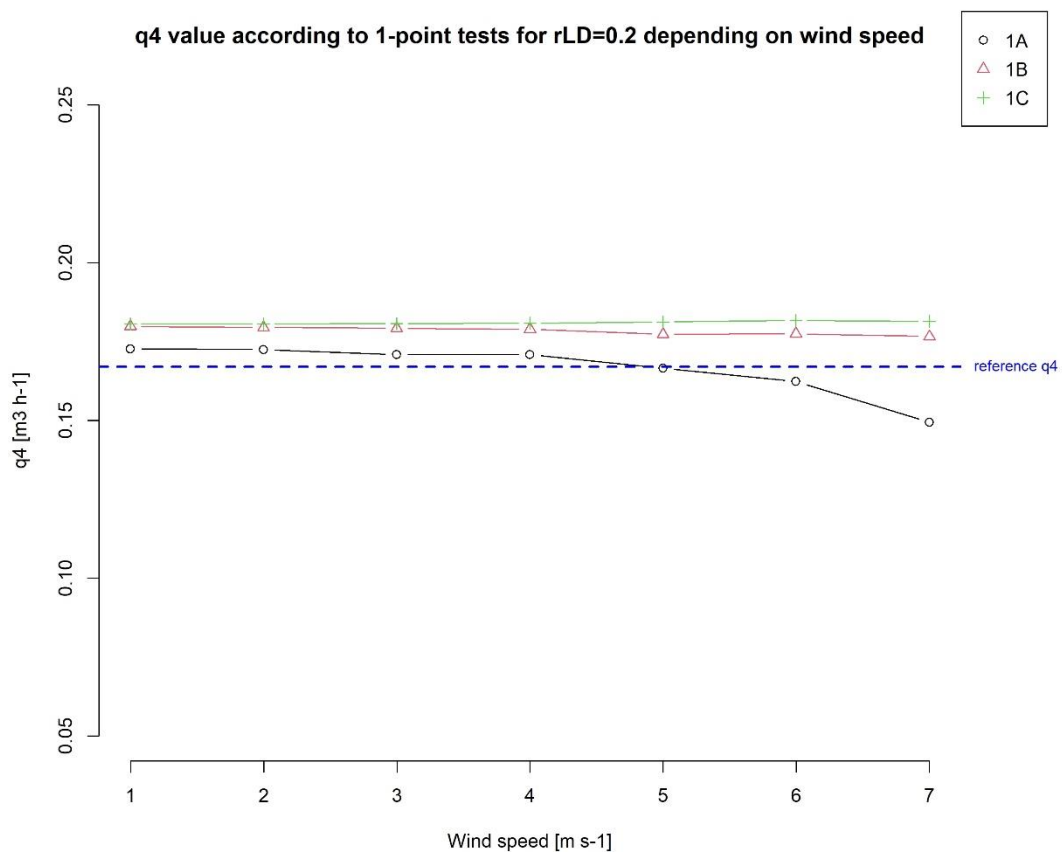
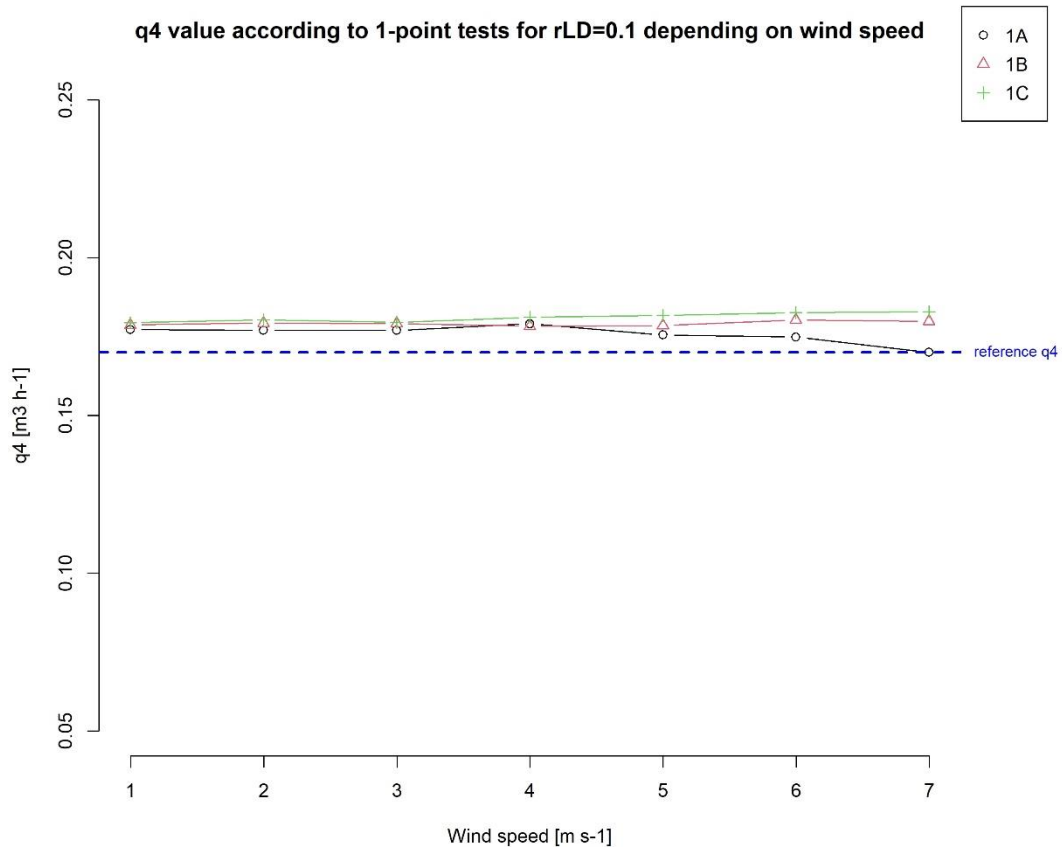
Error due to gravity simplification for the evaluation of the pressure difference on a windward leak in depressurization

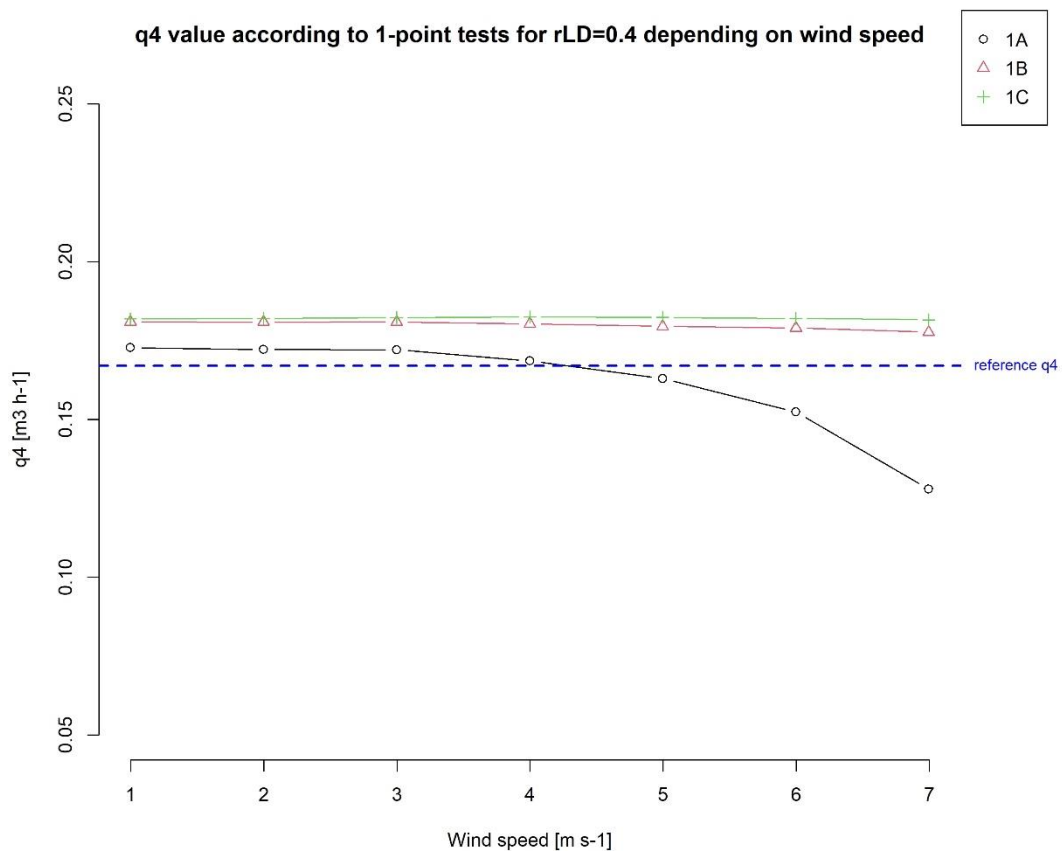
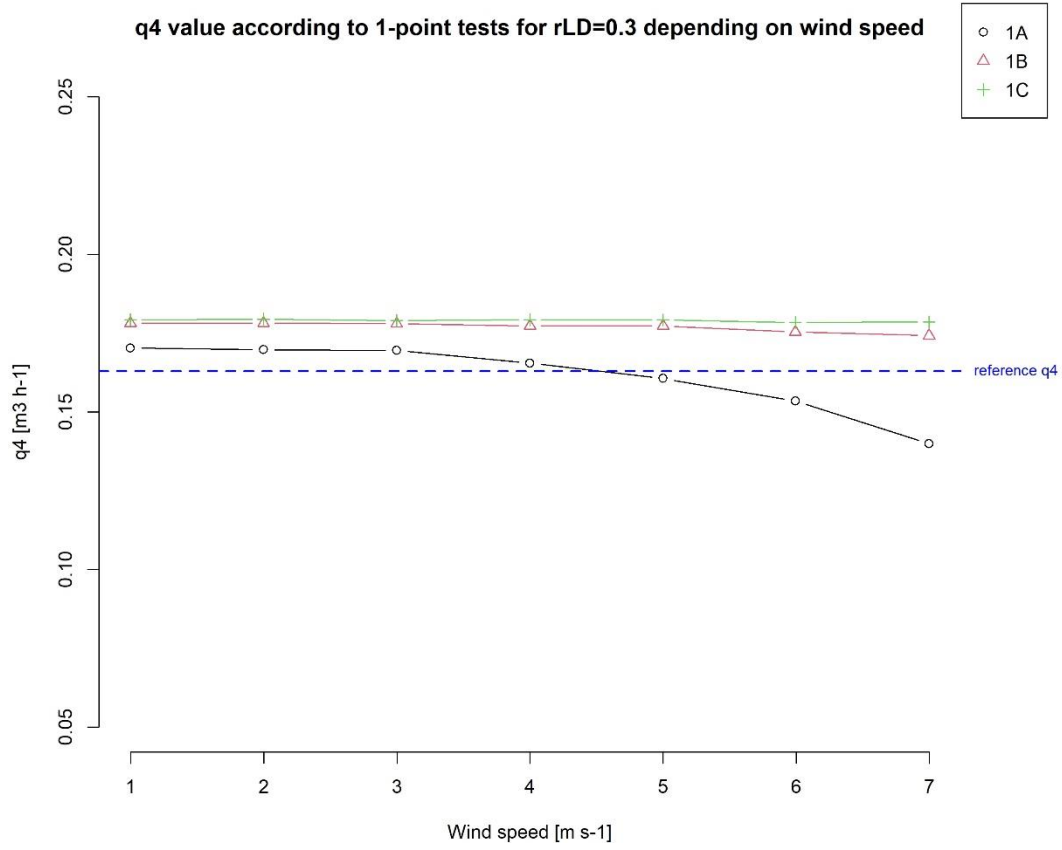
U (m s <sup>-1</sup> )	p <sub>i</sub> = -10 Pa			p <sub>i</sub> = -70 Pa		
	z=0,1 m	z=1 m	z=2,5 m	z=0,1 m	z=1 m	z=2,5 m
0	0,001%	0,012%	0,029%	0,001%	0,012%	0,029%
1	0,001%	0,011%	0,028%	0,001%	0,012%	0,029%
2	0,001%	0,010%	0,026%	0,001%	0,011%	0,029%
3	0,001%	0,009%	0,023%	0,001%	0,011%	0,028%
4	0,001%	0,008%	0,020%	0,001%	0,011%	0,027%
5	0,001%	0,007%	0,017%	0,001%	0,011%	0,026%
6	0,001%	0,006%	0,014%	0,001%	0,010%	0,025%
7	0,000%	0,005%	0,012%	0,001%	0,010%	0,024%
8	0,000%	0,004%	0,010%	0,001%	0,009%	0,023%
9	0,000%	0,003%	0,008%	0,001%	0,009%	0,022%
10	0,000%	0,003%	0,007%	0,001%	0,008%	0,020%
11	0,000%	0,003%	0,006%	0,001%	0,008%	0,019%
12	0,000%	0,002%	0,005%	0,001%	0,007%	0,018%

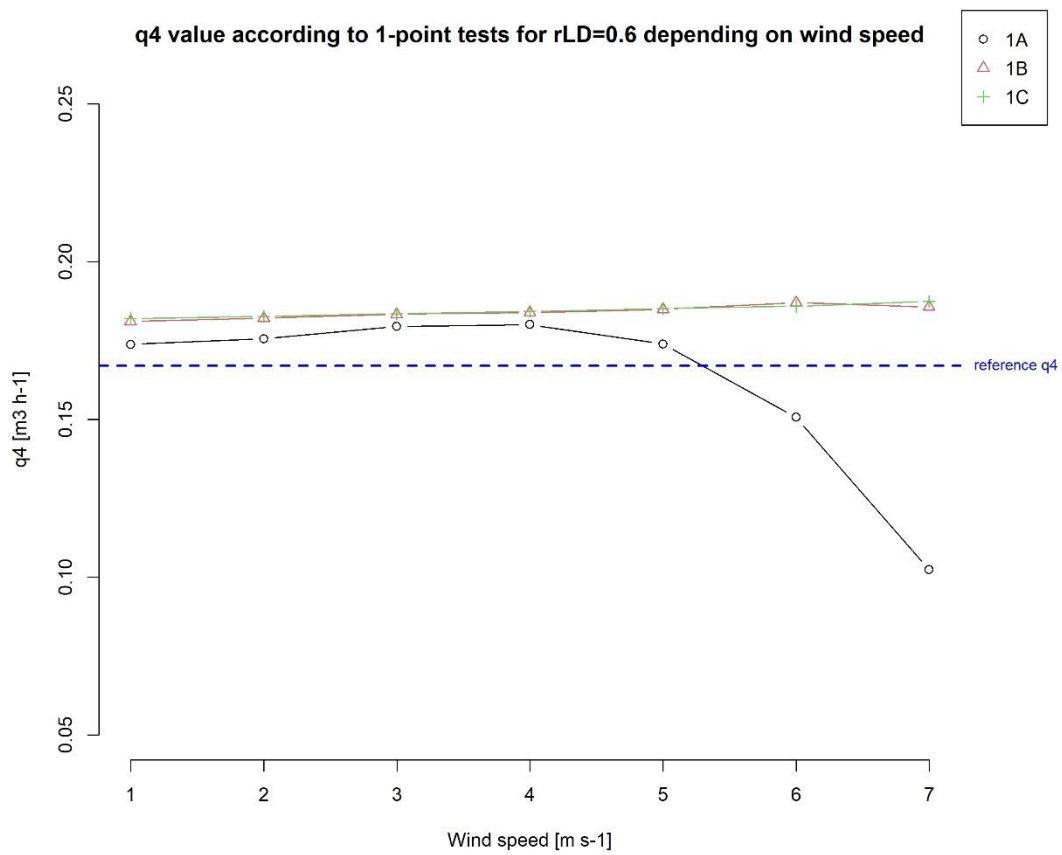
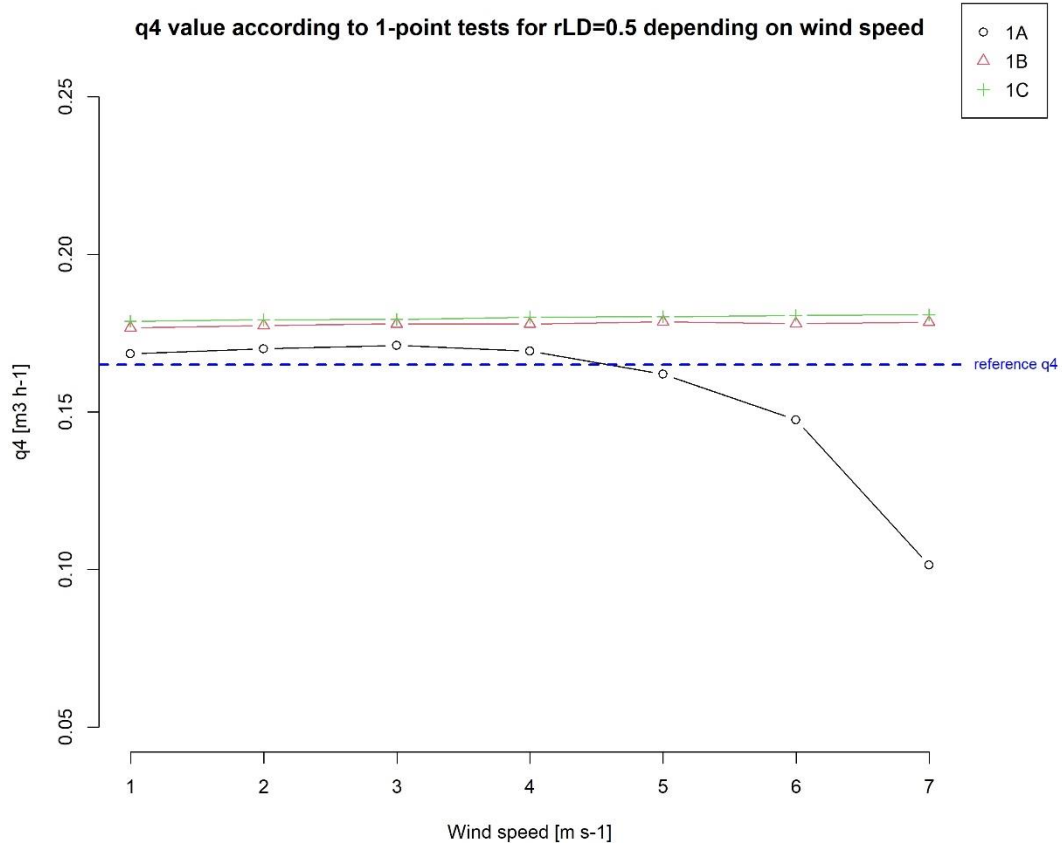
Error due to gravity simplification for the evaluation of the pressure difference on a windward leak in pressurization

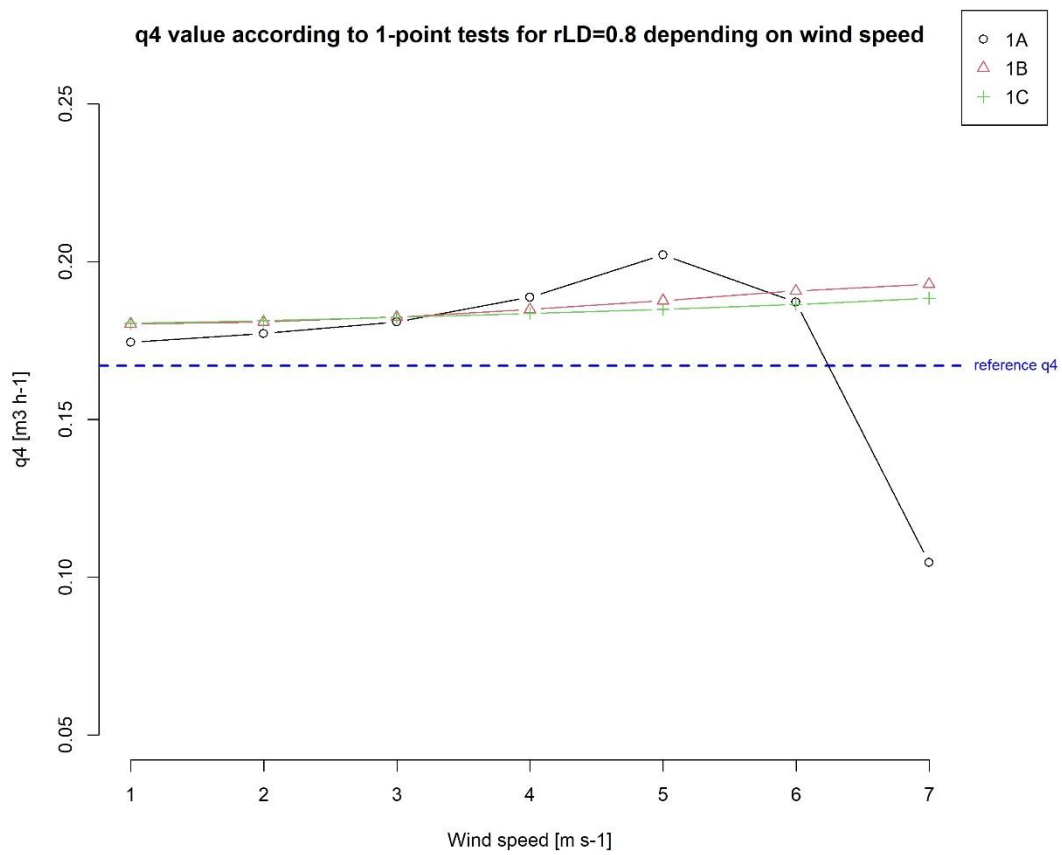
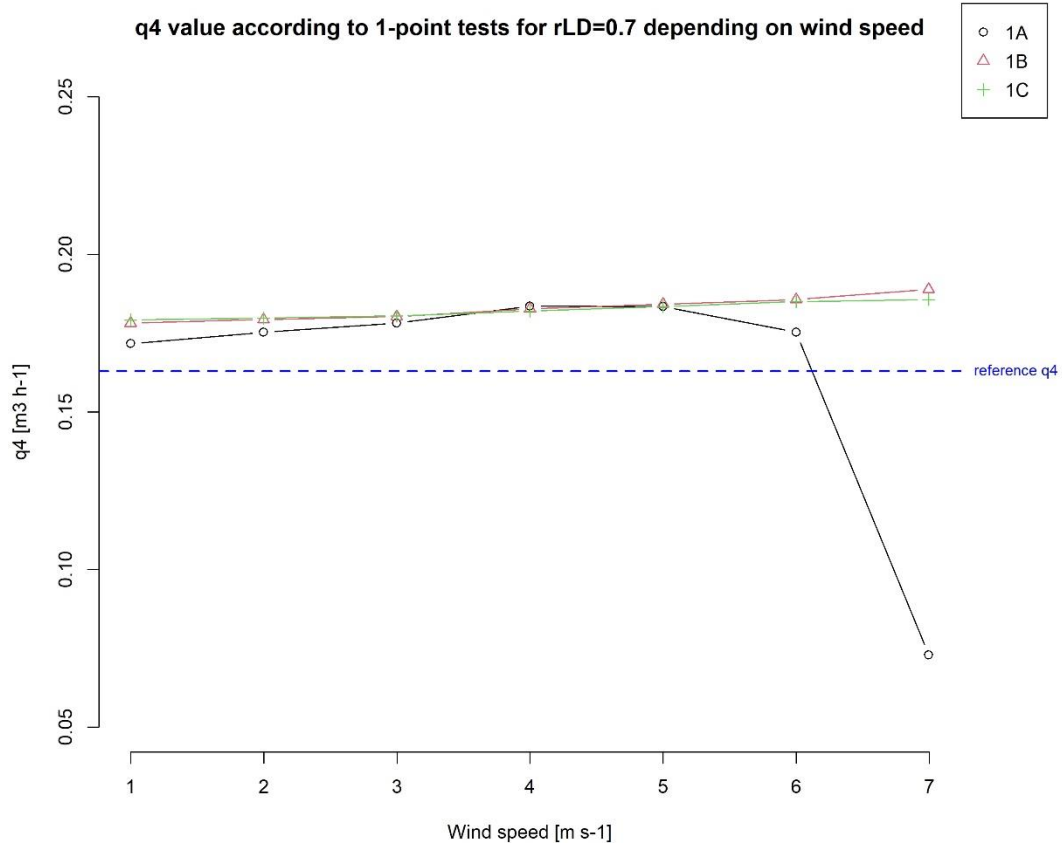
U (m s <sup>-1</sup> )	p <sub>i</sub> = 10 Pa			p <sub>i</sub> = 70 Pa		
	z=0,1 m	z=1 m	z=2,5 m	z=0,1 m	z=1 m	z=2,5 m
0	0,001%	0,012%	0,029%	0,001%	0,012%	0,029%
1	0,001%	0,012%	0,030%	0,001%	0,012%	0,029%
2	0,001%	0,013%	0,033%	0,001%	0,012%	0,030%
3	0,002%	0,016%	0,040%	0,001%	0,012%	0,030%
4	0,002%	0,023%	0,056%	0,001%	0,013%	0,031%
5	0,005%	0,047%	0,118%	0,001%	0,013%	0,033%
6	-0,014%	-0,138%	<b>-0,345%</b>	0,001%	0,014%	0,035%
7	-0,002%	-0,025%	-0,061%	0,001%	0,015%	0,037%
8	-0,001%	-0,013%	-0,031%	0,002%	0,016%	0,040%
9	-0,001%	-0,008%	-0,020%	0,002%	0,018%	0,045%
10	-0,001%	-0,006%	-0,014%	0,002%	0,020%	0,051%
11	0,000%	-0,004%	-0,011%	0,002%	0,024%	0,061%
12	0,000%	-0,003%	-0,009%	0,003%	0,031%	0,077%

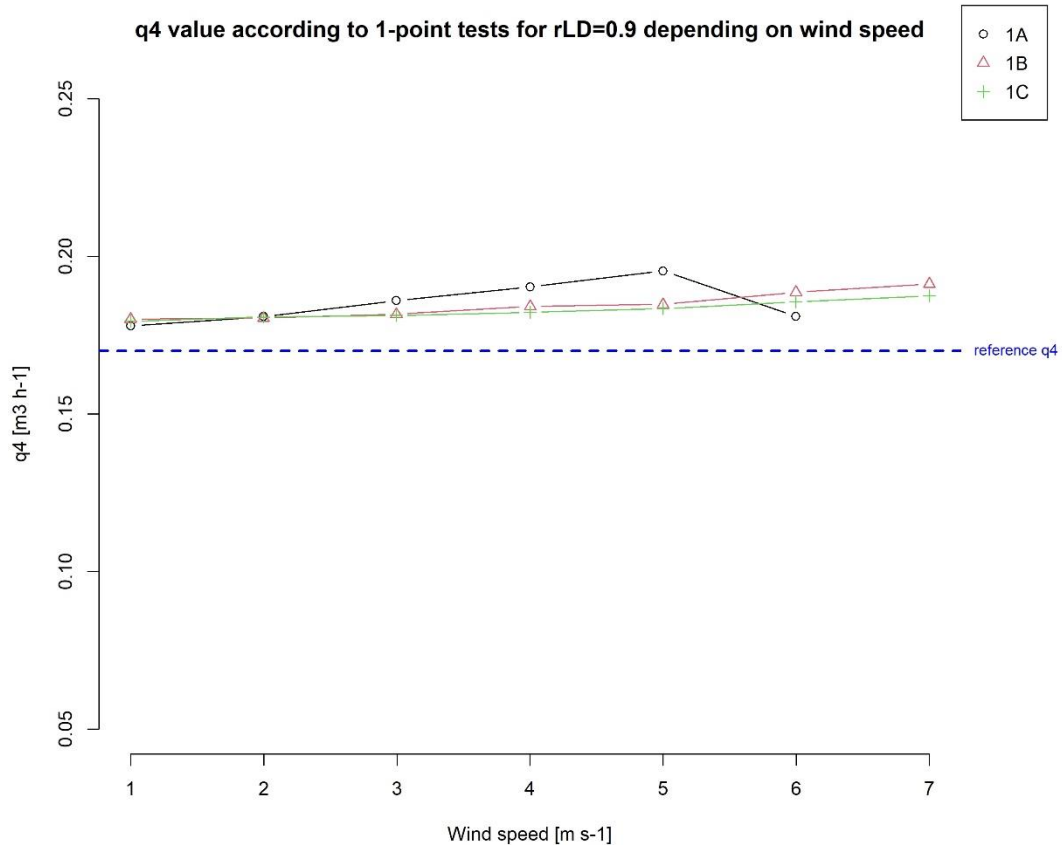
# Annex B 1-point test results: $q_4$ values



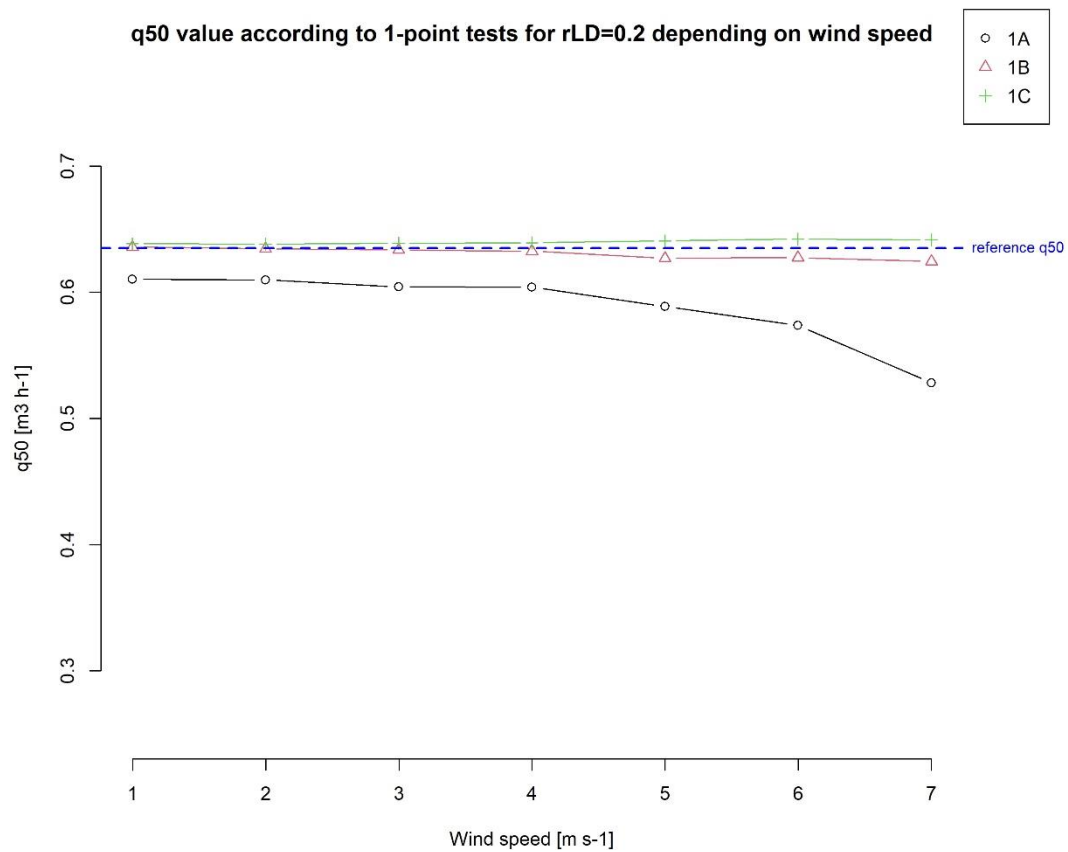
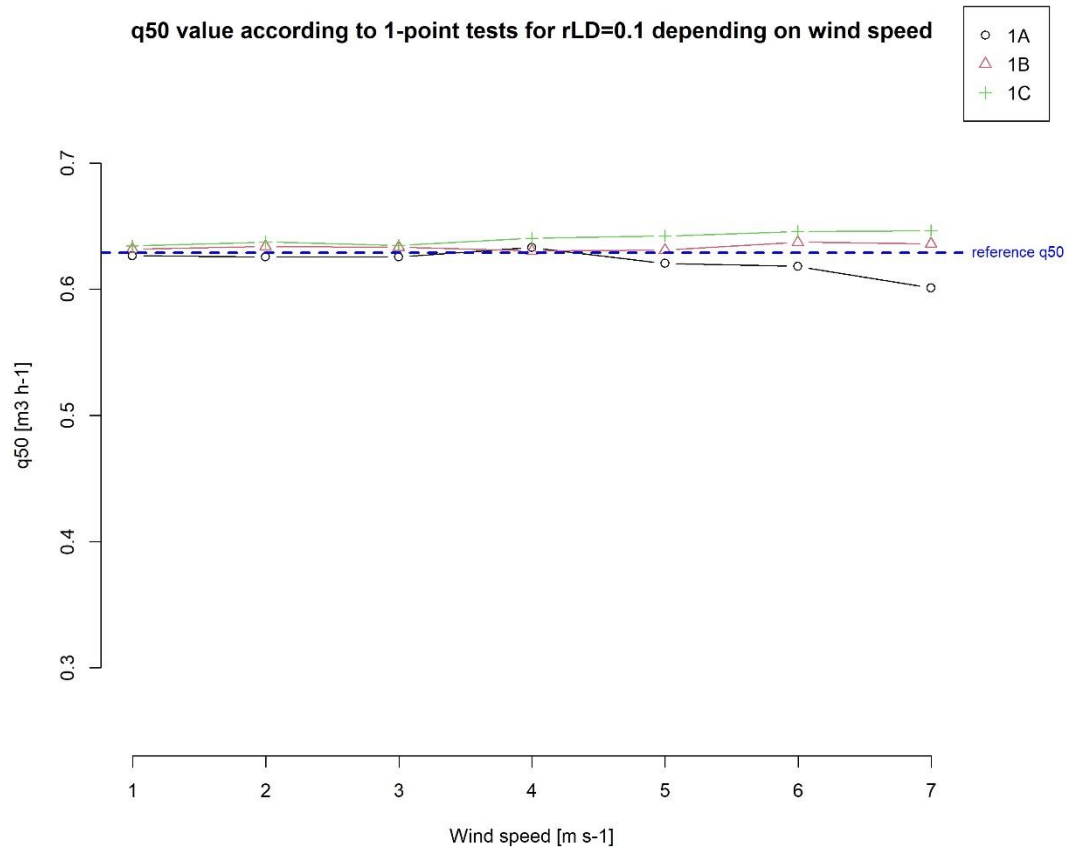




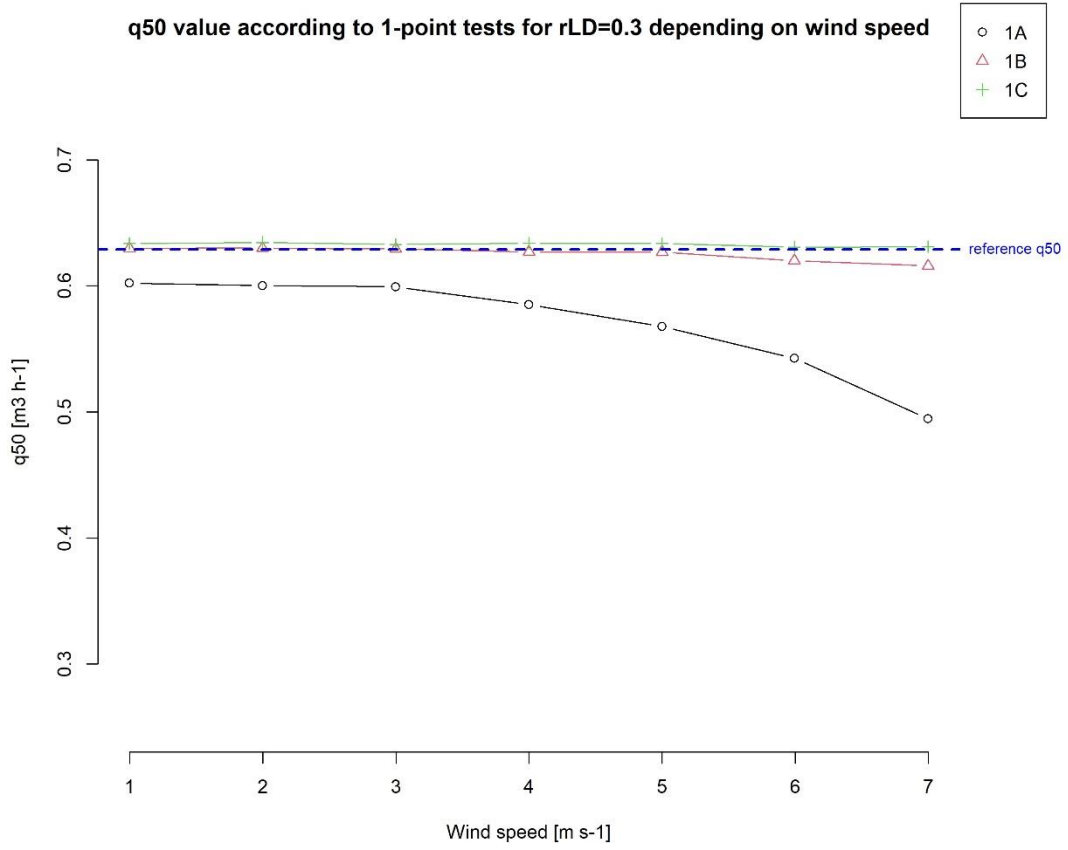




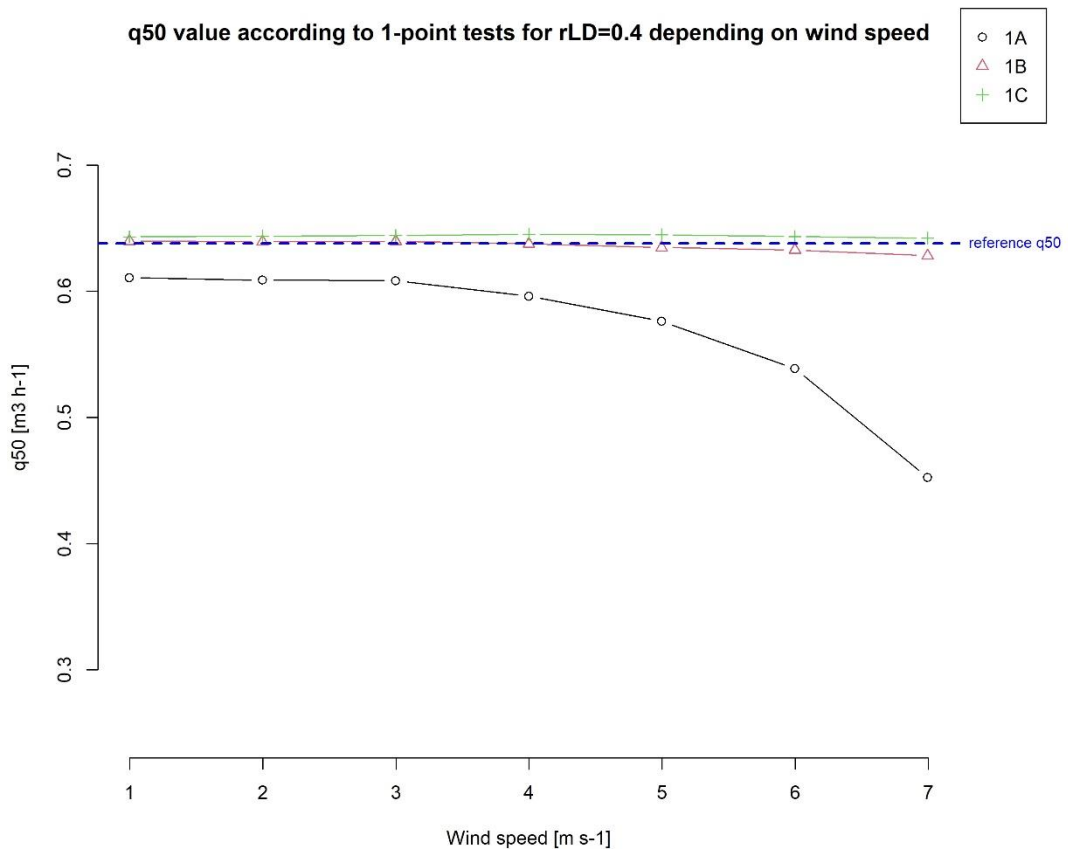
# Annex C 1-point test results: q<sub>50</sub> values



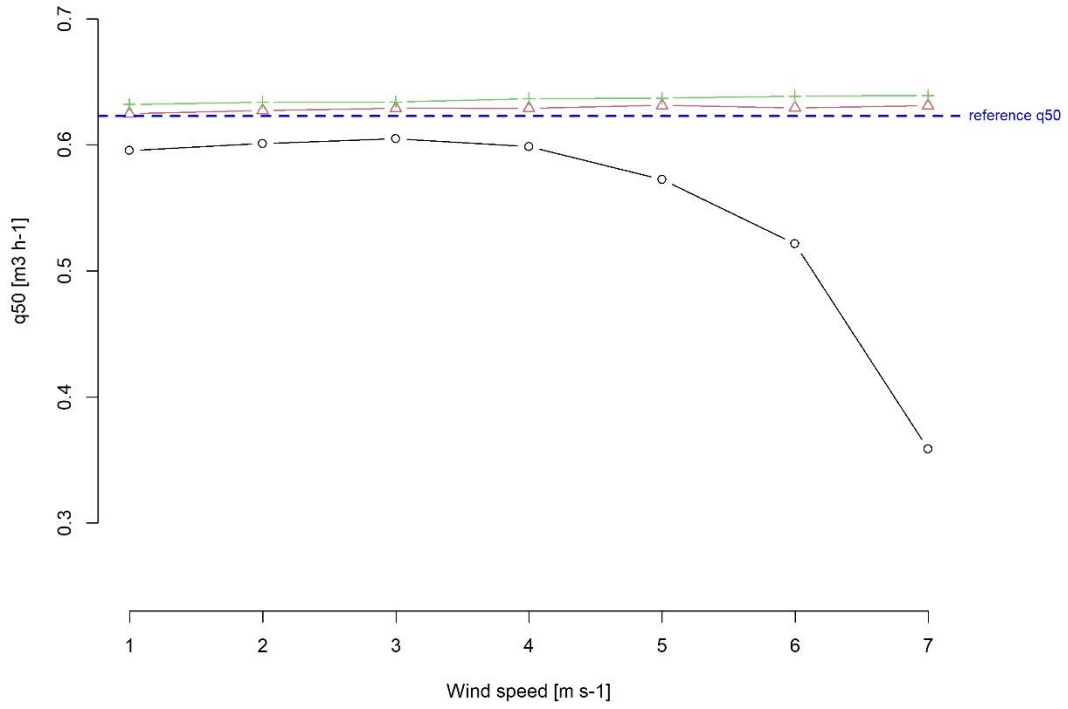
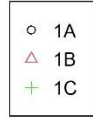
q50 value according to 1-point tests for rLD=0.3 depending on wind speed



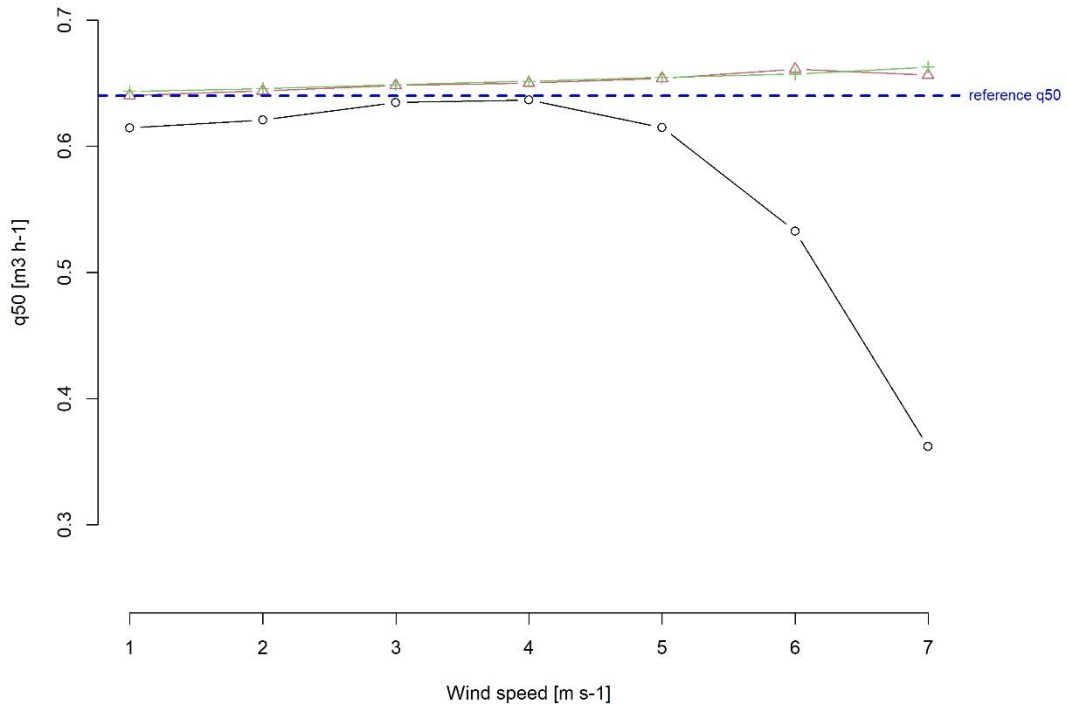
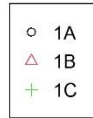
q50 value according to 1-point tests for rLD=0.4 depending on wind speed



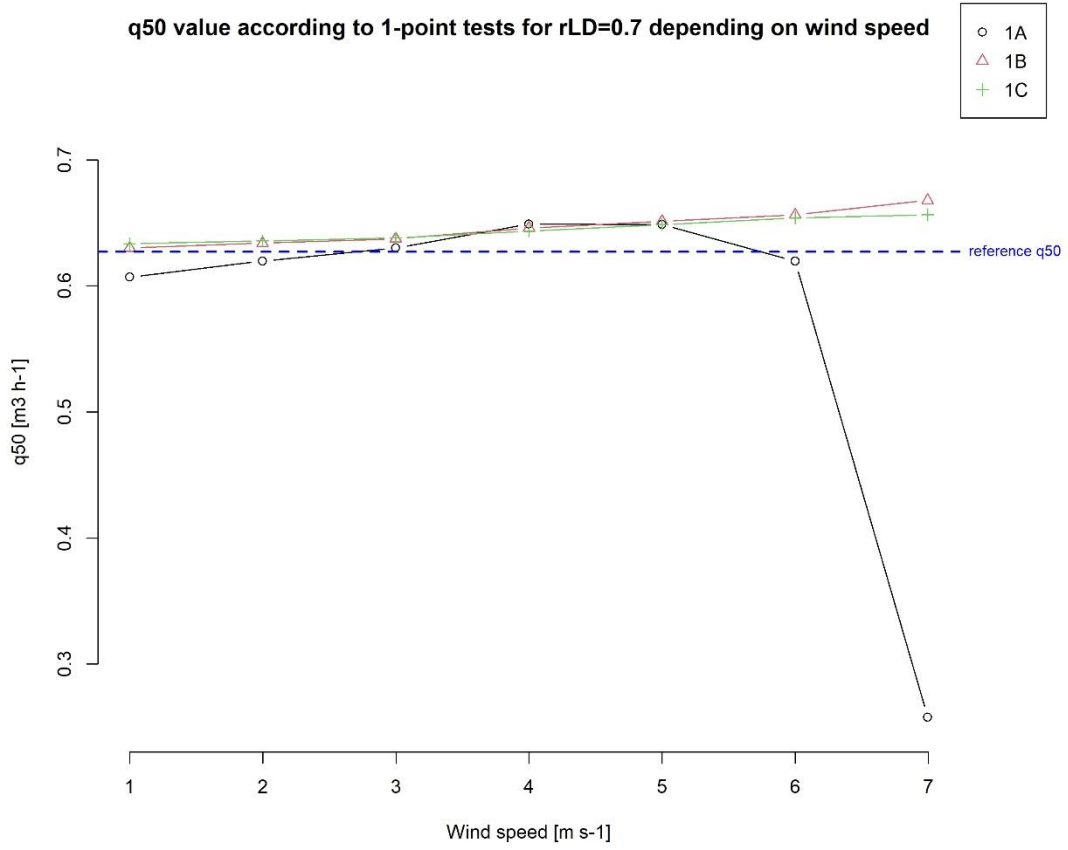
q50 value according to 1-point tests for rLD=0.5 depending on wind speed



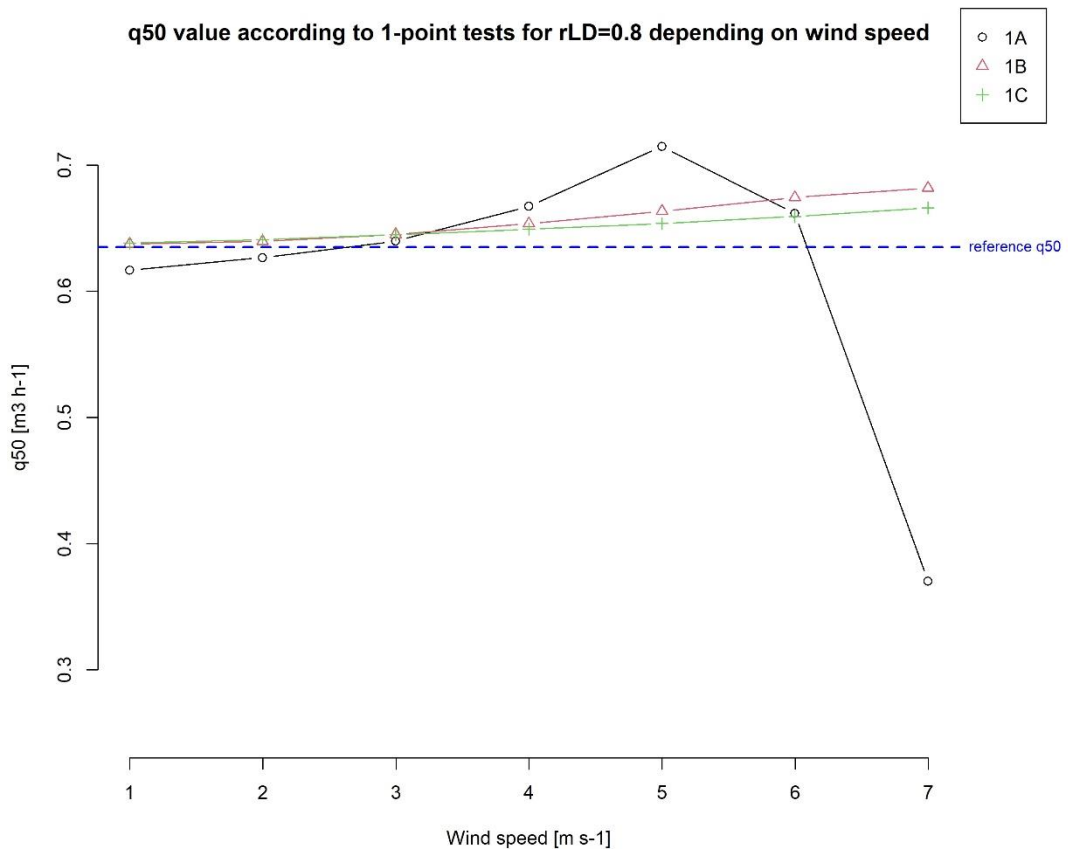
q50 value according to 1-point tests for rLD=0.6 depending on wind speed



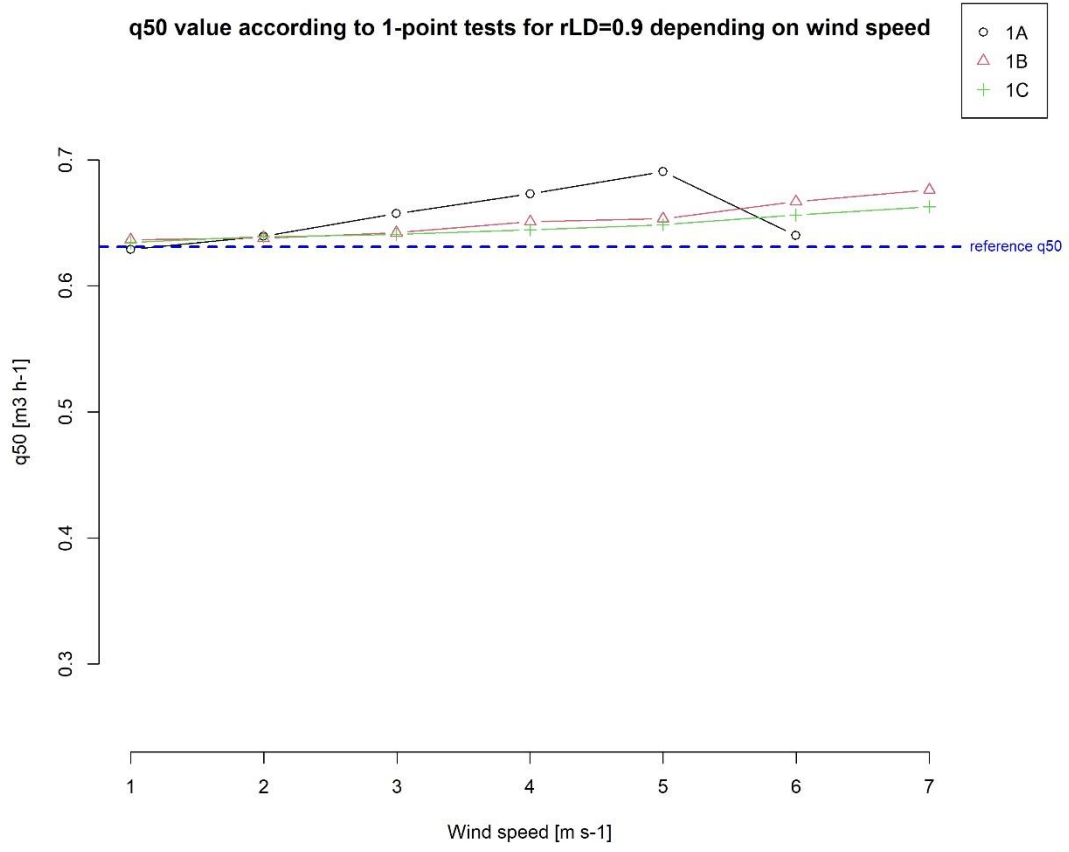
q50 value according to 1-point tests for rLD=0.7 depending on wind speed



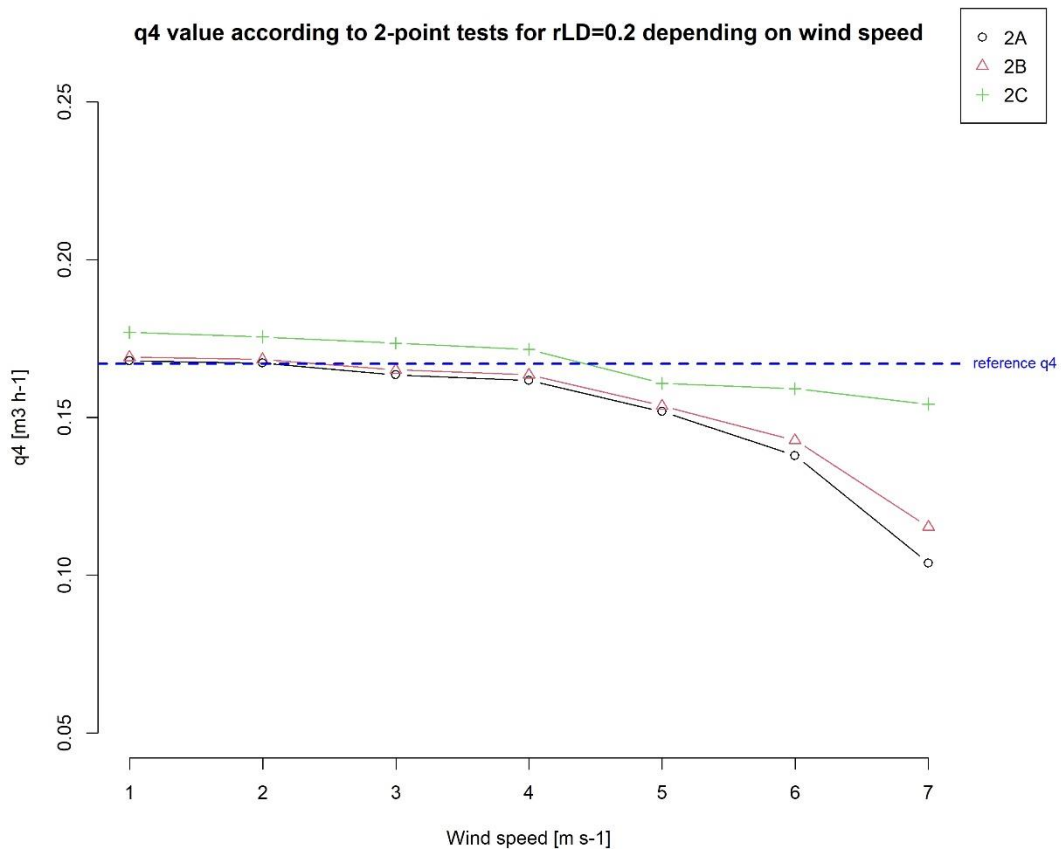
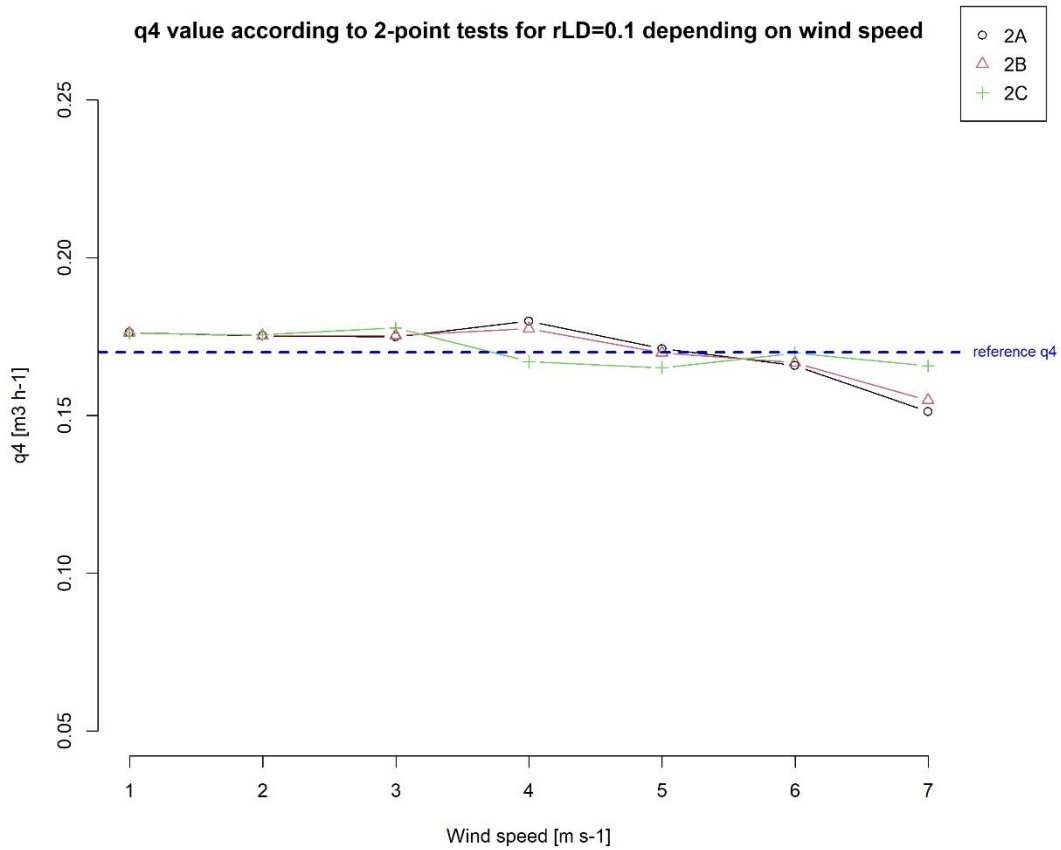
q50 value according to 1-point tests for rLD=0.8 depending on wind speed

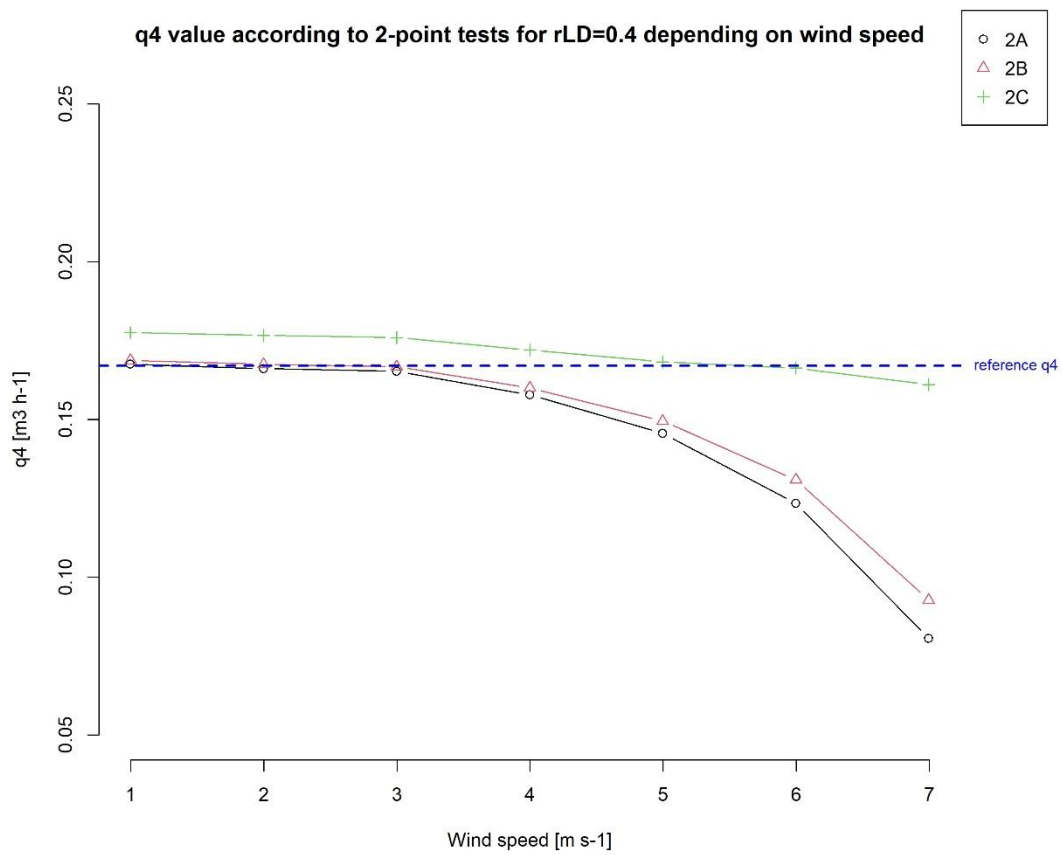
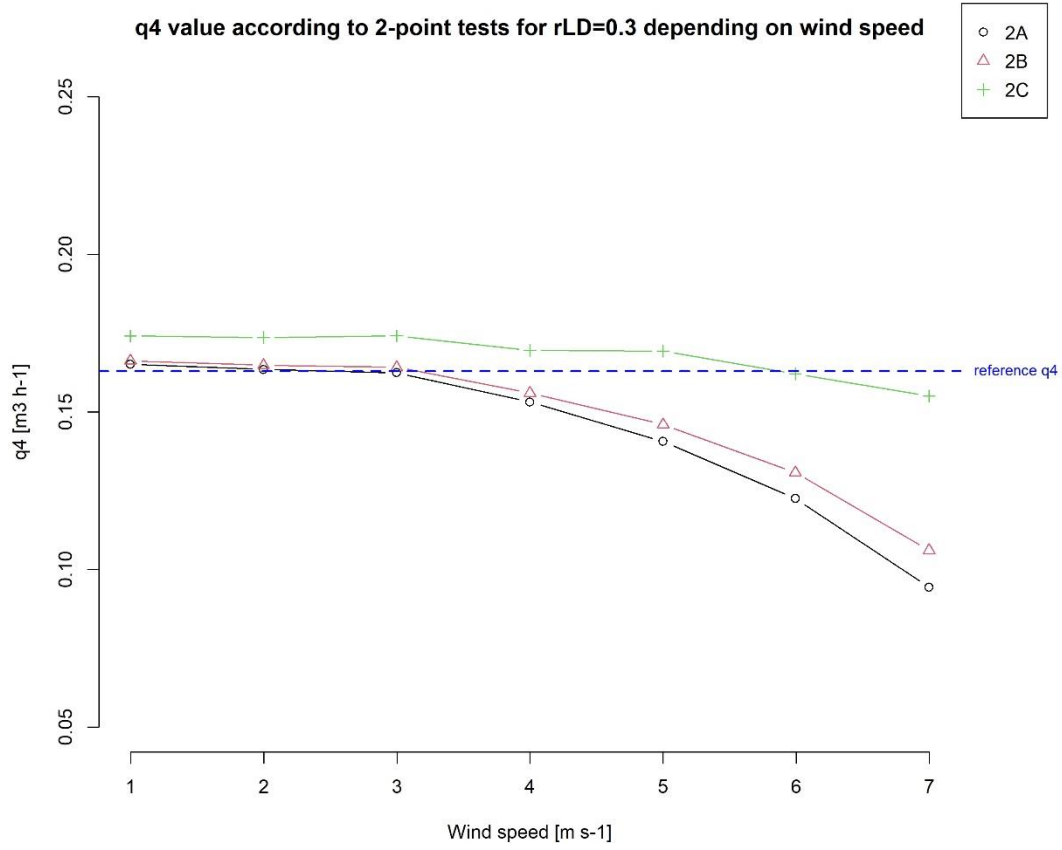


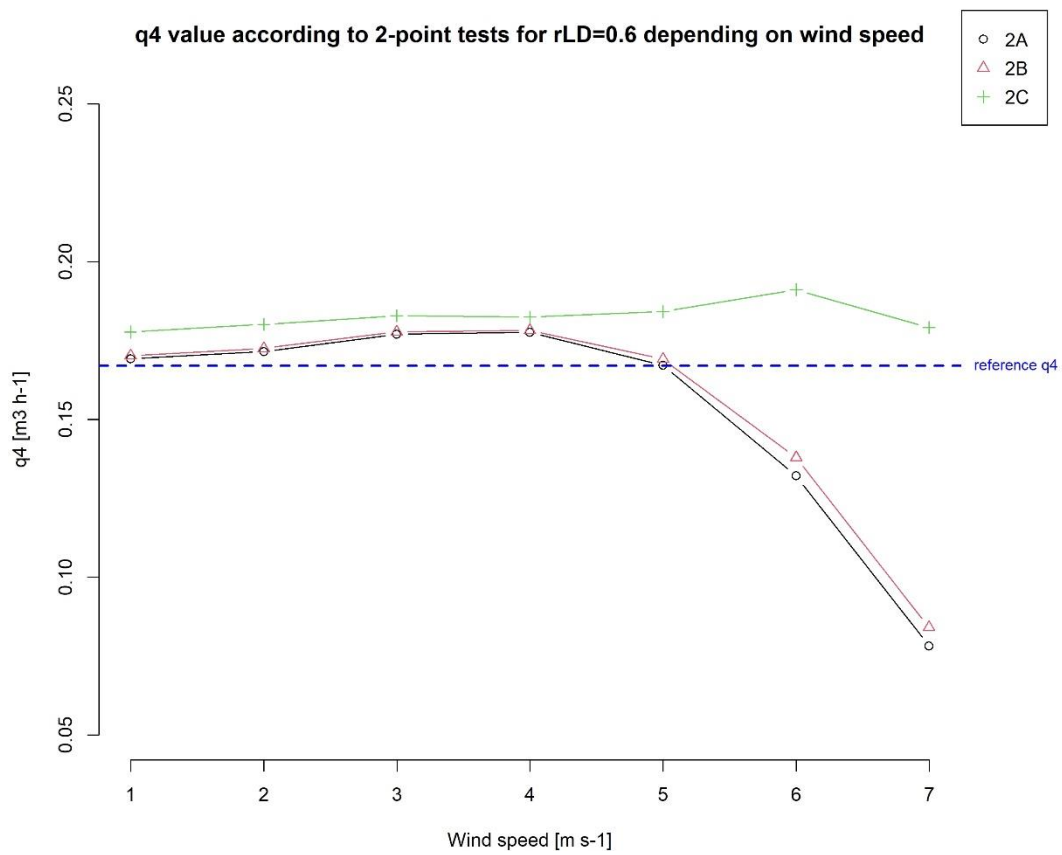
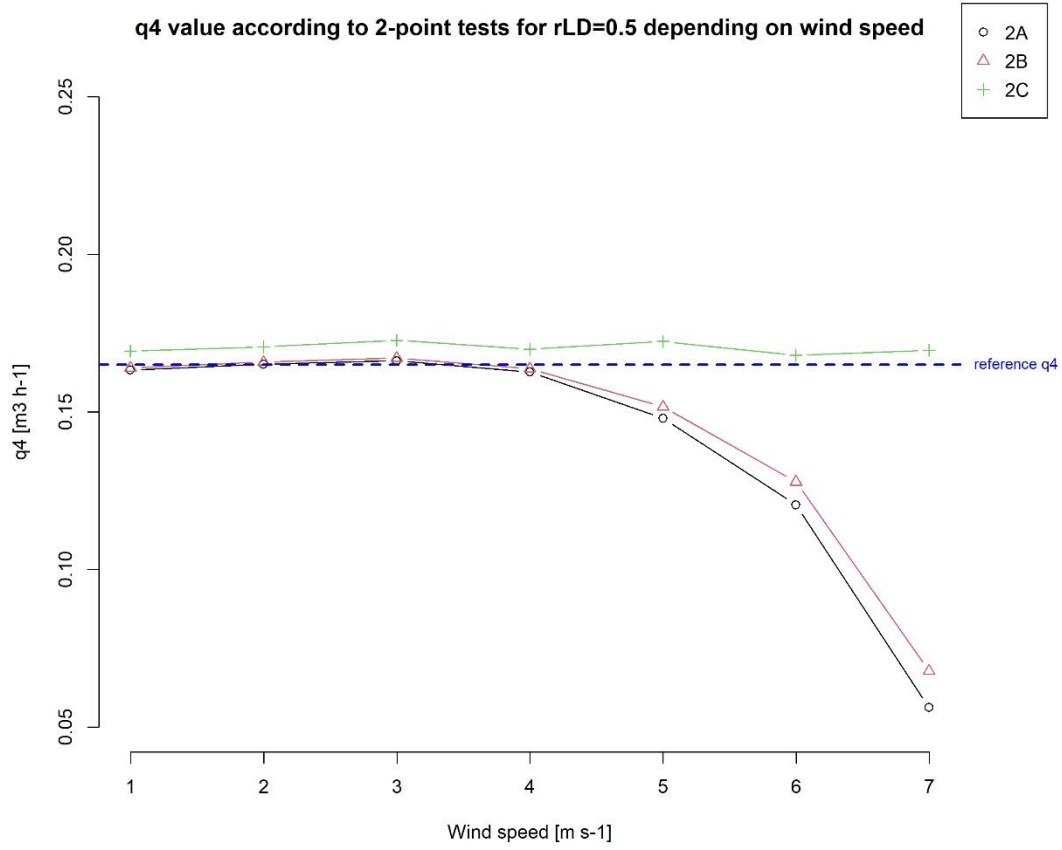
q50 value according to 1-point tests for rLD=0.9 depending on wind speed

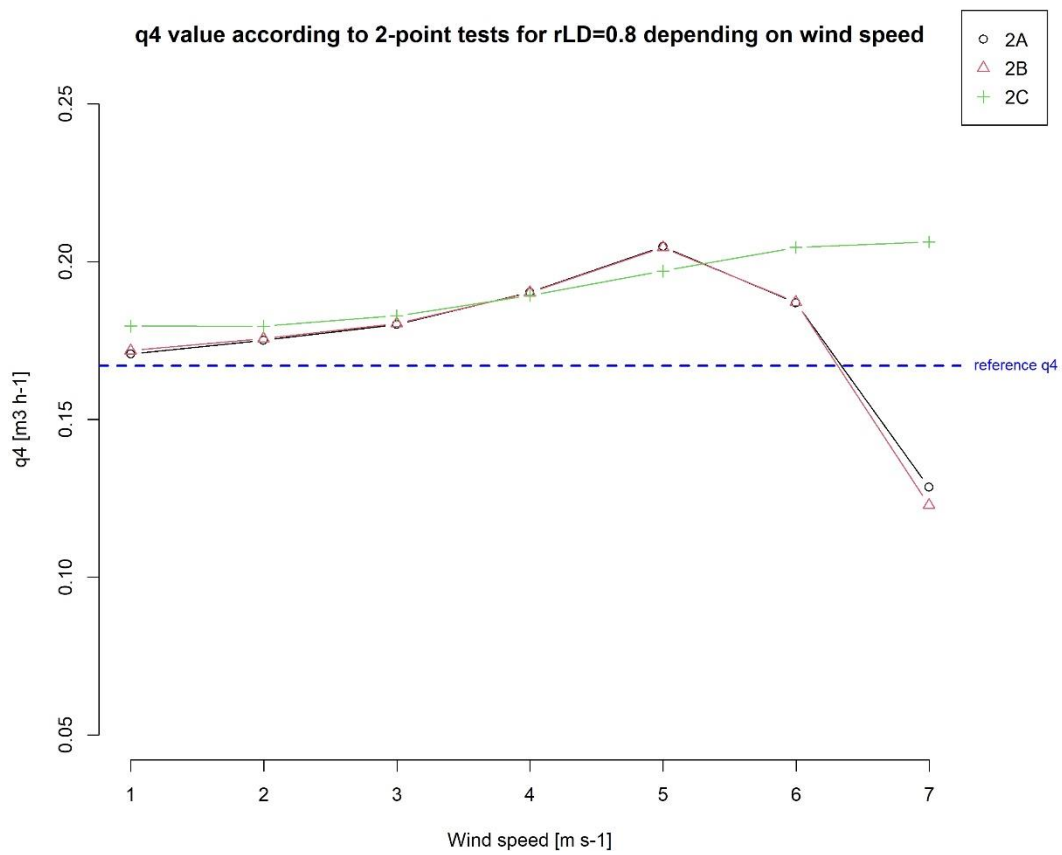
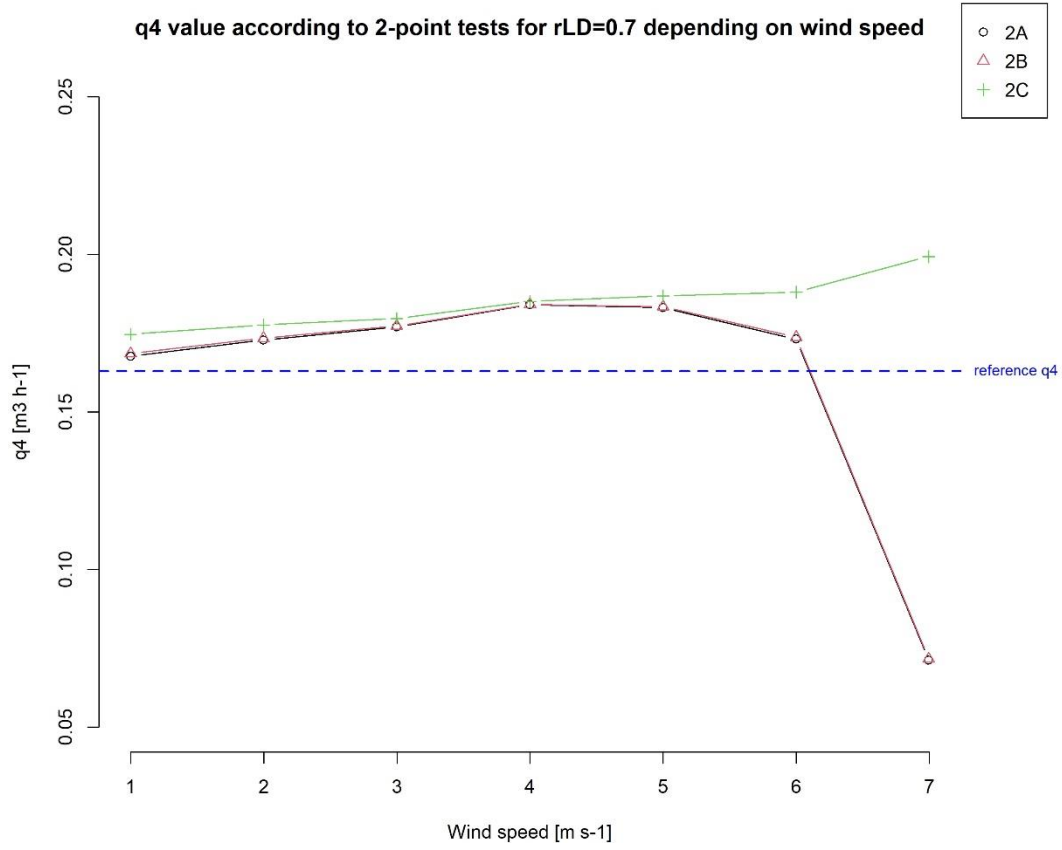


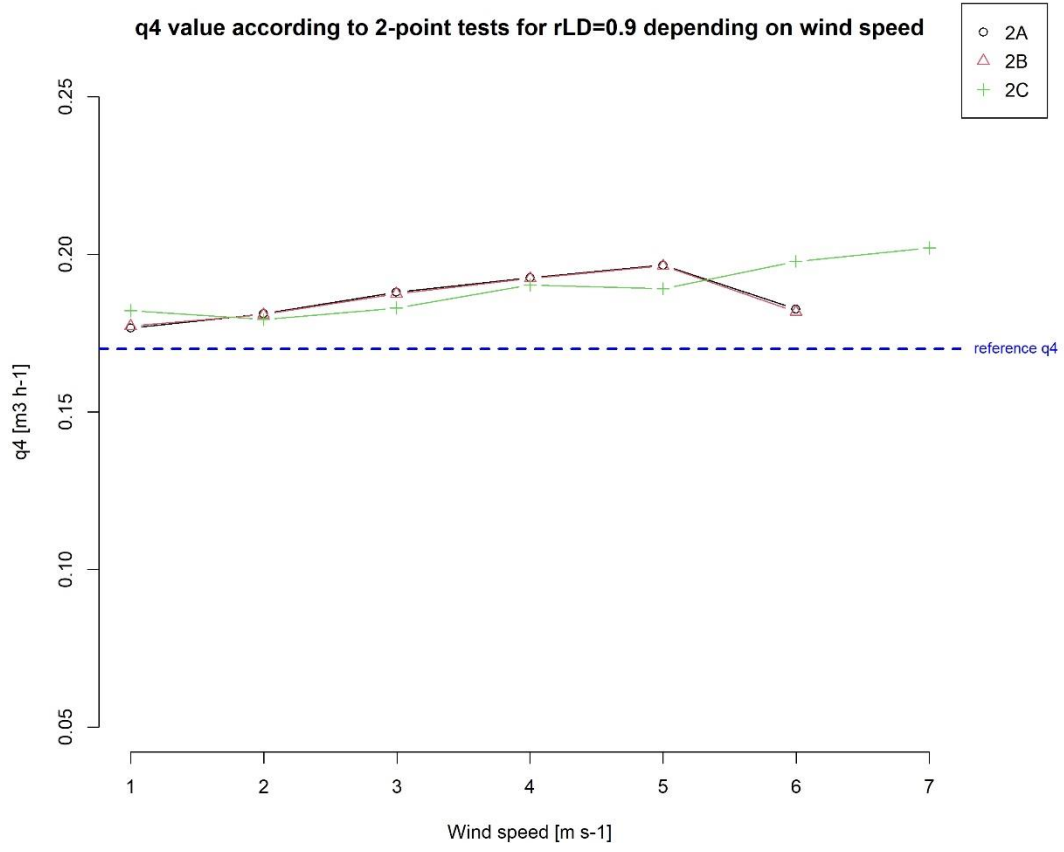
# Annex D 2-point tests result: $q_4$ values



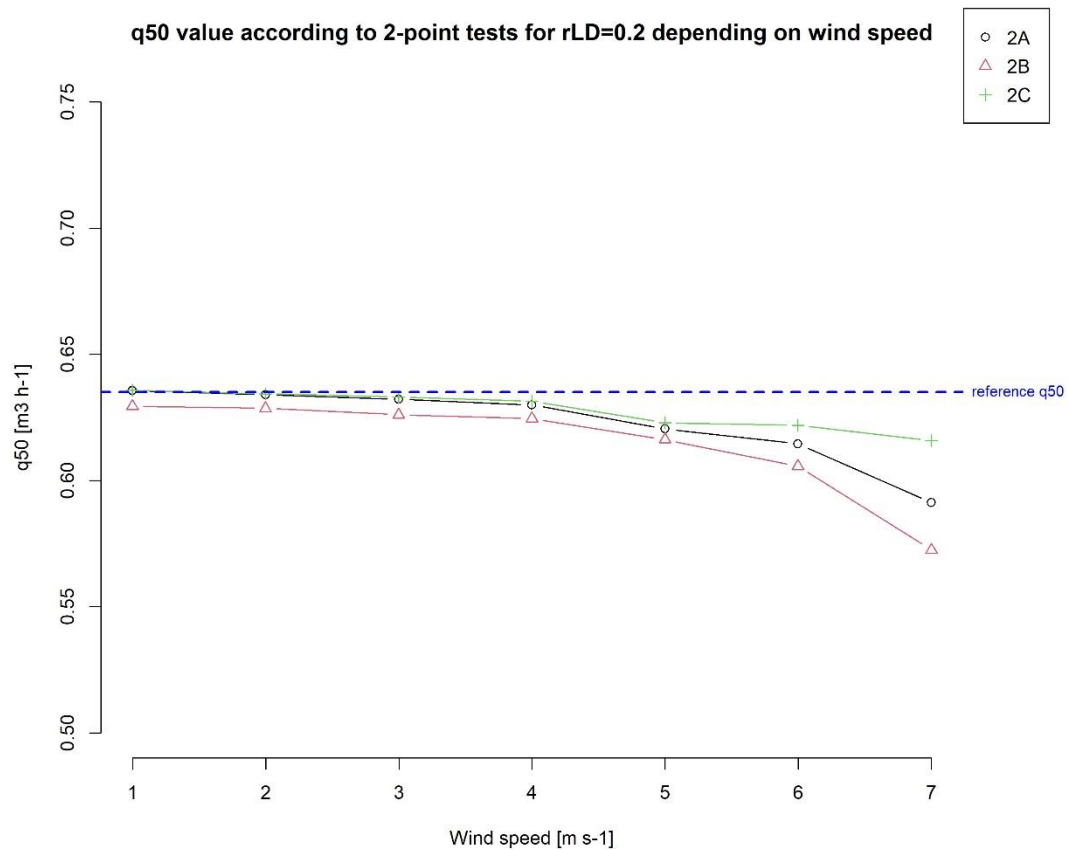
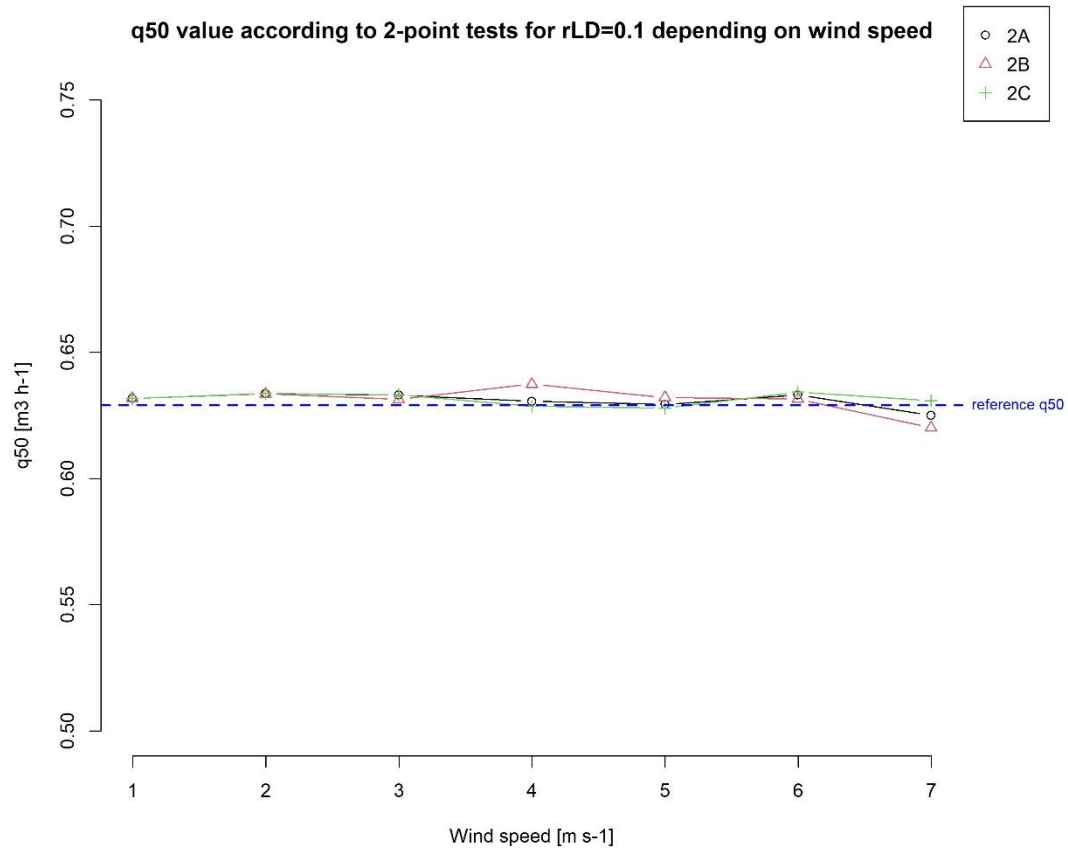


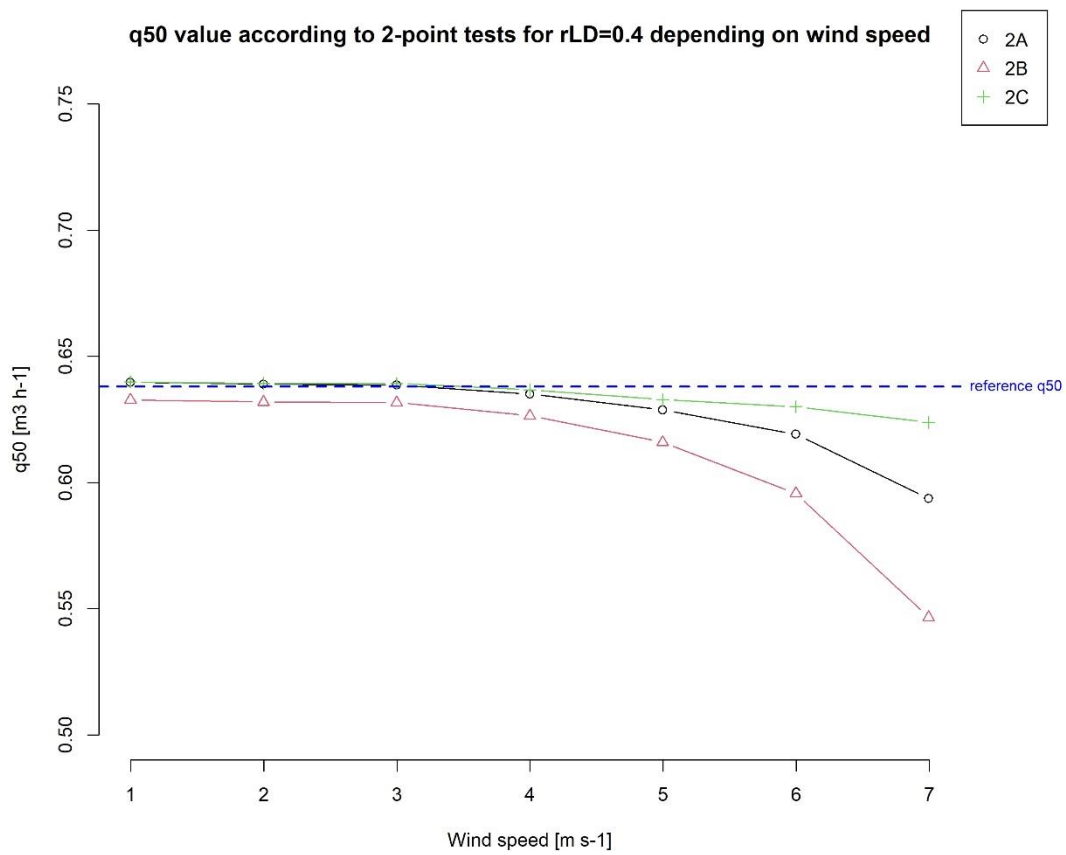
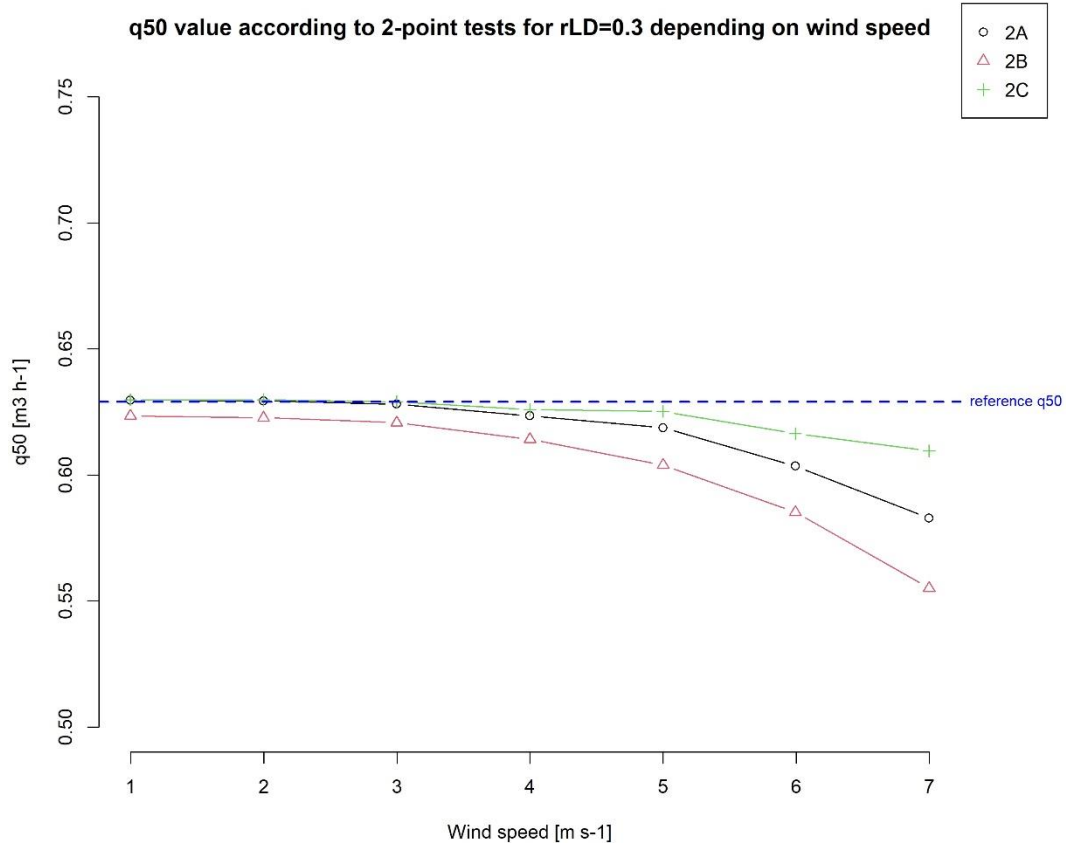


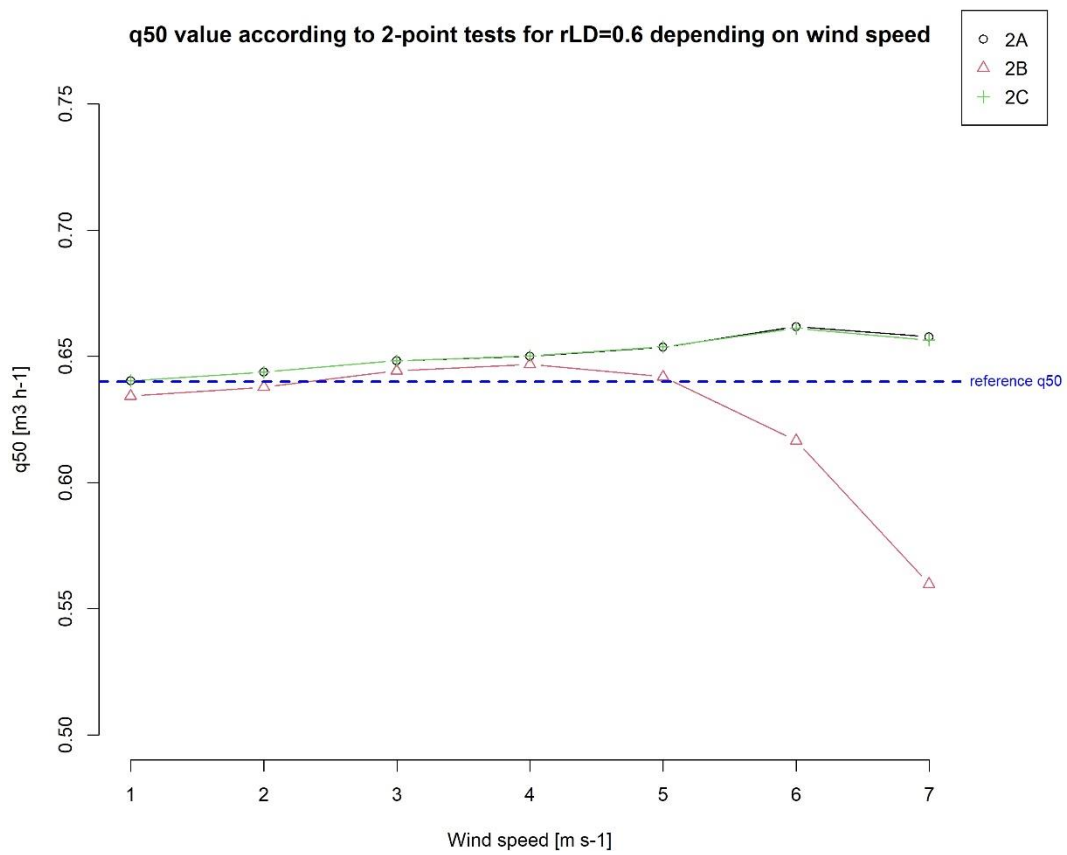
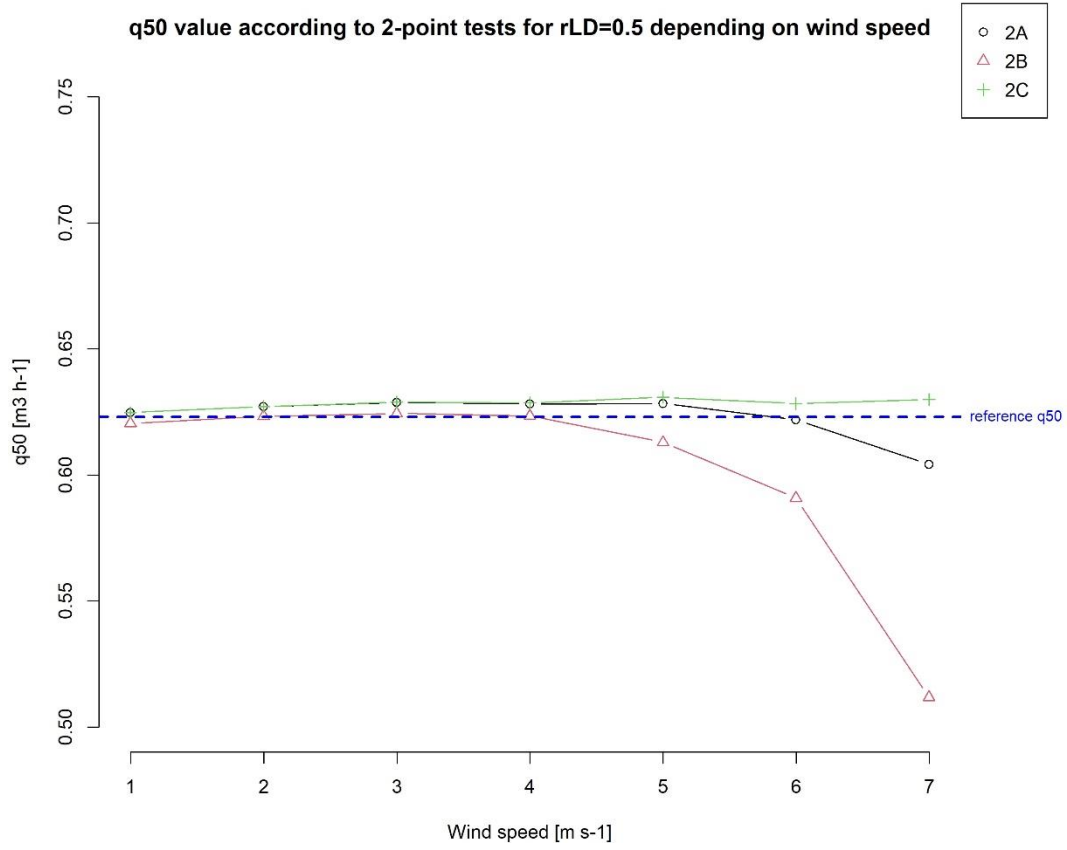


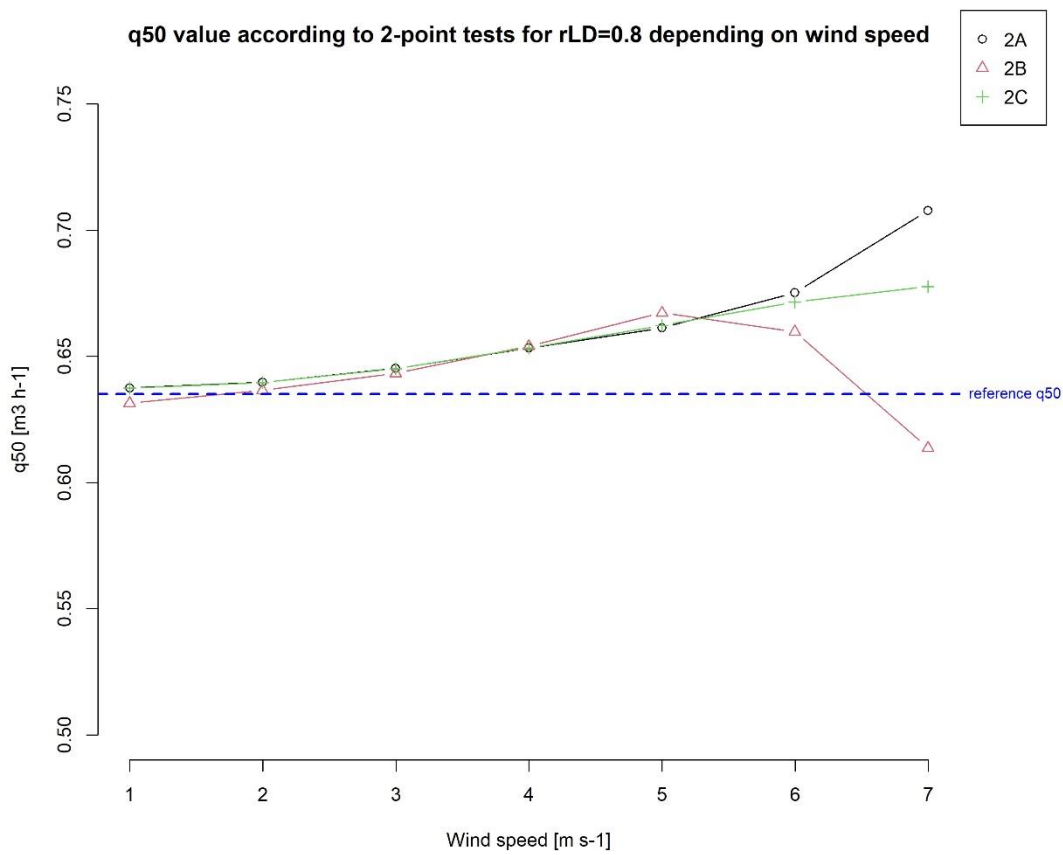
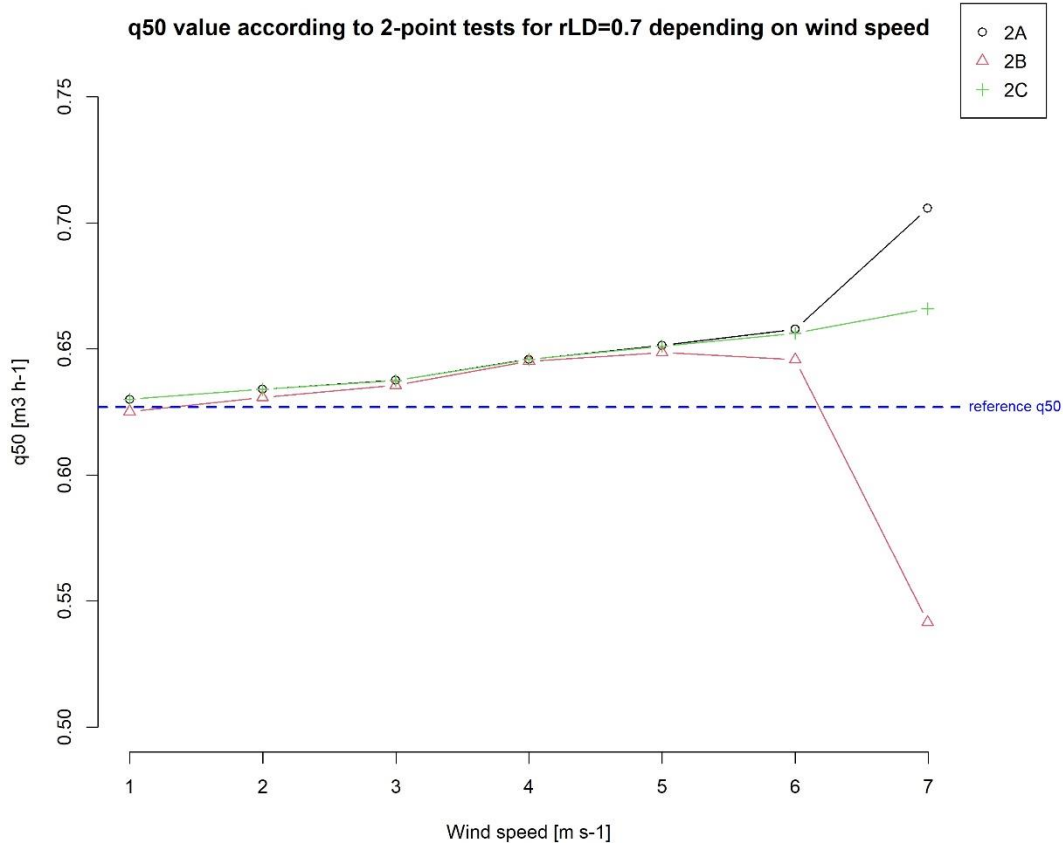


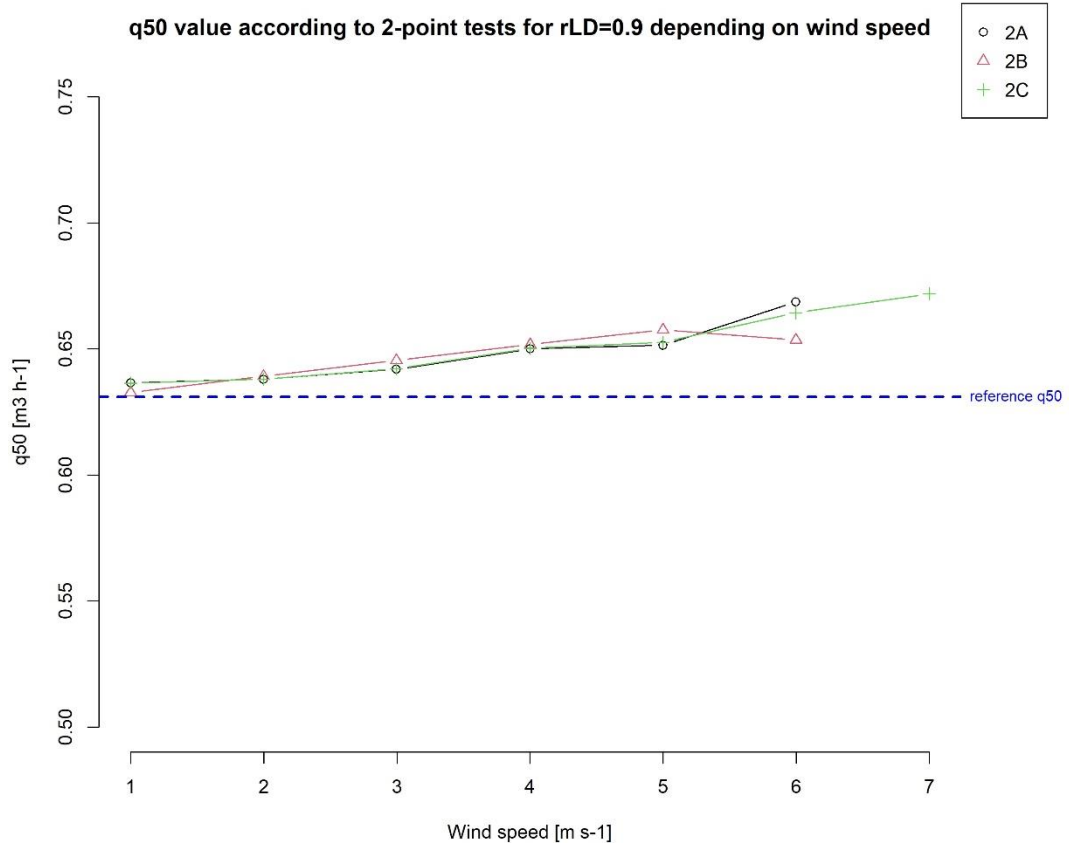
# Annex E 2-point test results: $q_{50}$ values





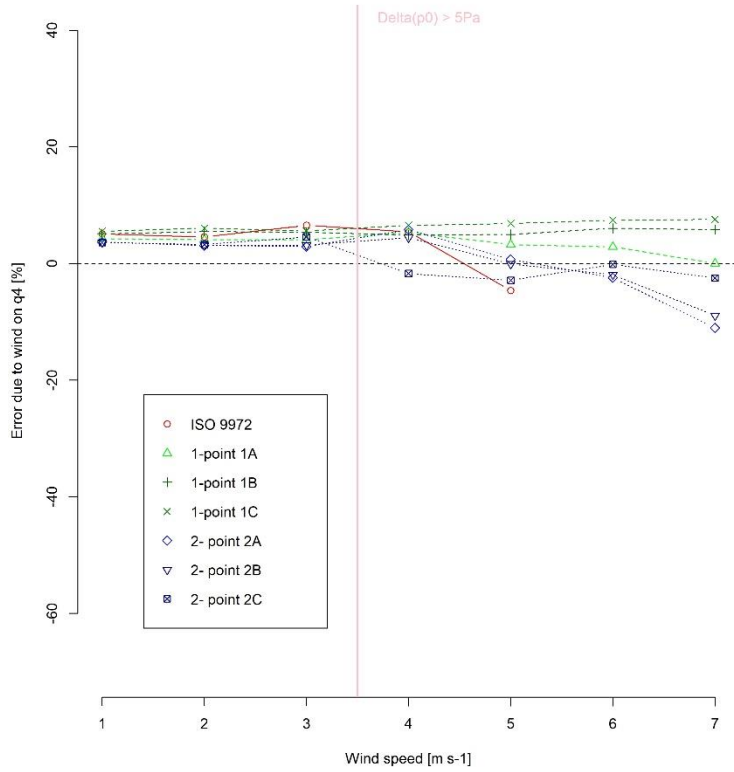




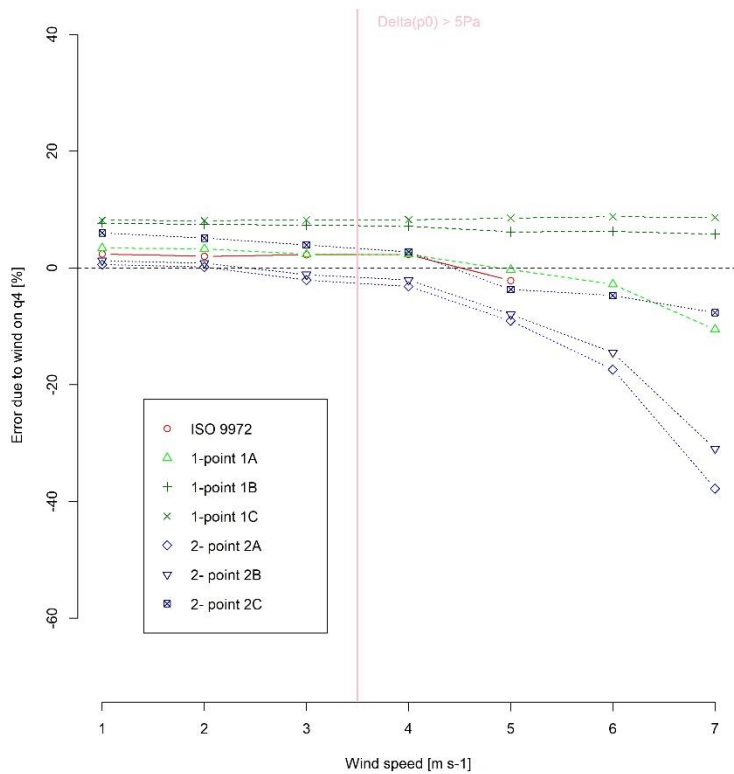


# Annex F Comparison of error on $q_4$ for different analysis methods

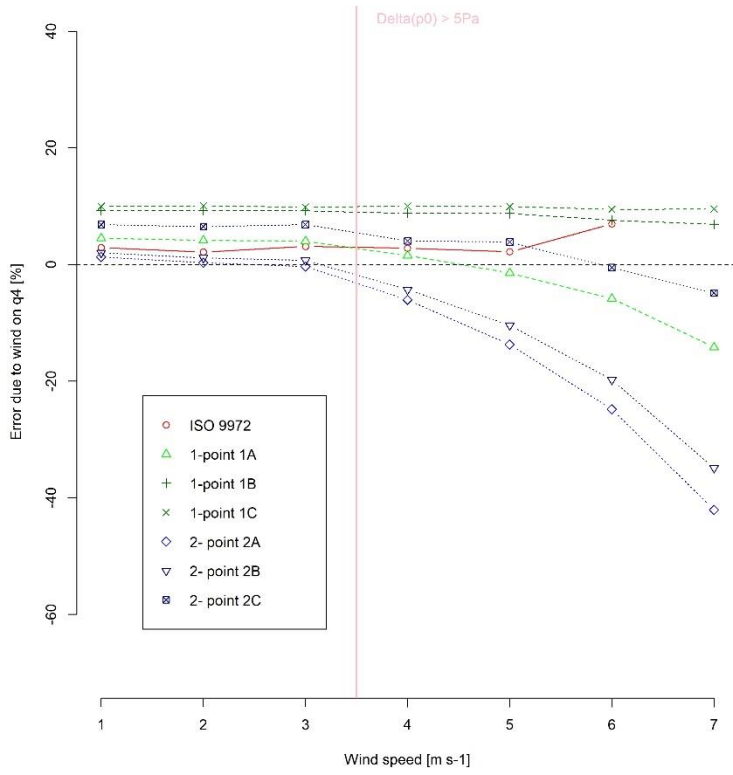
Error due to wind on  $q_4$  depending on the analysis method for  $rLD=0.1$



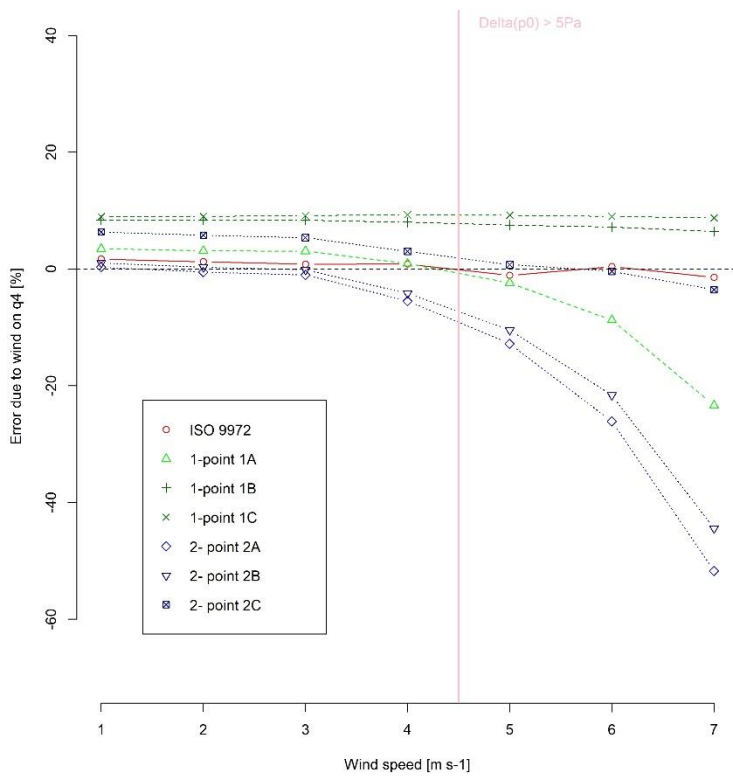
Error due to wind on  $q_4$  depending on the analysis method for  $rLD=0.2$



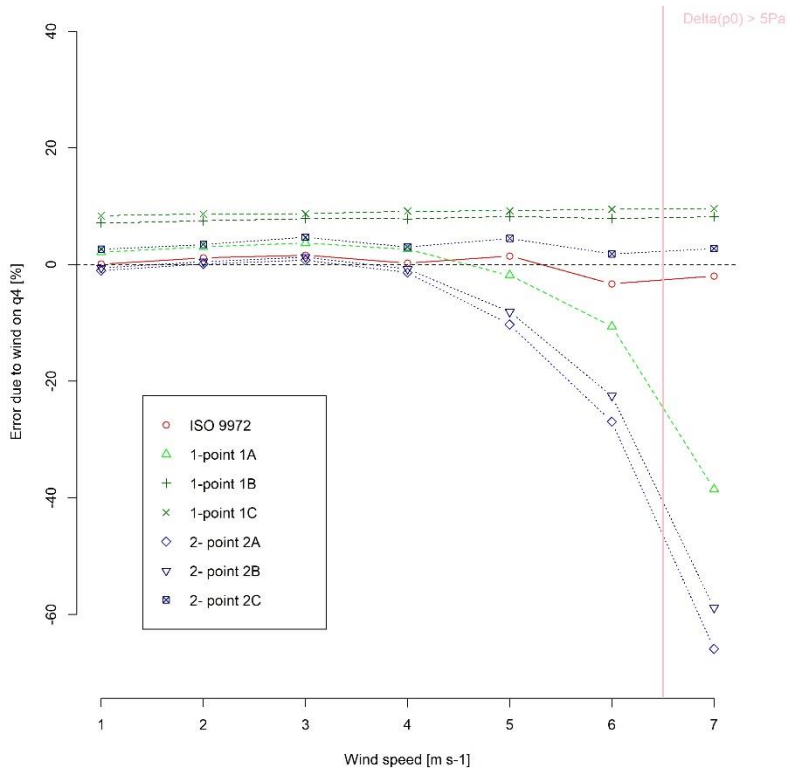
Error due to wind on q4 depending on the analysis method for rLD=0.3



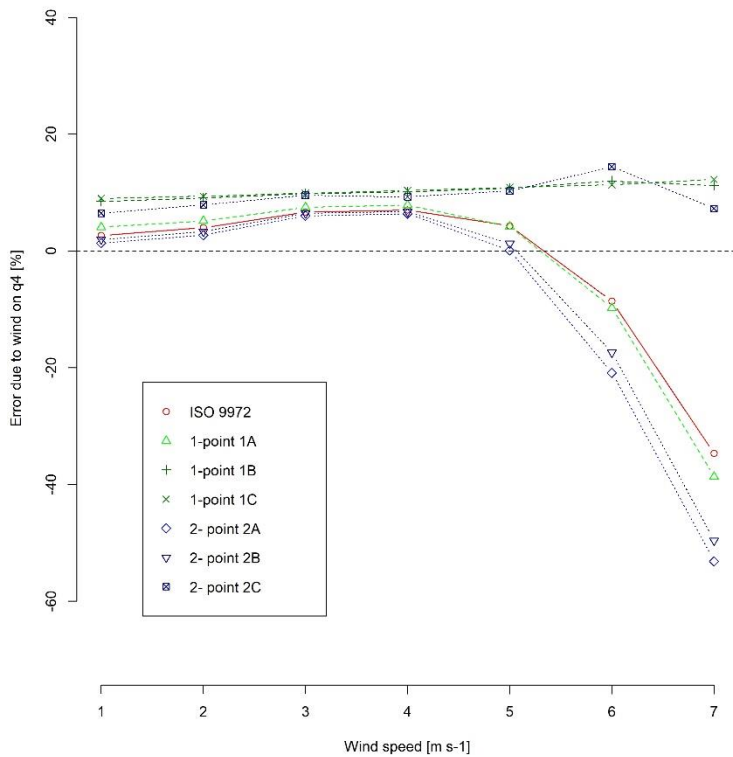
Error due to wind on q4 depending on the analysis method for rLD=0.4



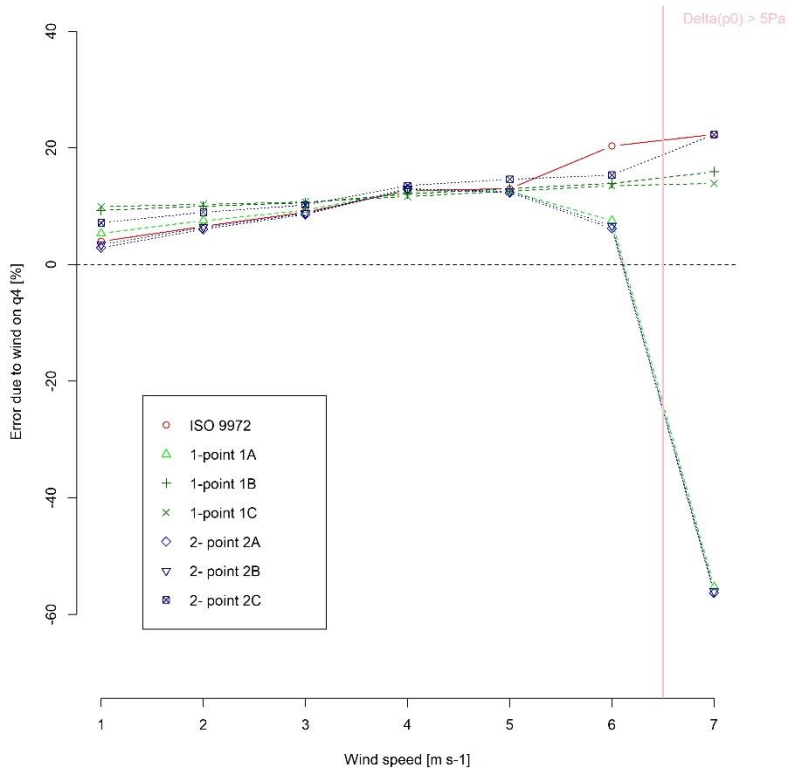
Error due to wind on q4 depending on the analysis method for rLD=0.5



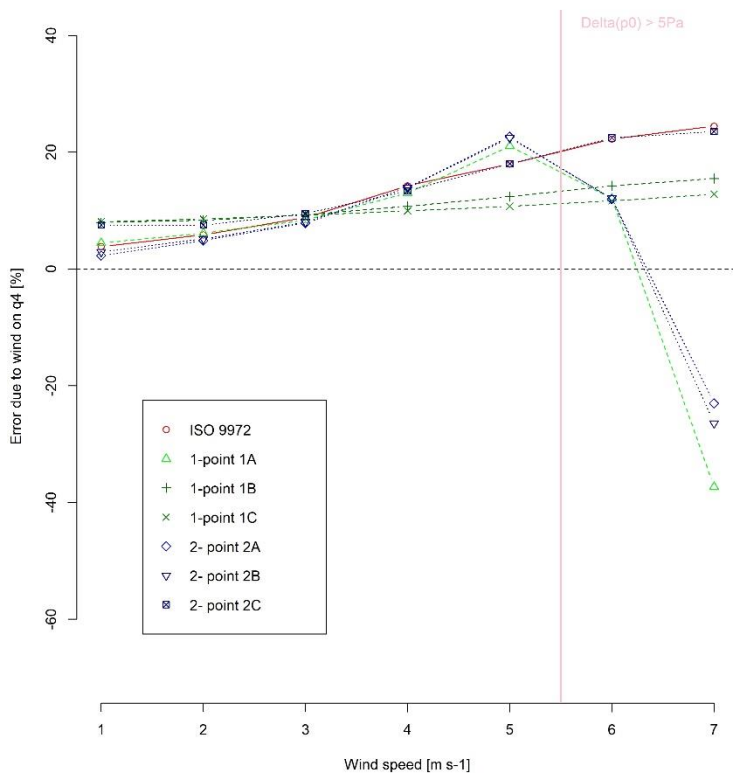
Error due to wind on q4 depending on the analysis method for rLD=0.6



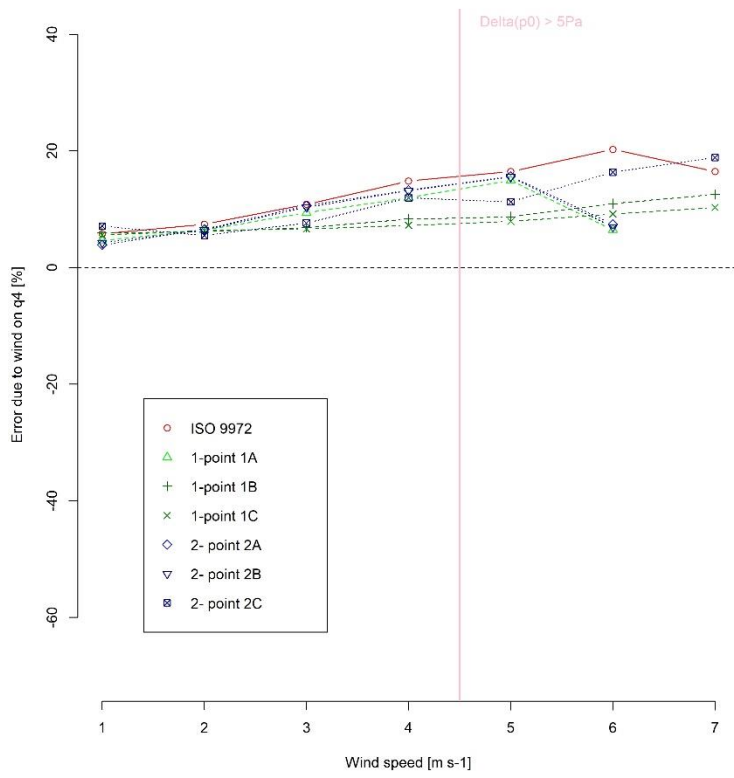
Error due to wind on q4 depending on the analysis method for rLD=0.7



Error due to wind on q4 depending on the analysis method for rLD=0.8

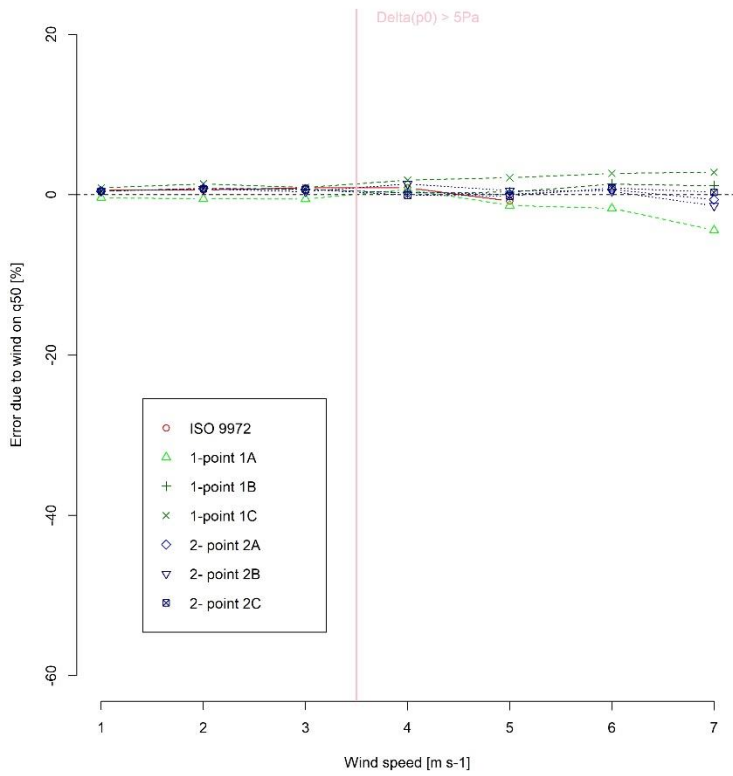


Error due to wind on q4 depending on the analysis method for rLD=0.9

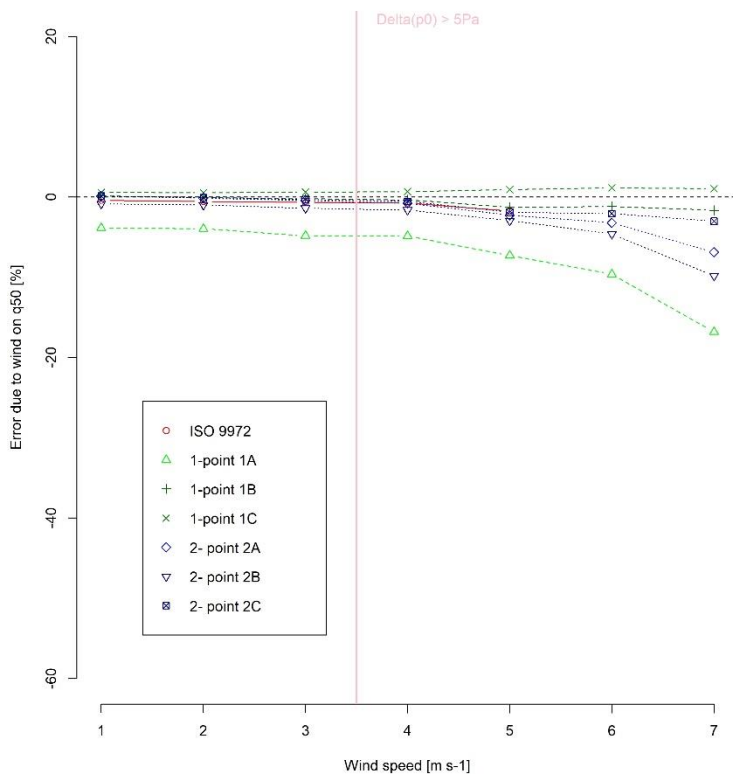


# Annex G Comparison of error on $q_{50}$ for different analysis methods

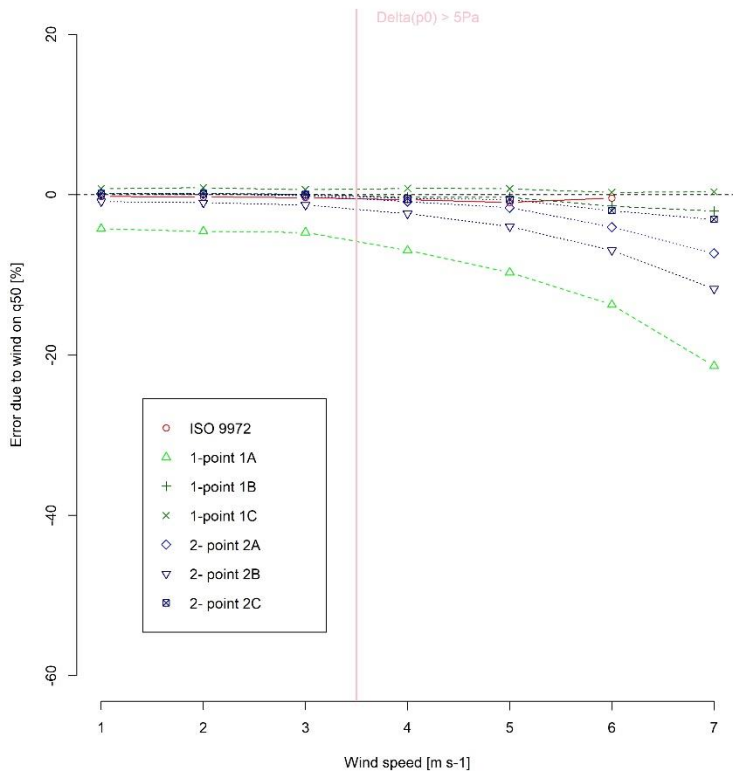
Error due to wind on  $q_{50}$  depending on the analysis method for  $rLD=0.1$



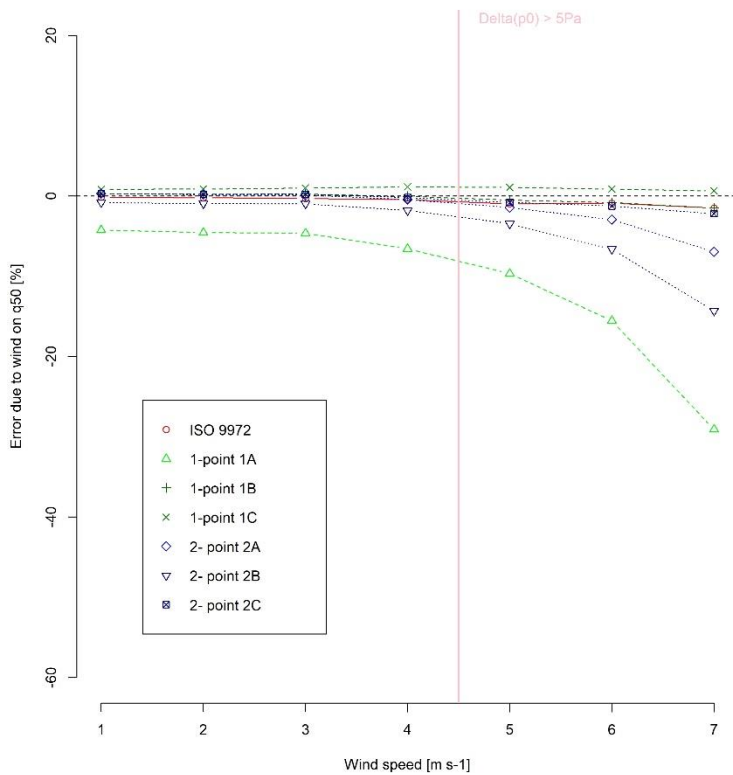
Error due to wind on  $q_{50}$  depending on the analysis method for  $rLD=0.2$



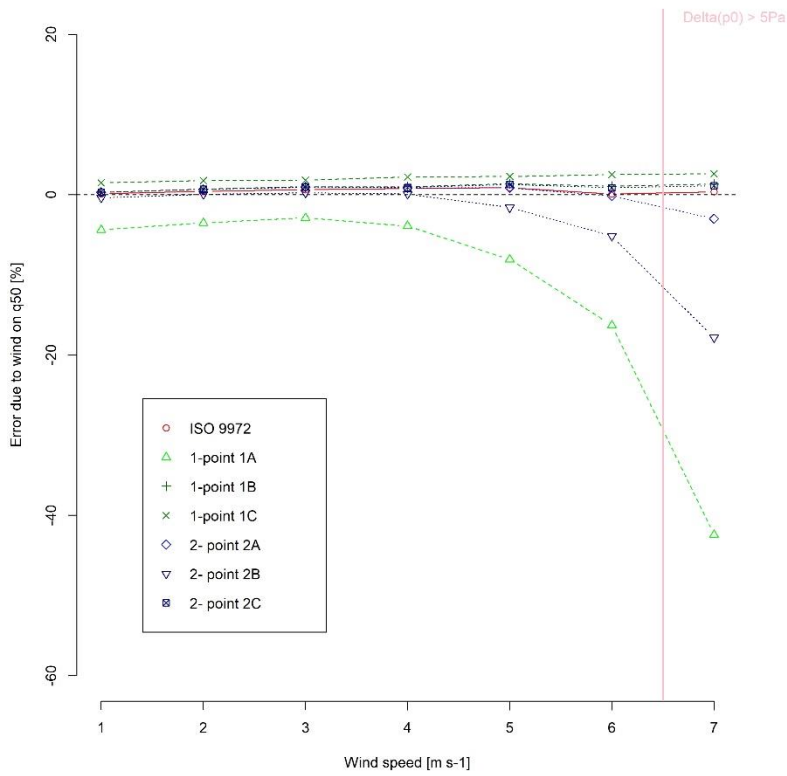
Error due to wind on q50 depending on the analysis method for rLD=0.3



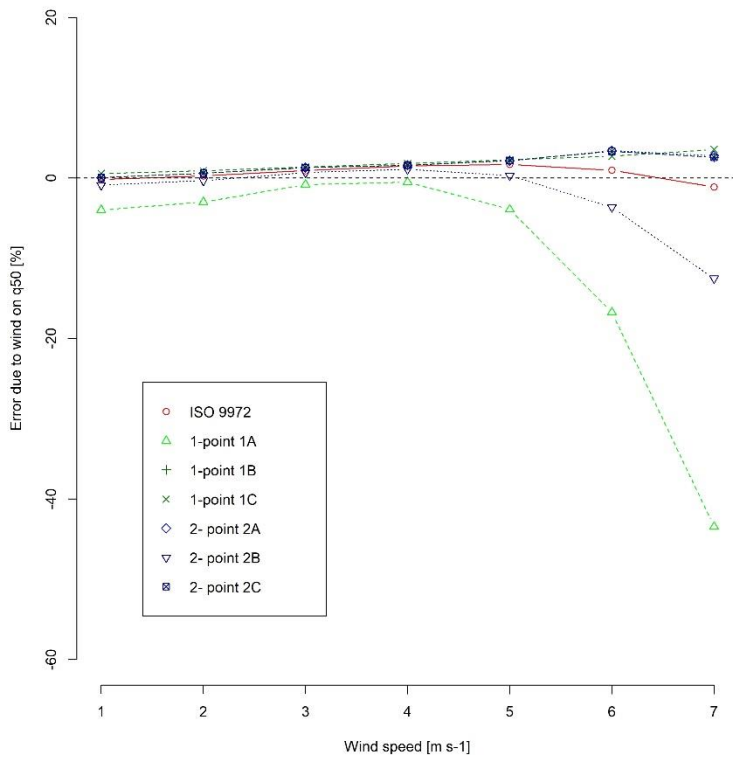
Error due to wind on q50 depending on the analysis method for rLD=0.4



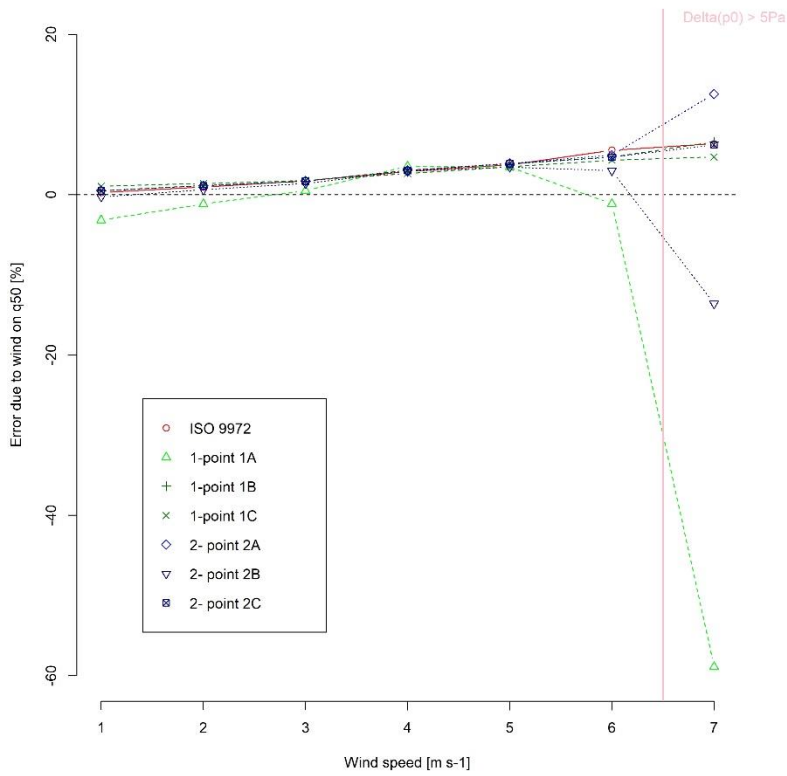
Error due to wind on q50 depending on the analysis method for rLD=0.5



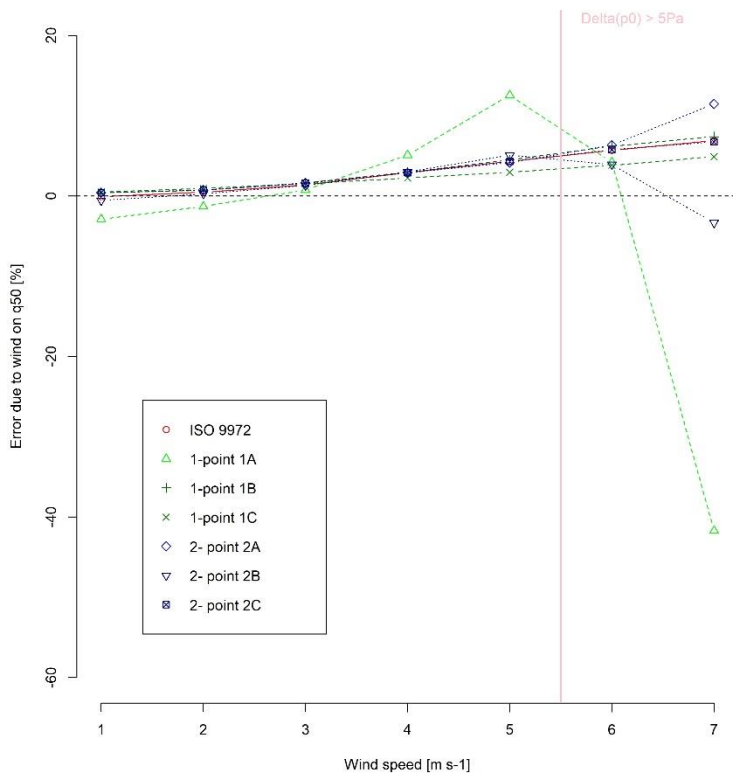
Error due to wind on q50 depending on the analysis method for rLD=0.6



Error due to wind on q50 depending on the analysis method for rLD=0.7



Error due to wind on q50 depending on the analysis method for rLD=0.8



Error due to wind on q50 depending on the analysis method for rLD=0.9

